Turkey Flat, USA

Site Effects Test Area

REPORT 2

Site Characterization

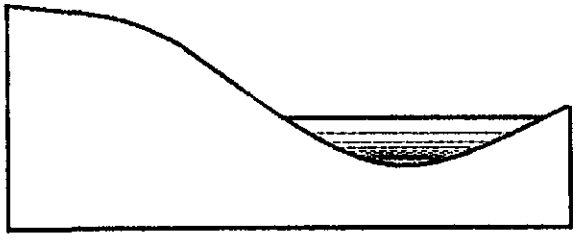

MARCH 1988

TECHNICAL REPORT NO. 88-2

CALIFORNIA DEPARTMENT OF CONSERVATION

DIVISION OF MINES AND GEOLOGY

EARTHQUAKE SHAKING ASSESSMENT UNIT

The Turkey Flat site effects test area is one of a series of international test areas endorsed by the International Association of Physics of the Earth's Interior and the International Association of Earthquake Engineers.

Members of the Turkey Flat Site Effects Test Area Geotechnical Planning Committee:

Mr. LeRoy Crandall (Chairman)
LeRoy Crandall and Associates

Dr. P.Y. Bard
LGIT-IRIGM, France

Dr. C.Y. Chang
Geomatrix Consultants, USA

Dr. Neville C. Donovan
Dames & Moore, USA

Mr. James H. Gates
California Department of Transportation, USA

Dr. I.M. Idriss
Woodward-Clyde Consultants, USA

Mr. Fumio Kaneko
OYO Corporation, Japan

Dr. Marshall Lew
LeRoy Crandall and Associates, USA

Dr. Satoru Ohya
Oyo Corporation, USA

Mr. Maurice S. Power
Geomatrix Consultants, USA

Mr. Charles R. Real
California Division of Mines and Geology, USA

Mr. Bruce Redpath
Qest Consultants, USA

Dr. Wolfgang Roth
Dames & Moore, USA

Dr. Anthony F. Shakal
California Division of Mines and Geology, USA

Dr. Jogeshwar P. Singh
Geospectra, USA

Dr. Brian E. Tucker
California Division of Mines and Geology, USA

Mr. John Vrymoed
California Department of Transportation, USA

The Turkey Flat site effects test area is one of a series of international test areas endorsed by the International Association of Physics of the Earth's Interior and the International Association of Earthquake Engineers.

Members of the Turkey Flat Site Effects Test Area Geotechnical Planning Committee:

TURKEY FLAT, USA
SITE EFFECTS TEST AREA

Report 2

SITE CHARACTERIZATION

Prepared by

Charles R. Real

With Contributions From:

Dames and Moore

Harding Lawson Associates

Kajima Corporation

LeRoy Crandall and Associates

OYO Corporation

Qest Consultants

Woodward-Clyde Consultants

MARCH 1988

TECHNICAL REPORT NO. 88-2
CALIFORNIA DEPARTMENT OF CONSERVATION
DIVISION OF MINES AND GEOLOGY
EARTHQUAKE SHAKING ASSESSMENT UNIT

TURKEY FLAT, USA
SITE EFFECTS TEST AREA

OVERVIEW

NEEDS The 1985 Mexico City earthquake is our most recent reminder that local ground conditions can have a strong impact on where damage will occur in urbanized areas during an earthquake, and underscores the need to incorporate seismic shaking potential in land use decisions. Although several different methods for making such assessments are currently in use, their accuracy and regional application costs are generally not known. This information is necessary before their results can form a sound basis for safer land-use and construction practices.

GOALS The principal goals of the Turkey Flat Site Effects Test Area are to systematically compare and test the reliability of contemporary methods used to estimate the effect of local geology on earthquake shaking, and to test the linearity of shallow stiff-soil site response.

OBJECTIVES Principal objectives are to collect high quality weak- and strong-motion data at several locations in the test area produced by local and regional earthquakes, quantify the site geology in terms of its geotechnical properties, and distribute the information to experts around the world.

APPROACH Using the acquired data, a series of "blind" predictions will be made by ground motion experts for test area locations where the response will be known, but not be available until all predictions have been received. Results of each prediction will be compared with one another and with actual observed ground motion.

PRODUCTS A series of reports describing each principal phase of the project will be available as the work progresses. An evaluation of all site response estimation methods will be prepared with recommendations as to suitability and cost of routine application for urban earthquake shaking hazard assessment.

Acknowledgments

Without the information provided in this report, the goals of this experiment cannot effectively be achieved. Special recognition is due the following companies and corporations for their voluntary contributions which have made the acquisition of this information possible: LeRoy Crandall Associates, Dames & Moore, Geomatrix Consultants, Harding Lawson Associates, Kajima Corporation, Lawrence Livermore National Laboratory, Pitcher Drilling Company, Qest Consultants, and Woodward-Clyde Consultants. We are especially indebted to OYO Corporation of Japan, who traveled great distances at great expense to contribute to the site characterization effort and share their technologies. We also wish to thank the California Department of Transportation for their assistance in field operations, and Edward Bortugno, geologist with the Bay Area Regional Earthquake Preparedness Project, who prepared the geologic map of the test area.

Most of all, we are grateful for the generosity and kindness of the land owners, Donald and Nila McCornack, and adjacent residents Melvin and Ruth Taylor, who persevered weeks of having the solitude of their setting disrupted. Their sincere interest in the future of mankind has made this important experiment possible.

TABLE OF CONTENTS

(CONTINUED)

ILLUSTRATIONS

Figures

Plates

TABLES

Tables

PART 1
STANDARD MODEL

STANDARD GEOTECHNICAL MODEL FOR THE TURKEY FLAT, USA SITE EFFECTS TEST AREA

Tables 1 and 2 summarize the geotechnical properties of the near surface geology at four site locations in the test area, where ground motion data are being acquired in an effort to validate methods of estimating the effects of local geology on earthquake ground motion for shallow stiff-soil sites. Figure 1 shows the locations of each site and three lines of profile. Figure 2 shows a cross sectional view along the three lines of profile to provide some knowledge of the three-dimensional structure of the test area.

The standard model was derived by a systematic procedure of data acquisition, analysis, and interpretation involving seven U.S. and two Japanese geotechnical firms and the California state government. Results of extensive field and laboratory tests, including state-of-the-art geophysical surveys, were selectively evaluated by members of an oversight committee of experts, leading to an average model of the test area that was reached by a consensus.

While this model represents a consensus of several experts in the geotechnical industry, it is not necessarily the most "accurate" model possible from the available data. Nonetheless, it serves as a standard against which various ground motion prediction methods

can be compared with one another. For this reason each participant in the prediction phase of the experiment is being asked to make one set of predictions using this model. Investigators wishing to make additional predictions using their own alternative models based on the geotechnical data collected may do so at their own discretion. For this reason, individual geotechnical reports by each contributor are included in the appendices.

The remainder of this report provides a brief overview of the project, a more detailed description of the site characterization program, the regional geologic setting and local geology of the site, and a brief narrative on the geotechnical properties of the Turkey Flat Test Area.

Table 1A. Dynamic Soil Properties at Valley Center and Valley North (G-curve I).

% Shear Strain	G/Gmax	% Damping
10^{-4}	1.00	1.5
10^{-3}	0.96	2
10^{-2}	0.75	4
$3x10^{-2}$	0.60	6.5
10^{-1}	0.40	10
$3x10^{-1}$	0.22	13

Table 1B. Seismic Velocities at soil site Valley Center.

Depth Range (m)	Shear Wave Velocity (m/sec)	Compression Wave Velocity (m/sec)	Density (gm/cm^3)
0 - 2.4	135	320	1.50
2.4 - 7.6	460	975	1.80
7.6 - 21.3	610	975	1.90
Below 21.3	1340	2715	2.20

Table 1C. Seismic Velocities at soil site Valley North.

Depth Range (m)	Shear Wave Velocity (m/sec)	Compression Wave Velocity (m/sec)	Density (gm/cm^3)
0 - 2.1	150	305	1.55
2.1 - 5.5	275	915	1.75
5.5 - 11.0	610	975	1.90
Below 11.0	1340	2715	2.20

Table 2A. Dynamic Rock Properties at Rock South and Rock North (G-curve II).

Parameter	Value	Shear Strain
G/Gmax	1	all strain levels
Damping	1%	all strain levels

Table 2B. Seismic Velocities at Rock South and Rock North.

Depth Range (m)	Shear Wave Velocity (m/sec)	Compression Wave Velocity (m/sec)	Density (gm/cm^3)
0 - 2.4	825	1980	2.10
Below 2.4	1340	2715	2.20

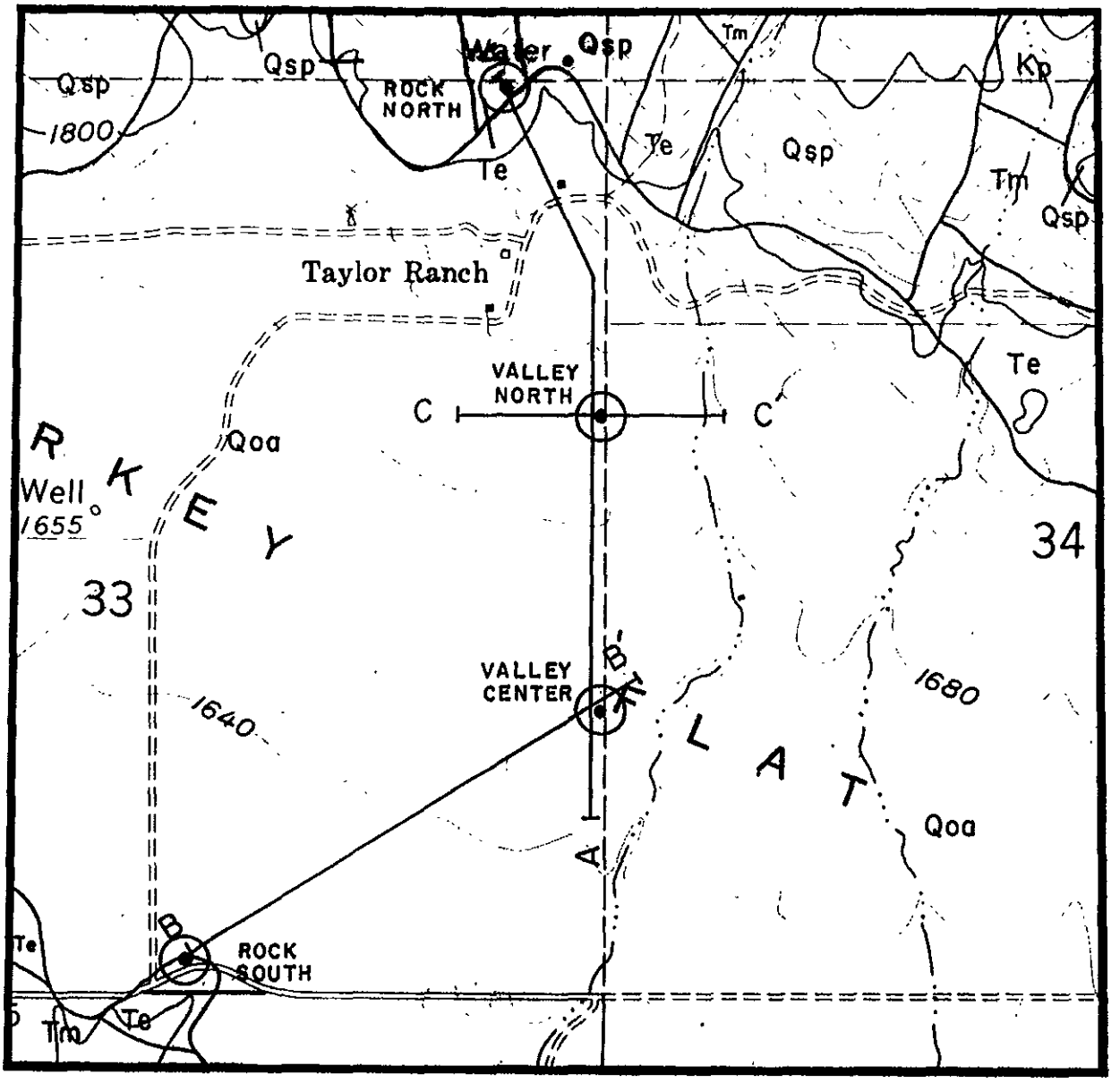

Figure 1. A map of the Turkey Flat Site Effects Test Area showing locations of the four ground motion recording sites, and three lines of profile that correspond to the cross sections shown in figure 2. At these locations, numerous geophysical surveys and laboratory testing of rock and soil samples have been conducted for the purpose of characterizing the test area for analysis of ground response. The remainder of this report describes the site characterization program and its findings in more detail.

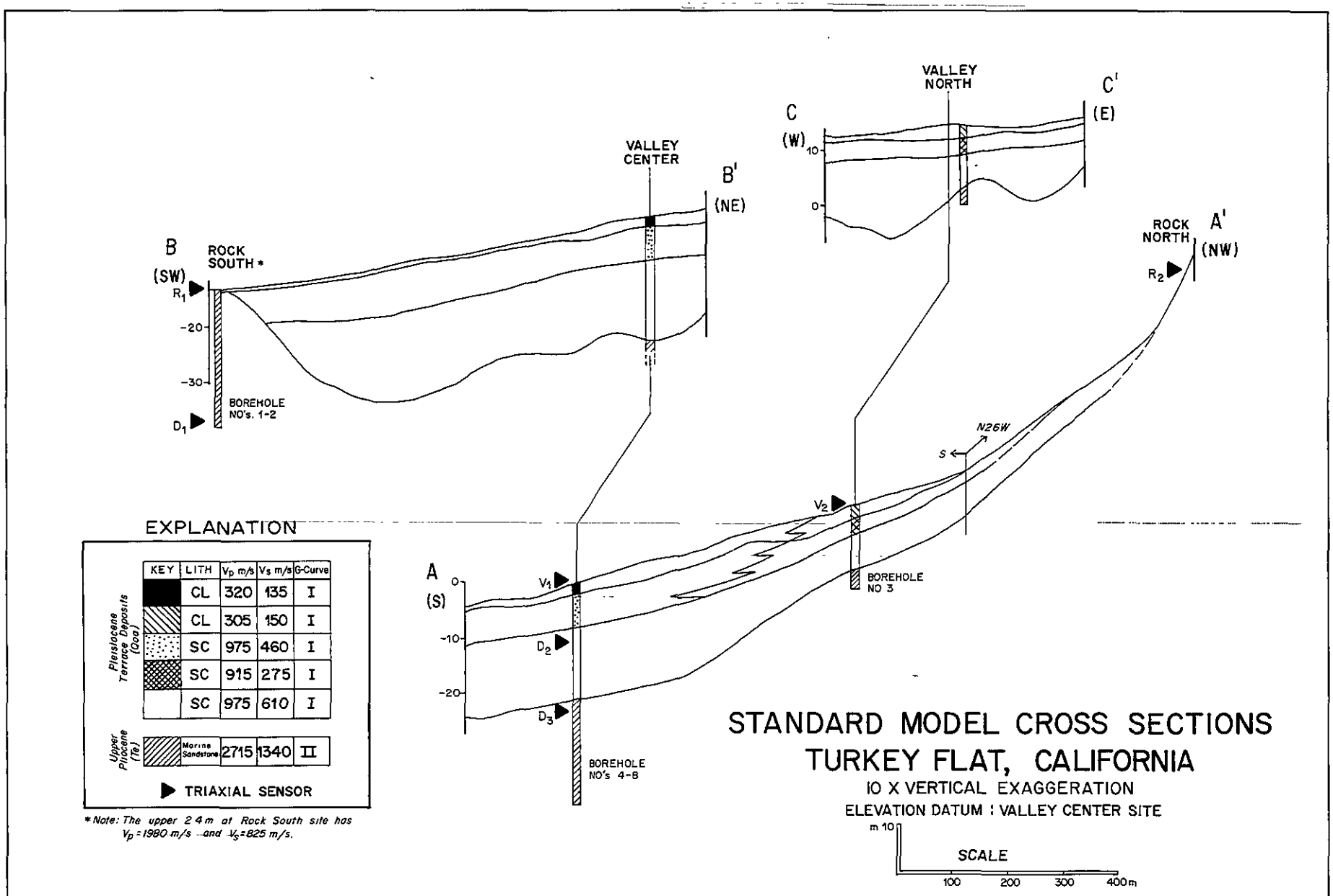
VALLEY NORTH
C'
(E)
C
(W)
10
0
VALLEY CENTER
B'
(NE)
B
ROCK SOUTH *
(SW)
R1
-20
-30
D1
BOREHOLE NO's. 1-2
ROCK NORTH
A'
(NW)
R2
N26W
S
V2
BOREHOLE NO 3
A
0
(S)
V1
-10
-20
D2
D3
BOREHOLE NO's 4-8
EXPLANATION
KEY
LITH
Vp m/s
Vs m/s
G-Curve
Pleistocene Terrace Deposits (Qoa)
CL 320 135 I
CL 305 150 I
SC 975 460 I
SC 915 275 I
SC 975 610 I
Upper Pliocene (Tp)
Marine Sandstone 2715 1340 II
TRIAXIAL SENSOR
* Note: The upper 2.4 m at Rock South site has Vp = 1980 m/s and Vs = 825 m/s.
STANDARD MODEL CROSS SECTIONS
TURKEY FLAT, CALIFORNIA
10 X VERTICAL EXAGGERATION
ELEVATION DATUM : VALLEY CENTER SITE
m 10
SCALE
100
200
300
400 m

PART 2

SITE CHARACTERIZATION PROGRAM

INTRODUCTION

IASPEI/IAEE Joint Working Group

At the 1985 meeting of the International Association of Seismology and Physics of the Earth's Interior (IASPEI), held jointly with the International Association of Earthquake Engineering (IAEE) in Tokyo, Japan, a resolution was passed forming the IASPEI/IAEE Joint Working Group on The Effects of Local Geology on Seismic Motion. The purpose of this group is to coordinate the establishment of an international series of test areas designed to provide a data base for comparing and testing contemporary methods, and developing new methods, to predict the effects of local geology on ground motion caused by earthquakes. The 1985 Mexico earthquake is only the most recent reminder that local ground conditions can have a major influence on where damage will occur in major earthquakes. Although methods for assessing site effects are being used to construct critical facilities around the world, the reliability of these methods has not been rigorously tested. It is the goal of this international program to fulfill this serious need. An international program provides a forum for experts around the world to

exchange ideas, and significantly increases the prospects of acquiring the necessary data soon.

Turkey Flat Experiment

The California Department of Conservation's Division of Mines and Geology (CDMG) has, among other mandates, the responsibility to look after the interest of the State and its people with regard to seismic and geologic hazards and promote safe utilization of the state's terrain. Safety analyses of critical facilities such as nuclear power plants, liquid natural gas repositories, and hospitals, as well as provision of hazard information to local governments for planning and development, require application of state-of-the-art techniques in predicting ground motion expected from future earthquakes; however, contemporary methods have not been thoroughly validated. When asked why microzonation has not been implemented in the U.S., the answer is often: "If you ask ten different experts how the ground might shake at a specific site during an earthquake, you will get ten different answers". We see a strong need to identify those methods that are reliable and those that are not, and to establish guidelines and procedures that insure repeatability, in order to effectively carry out our mandates. As a consequence, we have established a test area in Turkey Flat, California where a series of experiments will help answer this need.

Our general perceptions and experiment objectives echo those of IASPEI/IAEE's Joint Working Group. In their first workshop, held during the XIX Assembly of the International Union of Geodesy and Geophysics in Vancouver, British Columbia, Canada in August of 1987, a resolution was passed incorporating the experiment at Turkey Flat into the international program.

The principal objectives of the Turkey Flat Experiment are to systematically test and compare all methods of estimating the influence of local geology on ground motion during earthquakes, in order to determine the reliability and cost effectiveness of each. Secondary objectives are to generate a data base for the improvement of these methods, or the development of new methods, and to address the long standing debate on the linearity of site response. The approach is to collect high quality weak and strong ground motion data, and geotechnical data, and carry out a series of "blind predictions". Experts from around the world will be invited to use their preferred method and the acquired data to predict ground motion at a location where the actual response will be known but held in confidence until all predictions have been submitted.

The experiment is being conducted in a number of phases, and this report constitutes the results of phases I and II, Site Selection

and Characterization. A more detailed description of the overall experiment is available as Report 1, Turkey Flat Site Effects Test Area: Needs, Goals and Objectives. It is anticipated that several additional reports will be generated that cover other aspects of the experiment as it progresses.

This report is organized in three principal parts: 1) a summary, where a standard (consensus) geotechnical model of Turkey Flat is provided for easy access, 2) the body, where the site characterization program, regional geology, and local site conditions are discussed in more detail, and 3) a series of appendices that contains contributor's original reports or summaries. Part 3 is intended for those participants in the prediction phase who choose to do additional analyses using their own alternative models derived from the basic geotechnical data.

SITE CHARACTERIZATION PROGRAM

Siting

The principal requirements for the location of a site effects test area are 1) a site likely to experience strong-motion (>.25 g) in the next few years, 2) a site where ground motion is expected to be affected by the local geology to such a degree that it is measurable, and 3) a site not too unlike that commonly used for urban and industrial development. To the extent possible, the site characteristics should be favorable to discriminating between the various methods that will be tested. The Parkfield, California region was immediately chosen because it lies along that segment of the San Andreas fault where the only officially recognized U.S. earthquake prediction is pending (Bakun and McEvilly, 1984). This 30 km segment, known as the Parkfield segment, ruptured in a moderate size earthquake (M5-6) in 1966, producing a record acceleration of 1/2 g. This event is expected to repeat by 1992 with a 90% confidence. Having chosen the general area on this basis, the siting task was reduced to finding a relatively flat alluvial valley in the immediate Parkfield region.

Preliminary selection of the Turkey Flat site was based on its proximity to the San Andreas fault: close enough (5 km) to expect strong motion from a moderate earthquake, but not so close as to be dominated by source effects that might over shadow any local site effects. A series of preliminary seismic refraction profiles indicated a maximum sediment depth of about 25 meters over bedrock, with a velocity contrast of about three. Final selection was based on this information and the results of a spectral analysis of weak motion from large regional events and small local events recorded at several locations across the valley, which indicated a measurable site effect. Some 36 sensors were deployed across the valley and valley margins and were digitally telemetered to an automated data acquisition and analysis system located in the field, thus permitting rapid assessment of the relative weak-motion response of the site. This system was kindly provided by Lawrence Livermore National Laboratory, and is described in more detail by Jarpe and others (1988).

Objectives

The principal objective of the site characterization program is to provide a geotechnical model of the test area that will provide the input parameters necessary to estimate the seismic response of the valley, and permit execution of the prediction phase of the experiment. Because the principal goal of the experiment is to

test and compare a variety of methods currently used to estimate site effects, it is important to give careful consideration to what parameters should be measured, the techniques to be used, where and how often measurements should be made, and how to judge the reliability of the measurements. While on the one hand, the accuracy and precision of input parameters should be high to conclusively test and discriminate between the various prediction techniques, it is desirable to use industry standard procedures as they are used in routine application for ground response assessments. Such an approach provides a test of those parts of the routine site response estimation procedures in current practice that are exclusive of source and path considerations. As a final note, it will therefore be important to separate the variance from observations due to inaccuracies in the input data from that due to the various prediction techniques themselves. For this reason, uncertainties in the geotechnical data must eventually be assessed.

Organization

With the above desirability in mind, the geotechnical industry was invited to participate for the following reasons: 1) standard industry practice would be assured: CDMG does not have the geotechnical expertise nor resources to carry out the necessary work independently, 2) many of the participants in this phase are

also participants in the prediction phase of the experiment and would benefit from the continuity of the tasks, while at the same time contribute to the success of the experiment through high quality dedicated work, and finally, and perhaps most importantly, 3) the very industry that stands to be impacted most by the outcome of the experiment would be directly involved, greatly expediting application of findings to the benefit of society. The response by industry went beyond expectations, and included voluntary field and laboratory work.

To maximize the benefit from industry, a Geotechnical Planning Committee (GPC) was formed of individuals representing several geotechnical consulting firms from the U.S. and Japan (inside cover). The purpose of this committee was to plan, help organize, and assist in carrying out the site characterization program. Technical advice was provided throughout. The program that resulted was a joint U.S./Japan effort: a government-industry partnership in the U.S., and an academia-industry partnership in Japan (figure 3). Although carried out independently, both groups coordinated their work through CDMG under general guidance by the GPC.

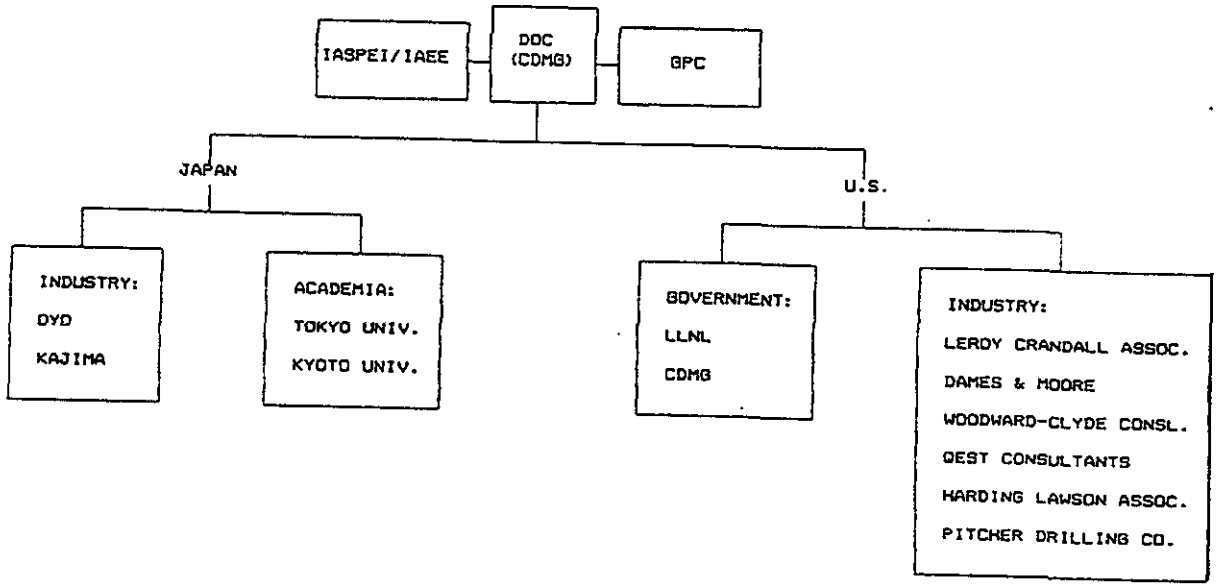

Figure 3. Organization of the Turkey Flat, USA Site Effects Test Area site characterization team.

Principal Tasks

The objectives set forth in the site characterization program required site drilling and sampling, laboratory measurements, *in situ* measurements using geophysical field surveys, and subsequent data reduction and interpretation. The principal parameters sought are P- and S-wave velocities, modulus reduction curves, and damping as a function of depth at each site where ground motion observations/predictions will be made. For those participants that might consider 2- or 3-dimensional models, it is desirable to obtain some knowledge of the spatial variability of parameters. More than one method of measuring a particular parameter was used as a means of cross-checking reliability, particularly for new techniques. Even in the case where standard procedures were used, such as for downhole velocity measurements, several surveys were repeated by different investigators as a means of obtaining the best possible data, and for estimating uncertainties. The various field surveys and laboratory tests made by each participant are shown in tables 3 and 4 respectively.

The final task of the site characterization program was to derive a "consensus" model of the test area to serve as a standard against which all ground motion site effect estimation methods can be compared. This was accomplished in the following way. Upon completion of analysis, individual investigators submitted a brief

Table 3. Geotechnical field tests.

FIELD TESTS	CDMG	HLA	LCA	QEST	WCC	PDC	OYO	KC
DRILLING AND SAMPLING	■		■		■	■	■	
STANDARD PENETRATION TEST	■		■		■	■		
WATER TABLE DEPTH	■							
CALIPER		■					■	
BOREHOLE DEVIATION	■							
ELECTRICAL							■	
DENSITY (GAMMA-GAMMA)		■						
NATURAL GAMMA		■						
BOREHOLE LATERAL LOAD TEST							■	
DOWNHOLE VP/VS	■		■	■	■		■	
CROSSHOLE VP/VS		■						
SUSPENSION VP/VS							■	
DOWNHOLE Q (P&S)	■			■			■	■
VERTICAL SEISMIC PROFILING							■	
SEISMIC REFLECTION (P&S)							■	
SEISMIC REFRACTION (P&S)	■						■	

CDMG - Calif. Dept. of Conservation
Division of Mines and Geology
HLA - Harding Lawson Associates
KC - Kajima Corporation
LCA - LeRoy Crandall and Associates
OYO - OYO Corporation
PDC - Pitcher Drilling Co.
QEST - QEST Consultants
WCC - Woodward-Clyde Consultants

Table 4. Geotechnical Laboratory Tests

LABORATORY TESTS	D & M	L C A	O Y O
SOIL CHARACTERISTICS*	■	■	■
CONSOLIDATION TEST		■	
DIRECT SHEAR TEST		■	
DYNAMIC TRIAXIAL TEST	■		
RESONANCE COLUMN TEST			■
DYNAMIC TORSION TEST			■
TRIAXIAL ULTRASONIC WAVE VELOCITY			■

* Grain size, specific gravity, moisture content, unit weight, liquid limit, and plastic limit.

D&M - Dames & Moore
LCA - LeRoy Crandall and Associates
OYO - OYO Corporation

report of their results to one of three subcommittees formed by GPC: 1) Geology Group, 2) Soils Group, and 3) Geophysics Group. Each group reviewed the results from individual participant reports in their discipline, and, by working with each participant, attempted to resolve significant differences. In some instances this required reinterpreting, remeasuring, or even discarding the data. Having eventually synthesized the contributions from each participant in their discipline, each group then recommended a model for the test area. The three group representatives met to resolve differences based on examination of all data combined, thereby resulting in a final "consensus" model melding results from the soils, geology and geophysics groups. This model was then reviewed by all GPC members for concurrence.

Schedule

In accordance with the overall project schedule (Report 1), siting was completed in the spring of 1986, and site characterization began in the fall of 1986. The intent was to begin the first round of ground motion predictions in the fall of 1987. Because both the geotechnical data synthesis and report generation, and the acquisition of weak motion data has taken longer than expected, the first round of ground motion predictions will begin late spring or early summer 1988.

The U.S. field and laboratory work was conducted during the fall of 1986 and spring of 1987. Individual reports were completed and submitted for review prior to a workshop held in June 1987.

The field and laboratory work carried out by Japan's industry was conducted independently during the spring of 1987. This effort, led by OYO Corporation, was considerably greater in scope than the U.S. counterpart, and involved the efforts of nearly 100 persons to be accomplished in this time frame. Being both a service oriented company and instrument manufacturer, OYO applied a number of conventional as well as innovative techniques and equipment to further internal research and development. The Turkey Flat test area served as a convenient test bed for company purposes while allowing the experiment to mutually benefit from the comprehensive work. This effort resulted in an extensive report prepared by OYO, only part of which is reproduced in appendix F. Those interested in the full report can obtain a copy directly from OYO Corporation. Two additional OYO reports, one on deep seismic reflection and the other on rock laboratory testing, are reproduced in their entirety in appendix F.

A second field program was conducted by researchers from Japan's Earthquake Research Institute of Tokyo University, and the Disaster Prevention Institute of Kyoto University during late summer 1987. This work involved application of microtremor surveys to de-

termine velocity structure. Because of its experimental nature, the results were not used in developing the geotechnical model for the prediction phase. The microtremor work stands alone as an ancillary validation experiment for a new geophysical site exploration tool. Consequently, microtremor results will be compared with those derived from conventional means and will be reported on separately.

In order to integrate the results of the U.S. and Japan programs, a geotechnical workshop was held in June 1987, where presentations were made summarizing each other's findings. During the workshop discrepancies were identified, and results from both the American and Japanese teams were distributed to each of the three sub groups identified previously. The workshop served two important functions: 1) to review results and point out problems, and 2) provide the forum needed to develop the procedure that would eventually lead to a consensus model. The consensus model was completed by November 1987. The following section is based on the geotechnical work and characterizes the regional and local site geology of the Turkey Flat Test Area.

TEST AREA SITE CONDITIONS

Regional Geologic Setting

Parkfield lies along the San Andreas fault in the central California Coast Ranges, a region characterized by a 100 kilometer wide belt of northwest trending ridges and valleys having a maximum relief of about 1500 meters (Plate 1 in pocket). In this region, the San Andreas fault forms a rift valley that separates the mobile Franciscan basement complex of the Diablo Range to the east from the contrasting rigid granitic basement of the Gabilan Range to the west. The granitic terrain, often referred to as the Salinian block, is unconformably overlain in this region by a relatively thin (1500 m) undisturbed sequence of Tertiary strata of marine and continental origin. This is in marked contrast to a much thicker (5500 m) sequence of highly deformed Tertiary marine and terrestrial strata that overlie the Franciscan rocks to the east (Plate 2 in pocket). Tertiary strata on both sides of the San Andreas fault are overlain by about 1000 meters of terrestrial gravels, sands, silts, and clays of Quaternary age, derived mainly from erosion of the Tertiary strata and the older exposed Franciscan rocks.

In the Parkfield region, the San Andreas fault zone is easily recognized as the prominent rift that forms Chalome Valley. Most of

the recent alluvium in the area is confined to Chalome Valley, and is a product of intermittent deposition from Chalome Creek and its tributaries. The segment of the fault zone that passes through Chalome Valley has ruptured at least 5 times in historic time with an average recurrence interval of 22 years. It last ruptured in 1966, and thus is expected to rupture again in the near future.

The structural history of this region is complex, resulting from two distinctly different episodes of tectonism over the past 60 million years. The Franciscan rocks are a highly sheared *melange*, and are believed to have formed in a subduction environment during the late Mesozoic. Subduction ceased about 20 million years ago, giving way to a transform regime that has continued to present time. Along the present and ancestral San Andreas fault, relative motion between the Pacific and North American Plates has transported the Salinian block, once part of the southern Sierran granitic batholith, several hundred kilometers north to its present position in the central Coast Ranges.

Because of the strong convergence of plate motion relative to the trend of the plate boundary, Neogene structural deformation in the region is a consequence of large-scale convergent transform tectonics, characterized by compressional basins, en echelon folds, northwest trending strike-slip faults and general uplift of the Coast Ranges (Page, 1981). While contemporary slip along the San

Andreas fault accounts for about 60% of the relative plate motion, the remainder is presumably taken up by slip along other secondary faults and plastic deformation over a broad zone hundreds of kilometers either side of the San Andreas plate boundary. The markedly contrasting rigidities of the granitic and Franciscan basements have given rise to different crustal responses, and accounts for the greater structural complexity of the Diablo Range.

Continued uplift of the Coast Ranges throughout the Quaternary was accompanied by extensive erosion, particularly during wetter periods of the Pleistocene. This has given rise to widely distributed surficial deposits of older alluvium such as that present in the Test Area. As uplift in the Coast Ranges continues, deposition of recent alluvium is confined mainly to the larger streambeds and floodplains throughout the region.

Local Site Geology

The Test Area lies in Turkey Flat, a shallow northwest trending elongated valley located about 5 kilometers east of the San Andreas fault and eight kilometers southeast of the town of Parkfield (Plate 1). The valley is approximately 6.5 kilometers long and 1.6 kilometers wide and is bounded on the north and east by the steep west flank of Table Mountain, part of the southern Diablo Range, and on the south and west by a gentle topographic

high. The elevation of the valley floor is about 500 meters above sea level, and lies about midway between Castle mountain to the north (elevation 1325 m) and Chalome Valley (elevation 380 m) which are separated by a distance of about 15 kilometers. The valley floor dips gently (1-2 degrees) to the southwest.

Turkey Flat lies nearly coincident with the axis of the southwest plunging Parkfield syncline, and is structurally bounded by northeast dipping faults on each side (Plates 1 and 2). Approximately 1 kilometer of Upper Cretaceous and Tertiary strata overlying Franciscan basement are steeply folded into a "U" shape having a dip of about 50 degrees on the southwest flank, and about 70 degrees on the northwest flank. A general description of the rock units composing the syncline and the surficial sedimentary cover throughout the test area follows. A discussion of geotechnical properties will follow in subsequent sections.

Principal Rock Units

Franciscan - The Franciscan formation consists of a highly sheared assemblage of chert, graywacke, and ophiolites in a matrix of argillaceous shale or claystone. Throughout the Franciscan occur bodies of serpentinite believed to be of diapiric origin (Dickenson, 1966). Owing to the wide variation in composition, the physical properties of the Franciscan vary widely. Though the

average bulk density of this unit ranges from 2.65 to 2.70 gm/cm^3, the total range in density reported for Franciscan lithologies is from 2.0 to 3.2 gm/cm^3 (Hanna et al., 1972).

Upper Cretaceous - Above the Franciscan formation lie marine sedimentary rocks of the Great Valley Sequence (Bailey et al., 1964, Dibblee, 1972). Although the total thickness of this sequence beneath Turkey Flat is not known, it can reach over 3 kilometers elsewhere in the region. The sequence is composed mainly of argillaceous shale and sandstone with some thin beds of graywacke and conglomerate. Hanna and others (1972) assigned this sequence an average density comparable to that for the Franciscan.

Middle and Upper Tertiary - Overlying the Great Valley Sequence are about 1 to 1.5 kilometers of marine sedimentary rocks. They are composed of semifriable arkosic sandstone, claystone and basal conglomerate of the Temblor formation; siliceous shale, clay shale, and siltstone of the Monterey formation; and sandstone and shale of the Etchegoin formation. The Etchegoin sandstone underlies the sediments of Turkey Flat, and crops out along the northern and southern margins of the valley. Hanna and others (1972) assigned a range in average bulk density of 2.2 to 2.3 gm/cm^3 for this sequence.

A deep seismic reflection survey conducted by OYO Corporation

proved useful in estimating thicknesses and seismic velocities of the Middle and Upper Tertiary Units (appendix F). In their survey a unique high energy airgun was used to generate and record reflections using a 48-channel exploration type recording system. Lithologic and sonic logs were obtained from a 1600 meter exploration well located approximately 10 kilometers up strike on the flank of Parkfield syncline (Phillips Petroleum Varian # 1, 1981). A synthetic seismogram was prepared from the sonic log and used to correlate reflections with geologic horizons. Compressional wave velocities used to compute depth were taken from refraction surveys and the sonic log, and are: 1 km/s for unconsolidated sediments, and 3 km/s for the underlying rock units. The agreement between the synthetic seismogram and the reflection time section is very good, and the results of this project indicate a depth to the base of the Etchegoin sandstone of 600 meters, and a thickness of about 300 meters for the upper member of the Monterey formation (McClure shale, (Tm on plate 1)). A strong reflector appears about half way through the Etchegoin formation, which is also indicated on the sonic log by a pronounced decrease in velocity. The origin of this reflector is believed to be a known regional unconformity that occurs about mid-section within the Etchegoin formation.

Surficial Deposits

Sediments in Turkey Flat are composed mainly of clayey sand and sandy clays with intermittent layers of gravel, and occasional strands of boulders having clasts that can exceed 30 cm (see borehole logs in appendix B). These sediments were principally derived from erosion along the west flank of Table mountain, during wetter climatic periods of late Pleistocene and Holocene. Source materials for these sediments consist of all of the above described rock units. Direction of sediment transport is believed to have remained relatively constant, toward the present southwest gradient. Sediment texture grades laterally across the valley in this same direction from coarser to finer. The extensive drilling program undertaken for this project determined a maximum thickness of valley sediments of less than 30 meters in the immediate test area, which probably does not exceed that amount throughout the remainder of Turkey Flat.

Erosion appears to be the predominant landform process operating in Turkey Flat in recent time. The sediments comprising the valley fill consist of older alluvium, and there appears to have been no extensive deposition over the last few thousand years. During infrequent periods of heavy rain, torrents of water travel down narrow canyons along the west flank of Table Mountain, carrying down large boulders and finer debris and depositing it along the base

of the slope as small fan deposits. Most of this debris comes from landslides and surficial rubble. Nearly all of the western flank of Table Mountain is covered with rubble derived from the landslide prone Franciscan rocks higher up the mountain front. Field inspection has revealed many generations of landslides, one on top of another, with the underlying older debris having lithified into a hard breccia while the most recent slides are of a fresh, soft nature. While this form of degradation has undoubtedly been going on for the past several thousand years, it is believed not to have contributed significantly to sediment accumulation at Turkey Flat. Where torrential waters flow out onto Turkey Flat, deep gullies (2 m) have been incised that show clear evidence of headward erosion, indicative of the rapid uplift and rejuvenation occurring throughout the region.

In summary, local site conditions at the Turkey Flat Test Area can be best described as a "shallow stiff-soil site". Although erosional processes appear to have dominated recent time, there is no evidence of substantial sediment removal in Turkey Flat. Consequently, it is unlikely that sediment thickness was appreciably greater in the past. Consolidation from overburden, therefore, cannot adequately explain the stiff nature of the soil. It is more likely a result of age and composition.

A description of the principal soil properties at each site, based

on extensive field and laboratory work, follows. The descriptions will be of a summary nature reflecting the synthesis of all data acquired. The appendices contain the results of all geotechnical tests (refer to appendix A to locate results of laboratory or field tests related to specific boreholes). Results from the different laboratory tests and field surveys will not be compared and contrasted in any detail here. Although such an analysis is both valuable and necessary, it is beyond the scope of this report and, consequently, will be presented in a separate report.

Physical Properties

The following is a summary of the principal geotechnical properties of the various rock and soil units: lithology, seismic velocities, seismic attenuation, layer geometry, and density. Variations in these properties at each site are presented under two general sections, bedrock and valley fill. It will be useful to refer to figures 1 and 2 of the Standard Model while reading this summary. While the summary synthesizes all of the data, the results of specific tests at each site can be found in the appendices. As a final note, because the physical properties of the geologic materials will vary depending on the degree of saturation, the depth to water table has been measured to determine its degree of fluctuation. Measurements taken in the winter and summer show a variation of about 3 meters at valley center. The measure-

ments made thus far are as follows: a) Rock South: winter-8.5 m, summer- no measurements, b) Valley Center: winter-23 m, summer-26 m, c) Valley North: winter and summer- an unknown depth below the bottom of the borehole (>14 m). Measurements will continue to be made.

Etchegoin sandstone - This formation crops out along the margins of the valley and underlies the sediments. Two boreholes (TF-1, TF-2), each 25 meters deep, were drilled into the sandstone outcrop at Rock South site, and five additional boreholes penetrated the sandstone beneath the valley sediments from three to 15 meters (TF-3 through TF-6, and TF-8). A summary of all tests conducted in the boreholes is provided in table (appendix A).

Lithology - Core samples taken at various depths indicate a medium brown to tan highly friable sandstone with sub-angular to rounded, well-sorted grains composed of about 50% quartz. A distinct color change to a blueish-gray occurs at a depth of about 14 meters into the sandstone at rock south site. This change is believed to represent the boundary below which the sandstone remains saturated.

Seismic Velocities - Three different methods were used to measure P- and S-wave velocity: 1) downhole, 2) crosshole, and 3) suspension logging. The results indicate two principal layers: an upper

compressional velocity of 900 m/s to 1100 m/s, and a range in shear velocity of 200 m/s to 800 m/s; and the lower having a range in compressional velocity of 1400 m/s to 3400 m/s, and a range in shear velocity of 700 m/s to 1500 m/s. Careful review of recorded waveforms, remeasurement in a few cases, and elimination of one downhole survey (the equipment used was designed for a smaller diameter borehole so the results were judged questionable by the contributor, (appendix B)), resulted in much less scatter and led to the final adopted values in Table 2.

Laboratory ultrasonic velocity measurements of several samples taken from borehole TF-1 show considerable variation depending on the state of saturation (appendix F). Unfortunately, several months lapsed before the laboratory measurements were made, so the *in situ* state of saturation could not be reliably reproduced in the laboratory. In all cases however, the laboratory results yielded higher velocities by a factor of 1.5 to 2.

Seismic Attenuation - The attenuation parameter Q was measured along the southern valley margin and beneath the valley sediments using several techniques. The results indicate generally very low constant Q values ranging from 13 to 21 for Qp (compressional wave) and from 5 to 12 for Qs (shear wave). These values correspond to signals in the frequency range 25 Hz to 70 Hz.

Density - Laboratory determinations of dry density of many samples taken from depths of 1 meter to 20 meters within the sandstone show a range from 1.90 to 1.95 gm/cm^3. Measurements made of the samples in a saturated state range from 2.20 to 2.23 gm/cm^3 (appendix F). In either case there is no significant difference in density between the upper and lower sandstone layers as defined above. *In situ* measurements of density using a gamma-gamma logging tool in borehole TF-8 indicate a higher value of 2.35 gm/cm^3, which shows little variance throughout the sampled section (appendix D).

Valley sediments - The variation of sediment thickness at the test area was determined by seismic refraction and reflection, and the drilling of a dozen boreholes. Three layers have been identified within the sediment deposits based on seismic velocities, density, and lithology (figure 2). The upper two layers show a lateral gradation from coarser to finer sediment toward the southwest, while the lower layer appears relatively constant throughout the valley.

Lithology - All subsequent descriptions of sediment deposits are based on the Unified Soil Classification System. The top layer consists of a dark brown sandy clay at the Valley North site, laterally changing to a dark brown silty clay at the Valley Center site. The second layer consists predominantly of a clayey sand having higher concentrations of gravel and sandy clay below the

Valley North site. The third layer consists of fine to medium clayey sand with gravel at both the Valley North and Valley Center sites.

Seismic Velocities - The final values for compressional and shear wave velocities are based on a synthesis of downhole, crosshole, suspension logging, and refraction surveys. Compressional wave velocity for the upper layer varies from 320 m/s at Valley North to 305 m/s at Valley Center, while shear wave velocity varies from 135 m/s at Valley North to 150 m/s at Valley Center. This corresponds to an increase in Poisson's ratio from .34 at the Valley North site to .39 at the Valley Center site.

Compressional wave velocity for the middle layer varies from 915 m/s at Valley North to 975 m/s at Valley Center, while shear wave velocity varies from 275 m/s to 460 m/s. This corresponds to a decrease in Poisson's ratio from .45 at the Valley North site to .36 at the Valley Center site.

Both compressional and shear wave velocity for the bottom sediment layer are constant at Valley Center and Valley North and are 975 m/s and 610 m/s respectively. Poisson's ratio for this layer is .18.

Seismic Attenuation - The seismic attenuation parameter Q of the

sediments was measured using the same variety of methods as for the rock measurements. Again, the results indicate very low values of Q: a compressional wave Qp of about 10, and a Qs for shear waves ranging from about 5 to 25. These values correspond to signals having frequencies between 25 Hz and about 70 Hz.

Density - Laboratory estimates of bulk density for the sediments varied greatly (1.3 to 1.9 gm/cm^3) depending on the degree of saturation and consolidation: the higher values for a given set of conditions were generally obtained from samples taken at greater depths. *In situ* measurements using a nuclear logging tool are about 20% higher than the laboratory estimates, and yield densities of less than 1.6 gm/cm^3 for the upper layer, about 2.0 gm/cm^3 for the middle layer, and about 2.1 gm/cm^3 for the bottom layer just above the sandstone. The seismic and density data obtained show some degree of correspondence. When the layer boundaries, as determined from the seismic data, are superimposed on the nuclear log, there is a noticeable stability of log signature within a given layer, and a distinct change in signature at layer boundaries.

Conclusions

The Turkey Flat site effects test area is best classified as a "shallow stiff-soil site". Specific geotechnical properties have

been determined by extensive field and laboratory tests, using equipment and techniques commonly employed in the U.S. and Japan. Experts from these countries have been involved in the collection, analysis, and interpretation of data from Turkey Flat, and have generated a "standard" model based on an organized procedure of synthesis. The standard model is believed to represent an "average" model of the geotechnical properties, which has been reached by consensus. While this model may not be the most accurate representation possible based on the data collected, it represents a common standard against which the various methodologies for estimating the effect of local site properties on ground shaking can be compared with one another given a common set of input motions. Consequently, as this comparison is one principal objective of the experiment, all participants in the prediction phase must estimate ground response using the "standard" model.

Other models not encumbered by the data are undoubtedly possible, and more "accurate" models are perhaps possible as well. Recognizing that a second principal objective of the experiment is to compare the results of each ground motion prediction with actual observed ground motions in order to test the reliability of the method, some investigators may wish to derive their own model and make separate predictions of response in the test area using their "Preferred" model. For this reason, the results of all field and laboratory tests are included in the following appendices of

report. It is important to refer first to appendix A, as it serves as an index to the various tests performed in each of the boreholes by the different investigators.

REFERENCES

Bailey, E.H., Irwin, W.P., and Jones, D.L., 1964, Franciscan and related rocks and their significance in the geolory of western California: California Div. Mines and Geology Bull. 183, 177p.

Bakun, W.H. and McEvilly, T.V., 1984, Recurrence Models and Parkfield, California, Earthquakes: Journal of Geophysical Research, v. 89, n. B5, p. 3051-3058.

Dibblee, T.W. Jr., 1972, Stratigraphy of the southern Coast Ranges near the San Andreas fault from Chalome to Maricopa, California: USGS Prof. Paper 764.

Dickenson, W.R., 1966, Table Mountain serpentinite extrusion in California Coast Ranges: Geol. Soc. America Bull., v. 77, n. 5, p. 451-471.

Hanna, W.F., S.H. Burch, and Dibblee, T.W. Jr., 1972, Gravity, Magnetics, and Geology of the San Andreas Fault Area Near Chalome, California: USGS Prof. Paper 646-C, p. 29.

Jarpe, S.P., Cramer, C.H., Tucker, B.E., and A.F. Shakal, 1988, A Comparison of Observations of Ground Response to Weak and Strong

Ground Motion at Coalinga, California: Bull. Seism. Society of Am. v. 78, n. 2, p. 421-435.

Page, B.M., 1981, The southern Coast Ranges, in Ernst, W.G., ed., The geotectonic development of California: Englewood Cliffs, New Jersey, Prentice-Hall, p. 329-417.

PART 3
APPENDICES

APPENDIX A
Guide

APPENDIX A

GUIDE TO RESULTS OF LABORATORY AND FIELD TESTS

Appendices B through I consist of individual reports from participants in the site characterization program, and contain all of the basic geotechnical data acquired in the field and laboratory. Because of the number of participants involved, and the fact that not all tests were performed in all boreholes by the same participants, it was felt that some indexing would make the acquired data more accessible. The purpose of this appendix is to identify the appendices that have information on specific tests (geotechnical parameters) for a specific borehole (location). This is accomplished by figure 1, which shows the location of the boreholes, and table 1, which cross-references the appendices with geotechnical measurements and boreholes.

Figure 1 shows the location of the eight boreholes (TF-1 through TF-8) in which samples were taken or geophysical tests performed, and lists the specifications of each borehole. All of the boreholes were drilled using a rotary-wash drill rig and tri-cone bit. Sediment samples were taken either by a Pitcher barrel sampler or a Crandall sampler and are indicated on the borehole drill

logs. Rock samples were obtained using a diamond core.

Table 1 is a matrix having geotechnical measurements by each participant in rows, and borehole identification in columns. At each point of intersection is the letter of the appendix containing the information depending on whether the corresponding data exist. There are at least four levels of geotechnical data depending on the degree of interpretation: 1) basic instrument readings, 2) reduced instrument data, 3) interpreted data, and 4) synthesized interpretations. It should be noted that all reports do not provide all levels of data. Furthermore, the size and complexity of reports does not, in any way, reflect the quality of each participants work, but rather the extent of their field investigation and involvement in the project. Most of the reports provide data levels two and three.

Oyo Corporation's field investigation was very extensive, and consequently resulted in a large report containing all four levels of data: too large, in fact, to be reproduced here. Instead, summary figures for each principal measurement is presented, as well as figures and tables summarizing synthesized results. A copy of the full OYO report entitled "Report of A Geotechnical Investigation of the Effects of Surface Geology on Seismic Motion" (June 1987), can be obtained from OYO Corporation.

Finally, while table 1 of this appendix is aimed at locating results of borehole related tests, tables 3 and 4 of Part 2 (pages 17 and 18) can be used to assist in searching for the results of specific laboratory tests, and geophysical surveys not associated with boreholes.

Table 1. Geotechnical data associated with boreholes (letter in box indicates appendix containing data).

GEOTECHNICAL ACTIVITY	BOREHOLE TF-							
	1	2	3	4	5	6	7	8
LOGGED, SAMPLED, SPT:								
LCA				B				
WCC			B			B		
CDMG	B							
WATER TABLE DEPTH:								
CDMG	H		H			H		H
CALIPER LOG:								
OYO								F
HLA								D
BOREHOLE DEVIATION:								
CDMG	H	H	H	H	H	H	H	
ELECTRICAL LOGS:								
OYO								F
DENSITY LOGS:								
HLA								D
NATURAL GAMMA:								
HLA		D			D			
BOREHOLE LATERAL LOAD TEST								
OYO								F
DOWNHOLE VP/VS:								
LCA		B			B			
WCC	I	I	I	I	I	I		
CDMG	H	H	H	H	H	H		H
QEST		G			G			
OYO		F	F		F			F

CONTINUED

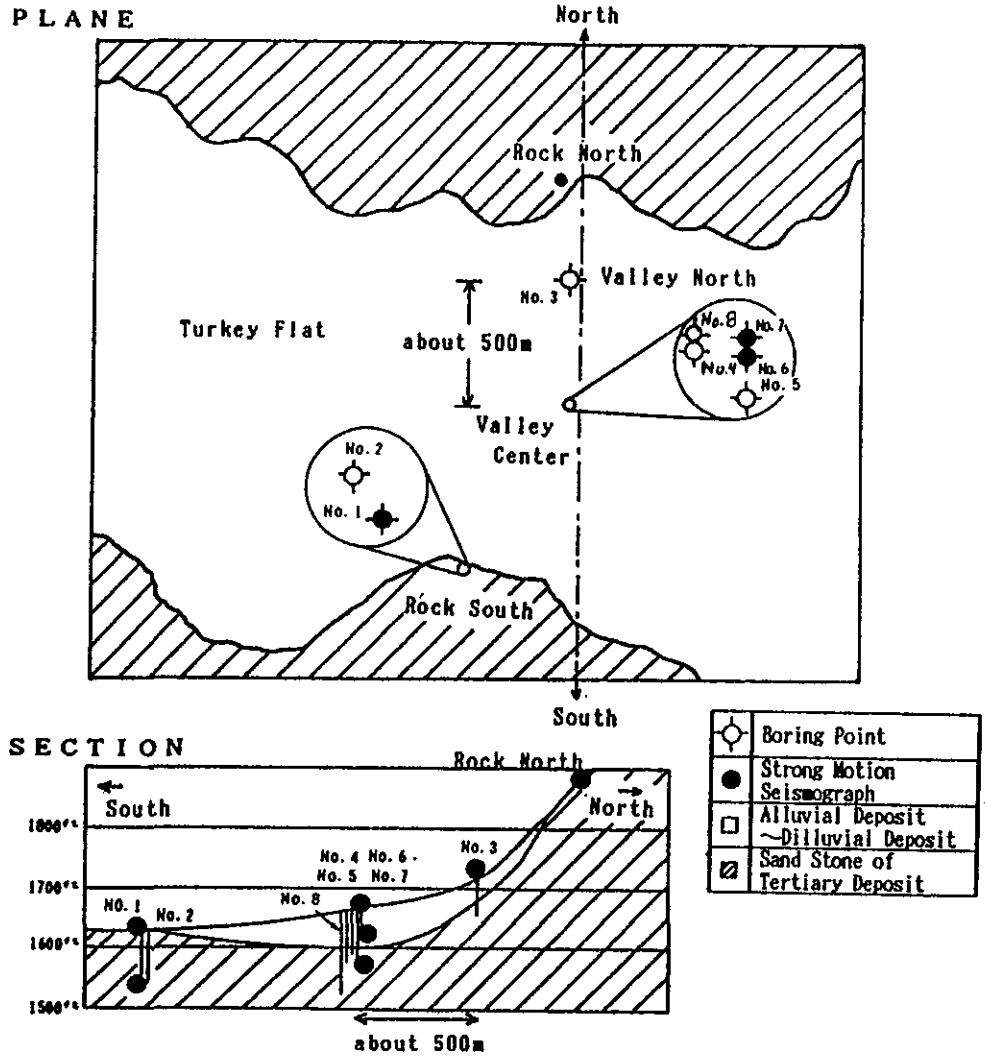

Description of Instrument and Test Borings

No.	Purpose	Depth (ft)	Diameter (inches)	Casing (inches)	Backfill
1	Test & Sensor	82	9	5-PVC	Pea Gravel[2]
2	Test	80	6	3.34-SINCO	Grout[1]
3	Test	47	9	5-PVC	Pea Gravel[2]
4	Test	73	8	5-PVC	Pea Gravel
5	Test	78	6	3.34-SINCO	Grout[1]
6	Test & Sensor	79	9	5-PVC	Pea Gravel[2]
7	Sensor	35	8	5-PVC	Pea Gravel
8	Test	132	3 1/8	Uncased	[2]

[1] A mixture of 5 parts cement to 1 part bentonite.
[2] A 3/4" piezometer tube installed in annulus.

Figure 1

Table 1. Geotechnical data associated with boreholes (letter in box indicates appendix containing data).

CONTINUED

GEOTECHNICAL ACTIVITY	BOREHOLE TF-							
	1	2	3	4	5	6	7	8
CROSSHOLE VP/VS:								
HLA	D	D		D	D	D		
SUSPENSION VP/VS:								
OYO		F			F			F
DOWNHOLE Q:								
QEST		G			G			
OYO								F
KC/CDMG	E		E	E		E		
VERTICAL SEISMIC PROFILING:								
OYO			F					F

CDMG - Calif. Dept. of Conservation Division of Mines and Geology
HLA - Harding Lawson Associates
KC - Kajima Corporation
LCA - LeRoy Crandall and Associates
OYO - OYO Corporation
PDC - Pitcher Drilling Co.
QEST - QEST Consultants
WCC - Woodward-Clyde Consultants

APPENDIX B
LeRoy Crandall and Associates

TURKEY FLAT PROJECT

GROUND RESPONSE STUDY

LeROY CRANDALL AND ASSOCIATES

BORING TF-1

DATE DRILLED: November 4, 1986

EQUIPMENT USED: 5"-Diameter Rotary Wash

DRILLER: PITCHER DRILLING COMPANY

ELEVATION 1621

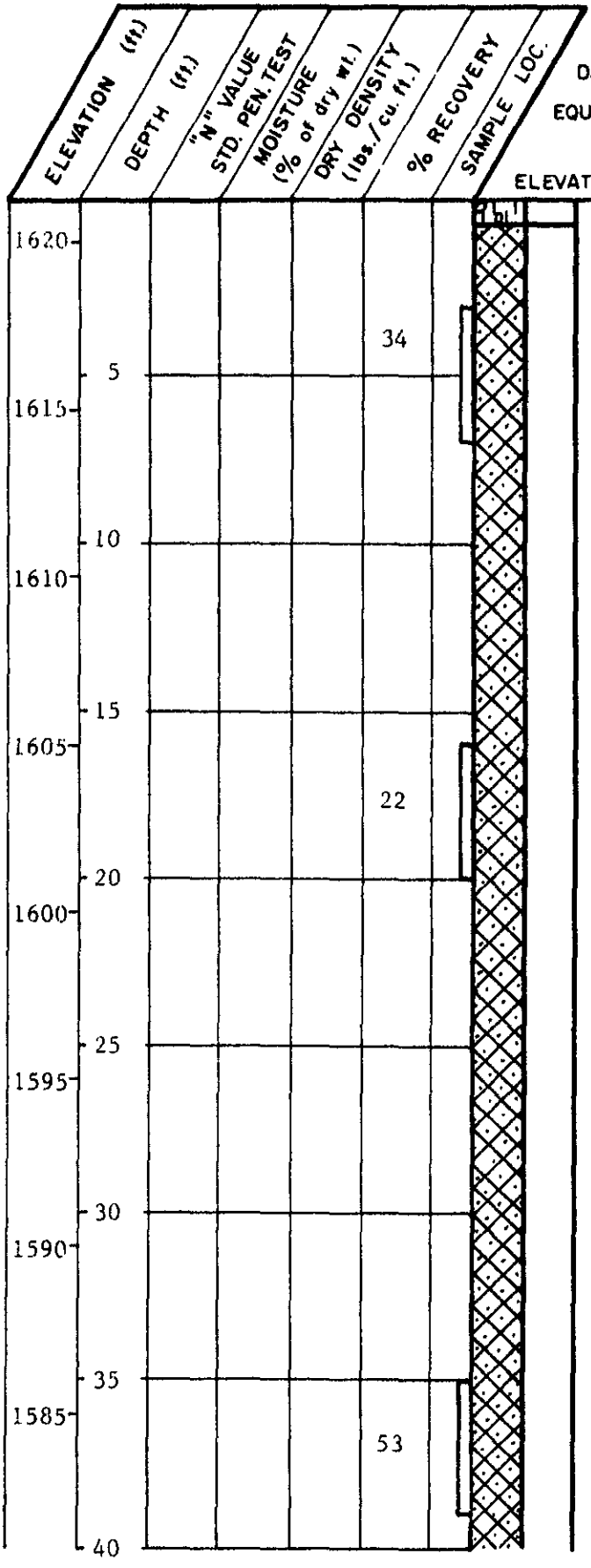

SILT and GRAVEL

SANDSTONE - weathered, light greyish brown

Boring logged by personnel of the California Division of Mines and Geology

NX CORE SAMPLE

(CONTINUED ON FOLLOWING PLATE)

NOTE: THE LOG OF SUBSURFACE CONDITIONS SHOWN HEREON APPLIES ONLY AT THE SPECIFIC BORING LOCATION AND AT THE DATE INDICATED. IT IS NOT WARRANTED TO BE REPRESENTATIVE OF SUBSURFACE CONDITIONS AT OTHER LOCATIONS AND TIMES.

LOG OF BORING

LeROY CRANDALL AND ASSOCIATES

BORING TF-1 (CONTINUED)

DATE DRILLED: November 4, 1986

EQUIPMENT USED: 5"-Diameter Rotary Wash
DRILLER: PITCHER DRILLING COMPANY

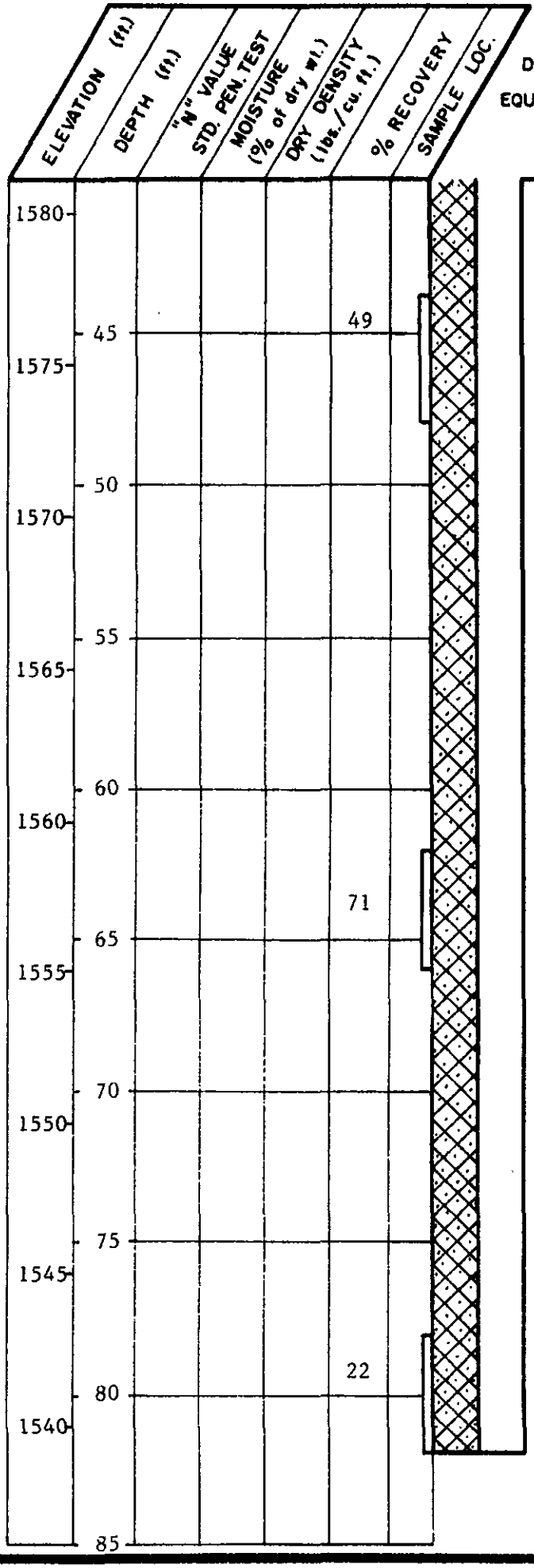

Bluish grey

Brownish grey

Bluish grey

NOTE: Drilling mud used in drilling process. Boring reamed to 8 3/4". Installed 5" diameter PVC pile to 82'. Annular spaced backfilled with pea gravel.

NOTE: THE LOG OF SUBSURFACE CONDITIONS SHOWN HEREON APPLIES ONLY AT THE SPECIFIC BORING LOCATION AND AT THE DATE INDICATED. IT IS NOT WARRANTED TO BE REPRESENTATIVE OF SUBSURFACE CONDITIONS AT OTHER LOCATIONS AND TIMES.

LeROY CRANDALL AND ASSOCIATES

BORING TF-3

DATE DRILLED: October 29, 1986

EQUIPMENT USED: 5"-Diameter Rotary Wash

DRILLER: PITCHER DRILLING COMPANY

ELEVATION 1708½

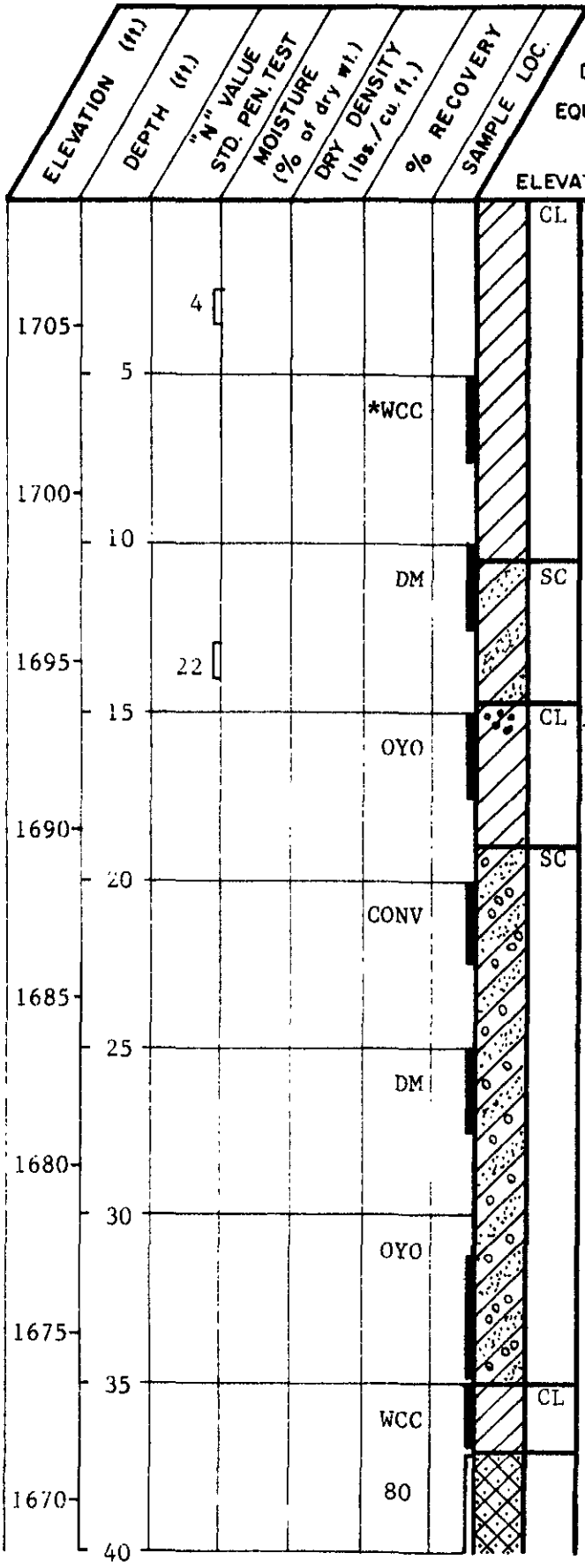

CL SANDY CLAY - dark brown

Boring logged by personell of Woodward-Clyde Consultants

*KEY TO DISTRIBUTION OF SAMPLES:
WCC - Woodward Clyde Consultants
DM - Dames & Moore
OYO - OYO Corporation
CONV - Converse

SC CLAYEY SAND - fine, dark brown

CL SANDY CLAY - brown
Lens of Gravel

SC CLAYEY SAND - fine, large amount of Gravel, light brown

More Gravel

Pitcher Sampler

NX Core Sample

Dark brown to black

CL SANDY CLAY - dark brown

SANDSTONE - grey

80% Recovery

NOTE: THE LOG OF SUBSURFACE CONDITIONS SHOWN HEREON APPLIES ONLY AT THE SPECIFIC BORING LOCATION AND AT THE DATE INDICATED. IT IS NOT WARRANTED TO BE REPRESENTATIVE OF SUBSURFACE CONDITIONS AT OTHER LOCATIONS AND TIMES.

LOG OF BORING

LeROY CRANDALL AND ASSOCIATES

97891

BORING TF-3 (CONTINUED)

DATE DRILLED: October 29, 1986

EQUIPMENT USED: 5"-Diameter Rotary Wash

DRILLER: PITCHER DRILLING COMPANY

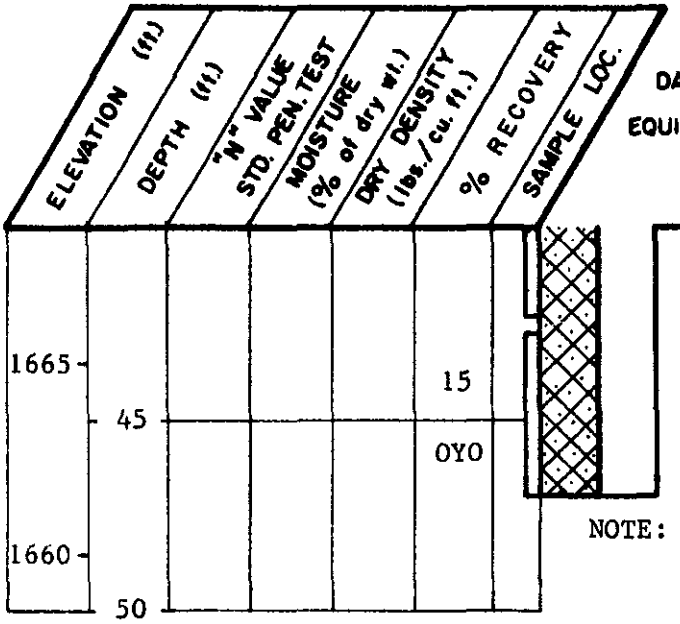

15% Recovery

NOTE: Drilling mud used in drilling process.

NOTE: THE LOG OF SUBSURFACE CONDITIONS SHOWN HEREON APPLIES ONLY AT THE SPECIFIC BORING LOCATION AND AT THE DATE INDICATED. IT IS NOT WARRANTED TO BE REPRESENTATIVE OF SUBSURFACE CONDITIONS AT OTHER LOCATIONS AND TIMES.

LOG OF BORING

LeROY CRANDALL AND ASSOCIATES

BORING TF-4

DATE DRILLED: October 20 & 21, 1986

EQUIPMENT USED: 5"-Diameter Rotary Wash

DRILLER: PITCHER DRILLING COMPANY

ELEVATION 1660

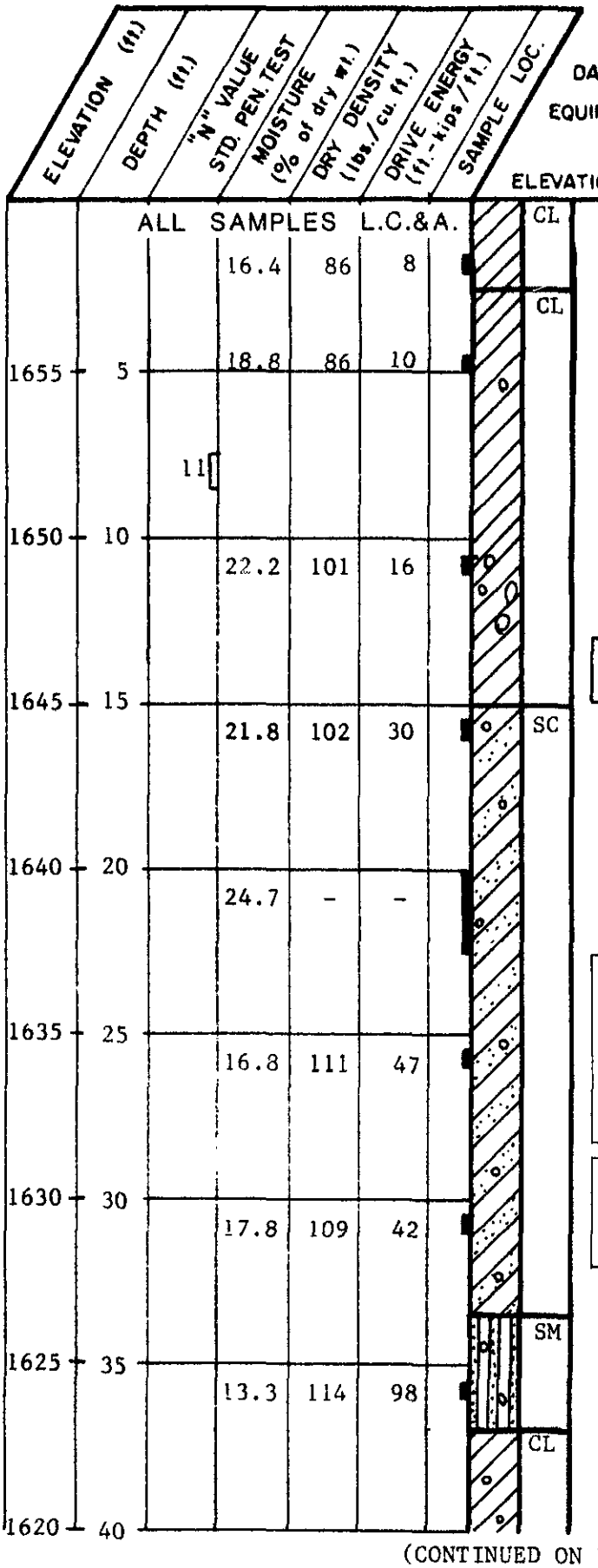

SILTY CLAY - dark brown

SANDY CLAY - light brown

Some Gravel

Some Gravel and Cobbles

Boring logged by LeRoy Crandall and Associates

CLAYEY SAND - fine to medium, some Gravel and Cobbles, light brown

90% Recovery
Few Gravel

8 ■ LC&A Sampler

└ Energy required to drive LC&A sampler 12", in ft. - kips per ft.:
Driving Weight = 325 lbs.
Stroke = 1½'

■ Pitcher Sampler

SILTY SAND - fine to coarse, some Gravel, light brown

SANDY CLAY - few Gravel, light brown

(CONTINUED ON FOLLOWING PLATE)

NOTE: THE LOG OF SUBSURFACE CONDITIONS SHOWN HEREON APPLIES ONLY AT THE SPECIFIC BORING LOCATION AND AT THE DATE INDICATED. IT IS NOT WARRANTED TO BE REPRESENTATIVE OF SUBSURFACE CONDITIONS AT OTHER LOCATIONS AND TIMES.

LOG OF BORING

LeROY CRANDALL AND ASSOCIATES

BORING TF-4 (CONTINUED)

DATE DRILLED: October 20 & 21, 1986

EQUIPMENT USED: 5"-Diameter Rotary Wash

DRILLER: PITCHER DRILLING COMPANY

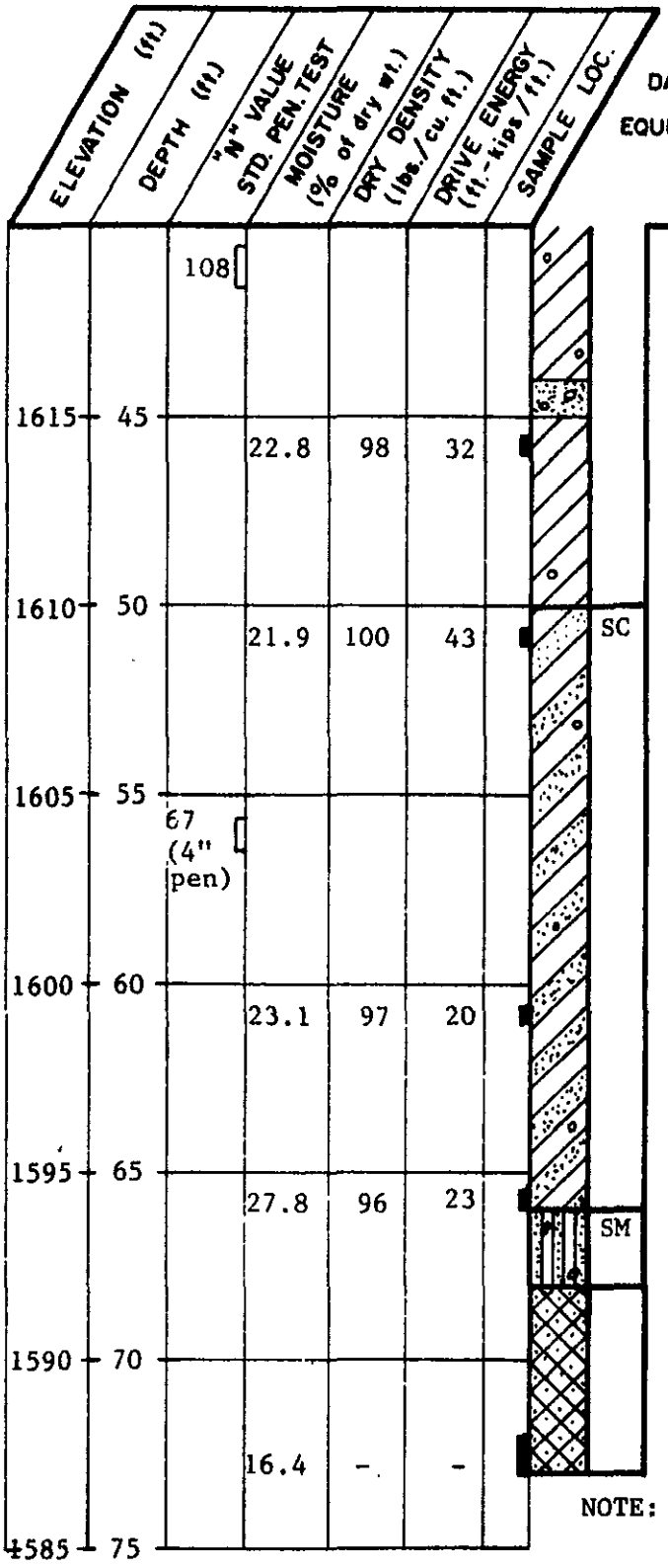

Layer of Sand and Gravel

CLAYEY SAND - fine to medium, few Gravel, light brown

SILTY SAND - fine, some Gravel, light brown

SANDSTONE - slightly fractured, greenish grey

79% Recovery

NOTE: Drilling mud used in drilling process. Boring reamed to 8". 5"-diameter casing and 1"-diameter perforated pipe installed. Annular space backfilled with Gravel.

NOTE: THE LOG OF SUBSURFACE CONDITIONS SHOWN HEREON APPLIES ONLY AT THE SPECIFIC BORING LOCATION AND AT THE DATE INDICATED. IT IS NOT WARRANTED TO BE REPRESENTATIVE OF SUBSURFACE CONDITIONS AT OTHER LOCATIONS AND TIMES.

LOG OF BORING

LeROY CRANDALL AND ASSOCIATES

BORING TF-6

DATE DRILLED: October 27, 1986

EQUIPMENT USED: 5"-Diameter Rotary Wash

DRILLER: PITCHER DRILLING COMPANY

ELEVATION 1660

ELEVATION (ft.)	DEPTH (ft.)	"N" VALUE STD. PEN. TEST	MOISTURE (% of dry wt.)	DRY DENSITY (lbs./cu. ft.)	% RECOVERY	SAMPLE LOC.		
							CL	SANDY CLAY - dark brown
							CL	SILTY CLAY - dark brown
		18						
1655	5						SC	CLAYEY SAND - fine, some Gravel, light brown
				OYO				
								Boring logged by personnel of Woodward-Clyde Consultants.
1650	10							
		58						
1645	15							Layer of Cobbles
							GC	CLAYEY GRAVEL - light brown
1640	20						SC	CLAYEY SAND - coarse, large amount of Gravel, light brown
		53						
								Layer of Cobbles
1635	25							Pitcher Sampler
				DM				NX Core Sample
							GC	CLAYEY GRAVEL - light brown
1630	30							
				WCC				
		50 (6" pen)					SC	CLAYEY SAND - coarse, some Gravel, light brown
1625	35	50 (5" pen)						
1620	40						CL	SANDY CLAY - large amount of Gravel, light brown

(CONTINUED ON FOLLOWING PLATE)

NOTE: THE LOG OF SUBSURFACE CONDITIONS SHOWN HEREON APPLIES ONLY AT THE SPECIFIC BORING LOCATION AND AT THE DATE INDICATED. IT IS NOT WARRANTED TO BE REPRESENTATIVE OF SUBSURFACE CONDITIONS AT OTHER LOCATIONS AND TIMES.

LOG OF BORING

LeROY CRANDALL AND ASSOCIATES

BORING TF-6 (CONTINUED)

DATE DRILLED: October 27, 1986

EQUIPMENT USED: 5"-Diameter Rotary Wash

DRILLER: PITCHER DRILLINC COMPANY

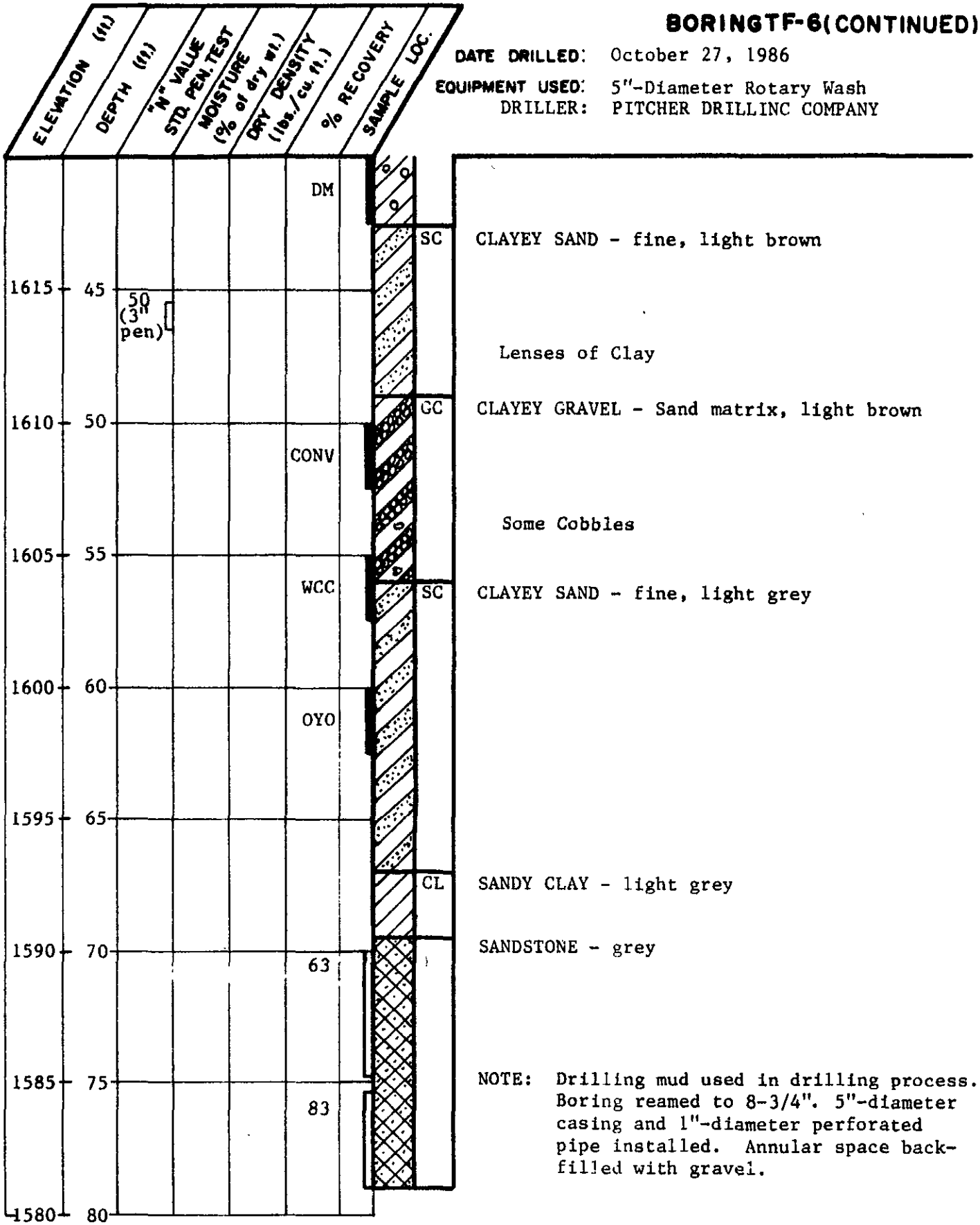

NOTE: Drilling mud used in drilling process. Boring reamed to 8-3/4". 5"-diameter casing and 1"-diameter perforated pipe installed. Annular space back-filled with gravel.

NOTE: THE LOG OF SUBSURFACE CONDITIONS SHOWN HEREON APPLIES ONLY AT THE SPECIFIC BORING LOCATION AND AT THE DATE INDICATED. IT IS NOT WARRANTED TO BE REPRESENTATIVE OF SUBSURFACE CONDITIONS AT OTHER LOCATIONS AND TIMES.

LOG OF BORING

LeROY CRANDALL AND ASSOCIATES

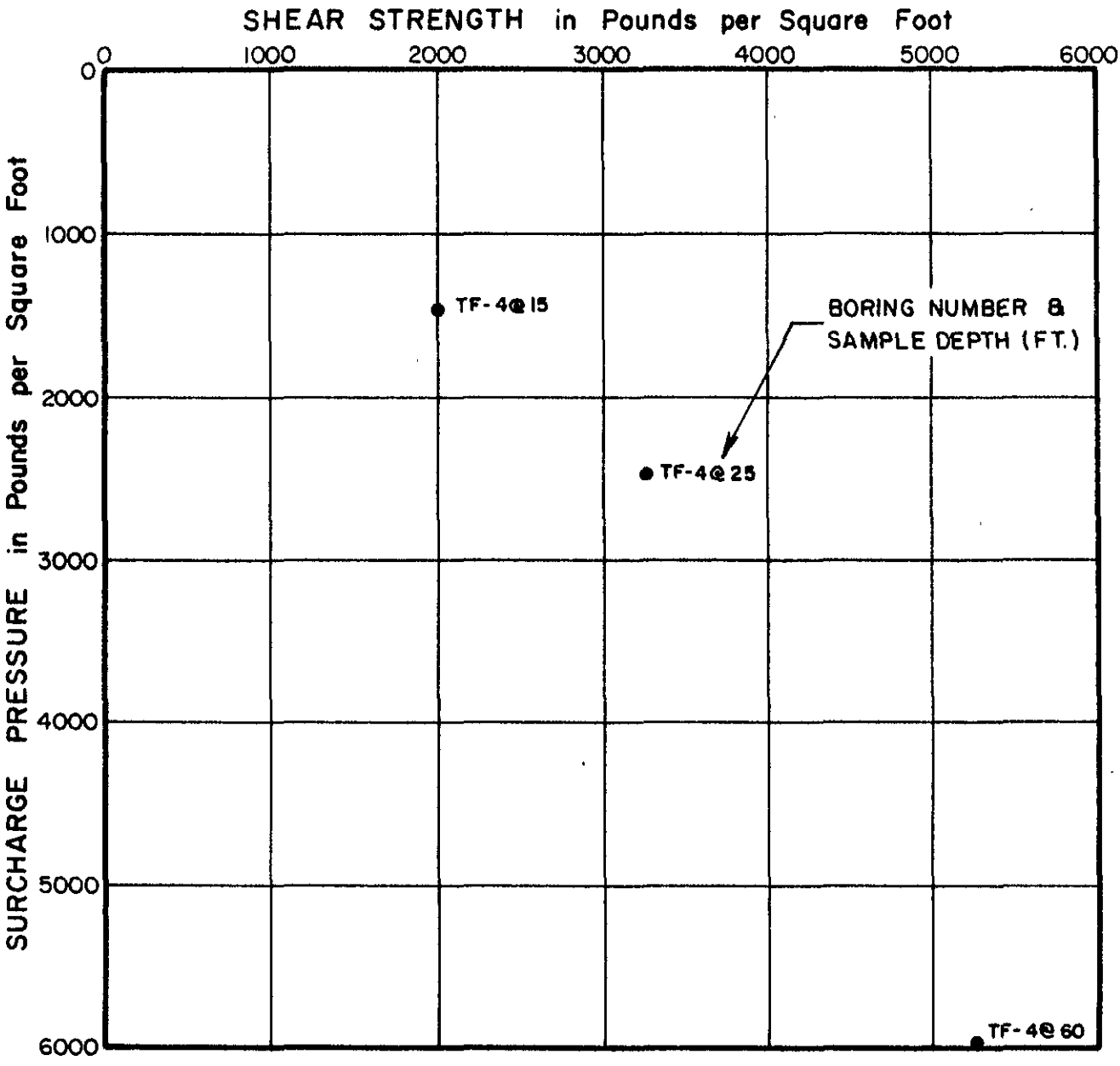

NOTE: All samples tested at field moisture content.

DIRECT SHEAR TEST DATA

LEROY CRANDALL & ASSOCIATES

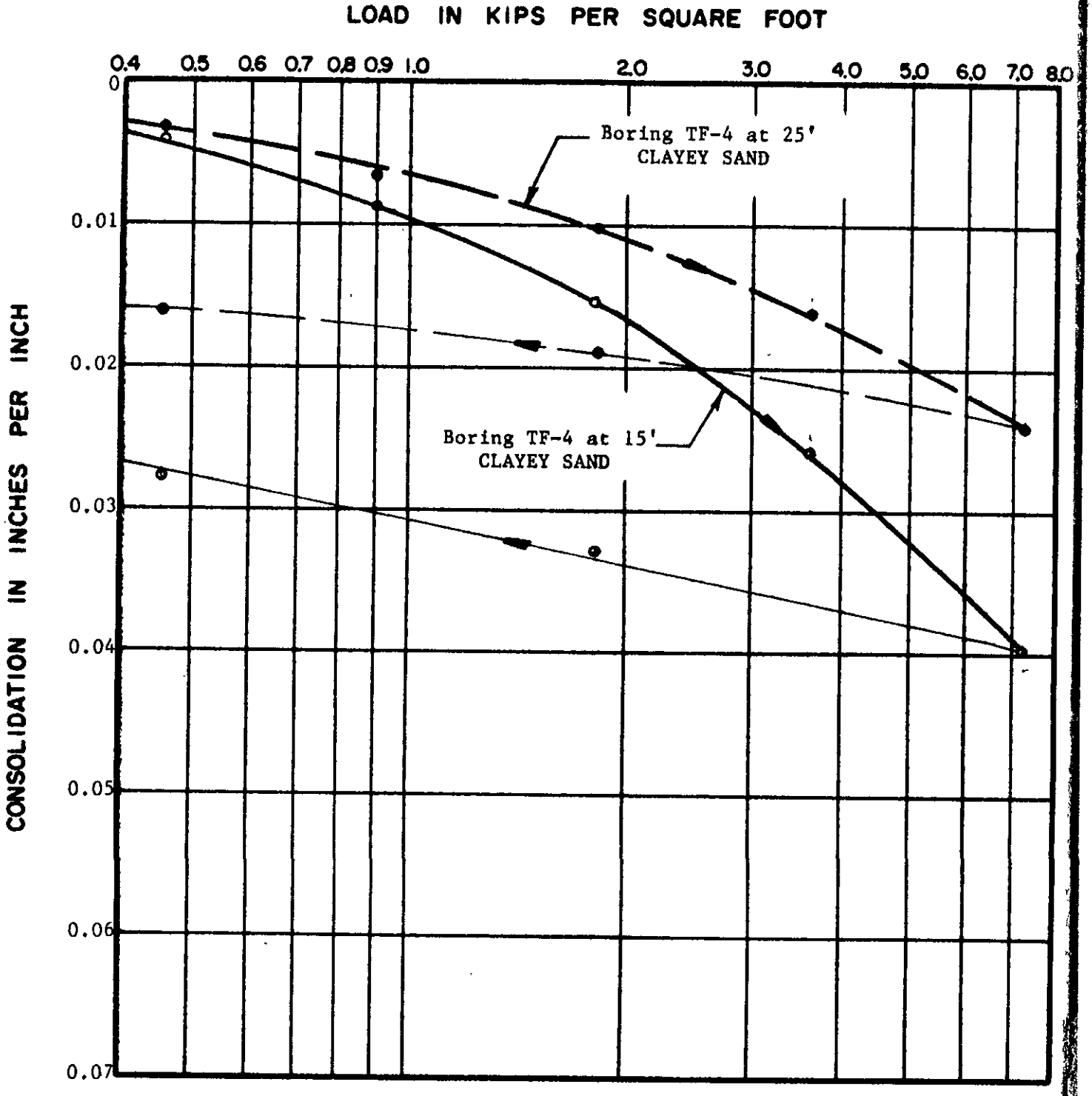

NOTE: Samples tested at field moisture content.

CONSOLIDATION TEST DATA

LeROY CRANDALL AND ASSOCIATES

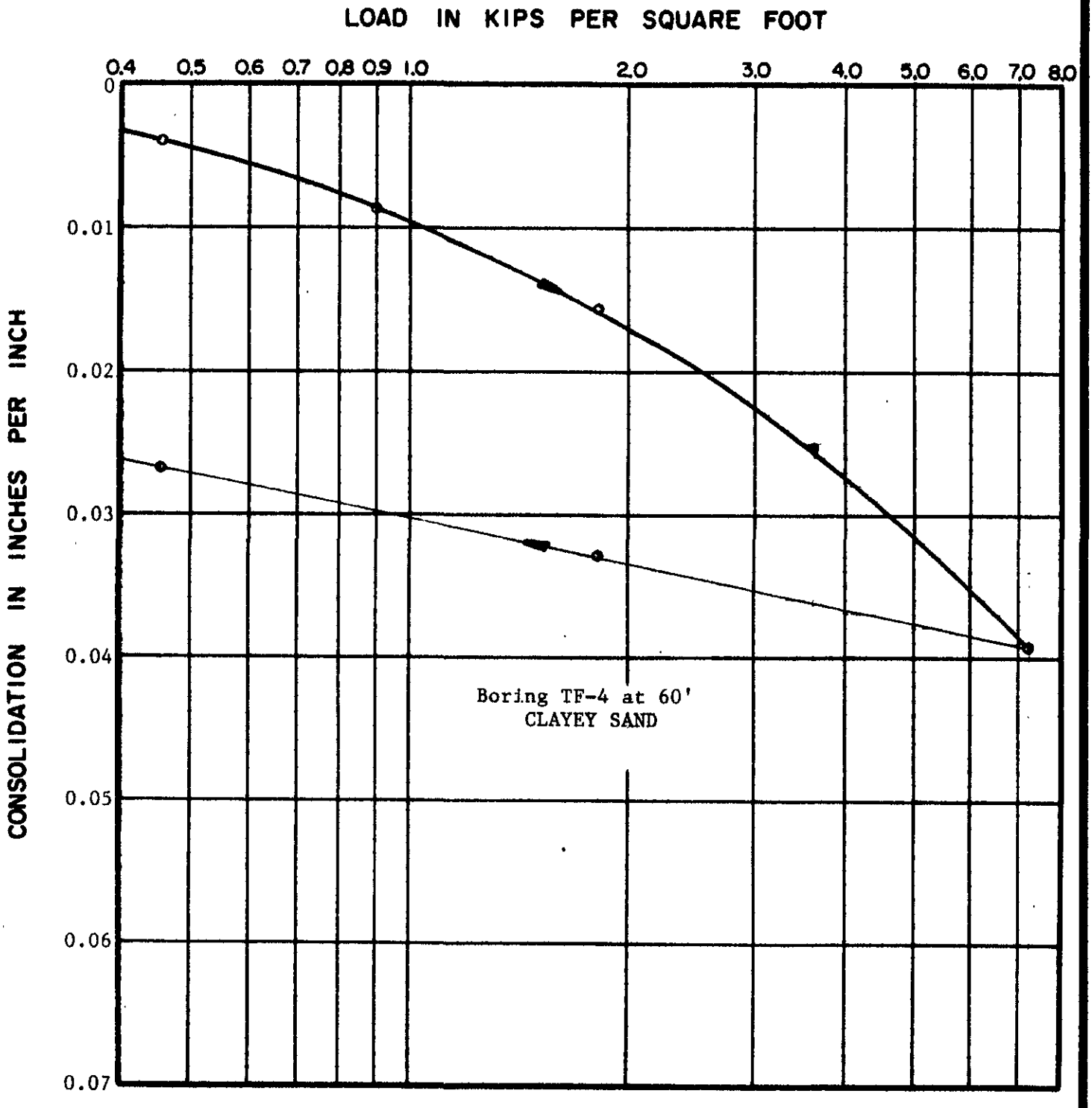

NOTE: Sample tested at field moisture content.

CONSOLIDATION TEST DATA

LeROY CRANDALL AND ASSOCIATES

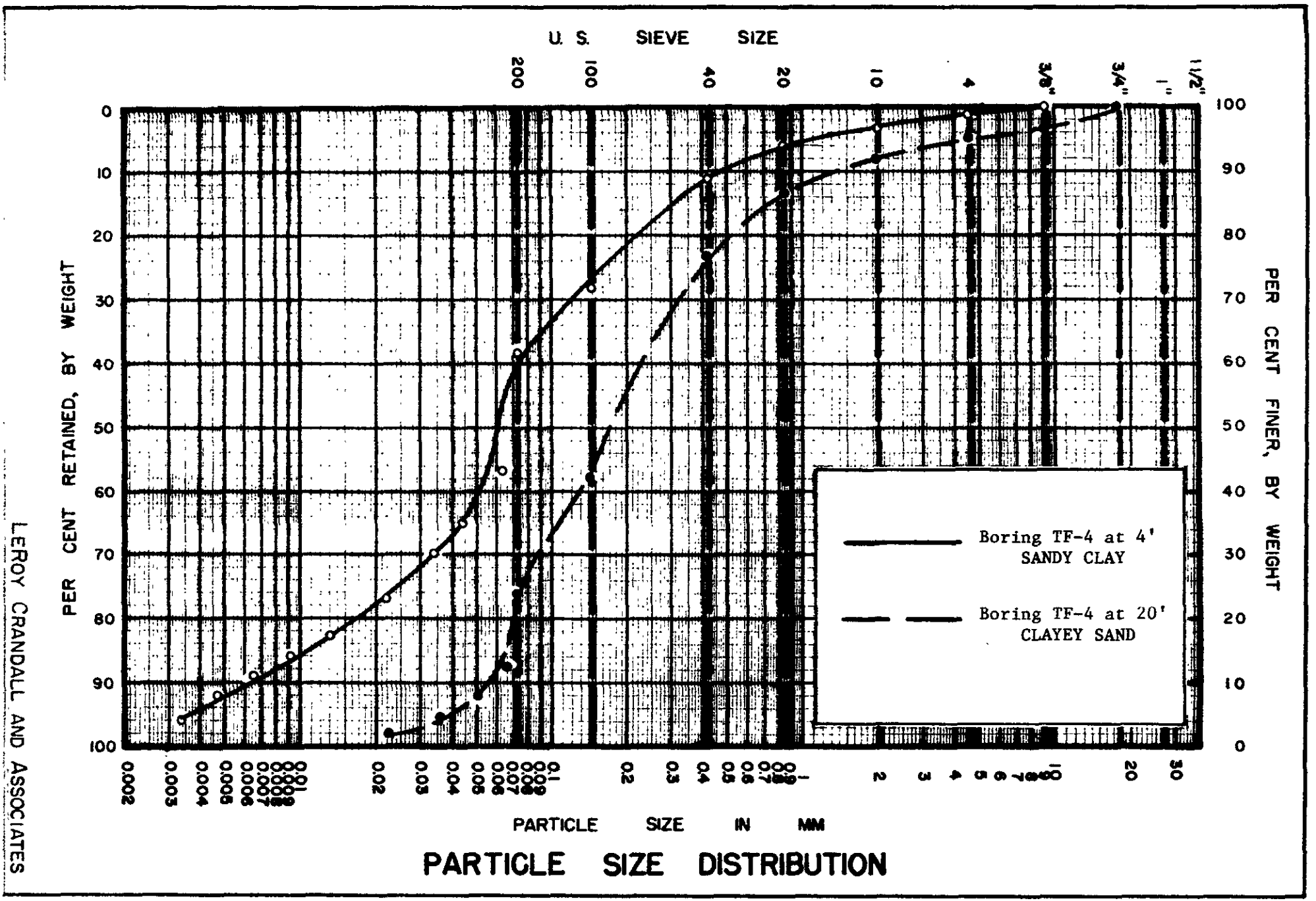

PARTICLE SIZE DISTRIBUTION

LEROY CRANDALL AND ASSOCIATES

Form 12a

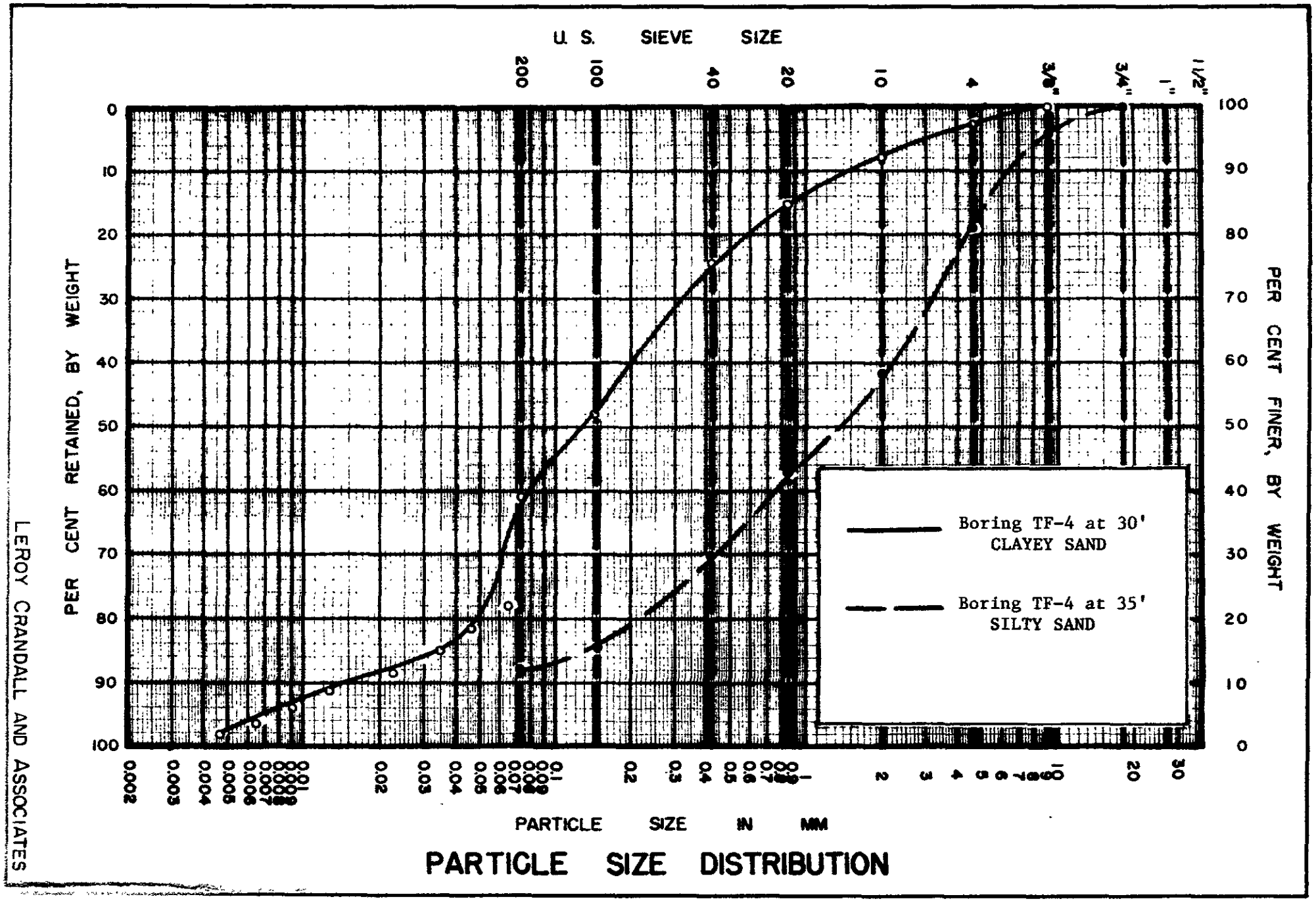

LEROY CRANDALL AND ASSOCIATES

PARTICLE SIZE DISTRIBUTION

F.... 12 JL ____ DAT ____ B. DM CHECKED ____

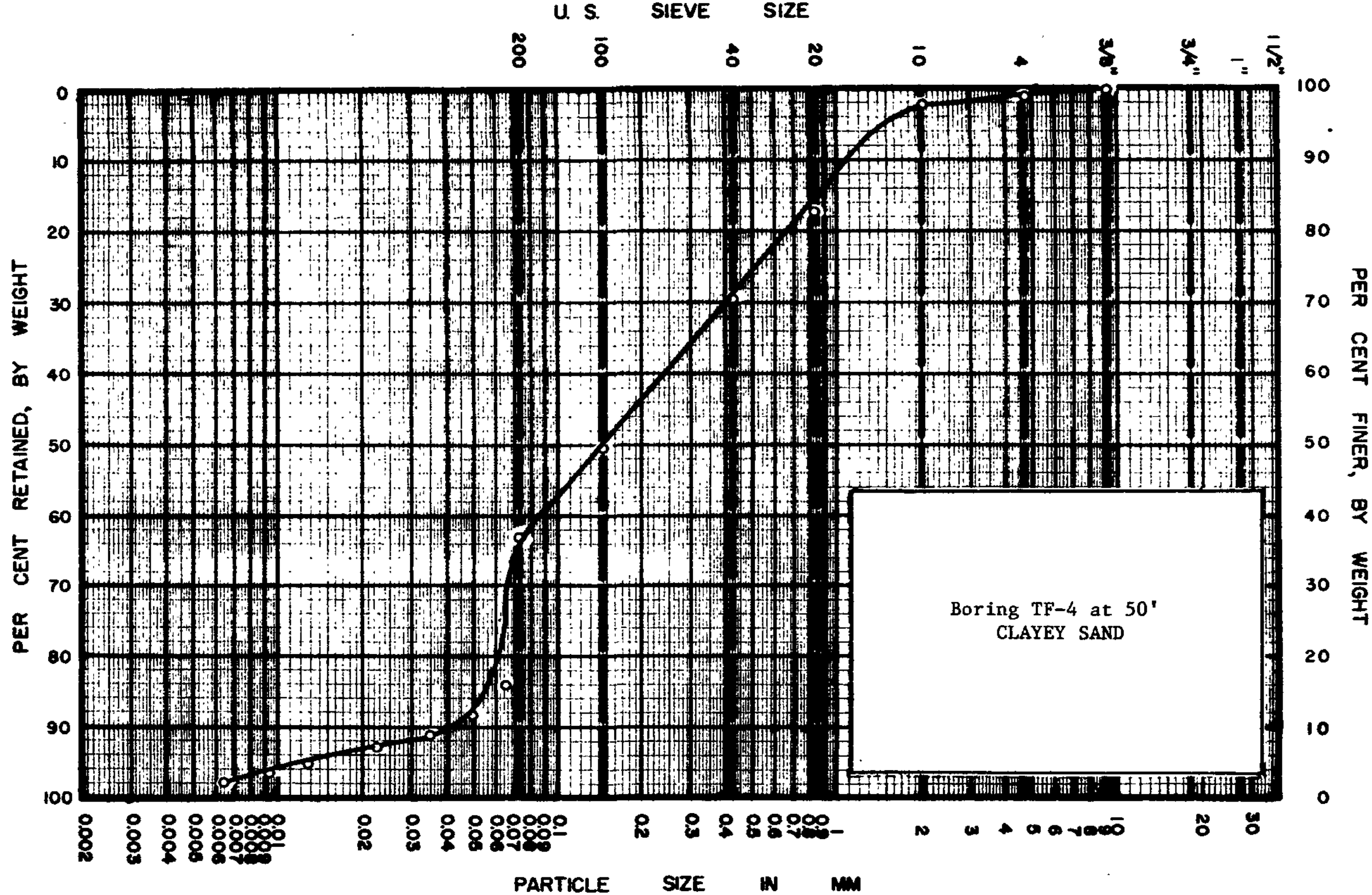

PARTICLE SIZE DISTRIBUTION

LEROY CRANDALL AND ASSOCIATES

BORING NUMBER AND SAMPLE DEPTH	SOIL TYPE	LIQUID LIMIT (%)	PLASTIC LIMIT (%)	PLASTICITY INDEX (%)
TF-4 at 4'	SANDY CLAY	49	25	24
TF-4 at 20'	CLAYEY SAND	29	21	8
TF-4 at 30'	CLAYEY SAND	36	23	13

ATTERBERG LIMITS TEST DATA

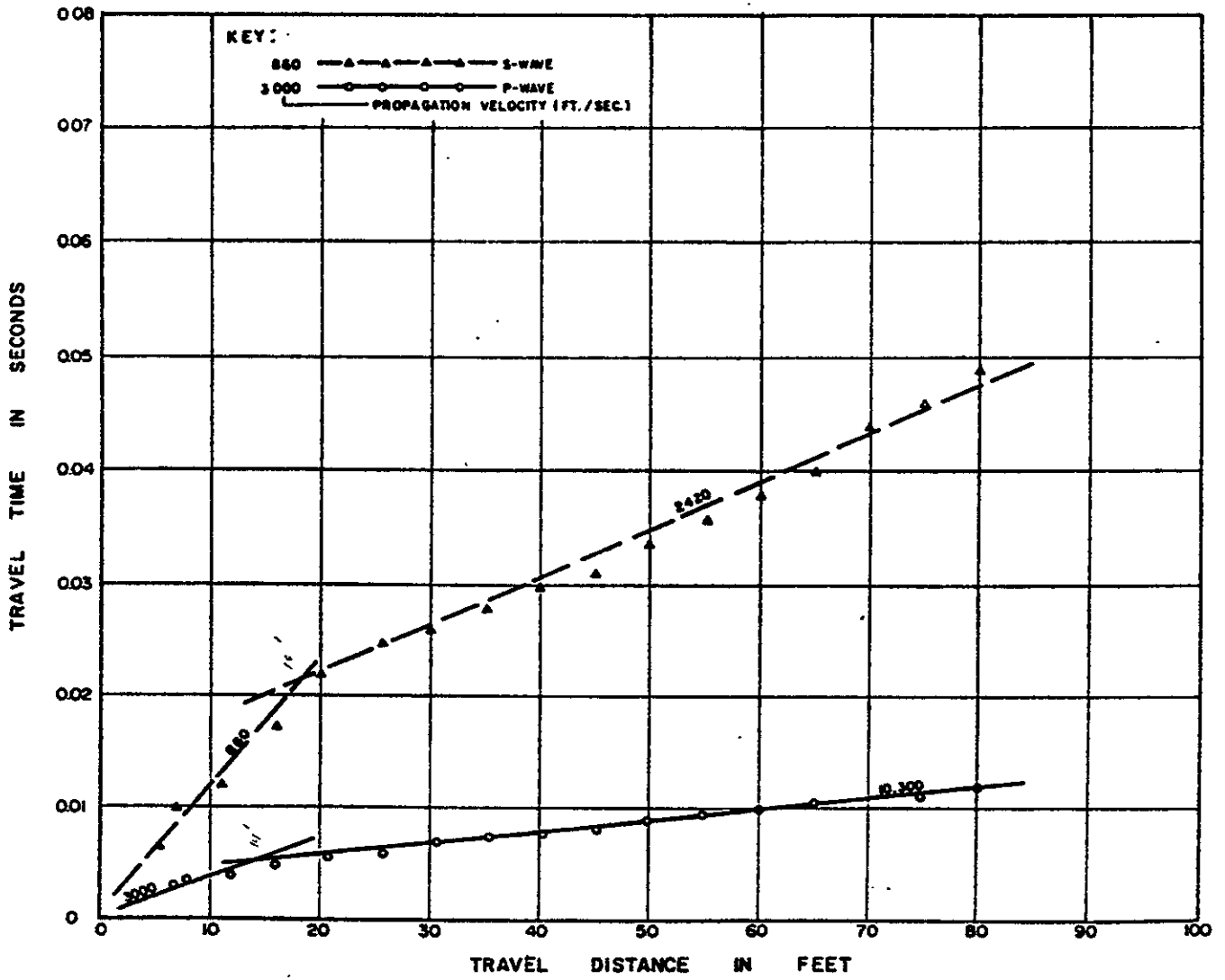

BORING TF-2

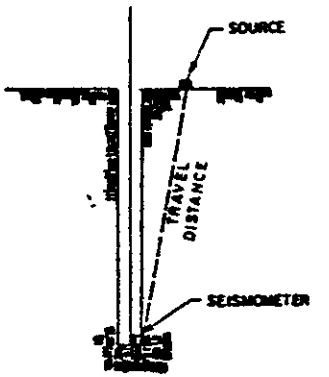

SECTION

NOTE:
VELOCITY MEASUREMENTS MADE BY LeROY CRANDALL AND ASSOCIATES.

DOWNHOLE SEISMIC SURVEY

LeROY CRANDALL AND ASSOCIATES

PLATE

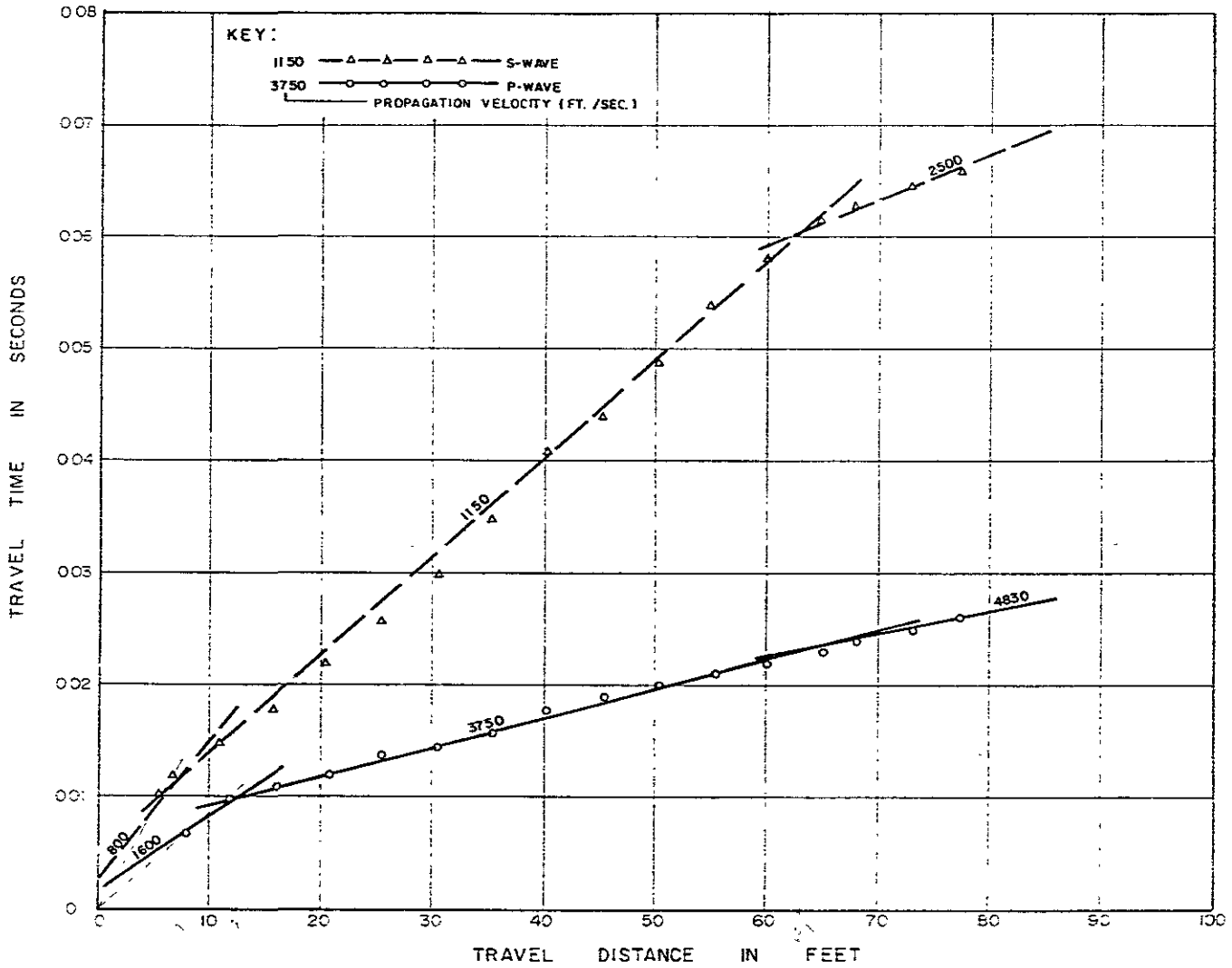

BORING TF-5

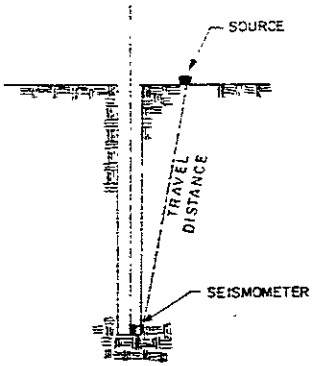

SECTION

NOTE:
VELOCITY MEASUREMENTS MADE BY LeROY CRANDALL AND ASSOCIATES.

DOWNHOLE SEISMIC SURVEY

LeROY CRANDALL AND ASSOCIATES

PLATE

APPENDIX C
Dames & Moore

TURKEY FLAT EXPERIMENT

Dynamic Triaxial Tests Performed by Dames & Moore

Dames & Moore performed two stage dynamic triaxial tests on 4 samples taken during the boring program in Turkey Flat. The samples were severely dessicated and somewhat disturbed so the results of the tests should be expected to present considerably lower dynamic properties than measured by in place geophysical test procedures.

Some classification tests were conducted on the samples tested. Grain size analyses were performed on the samples after testing so the sample description included with the test results are correct in accordance with the ASTM classification guidelines. Plasticity analyses were performed on the cohesive samples with the following results.

TF3 @ 10 feet	LL= 51 PL = 26	(CL/SM)
TF3 @ 25 feet	non-plastic	(GP/SP)
TF6 @ 25 feet	LL = 52 PL = 28	(CL)
TF6 @ 40 feet	LL = 48 PL = 30	(CL/ML)

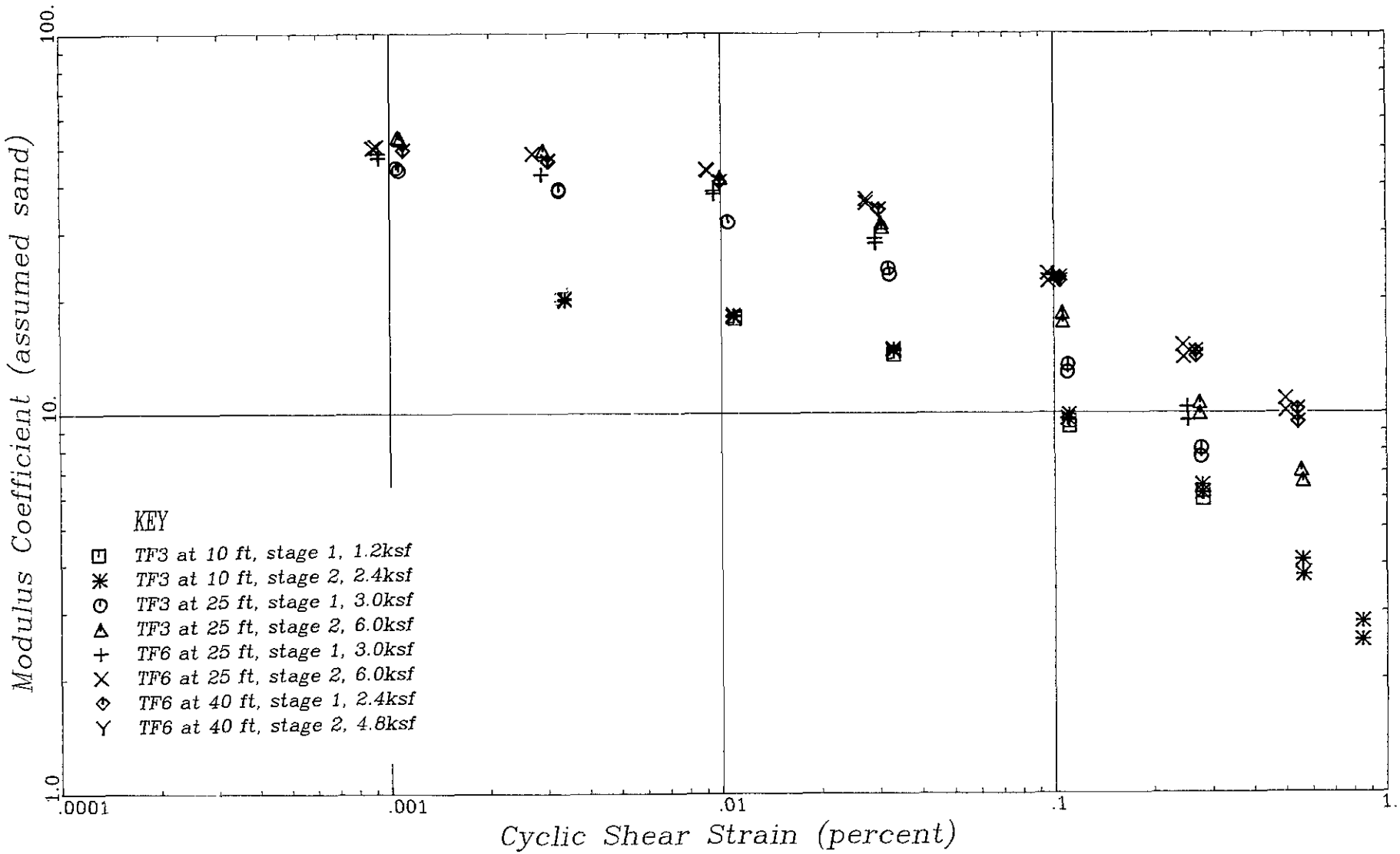

Parkfield Ground Response Test "Turkey Flat Experiment"
Summary plot of Cyclic Triaxial Tests performed by Dames & Moore

Dames & Moore

SHEAR MODULUS TEST RESULTS

2-FEB-87

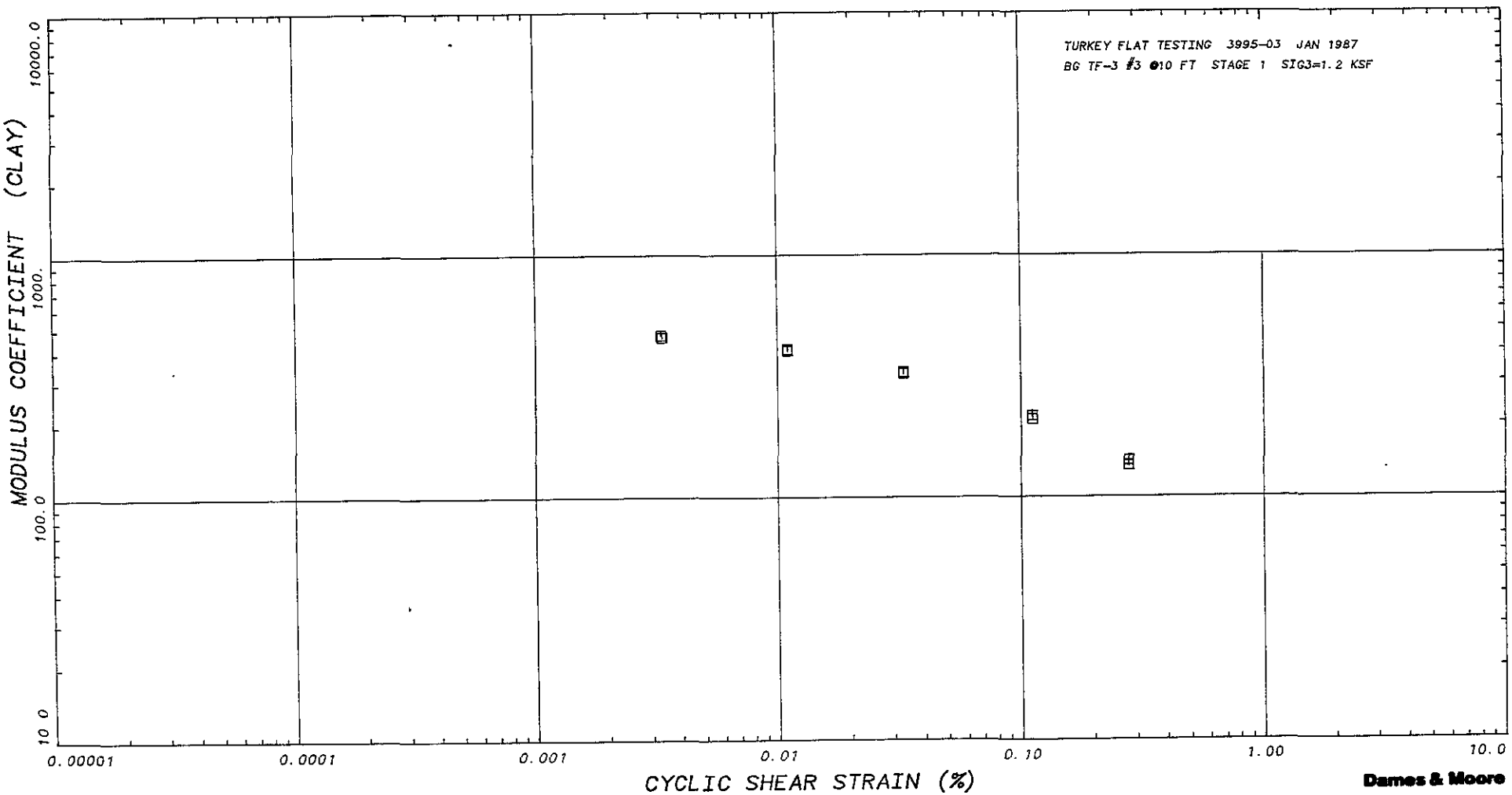

Dames & Moore

SHEAR MODULUS TEST RESULTS

2-FEB-87

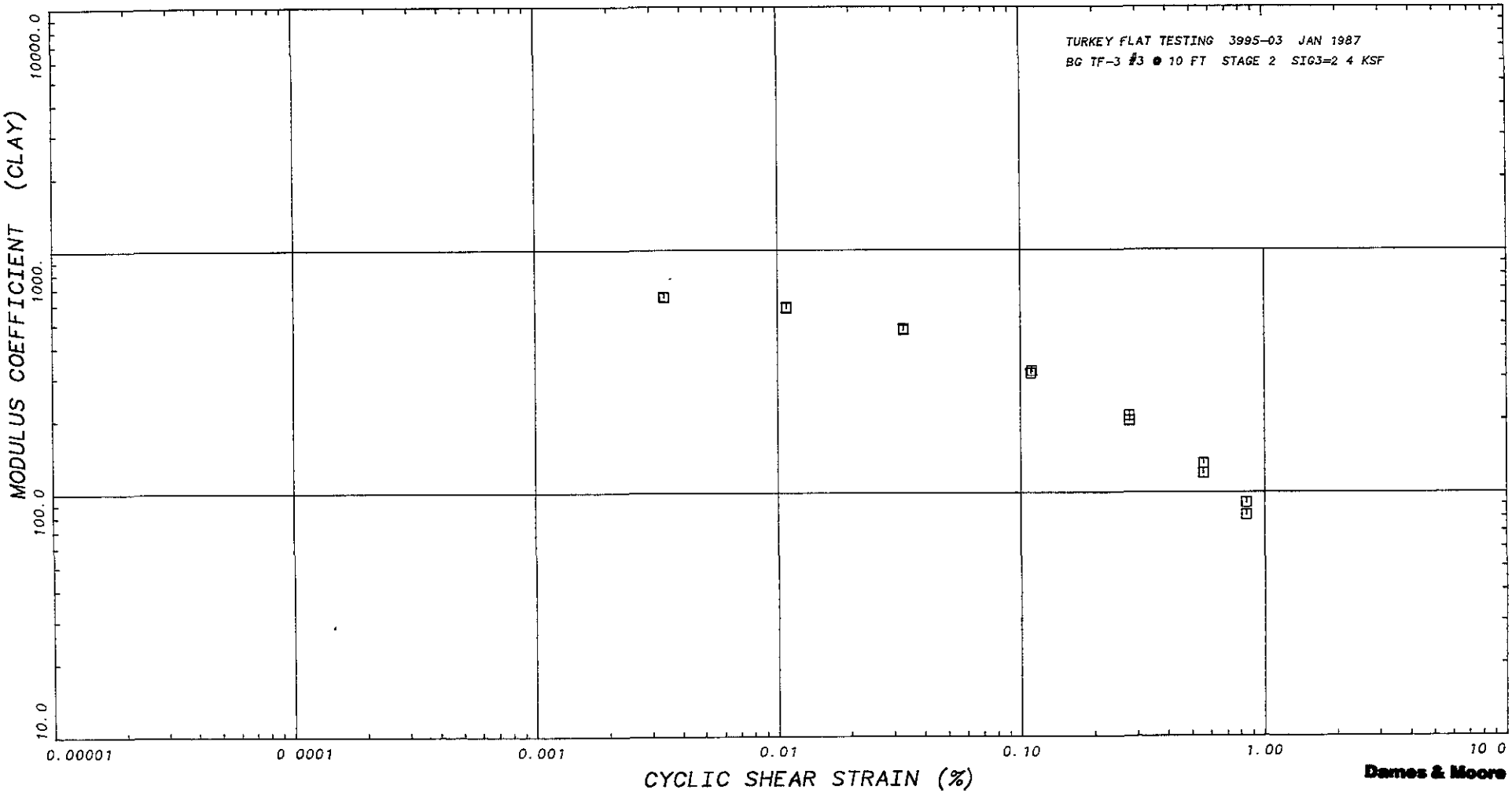

Dames & Moore

SHEAR MODULUS TEST RESULTS

2-FEB-87

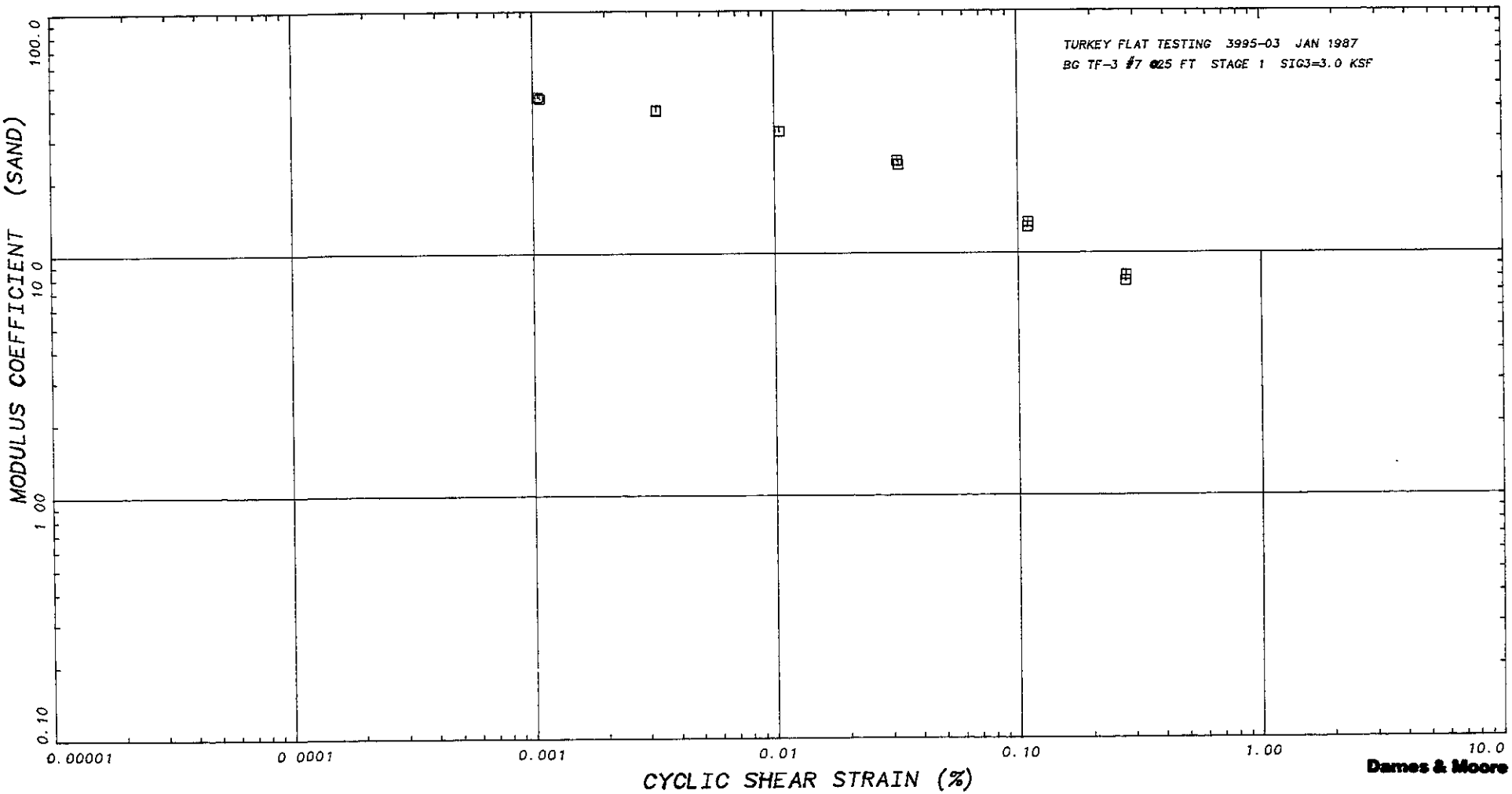

SHEAR MODULUS TEST RESULTS

2-FEB-87

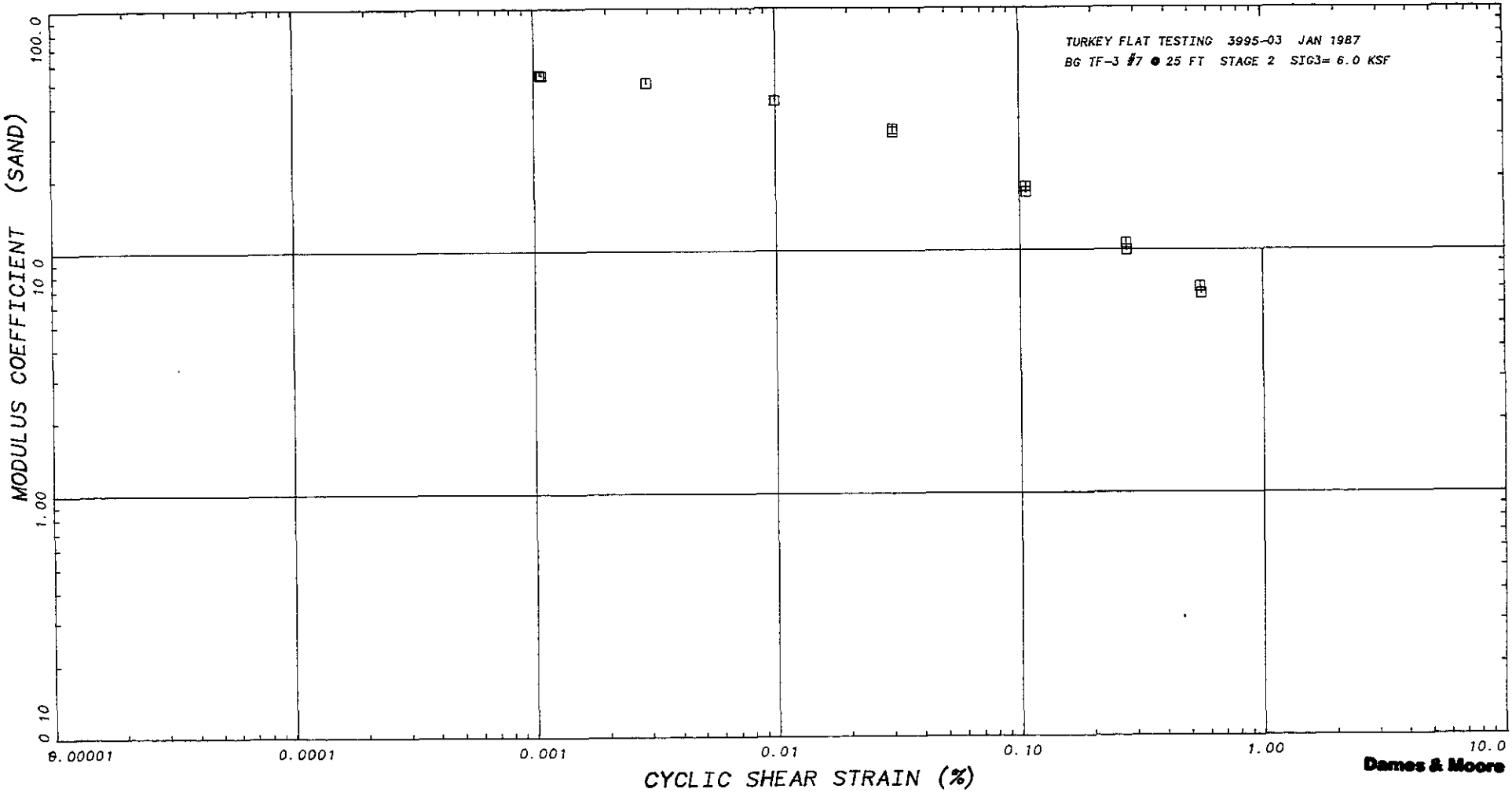

SHEAR MODULUS TEST RESULTS

30-JAN-87

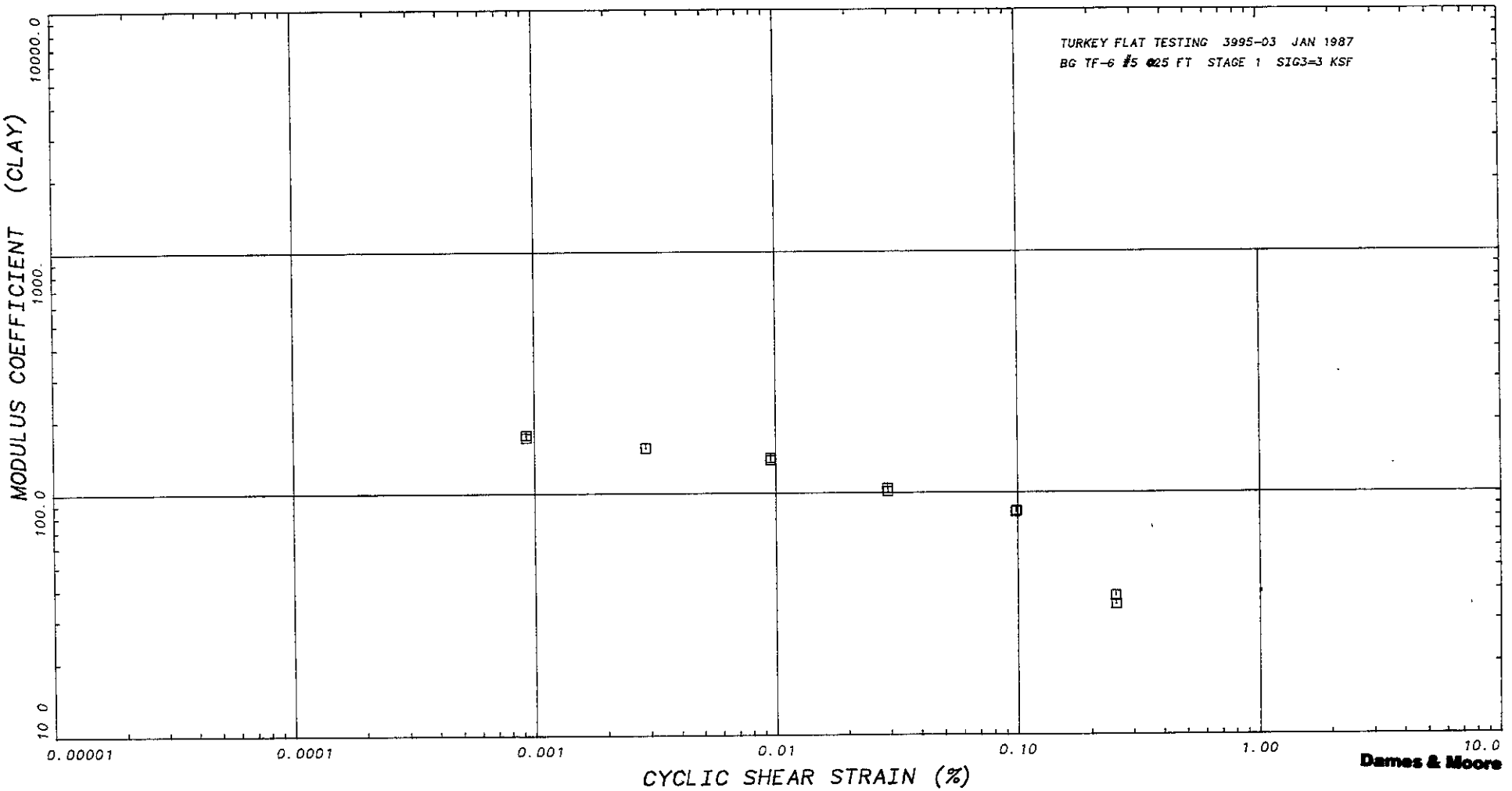

SHEAR MODULUS TEST RESULTS

30-JAN-87

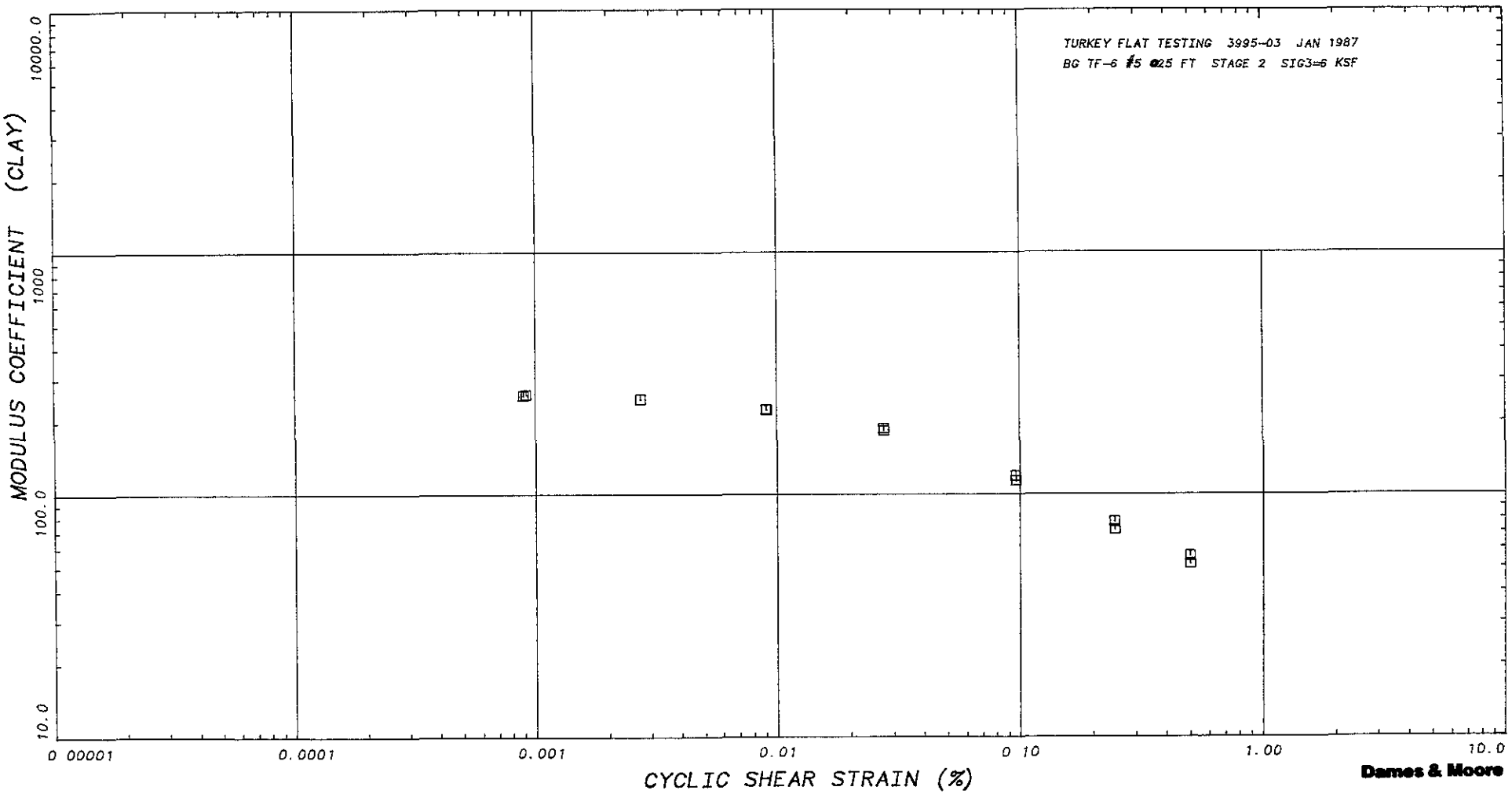

SHEAR MODULUS TEST RESULTS

2-FEB-87

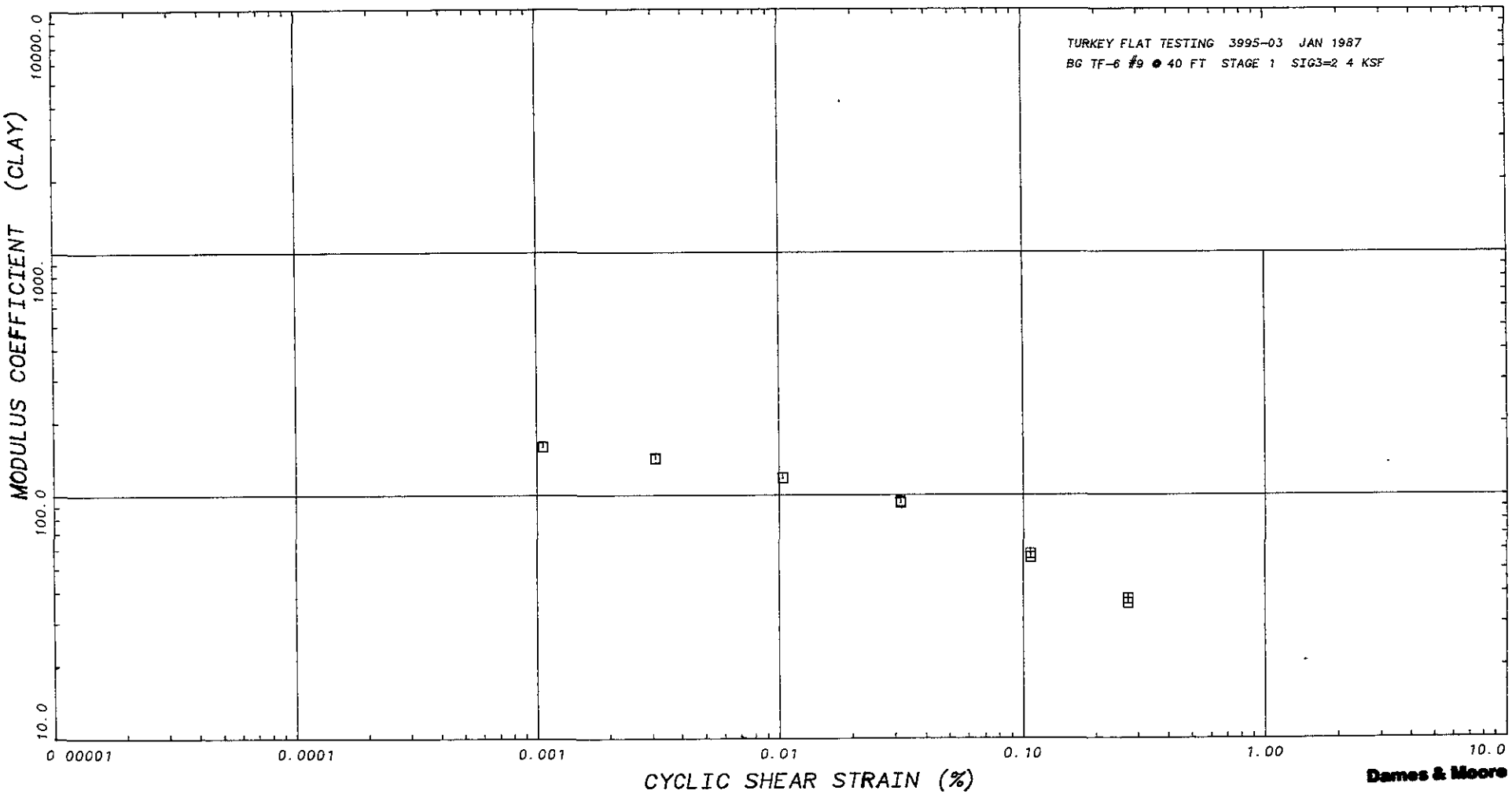

SHEAR MODULUS TEST RESULTS

2-FEB-87

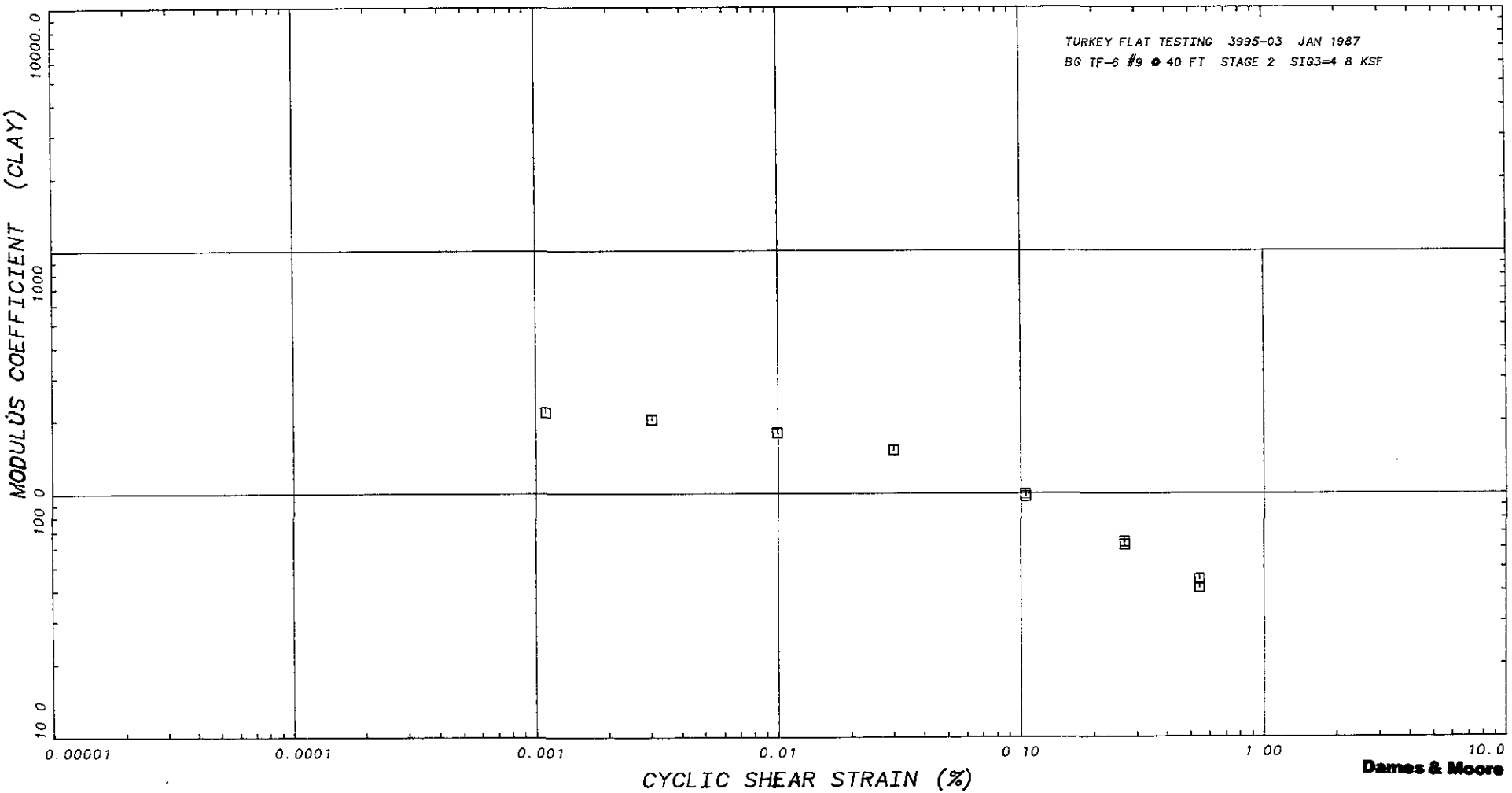

Dames & Moore

REVISIONS BY DATE

BY DATE FILE

CHECKED BY DATE

DYNAMIC SOIL PROPERTY TEST 2-FEB-87

TURKEY FLAT TESTING 3995-03 JAN 1987
BG TF-3 #3 @10 FT STAGE 1 SIG3=1.2 KSF
Dark Brown Sandy Silty Clay with a trace of fine gravel

INITIAL MOISTURE CONTENT	=	27.8	PERCENT
INITIAL DRY DENSITY	=	86.50	PCF
MOISTURE CONTENT AFTER CONSOL.	=	0.0	PERCENT
DRY DENSITY AFTER CONSOL.	=	87.70	PCF
SAMPLE HEIGHT AFTER CONSOL.	=	5.93	IN
SAMPLE DIAMETER AFTER CONSOL.	=	2.86	IN
CONSOLIDATION PRESSURE	=	1200.0	PSF
POISSON RATIO	=	0.35	(ASSUMED)

VALUES MEASURED AT CYCLE(S) 5 & 15

SYSTEM DEFORMATION CORRECTION CURVE -

LOAD (LB)	0.00	1000.00
DEFM (IN)	0.00000	0.00230

SYSTEM DAMPING CORRECTION CURVE -

LOAD (LB)	0.00	1000.00
DAMP (PCT)	0.000	0.000

DEVIATOR STRESS (PSF)	SINGLE AMPL CYCLIC STRAIN AXIAL (PERCENT)	SHEAR	YOUNGS MODULUS (KSF)	SHEAR MODULUS (KSF)	K	DAMPING RATIO (PERCENT)	SHEAR WAVE VELOCITY (FPS)
47.1	0.0024	0.0033	1926.	713.	467.7	3.7	511.71
46.6	0.0025	0.0030	1886.	698.	458.0	4.3	506.38
130.0	0.0082	0.0111	1685.	624.	409.2	4.4	478.67
136.3	0.0082	0.0111	1664.	616.	404.1	4.1	475.66
362.1	0.0245	0.0330	1355.	502.	329.2	6.5	429.37
367.6	0.0245	0.0330	1337.	495.	324.6	5.8	426.35
734.9	0.0826	0.1115	890.	330.	216.1	9.8	347.84
712.5	0.0826	0.1116	862.	319.	209.4	9.3	342.41
1206.1	0.2076	0.2807	581.	215.	141.1	12.3	281.09
1150.0	0.2077	0.2804	554.	205.	134.5	11.5	274.41

WHERE K IS GIVEN BY... K=G/SU
AND SU=UNDRAINED SHEAR STRENGTH = 1525.0 (PSF)

Dames & Moore

PLATE

946.7 (REV. 6-61)

REVISIONS BY DATE

BY FILE

BY DATE

CHECKED BY DATE

946.7 (REV. 6-61)

DYNAMIC SOIL PROPERTY TEST 2-FEB-87

TURKEY FLAT TESTING 3995-03 JAN 1987
BG TF-3 #3 @ 10 FT STAGE 2 SIG3=2.4 KSF

Dark Brown Sandy Silty Clay with a trace of fine gravel

INITIAL MOISTURE CONTENT	=	0.0	PERCENT
INITIAL DRY DENSITY	=	87.70	PCF
MOISTURE CONTENT AFTER CONSOL.	=	27.2	PERCENT
DRY DENSITY AFTER CONSOL	=	88.20	PCF
SAMPLE HEIGHT AFTER CONSOL.	=	5.92	IN
SAMPLE DIAMETER AFTER CONSOL.	=	2.85	IN
CONSOLIDATION PRESSURE	=	2400.0	PSF
POISSON RATIO	=	0.35	(ASSUMED)

VALUES MEASURED AT CYCLE(S) 5 & 15

SYSTEM DEFORMATION CORRECTION CURVE -

LOAD (LB)	0.00	1000.00
DEFM (IN)	0.00000	0.00230

SYSTEM DAMPING CORRECTION CURVE -

LOAD (LB)	0.00	1000.00
DAMP (PCT)	0.000	0.000

DEVIATOR STRESS (PSF)	SINGLE AMPL CYCLIC STRAIN AXIAL (PERCENT)	SHEAR	YOUNGS MODULUS (KSF)	SHEAR MODULUS (KSF)	K	DAMPING RATIO (PERCENT)	SHEAR WAVE VELOCITY (FPS)
66.4	0.0025	0.0034	2631.	975.	639.1	1.9	528.87
67.0	0.0025	0.0034	2655.	983.	644.8	2.2	531.23
194.7	0.0081	0.0107	2402.	890.	583.4	3.0	505.37
193.1	0.0081	0.0107	2380.	882.	578.1	2.9	503.03
479.5	0.0245	0.0330	1957.	725.	475.3	4.7	456.17
473.9	0.0245	0.0330	1933.	716.	469.6	4.7	453.35
1080.7	0.0826	0.1115	1309.	485.	317.9	8.6	373.00
1046.9	0.0818	0.1104	1280.	474.	310.9	8.2	368.87
1767.3	0.2070	0.2794	854.	316.	207.4	12.1	301.20
1688.5	0.2071	0.2796	815.	302.	198.0	11.4	294.37
2951.4	0.4162	0.5618	541.	200.	131.4	14.4	239.81
2060.0	0.4165	0.5623	495.	183.	120.1	13.7	229.30
2341.4	0.6271	0.8466	373.	138.	90.7	14.5	199.23
2093.8	0.6275	0.8471	334.	124.	81.0	14.5	188.33

WHERE K IS GIVEN BY... K=σ/SU
AND SU=UNDRAINED SHEAR STRENGTH = 1525.0 (PSF)

Dames & Moore

PLATE

REVISIONS BY DATE

BY DATE FILE

CHECKED BY DATE

946.7 (REV. 6-61)

DYNAMIC SOIL PROPERTY TEST 2-FEB-87

TURKEY FLAT TESTING 3995-03 JAN 1987
BORING B-3 #7 @25 FT STAGE 1 SIG3=3.0 KSF

Brown Gravelly Silty Sand

INITIAL MOISTURE CONTENT	=	11.7	PERCENT
INITIAL DRY DENSITY	=	117.40	PCF
MOISTURE CONTENT AFTER CONSOL.	=	0.0	PERCENT
DRY DENSITY AFTER CONSOL.	=	119.50	PCF
SAMPLE HEIGHT AFTER CONSOL.	=	5.91	IN
SAMPLE DIAMETER AFTER CONSOL.	=	2.86	IN
CONSOLIDATION PRESSURE	=	3000.0	PSF
POISSON RATIO	=	0.35	(ASSUMED)

VALUES MEASURED AT CYCLE(S) 5 & 15

SYSTEM DEFORMATION CORRECTION CURVE -

LOAD (LB)	0.00	1000.00
DEFM (IN)	0.00000	0.00200

SYSTEM DAMPING CORRECTION CURVE -

LOAD (LB)	0.00	1000.00
DAMP (PCT)	0.000	0.000

DEVIATOR STRESS (PSF)	SINGLE AMPL CYCLIC STRAIN AXIAL (PERCENT)	SHEAR (PERCENT)	YOUNGS MODULUS (KSF)	SHEAR MODULUS (KSF)	K	DAMPING RATIO (PERCENT)	SHEAR WAVE VELOCITY (FPS)
51.4	0.0008	0.0011	6476.	2399.	43.8	4.4	803.93
51.4	0.0008	0.0011	6581.	2437.	44.5	4.8	810.47
139.7	0.0024	0.0033	5774	2139.	39.0	4.6	759.10
138.6	0.0024	0.0033	5723.	2120.	38.7	4.6	755.75
368.8	0.0078	0.0105	4722.	1749.	31.9	5.5	686.46
368.8	0.0078	0.0105	4722.	1749.	31.9	5.1	686.46
843.9	0.0237	0.0320	3564.	1320.	24.1	9.0	596.36
821.5	0.0239	0.0329	3433.	1271.	23.2	7.9	585.37
1620.7	0.0817	0.1103	1983.	735.	13.4	12.9	444.90
1542.4	0.0814	0.1097	1894.	702.	12.8	11.7	434.77
2458.2	0.2060	0.2781	1194.	442.	8.1	14.2	345.15
2324.8	0.2052	0.2770	1133.	420.	7.7	12.8	336.20

WHERE K IS GIVEN BY... K=G/(1000.*SIG3**0.500)

Dames & Moore

PLATE

REVISIONS BY DATE

FILE

BY DATE

CHECKED BY DATE

DYNAMIC SOIL PROPERTY TEST 2-FEB-87

TURKEY FLAT TESTING 3995-03 JAN 1987
BORING B-3 #7 @ 25 FT STAGE 2 SIG3= 6.0 KSF

Brown Gravelly Silty Sand

INITIAL MOISTURE CONTENT	=	0.0	PERCENT
INITIAL DRY DENSITY	=	119.50	PCF
MOISTURE CONTENT AFTER CONSOL.	=	11.1	PERCENT
DRY DENSITY AFTER CONSOL.	=	120.20	PCF
SAMPLE HEIGHT AFTER CONSOL.	=	5.90	IN
SAMPLE DIAMETER AFTER CONSOL.	=	2.86	IN
CONSOLIDATION PRESSURE	=	6000.0	PSF
POISSON RATIO	=	0.35	(ASSUMED)
VALUES MEASURED AT CYCLE(S)		5 & 15	

SYSTEM DEFORMATION CORRECTION CURVE -

LOAD (LB)	0.00	1000.00
DEFM (IN)	0.00000	0.00730

SYSTEM DAMPING CORRECTION CURVE -

LOAD (LB)	0.00	1000.00
DAMP (PCT)	0.000	0.000

DEVIATOR STRESS (PSF)	SINGLE AMPL CYCLIC STRAIN AXIAL (PERCENT)	SHEAR	YOUNGS MODULUS (KSF)	SHEAR MODULUS (KSF)	K	DAMPING RATIO (PERCENT)	SHEAR WAVE VELOCITY (FPS)
60.6	0.0008	0.0011	11095.	4109.	53.0	3.9	995.37
60.1	0.0008	0.0011	11189.	4144.	53.5	4.3	999.60
224.4	0.0022	0.0027	10329.	3826.	49.4	4.0	960.45
224.4	0.0022	0.0027	10329.	3826.	49.4	3.8	960.45
645.1	0.0074	0.0100	8728.	3233.	41.7	4.6	882.86
645.1	0.0074	0.0100	8728.	3233.	41.7	4.4	882.86
1477.7	0.0226	0.0305	6629.	2455.	31.7	7.5	769.41
1464.1	0.0227	0.0306	6463.	2394.	30.9	6.9	759.73
3029.1	0.0790	0.1067	3834.	1420.	18.3	11.0	585.15
2883.3	0.0793	0.1070	3638.	1347.	17.4	10.3	569.90
4539.5	0.2039	0.2752	2223.	823.	10.6	12.9	445.60
4263.2	0.2043	0.2758	2087.	773.	10.0	11.8	431.67
6056.3	0.4108	0.5546	1475.	546.	7.1	12.5	362.91
5744.2	0.4156	0.5610	1382.	512.	6.6	11.3	351.33

WHERE K IS GIVEN BY...K=G/(1000.*SIG3**0.500)

Dames & Moore

PLATE

946.7 (REV. 6-61)

REVISIONS BY DATE

BY DATE

FILE

BY DATE

CHECKED BY

DYNAMIC SOIL PROPERTY TEST 30-JAN-87

TURKEY FLAT TESTING 3995-03 JAN 1987
BG TF-6 #5 @25 FT STAGE 1 S1@3=3 KSF
Brown Sandy Silty Clay (cemented)

INITIAL MOISTURE CONTENT	=	20.5	PERCENT
INITIAL DRY DENSITY	=	102.50	PCF
MOISTURE CONTENT AFTER CONSOL.	=	0.0	PERCENT
DRY DENSITY AFTER CONSOL.	=	104.00	PCF
SAMPLE HEIGHT AFTER CONSOL.	=	6.46	IN
SAMPLE DIAMETER AFTER CONSOL.	=	2.86	IN
CONSOLIDATION PRESSURE	=	3000.0	PSF
POISSON RATIO	=	0.35	(ASSUMED)

VALUES MEASURED AT CYCLE(S) 5 & 15

SYSTEM DEFORMATION CORRECTION CURVE -

LOAD (LB)	0.00	1000.00
DEFM (IN)	0.00000	0.00730

SYSTEM DAMPING CORRECTION CURVE -

LOAD (LB)	0.00	1000.00
DAMP (PCT)	0.000	0.000

DEVIATOR STRESS (PSF)	SINGLE AMPL CYCLIC STRAIN AXIAL (PERCENT)	SHEAR	YOUNGS MODULUS (KSF)	SHEAR MODULUS (KSF)	K	DAMPING RATIO (PERCENT)	SHEAR WAVE VELOCITY (FPS)
47.3	0.0007	0.0007	7158.	2651.	175.4	4.4	906.03
48.1	0.0007	0.0007	6978.	2584.	170.9	4.6	894.51
135.4	0.0021	0.0029	6313.	2338.	154.6	4.2	850.82
135.4	0.0021	0.0029	6313.	2338.	154.6	4.5	850.82
403.0	0.0071	0.0098	5707.	2114.	139.8	4.8	808.90
397.4	0.0071	0.0096	5605.	2076.	137.3	4.5	801.71
923.5	0.0216	0.0292	4275.	1584.	104.7	7.8	700.20
901.1	0.0217	0.0293	4150.	1537.	101.7	7.3	689.86
2524.2	0.0734	0.0991	3439.	1274.	84.2	11.6	627.99
2490.6	0.0731	0.0986	3409.	1263.	83.5	9.8	625.22
2865.6	0.1870	0.2525	1532.	567.	37.5	11.7	419.16
2664.1	0.1883	0.2542	1415.	524.	34.7	11.0	402.77

WHERE K IS GIVEN BY... K=G/SU
AND SU=UNDRAINED SHEAR STRENGTH =15119.0 (PSF)

Dames & Moore

PLATE

946.7 (REV. 6-61)

REVISIONS BY DATE

BY DATE

FILE

BY DATE

CHECKED BY

DYNAMIC SOIL PROPERTY TEST 30-JAN-87

TURKEY FLAT TESTING 3995-03 JAN 1987
BG TF-6 #5 @25 FT STAGE 2 SIG3=6 KSF
Brown Sandy Silty Clay (cemented)

INITIAL MOISTURE CONTENT	=	0.0	PERCENT
INITIAL DRY DENSITY	=	104.00	PCF
MOISTURE CONTENT AFTER CONSOL.	=	20.3	PERCENT
DRY DENSITY AFTER CONSOL.	=	104.50	PCF
SAMPLE HEIGHT AFTER CONSOL.	=	6.45	IN
SAMPLE DIAMETER AFTER CONSOL.	=	2.86	IN
CONSOLIDATION PRESSURE	=	6000.0	PSF
POISSON RATIO	=	0.35	(ASSUMED)

VALUES MEASURED AT CYCLE(S) 5 & 15

SYSTEM DEFORMATION CORRECTION CURVE -

LOAD (LB)	0.00	1000.00
DEFM (IN)	0.00000	0.00230

SYSTEM DAMPING CORRECTION CURVE -

LOAD (LB)	0.00	1000.00
DAMP (PCT)	0.000	0.000

DEVIATOR STRESS (PSF)	SINGLE AMPL CYCLIC STRAIN AXIAL (PERCENT)	SHEAR	YOUNGS MODULUS (KSF)	SHEAR MODULUS (KSF)	K	DAMPING RATIO (PERCENT)	SHEAR WAVE VELOCITY (FPS)
71.9	0.0007	0.0009	10560.	3911.	258.7	4.1	1000.87
69.6	0.0007	0.0009	10473.	3879.	256.6	4.9	996.70
204.3	0.0020	0.0027	10114.	3746.	247.8	3.9	979.51
204.3	0.0020	0.0027	10114.	3746.	247.8	3.8	979.51
617.5	0.0068	0.0091	9120.	3378.	223.4	3.7	930.13
617.5	0.0067	0.0091	9172.	3397.	224.7	4.0	932.81
1560.6	0.0204	0.0278	7654.	2835.	187.5	6.2	852.17
1567.6	0.0204	0.0276	7500.	2778.	183.7	5.7	843.50
3469.4	0.0712	0.0962	4870.	1804.	119.3	9.6	679.77
3523.4	0.0715	0.0965	4650.	1722.	113.9	9.3	664.19
5776.1	0.1818	0.2454	3150.	1167.	77.2	10.4	546.68
5344.4	0.1824	0.2462	2930.	1085.	71.8	10.4	527.21
6420.8	0.3703	0.5000	2274.	842.	55.7	8.8	464.44
7059.4	0.3712	0.5012	2117.	784.	51.9	8.7	448.15

WHERE K IS GIVEN BY... K=G/SU
AND SU=UNDRAINED SHEAR STRENGTH =15119.0 (PSF)

Dames & Moore

PLATE

946.7 (REV. 6-61)

REVISIONS BY DATE

BY DATE FILE

BY DATE

CHECKED BY

946.7 (REV. 6-61)

DYNAMIC SOIL PROPERTY TEST 2-FEB-87

TURKEY FLAT TESTING 3995-03 JAN 1987
RG TF-6 #9 @ 40 FT STAGE 1 SIG3=2.4 KSF

Brown Sandy Silty Clay (cemented)

INITIAL MOISTURE CONTENT	=	25.5	PERCENT
INITIAL DRY DENSITY	=	95.30	PCF
MOISTURE CONTENT AFTER CONSOL.	=	0.0	PERCENT
DRY DENSITY AFTER CONSOL.	=	96.30	PCF
SAMPLE HEIGHT AFTER CONSOL.	=	5.96	IN
SAMPLE DIAMETER AFTER CONSOL.	=	2.87	IN
CONSOLIDATION PRESSURE	=	2400.0	PSF
POISSON RATIO	=	0.35	(ASSUMED)

VALUES MEASURED AT CYCLE(S) 5 & 15

SYSTEM DEFORMATION CORRECTION CURVE -

LOAD (LB)	0.00	1000.00
DEFM (IN)	0.00000	0.00230

SYSTEM DAMPING CORRECTION CURVE -

LOAD (LB)	0.00	1000.00
DAMP (PCT)	0.000	0.000

DEVIATOR STRESS (PSF)	SINGLE AMPL CYCLIC STRAIN AXIAL (PERCENT)	SHEAR	YOUNGS MODULUS (KSF)	SHEAR MODULUS (KSF)	K	DAMPING RATIO (PERCENT)	SHEAR WAVE VELOCITY (FPS)
53.3	0.0008	0.0011	6762.	2505.	158.3	3.1	915.13
53.3	0.0008	0.0011	6762.	2505.	158.3	2.5	915.13
138.8	0.0023	0.0031	6045.	2239.	141.5	3.1	865.17
139.9	0.0023	0.0031	6087.	2254.	142.5	2.8	868.27
366.7	0.0077	0.0104	5039.	1866.	118.0	4.2	789.94
366.7	0.0077	0.0104	5039.	1866.	118.0	4.2	789.94
744.1	0.0234	0.0316	4034.	1494.	94.4	7.4	706.70
733.0	0.0235	0.0317	3976.	1473.	93.1	6.8	701.67
1954.9	0.0797	0.1076	2454.	909.	57.4	12.3	551.24
1868.2	0.0798	0.1077	2367.	877.	55.4	11.3	541.37
3243.3	0.2020	0.2727	1605.	595.	37.6	12.2	445.87
3110.0	0.2023	0.2731	1538.	569.	36.0	11.3	436.37

WHERE K IS GIVEN BY... K=G/SU
AND SU=UNDRAINED SHEAR STRENGTH =15819.0 (PSF)

Dames & Moore

PLATE

DYNAMIC SOIL PROPERTY TEST 2-FEB-87

TURKEY FLAT TESTING 3995-03 JAN 1987
BC TF-6 #9 @ 40 FT STAGE 2 SIG3=4.8 KSF
Brown Sandy Silty Clay (cemented)

INITIAL MOISTURE CONTENT	=	0.0	PERCENT
INITIAL DRY DENSITY	=	96.30	PCF
MOISTURE CONTENT AFTER CONSOL.	=	25.3	PERCENT
DRY DENSITY AFTER CONSOL.	=	96.60	PCF
SAMPLE HEIGHT AFTER CONSOL.	=	5.95	IN
SAMPLE DIAMETER AFTER CONSOL.	=	2.87	IN
CONSOLIDATION PRESSURE	=	4800.0	PSF
POISSON RATIO	=	0.35	(ASSUMED)

VALUES MEASURED AT CYCLE(S) 5 & 15

SYSTEM DEFORMATION CORRECTION CURVE -

LOAD (LB)	0.00	1000.00
DEFN (IN)	0.00000	0.00200

SYSTEM DAMPING CORRECTION CURVE -

LOAD (LB)	0.00	1000.00
DAMP (PCT)	0.000	0.000

DEVIATOR STRESS (PSF)	SINGLE AMPL CYCLIC STRAIN AXIAL (PERCENT)	SHEAR	YOUNGS MODULUS (KSF)	SHEAR MODULUS (KSF)	K	DAMPING RATIO (PERCENT)	SHEAR WAVE VELOCITY (FPS)
75.7	0.0008	0.0011	9256.	3428.	216.7	3.6	954.98
75.7	0.0008	0.0011	9256.	3428.	216.7	2.8	954.98
173.7	0.0022	0.0030	8621.	3193.	201.8	3.0	921.68
174.8	0.0022	0.0030	8678.	3214.	203.2	2.7	924.60
367.2	0.0074	0.0100	7615.	2820.	178.3	3.4	866.20
367.2	0.0074	0.0100	7615.	2820.	178.3	3.3	866.20
1436.1	0.0223	0.0301	6443.	2386.	150.9	5.4	796.77
1436.1	0.0223	0.0301	6443.	2386.	150.9	5.6	796.77
3295.3	0.0774	0.1046	4255.	1576.	99.6	10.2	647.40
3278.5	0.0776	0.1047	4162.	1542.	97.5	9.6	640.41
5392.4	0.1985	0.2680	2720.	1007.	63.7	11.7	517.64
5243.5	0.1988	0.2684	2637.	977.	61.7	11.1	509.77
7601.6	0.4025	0.5434	1908.	707.	44.7	9.8	433.64
7176.0	0.4035	0.5447	1766.	654.	41.3	9.3	417.13

WHERE K IS GIVEN BY... K=G/SU
AND SU=UNDRAINED SHEAR STRENGTH =15819.0 (PSF)

REVISIONS BY DATE

BY DATE FILE

CHECKED BY DATE

946.7 (REV. 6-61)

Dames & Moore

PLATE

APPENDIX D
Harding Lawson Associates

TWO PARTS:

1) **Radioactive Logging, and**
2) **Crosshole Velocity Surveys**

PART 1
RADIOACTIVE LOGGING

Appendix D

Harding Lawson Associates

Radioactive Logging

The logging tool used is a gamma-gamma "4-pi" device. That is, it is not focussed, but reads back scattered gamma radiation from a sphere of material surrounding the detector. As such, the log's measure of gamma radiation is affected by the position (centered, diagonal, sidewall) of the probe in the borehole. It was assumed that the probe had been pressed against the sidewall, especially in the lower half of the well bore as the boring was not drilled perfectly vertical. Calibration measurements, therefore, were taken with the probe pressed against the sidewall. Calibration was as follows.

The standard used was a 40 gallon drum filled with concrete having a 3 inch diameter PVC casing within. The concrete density was calculated to be 2.35 g/cm^3 from mass-volume considerations, and 2.33 g/cm^3 from a sample of concrete. Radiation measurements were made with water. A total of 4 calibration curves are plotted taking into consideration long-short spacing and dry-saturated inside casing conditions (see semi-log plot, figure 1).

The curve that probably has any relevance is the saturated-long spacing curve. The bulk density for sandstone (measured in borehole TF-8) is calculated to be 2.34 g/cm^3 (N=1500 cps, figure 2). This is a general average that is valid below the water table.

Figures 3 and 4 show natural-gamma and gamma-gamma logs for boreholes TF-2 and TF-5 respectively. They show only relative variations in the sediments or the grouting material. Because the boreholes are cased, the gamma-gamma logs for these boreholes reflect density changes in the backfill and casing as well. Consequently, these records cannot be used to estimate sediment density.

CALIBRATION CURVES
Bulk Density

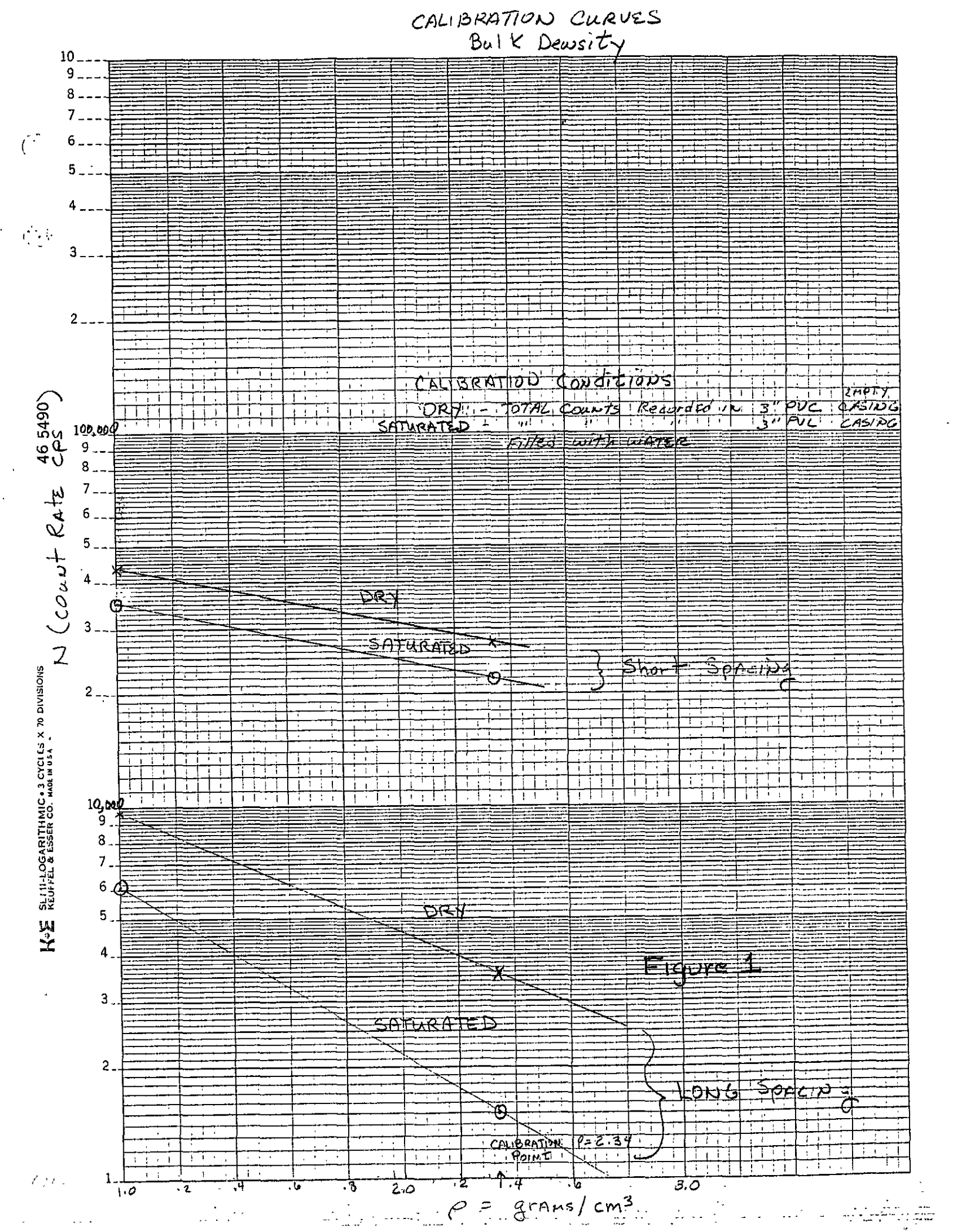

Figure 1

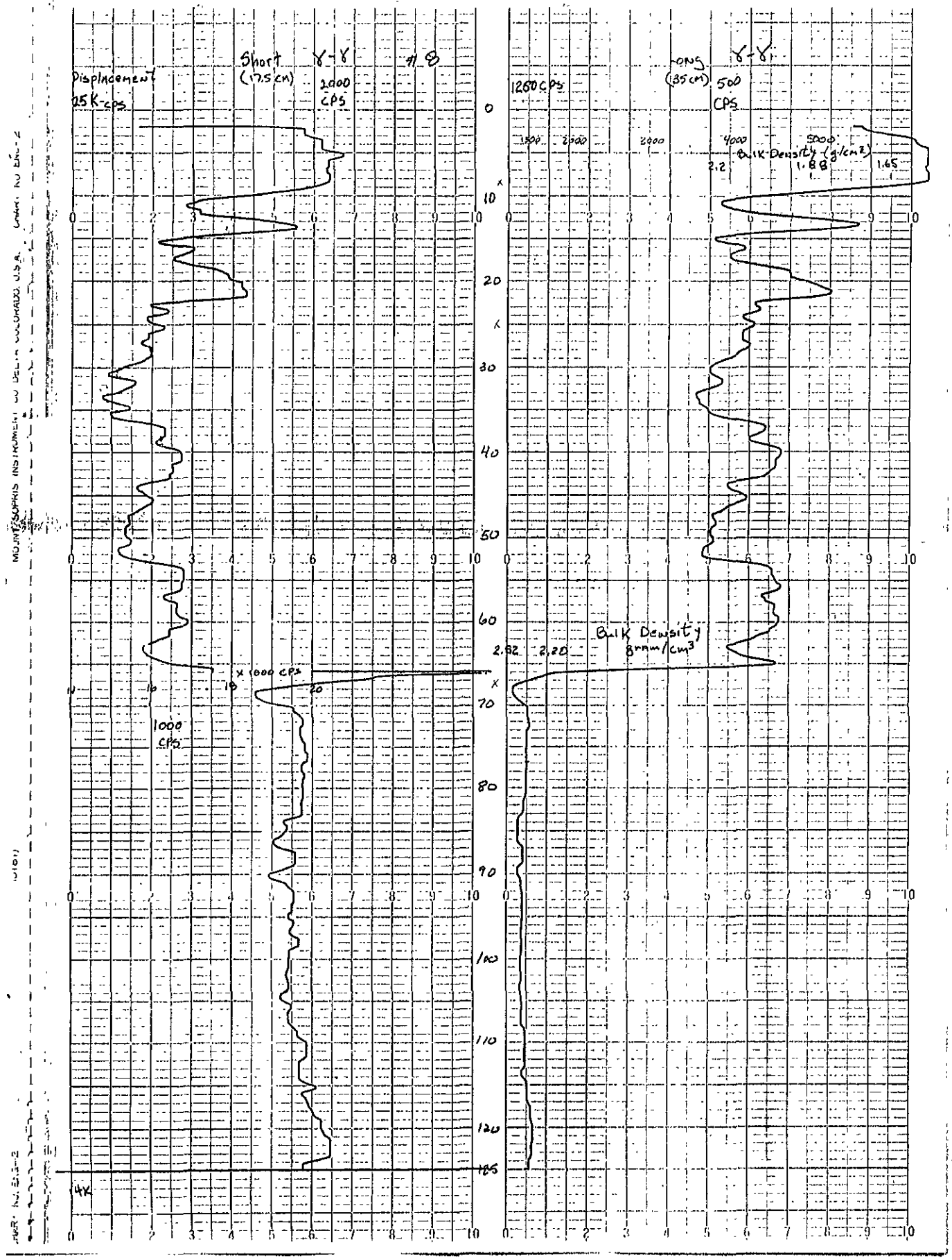
Displacement
25K-cps
Short γ-γ
(17.5 cm)
2000
CPS
#8
1000
CPS
X 1000 CPS
14K
Long γ-γ
(35 cm)
500
CPS
1200 CPS
Bulk Density (g/cm³)
2.2
1.88
1.65
Bulk Density
2.62
2.20
8 mm/cm³

Figure 2.

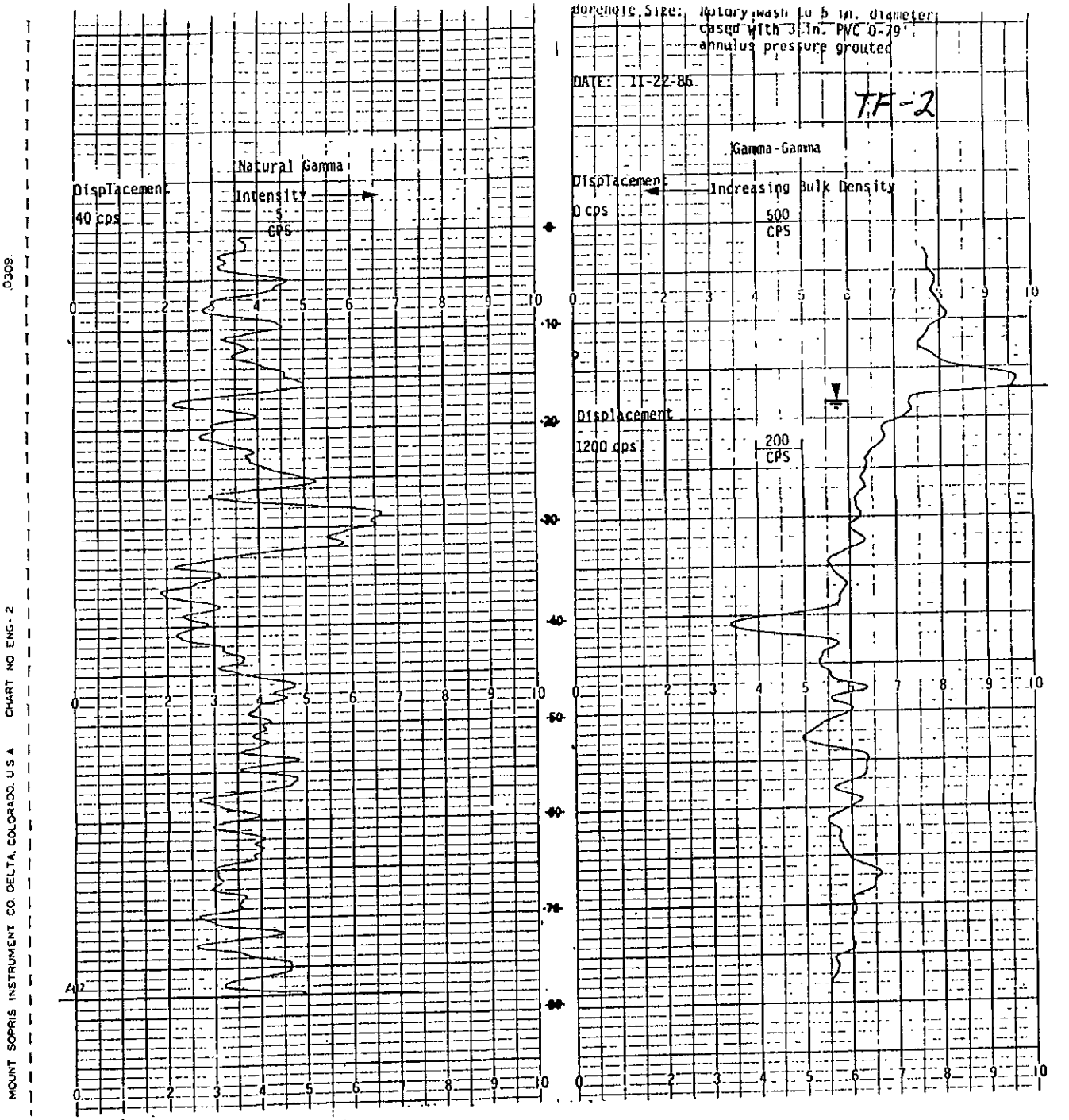
Borehole Size: Rotary wash to 6 in. diameter
cased with 3 in. PVC 0-79'
annulus pressure grouted
DATE: 11-22-86
TF-2
Natural Gamma
Intensity
5
CPS
Displacement
40 cps
0
Gamma-Gamma
Displacement
Increasing Bulk Density
0 cps
500
CPS
Displacement
1200 cps
200
CPS
MOUNT SOPRIS INSTRUMENT CO. DELTA, COLORADO, U.S.A. CHART NO ENG-2
0308

Figure 3

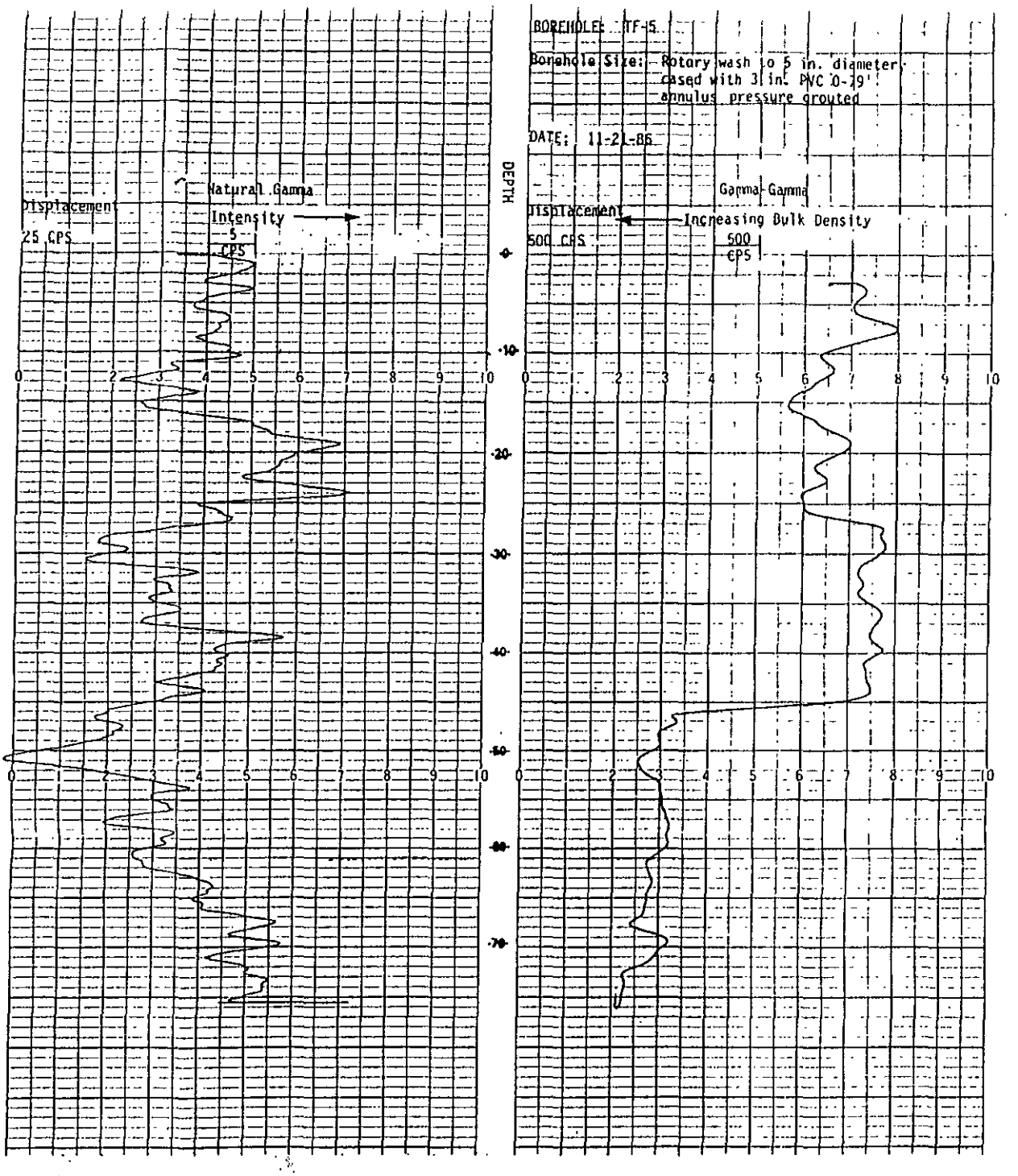
BOREHOLE: TF-5
Borehole Size: Rotary wash to 5 in. diameter cased with 3 in. PVC 0-79' annulus pressure grouted
DATE: 11-21-86
Natural Gamma
Displacement
Intensity
25 CPS
5
CPS
Gamma-Gamma
Displacement
Increasing Bulk Density
500 CPS
500
CPS
DEPTH
0
10
20
30
40
50
60
70

Figure 4

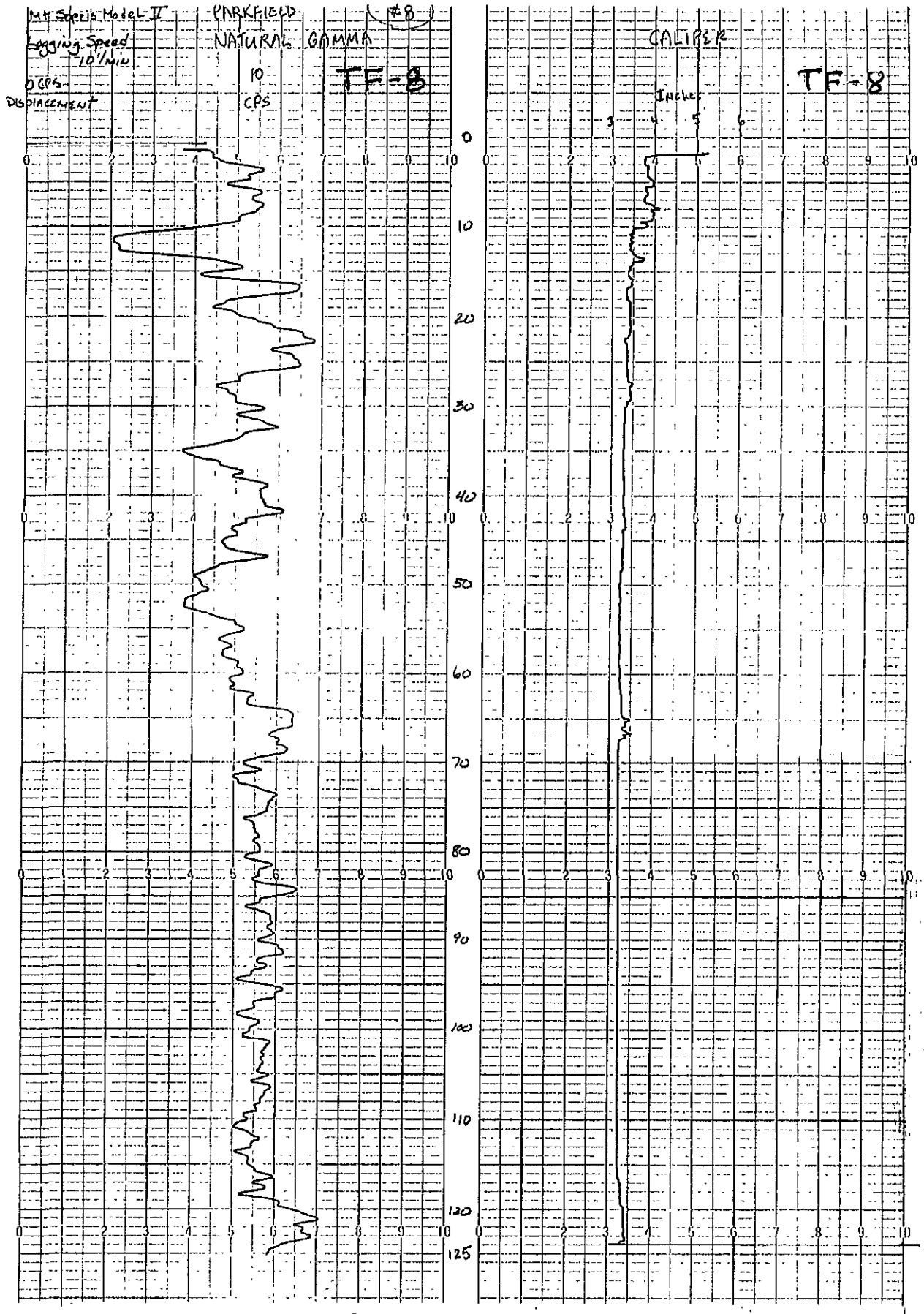
MT Sopris Model II
Logging Speed 10'/min
0 CPS
DISPLACEMENT
PARKFIELD
#8
NATURAL GAMMA
10
CPS
TF-8
CALIPER
INCHES
TF-8

Figure 5

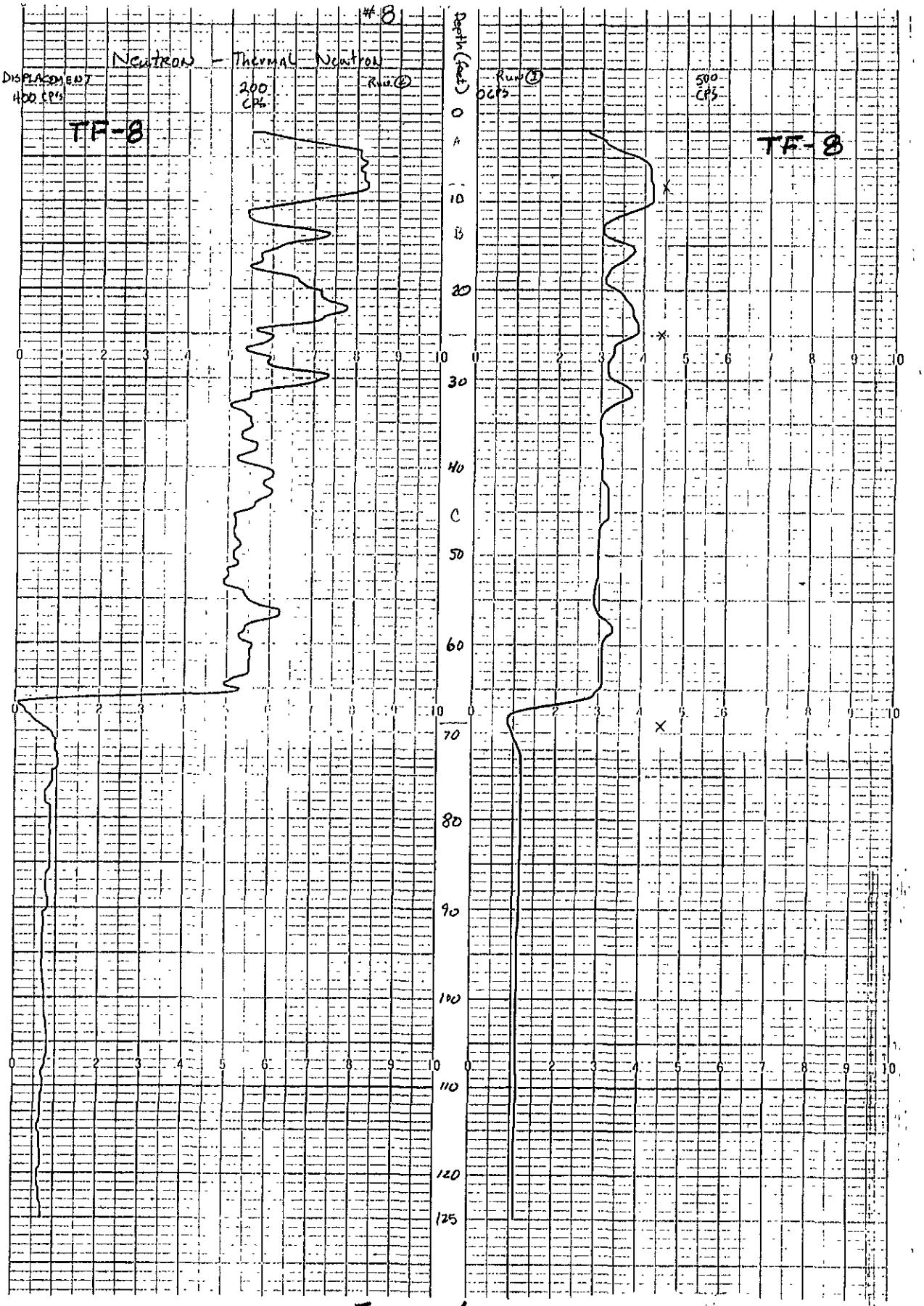
#8
Neutron – Thermal Neutron
DISPLACEMENT
400 CPS
200 CPS
Run ②
TF-8
Depth (feet)
0
A
10
B
20
30
40
C
50
60
70
80
90
100
110
120
125
Run ①
0 CPS
500 CPS
TF-8
MOUNT SOPRIS INSTRUMENT CO. DELTA COLORADO, U.S.A.
CHART NO ENG-2
(0181)

Figure 6

PART 2
CROSSHOLE VELOCITY SURVEYS

Harding Lawson Associates

March 16, 1987

Charles R. Real
Department of Conservation
Division of Mines & Geology
Sacramento District Office
Sacramento, CA 95814

Dear Chuck:

Enclosed is a table summarizing my cross-hole velocity survey at Parkfield, California. Qualitatively, data from Borehole TF-4 is not as good as TF-5, as TF-4 contained 5-inch-diameter casing which made coupling of the triaxial geophone very difficult. I was presented with a multitude of choices for S-wave arrival times for TF-2. We generally are confident of P-wave velocities, then count on Poisson's Ratio (1.9) to sight in on the most probable S-wave velocities for a given interval in hard rock (sandstone). However, in this case Poisson Ratios are high (2.5 to 3.0) for the reported velocities. Despite the fact TP-2 is in hard rock, we have seen departures from the ideal Poisson Ratio for hard rock in past surveys. Surficial rock formations generally exhibit wide variations in terms of dynamic moduli values, especially if the rock has been stressed and fractured. An added difficulty is the survey method itself which, because of variables such as source-receiver coupling, P-S wave mode conversion, and randomized geophone orientations make S-wave arrivals uncertain.

Please pass on my regards to Bruce Redpath. If there is anything else you need please let me know.

Yours very truly,

HARDING LAWSON ASSOCIATES

William J. Henrich
Senior Geophysicist

WJH/mg

Enclosure

PARKFIELD CROSS-HOLE SEISMIC VELOCITIES

DEPTH (FEET)	HORIZONTAL DISTANCE (FEET)	BOREHOLE ARRIVAL P-WAVE (MS)	TF-5 TIME S-WAVE (MS)	SEISMIC P-WAVE (FPS)	VELOCITY S-WAVE (FPS)	HORIZONTAL DISTANCE (FEET)	ARRIVAL P-WAVE (MS)	BOREHOLE TIME S-WAVE (MS)	TF-4 SEISMIC P-WAVE (FPS)	VELOCITY S-WAVE (FPS)
15	25.6	0.0	0.0	ERR	ERR	20.0	10.0	19.0	2000.0	1052.6
20	25.7	8.2	15.5	3134.1	1658.1	20.0	5.5	11.7	3636.4	1709.4
25	25.8	6.0	12.5	4300.0	2064.0	19.9	7.0	11.0	2842.9	1809.1
30	26.0	7.0	12.5	3714.3	2080.0	19.7	6.0	10.5	3283.3	1876.2
35	26.1	8.0	12.5	3262.5	2088.0	19.7	7.0	10.0	2814.3	1970.0
40	26.2	6.7	11.2	3910.4	2339.3	19.7	5.5	10.0	3581.8	1970.0
50	26.4	7.5	11.6	3520.0	2275.9	19.6	6.0	10.5	3266.7	1866.7
55	26.4	5.5	10.5	4800.0	2514.3	19.6	4.5	8.0	4355.6	2450.0
60	26.5	6.0	12.0	4416.7	2208.3	19.7	6.5	11.5	3030.8	1713.0
70	26.5	4.5	9.3	5888.9	2849.5	19.8	3.0	6.2	6600.0	3193.5
75	26.5	3.0	9.0	8833.3	2944.4	19.8	2.5	4.2	7920.0	4714.3

	BOREHOLE TF-2				
10.0	23.1	4.0	10.0	5775.0	2310.0
20.0	23.3	3.0	10.0	7766.7	2330.0
30.0	23.5	2.0	6.2	11750.0	3790.3
40.0	23.7	2.0	6.0	11850.0	3950.0
50.0	24.0	2.2	7.0	10909.1	3428.6
60.0	24.1	2.5	7.5	9640.	3213.3
70.0	24.2	2.2	7.0	11000.0	3457.1
75.0	24.3	2.2	6.2	11045.5	3919.4

APPENDIX E
Kajima Corporation

Evaluation of Q-Values obtained at Turkey Flat Near Parkfield, California, USA

Tokiharu Ohta[1], Katsuya Takahashi[2], Hiroshi Ishida[3],
Tomonori Ikeura[3], Ryuji Kubota[4],
Brian E. Tucker[5], Charles R. Real[6], and Chris H. Cramer[7]

1. Introduction

In November 1986, geotechnical investigations have been performed at Turkey Flat, California, USA, for the workshop of the effects of surface geology on seismic motion. For this task, P-S loggings for four boreholes were carried out by California Division of Mines and Geology (CDMG). Before these investigations were executed, Kajima Institute of Construction Technology (KICT), Japan, proposed to evaluate Q-values from the data of S-wave loggings obtained by CDMG. Consequently, KICT and CDMG agreed on a plan of collaboration for the Q-value investigations. This report describes the evaluation method and results of the Q-values for S-wave of Turkey Flat.

Locations of the S-wave loggings are shown in Fig. 1, and description of test holes are shown in Table 1.

2. Analytical method

The flow of this method to estimate the Q-values is as shown in Fig. 2.

2.1 S-wave logging

A specific S-wave logging is carried out to evaluate the changes of S-waves travelling vertically in the ground. In this logging, measurements are made with two geophones. During the measurements, one is placed close to the top of a borehole as a reference point and the other is moved in the hole at appropriate intervals. For each shot, the ground motions in two horizontal components are measured simultaneously at these two points without saturation.

2.2 Synthesis of S-wave

An S-wave motion is synthesized from two horizontal components of ground motions at each point. The direction, in which amplitude of synthesized S-wave is the maximum, is found in the particle orbit which is made from two horizontal components of measured ground motions. This direction is used as the direction of S-wave motion to synthesize waveform for each measurement. This process is conducted for records both at the reference point and at the measurement point in the hole.

2.3 Calculation of Fourier amplitude spectrum of S-wave

Fourier amplitude spectra of direct S-waves are calculated. To extract the portion of the direct S-wave from the synthesized one, the synthesized S-wave motion is multiplied by a time window of Gaussian type, of which gravity center is adjusted at the first zero crossing time point in the synthesized S-wave.

---

1) D.Eng., Chief Research Engineer, Kajima Institute of Construction Technology (KICT), Japan
2) Senior Research Engineer, KICT
3) Research Engineer, KICT
4) D.Sc., Seismic Processing Center of Kawasaki Geotechnical Engineering Co., Ltd.
5) Ph.D., Acting State Geologist, California Division of Mines and Geology (CDMG), USA
6) M.Sc., Senior Seismologist, CDMG
7) Ph.D., Associate Seismologist, CDMG

2.4 Calculation of spectral ratio

A ratio of the Fourier amplitude spectrum of S-wave in the hole to that of the reference point is calculated for each measurement. Since this spectral ratio is a normalized amplitude of direct S-wave, it is independent of strength of the generated wave from the source. Therefore, changes of the spectral ratios in vertical direction can be regarded as those of amplitude spectra of transfer functions for S-wave which travels downward in the ground.

2.5 Evaluation of attenuation of S-wave due to Q-value

Theoretical variations of amplitude of travelling S-wave in the ground due to transmission coefficients of boundaries and geometrical spreading of spherical wave from the point source in the multi-layered subsoil model are calculated by using informations regarding subsoil structure, such as thickness, density and S-wave velocity of layers, and the arrangement of the source and two geophones. Attenuation due to Q-value is evaluated by eliminating the theoretical variations of S-wave amplitude from the variations of the spectral ratio calculated from S-wave records.

Estimation of Q-values is performed by using the structure of the S-wave velocity and the soil weight per unit volume. In this method, the reliability of analytical results is dependent on the accuracy of parameters of subsoil structure and the validity of the assumption that the ground structure is a multi-layered medium. Therefore, it is possible that the analytical results may change sensitively, if the parameters are altered.

3. Results

3.1 Analytical Conditions

(1) Parameters of subsoil structure

Parameters of subsoil structure for four boreholes are shown in Fig. 3. The structure of S-wave velocity by the S-wave logging has been provided by CDMG, and that of the soil weight per unit volume was estimated empirically by KICT with reference to the boring logs for each borehole.

(2) Source Configuration

S-waves are originated by a single hammer blow on an end of a wooden plank at each measurement. The standard source configuration, which has been provided by CDMG, is shown in Fig. 4.

3.2 Results

The Q-values in the specified layer were obtained at 4.9 Hz frequency intervals from two sets, each from a hammer blow on each end of the plank, of S-wave records per borehole. Damping ratios h(=1/(2Q)) are shown in Figs. 5 to 8 with the normalized Fourier amplitudes of weighted synthesized records. The frequency ranges to be noted and values of 1/(2Q) evaluated in these ranges are also shown in these figures: Results of four boreholes are summarized in Table 2 and Fig. 9.

4. Conclusion

It can be seen from Fig. 8 and Table 2 that the results obtained from two sets of records for the hole #6 disagree both in magnitude and in frequency-dependency. Accordingly, they can be considered to be unreliable.

When considering the correspondence of Q-values to the S-wave velocity, Q-values of the high S-wave velocity layer and the low one can be estimated from the results of holes #1 and #6. The Q-values obtained by averaging the two values for each hole are shown in Table 3.

These results are considered to be useful for estimating Q-values of other similar layers. However, Q-values of the surface layer with the S-wave velocity of 130-220 m/s could not be estimated in this analysis. Since the estimated Q-values are very large for the layers of such S-wave velocities, it is necessary to compare these results with those of other investigations.

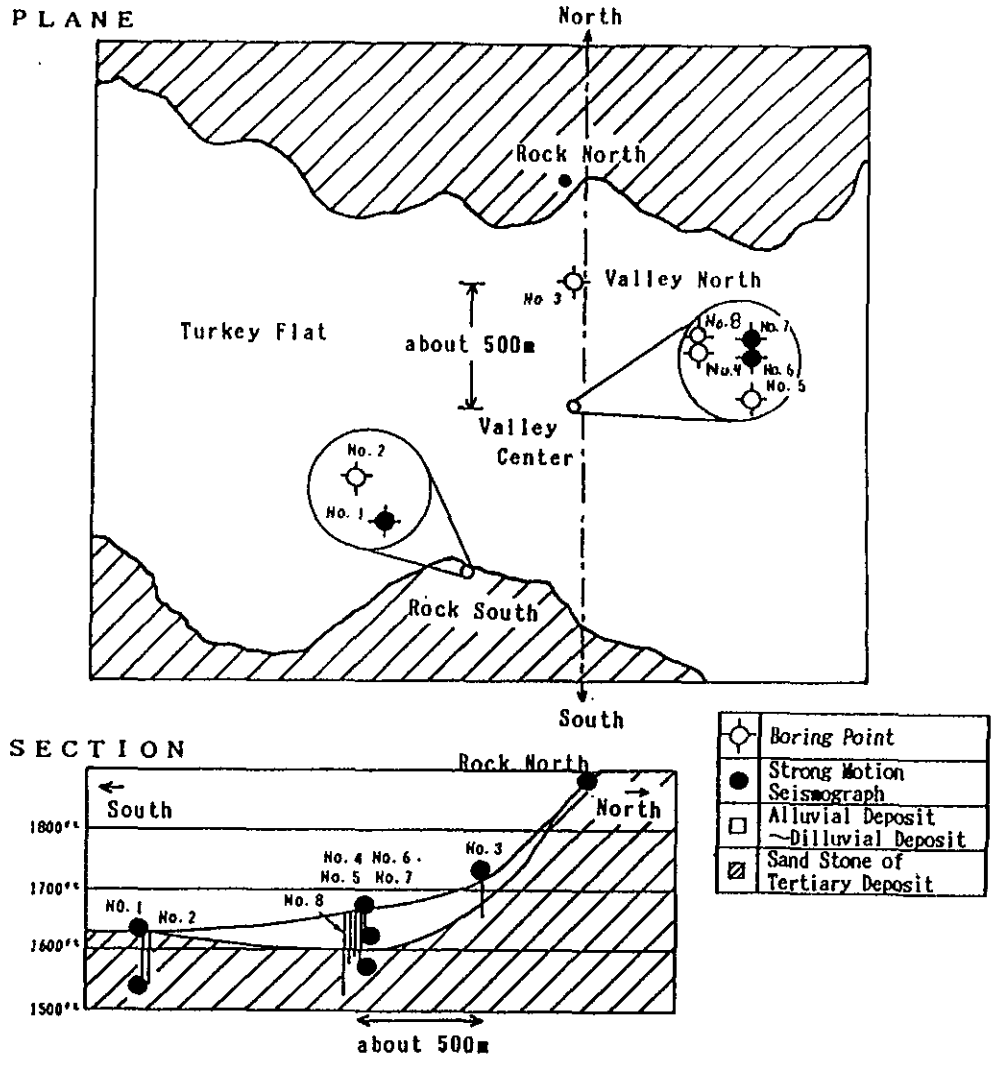

Description of Instrument and Test Borings

No.	Purpose	Depth (ft)	Diameter (inches)	Casing (inches)	Backfill
1	Test & Sensor	82	9	5-PVC	Pea Gravel[2]
2	Test	80	6	3.34-SINCO	Grout[1]
3	Test	47	9	5-PVC	Pea Gravel[2]
4	Test	73	8	5-PVC	Pea Gravel
5	Test	78	6	3.34-SINCO	Grout[1]
6	Test & Sensor	79	9	5-PVC	Pea Gravel[2]
7	Sensor	35	8	5-PVC	Pea Gravel
8	Test	132	3 1/8	Uncased	[2]

[1] A mixture of 5 parts cement to 1 part bentonite.
[2] A 3/4" piezometer tube installed in annulus.

Figure 1

1. S-wave logging

Two horizontal components of ground motions are measured at each point (Fig.1a).

2. Synthesis of S-wave

The direction of S-wave motion is determined from the particle orbit of horizontal ground motions (Fig.1b). An S-wave motion is synthesized from the records using the determined direction (Fig.1c).

3. Calculation of Fourier amplitude spectrum of S-wave

Fourier amplitude spectrum of S-wave is calculated by FFT (Fig.1e). To extract a direct wave, a part of first motion is enhanced by a Gaussian window (broken line in Fig.c) before FFT (Fig.1d).

4. Calculation of spectral ratio

Spectral ratio of S-waves of the measurement point in the hole to that of the reference point is calculated (Fig.1f).

The procedures from 1 to 4 is performed for all measurements which are made at given depth intervals.

5. Evaluation of Attenuation curve due to Q-value

Variation in Fourier amplitude with depth (solid circle in Fig.1g) is compared with theoretical variation which is due to transmission coefficient and geometrical spreading from the point source on the surface (solid lines in Fig.1g).

The difference between the analytical curve and the theoretical one corresponds to the attenuation due to Q-value (Fig.1h).

6. Evaluation of Q-values

The inclination of the attenuation curve (Fig.1h) is evaluated by Least Square Method. Damping ratio and Q-value are obtained from its result.

The procedures of 5 and 6 are performed at each frequency.

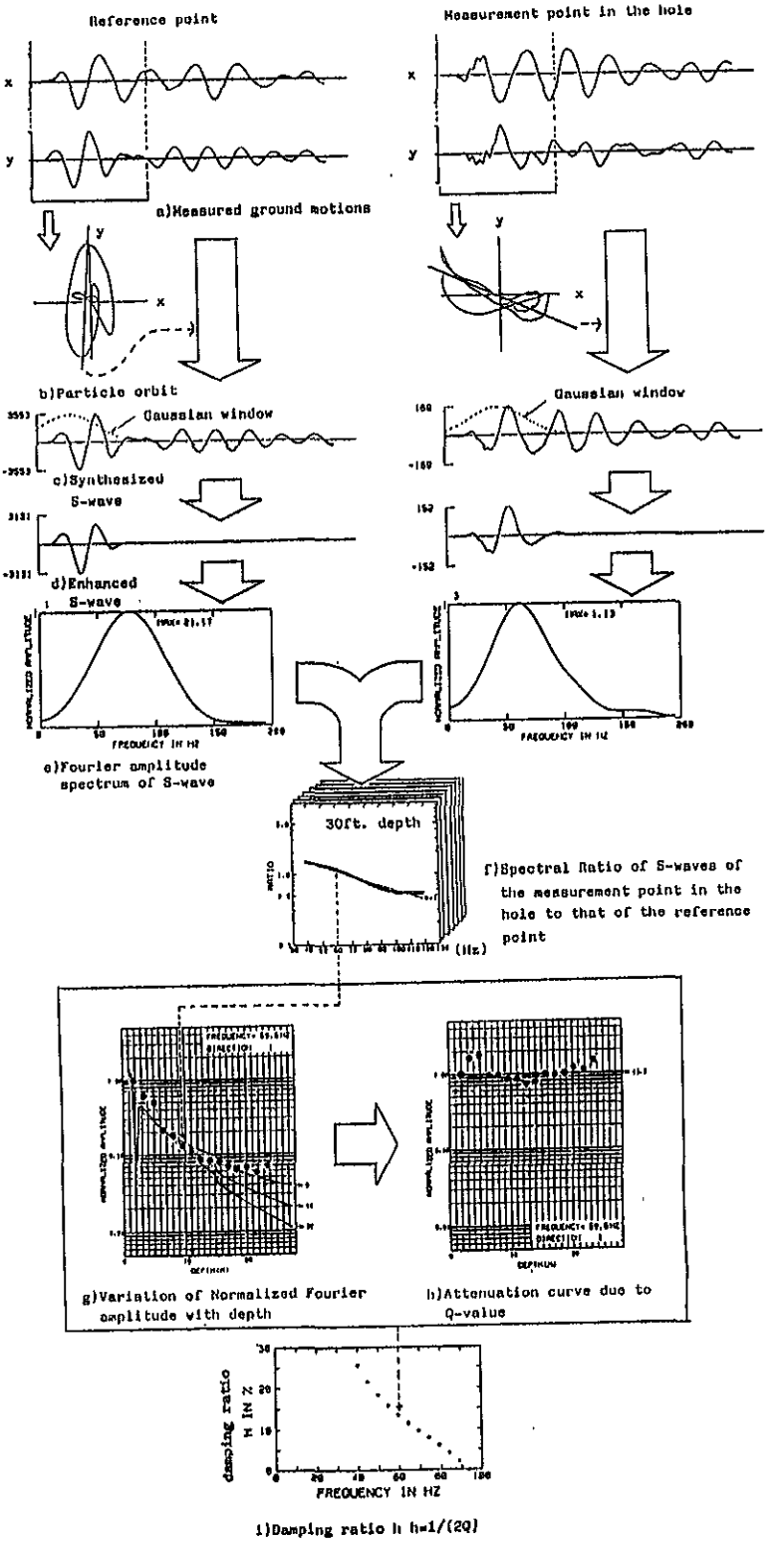

Fig.2 Flow of the Method

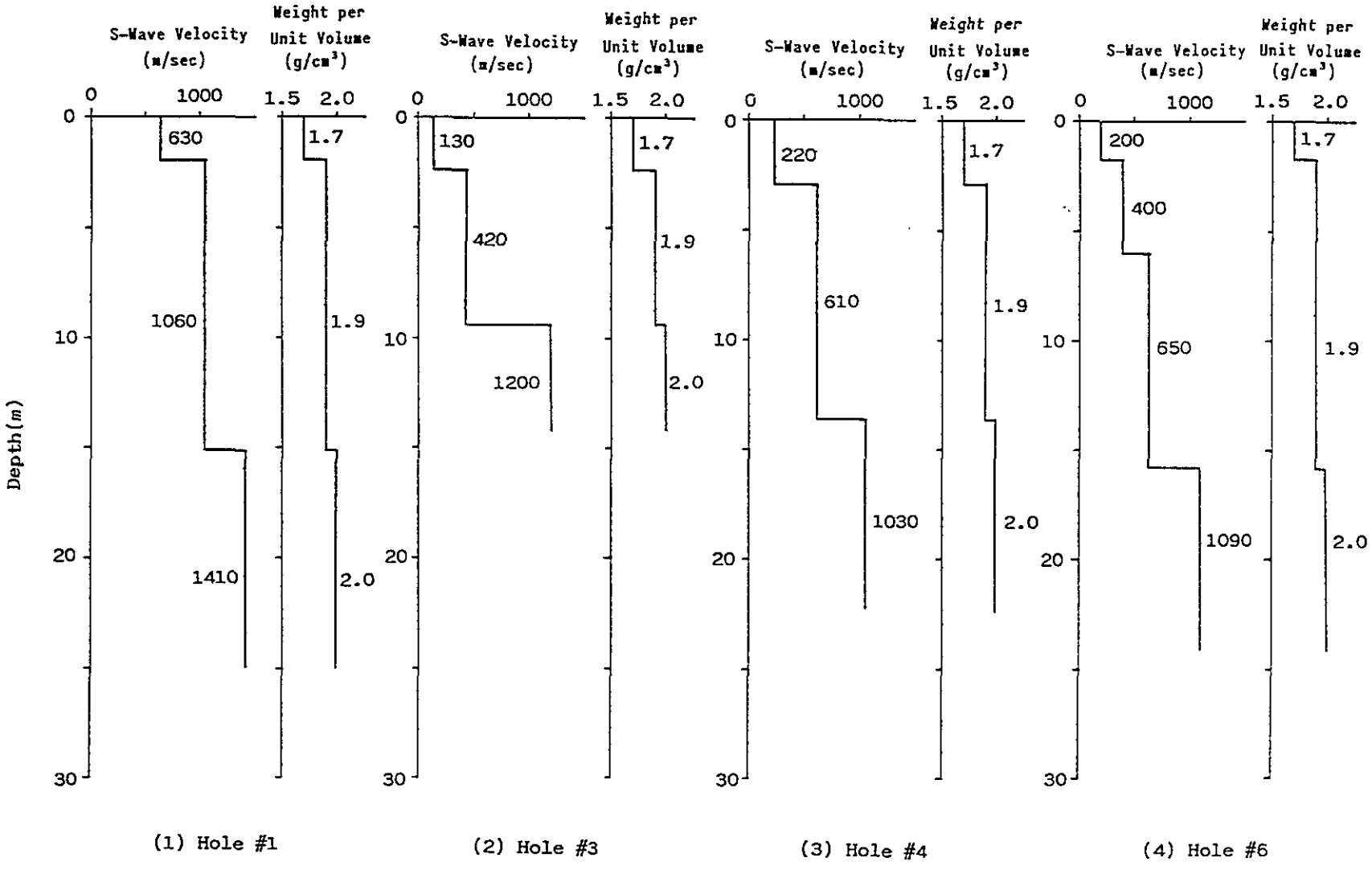

Fig. 3 Parameters of Subsoil Structure for Four Boreholes

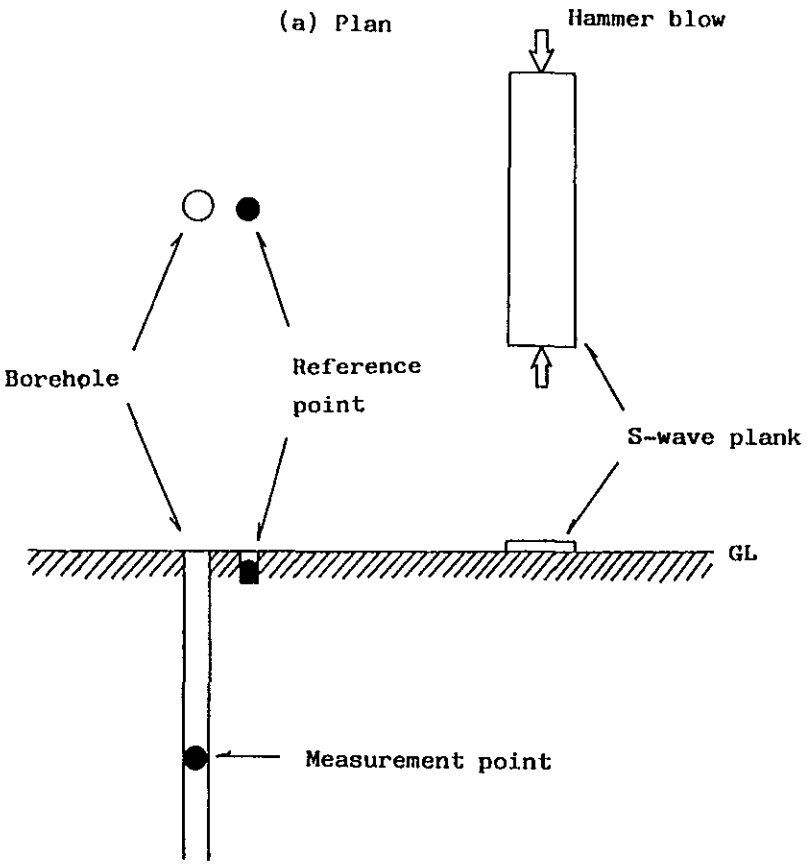

Fig. 4 Standard Source Configuration

Distance between the top of the borehole and the S-wave plank is about 3.05 meters (10 feet).

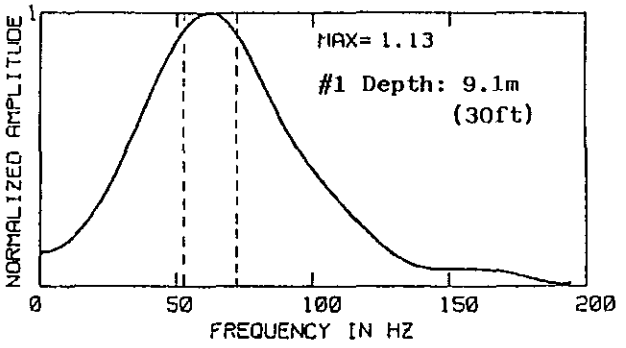

Normalized Fourier Amplitude of the Weighted Synthesized Record

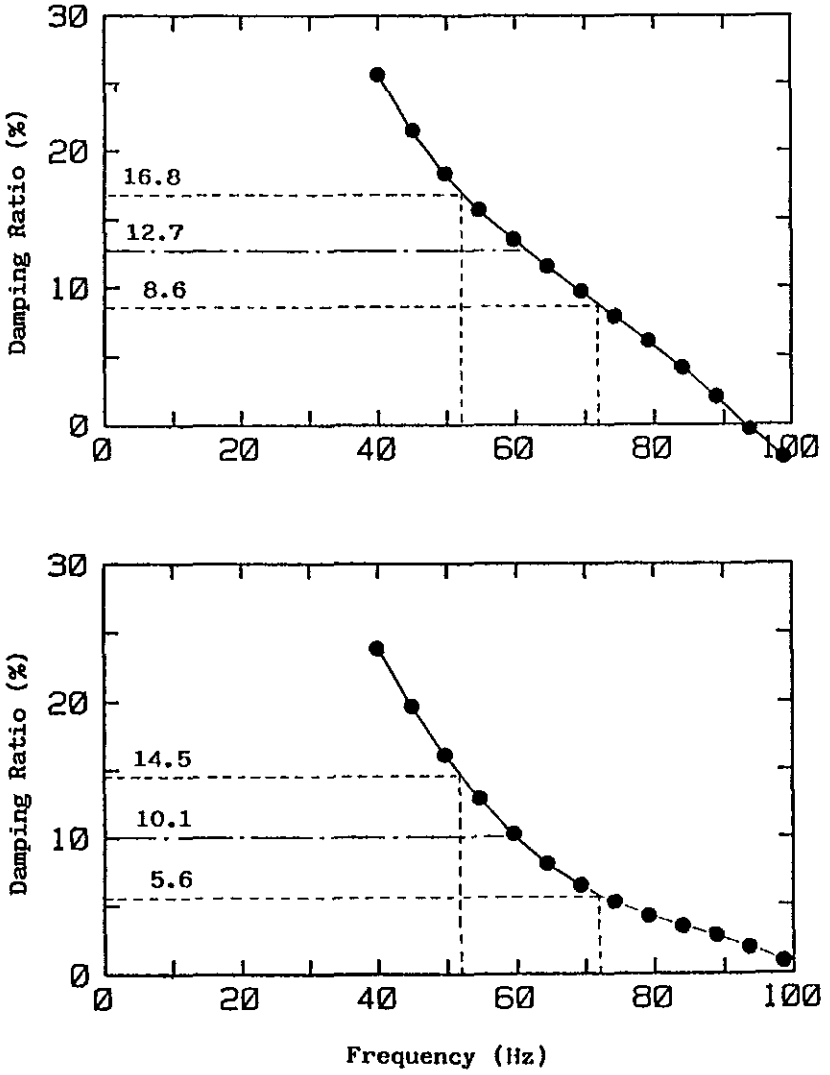

Fig. 5 Damping Ratios h(=1/2Q) of the 2nd Layer (6.4-14.0m) for Hole #1

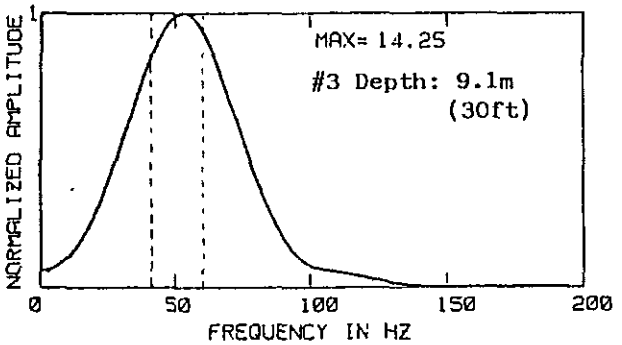

Normalized Fourier Amplitude of the Weighted Synthesized Record

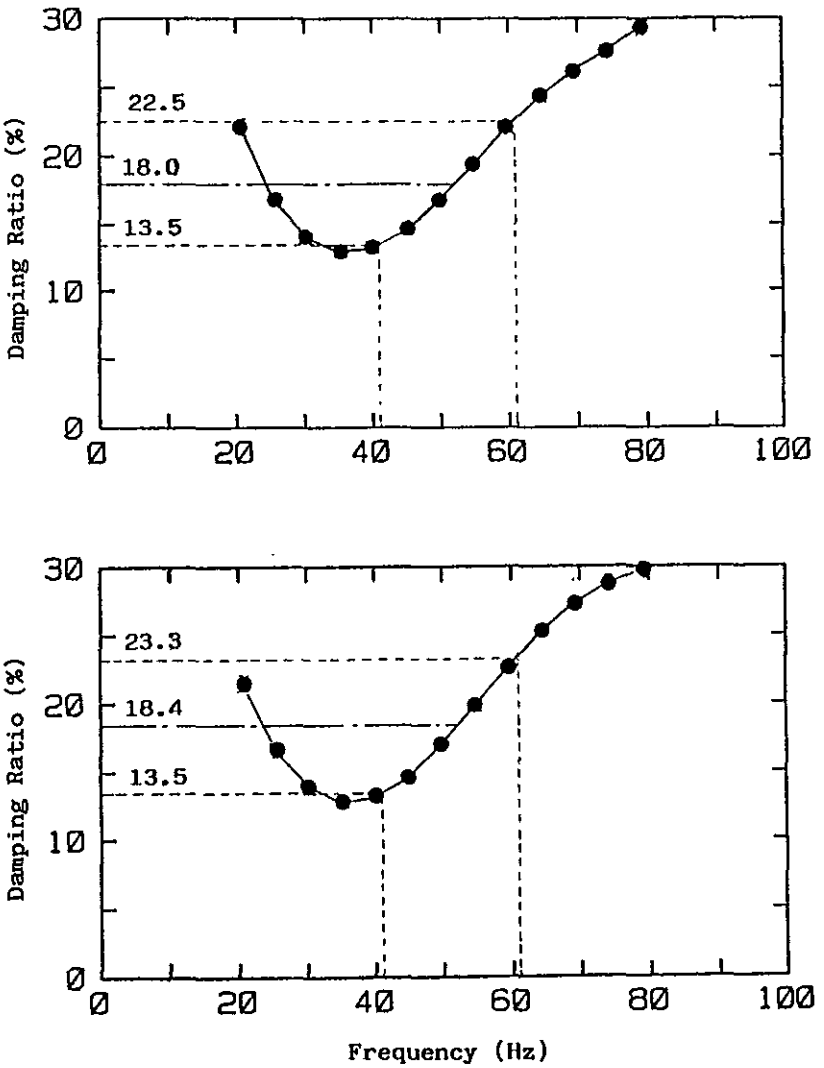

Fig. 6 Damping Ratios h(=1/2Q) of the 2nd and 3rd Layers (4.9-13.4m)for Hole #3

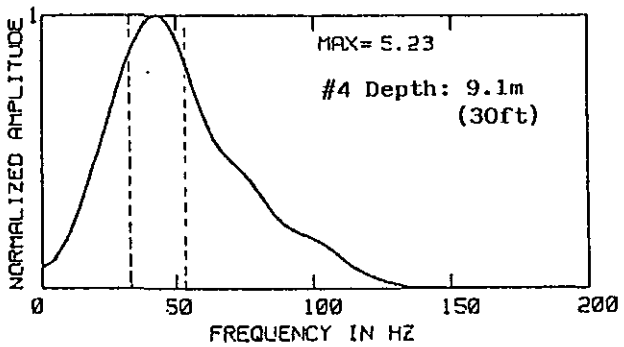

Normalized Fourier Amplitude of the Weighted Synthesized Record

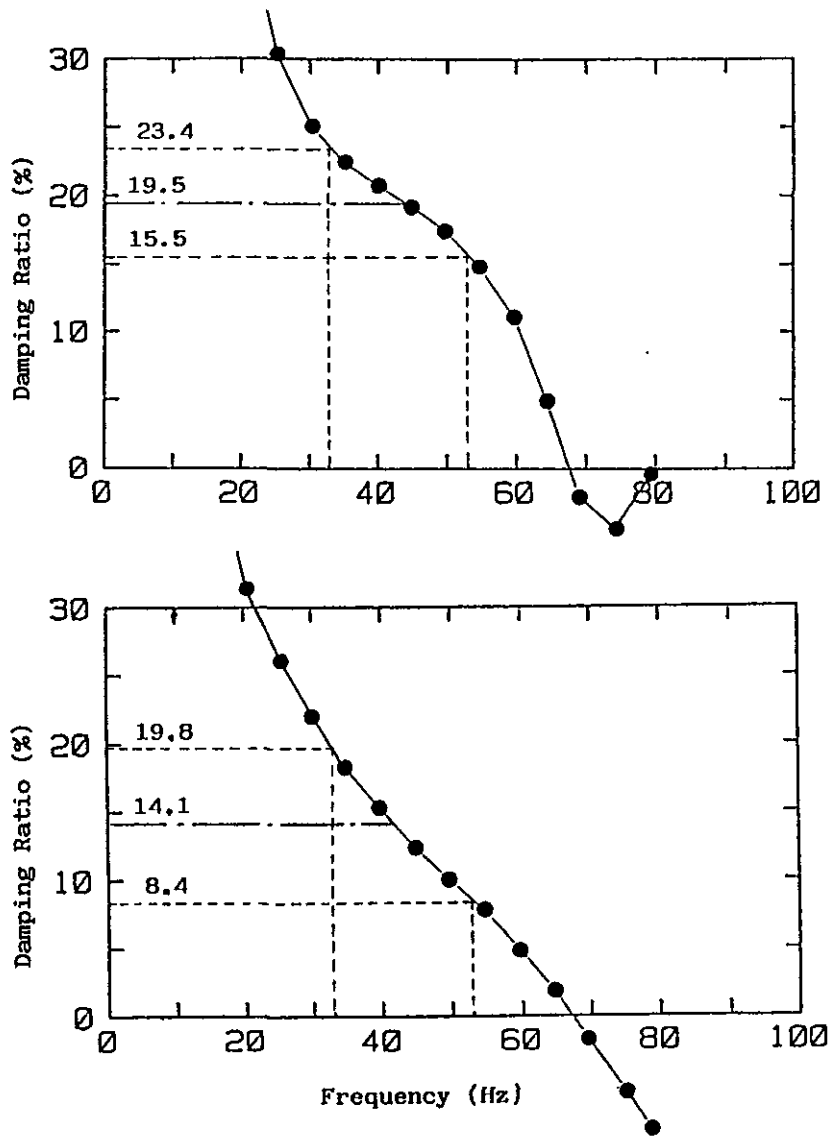

Fig. 7 Damping Ratios h(=1/2Q) of the 2nd Layer (4.9-12.5m) for Hole #4

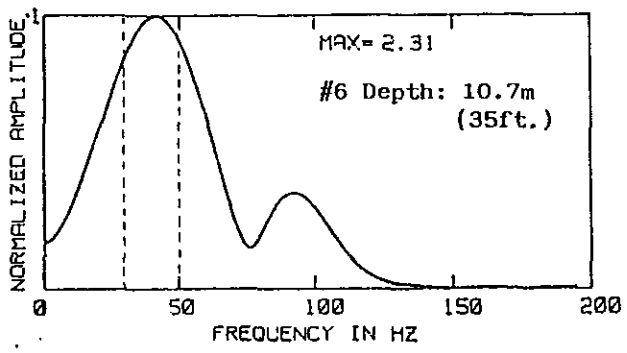

Normalized Fourier Amplitude of the Weighted Synthesized Record

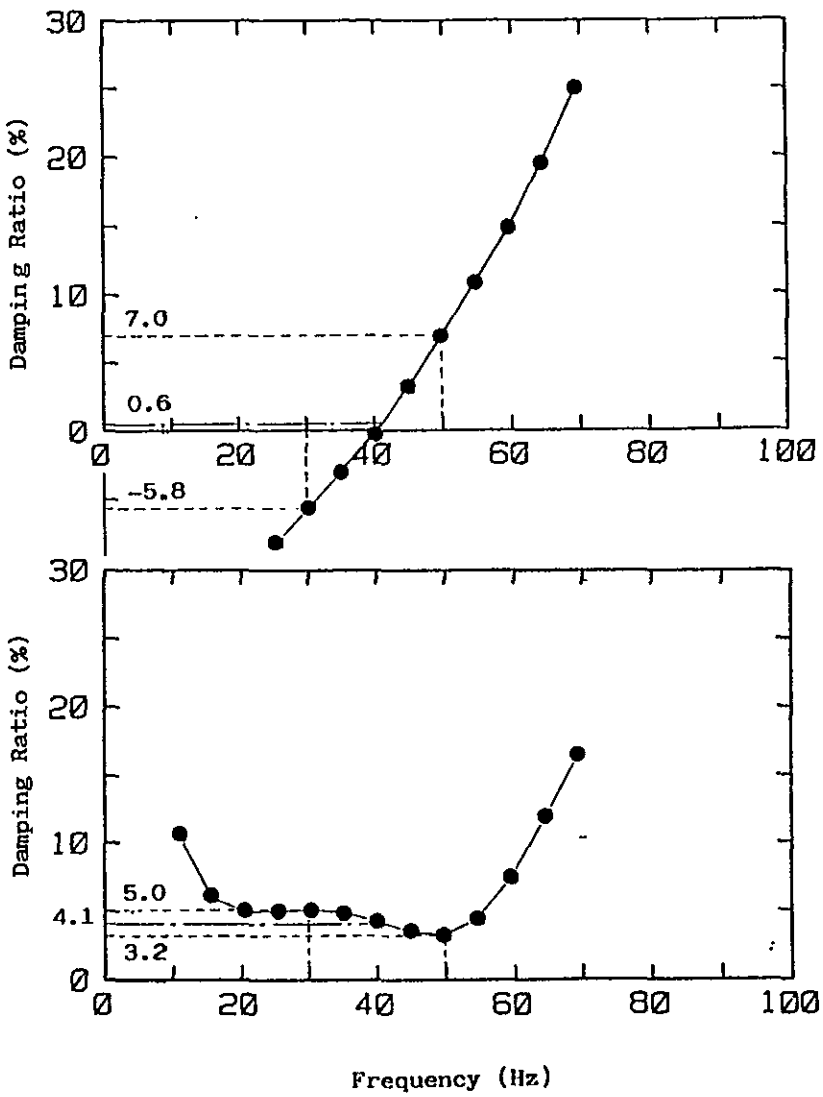

Fig. 8 Damping Ratios h(=1/2Q) of the 2nd Layer (6.4-14.0m) for Hole #6

Table. 2 Comparison of Results for Four Boreholes

Hole No.	Damping Ratio h(%) (h=1/2Q)	Frequency (Hz)	Depth (m)	S-wave Velocity (m/sec)
1	12.7 ± 4.1* 10.1 ± 4.5	52-72	6.4-14.0	1060
3	18.0 ± 4.5 18.4 ± 4.9	41-61	4.9-13.4	420 1200
4	19.5 ± 4.0 14.1 ± 5.7	33-53	4.9-12.5	610
6	0.6 ± 6.4 4.1 ± 0.9	30-50	6.4-14.0	650

*: Range width of damping ratio in the frequency range of 20Hz around the predominant frequency.

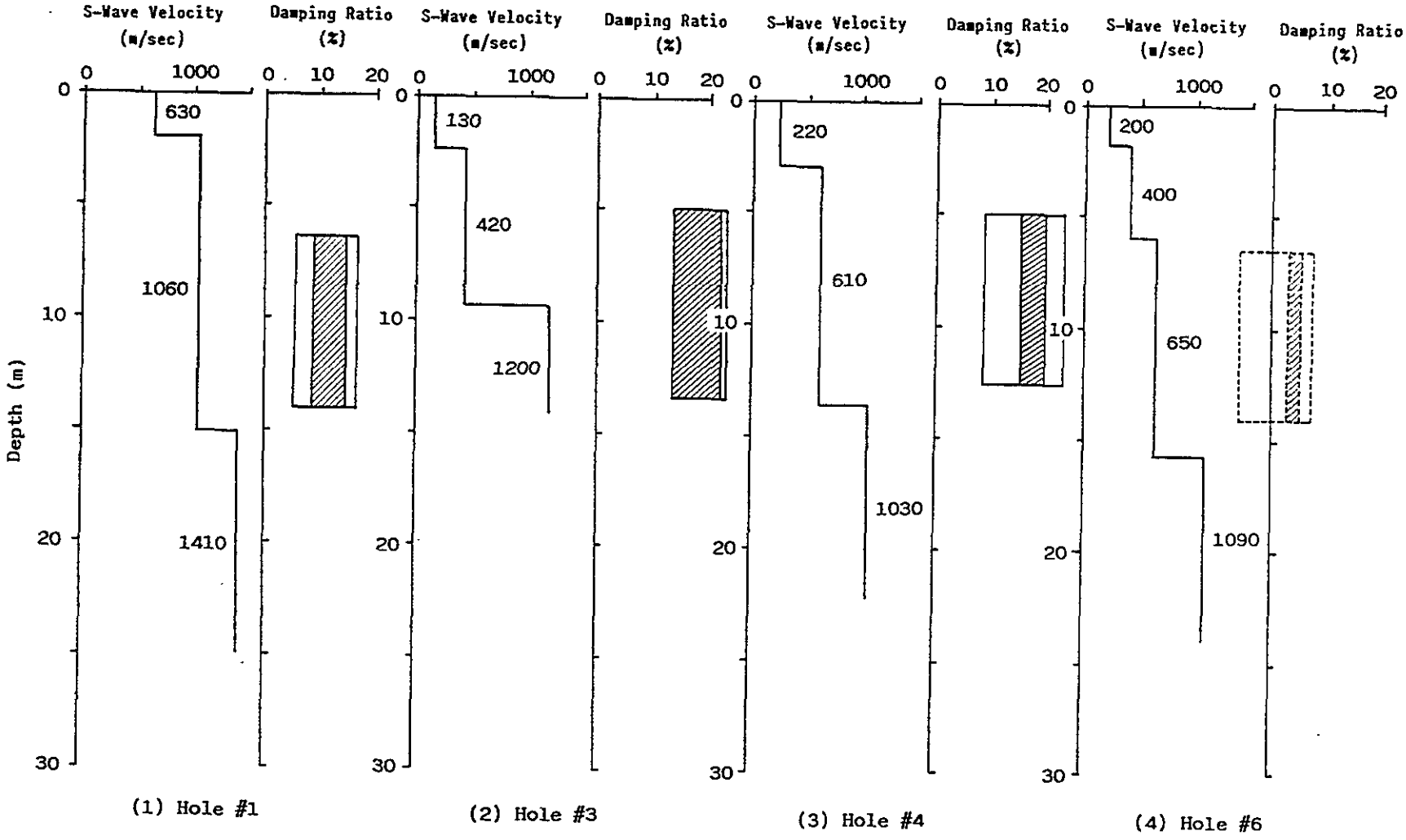

Fig. 9 Correspondence of Q-value to Layers

The hatched area covers results of two sets of S-wave records for each hole.

Table. 3 Correspondence of Q-value to S-wave Velocity

Hole No.	S-wave Velocity (m/sec)	Q-value
1	1060	4.5
4	610	5.9

APPENDIX

There is a method to estimate Q-values very roughly in time domain by examining variations of peak amplitude of travelling S-wave according to depth.

This method is the same as the method which is used in the text except following points :

1) Instead of Fourier amplitude spectrum of the method in the text, variations of S-waves in amplitude according to depth are estimated by using peak amplitude of second phase of synthesized S-wave motion (Fig. 2c in the text) which propagates in the ground with no significant transformation of its waveform.
2) An estimated Q-value is treated as the result for a representative frequency point, which is obtained by averaging the predominant frquencies of the Fourier amplitude spectra of the synthesized S-wave motions.

All other procedures, such as normalization (Fig. 2f in the text) and comparison of analytical variations with theoretical ones in amplitude with depth (Fig. 2g, 2h) and so on, are carried out as the method indicated in the text.

Estimation of Q-values by this method was performed by using the same data as those used in the text. Results are shown in table A1.

Table A1 Damping ratios h=1/(2Q), obtained by the method in time domain

hole No.	depth (m)	S-wave velocity (m/sec)	frequency (Hz)	damping ratio h=1/(2Q) (%)
1	6.4 - 14.0	1060	62	9.4 , 9.3
3	4.9 - 13.4	420 1200	51	19.9 , 20.9
4	4.9 - 12.5	610	43	19.5 , 8.0
6	6.4 - 14.0	650	40	7.4 , 29.7

APPENDIX F
OYO Corporation

THREE PARTS:

1) **Principal Geotechnical Investigation,**
2) **Deep Reflection Profiling, and**
3) **Laboratory Testing of Rock Samples.**

PART 1
PRINCIPAL GEOTECHNICAL INVESTIGATION

This section is a reduced version of the principal OYO report entitled "Report of a Geotechnical Investigation of the Effects of Surface Geology on Seismic Motion", June 1987. The complete report can be obtained upon request from OYO Corporation. The following is a table of contents for the reduced version.

CONTENTS

PREFACE

Japan is one of the world's earthquake prone countries. In 30 years of managing OYO Corporation's geotechnical consultant work, I have considered earthquake engineering to be a fundamental part of our technical capabilities. Accordingly, I have striven to develop a comprehensive system of technology in this field. Research in this direction includs seismological studies, geological, geophysical and geotechnical investigations and many kinds of analysis and simulations using data from the investigations.

In addition, it is my belief that in order to solve problems in earthquake engineering, there is much to be learned through study of actual damage caused by earthquakes. OYO investigation teams have conducted investigations of the sites of earthquakes that have caused major damage both in Japan and abroad, working to accumulate data and develop our technology. When the September, 1985 the Mexico Earthquake occurred, such a team was immediately dispatched. That investigation confirmed once again the deep relationship between surface geology and earthquake damage. Furthermore, we learned from it that interaction between the ground and structures results in complex patterns of damage. This gave us a painful awareness of the neccesity for still greater efforts towards the furthering research of earthquake engineering and microzonation.

The research on the Effects of Surface Geology on Seismic Motion conducted jointly by IASPEI and IAEE is very timely. When my

good friend, Professor Etsuzo Shima of the Earthquake Research Institute of the University of Tokyo, proposed that OYO participate in this project by conducting a geotechnical investigation, I thought it was a unique opportunity that would call for all the technology we have acquired. Not only would it be a good chance for OYO's technology to be appraised internationally, but it would also give OYO's young engineers valuable experience in technical exchanges with their American counterparts at the site. I believe this experience would broaden their vision both from a technical and human standpoint, and provide a fresh inspiration to their research efforts.

Financially, the comprehensive site investigation we conducted in California was quite burdensome. Fortunately, the very substantial cooperation of Dr.Tucker and Dr.Real of CDMG made it possible to bring the planned items of the investigation to a successful conclusion.

It is my hope that OYO's investigation data is useful to the progress of this research project. I look forward to further opportunities in the future for OYO to actively join research and investigation projects like this one.

I wish to express my sincere thanks to Prof. Shima and Dr. Kudo of the University of Tokyo, Dr. Tucker and Dr. Real of CDMG, and Prof. Iwan of CIT for their leadership and help in the planning and execution of this investigation.

Kunio Suyama
President, OYO Corporation
June 10, 1987

(3) Procedure

The heart of OYO's investigation was to grasp the physical and mechanical properties of the test field ground, as well as the dynamic properties, for the sake of forecasting seismic motion. Thus, since the existing boreholes were cased, OYO drilled new boreholes, in which borehole lateral load testing, electrical logging, caliper logging, P & S-wave velocity logging (downhole method, suspension method) and offset V.S.P.were conducted, as a means of obtaining a more comprehensive picture of the physical properties of the ground, as close as possible to reality. Also, in addition to the investigation using boreholes, shallow seismic reflection prospecting and seismic refraction prospecting were conducted, in order to obtain in detail the velocity layer structure of the entire test filed. In addition, analysis of Q-value, indispensable to seismic motion forecast were conducted according to a number of methods. Though, OYO's investigation did not attempt to take core samples, samples from pervious investigations were available, so we conducted such laboratory soil testing as physical testing, dynamic deformation characteristics testing and triaxial ultrasonic wave velocity measurement. Finally, the results from these investigations were examined to determine the physical properties of the ground, and a ground model of the site was proposed.

Fig. 5 is a flow chart of the entire investigation.

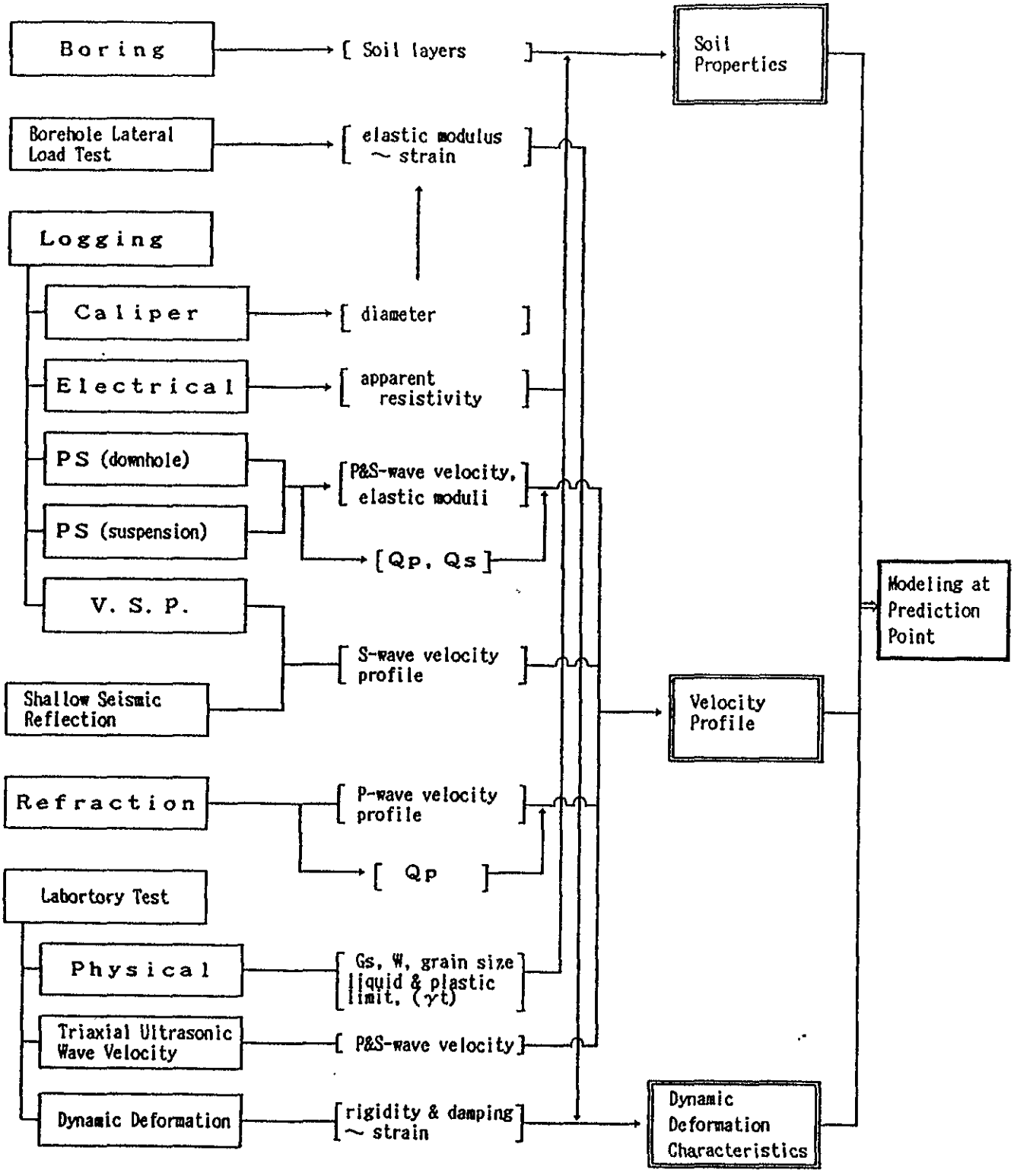

Fig. 5 Flowchart of Investigation

Table 2 Summary of OYO's Planning of Investigation

Investigation	Quantity	Breakdown	Remarks
1) Boring	40m (1 hole)	No.8	・diameter 3 1/8 inches
	30m (8 holes)	No.a ～ No.h	・diameter 3 7/8 inches
2) Borehole Lateral Load Testing	3 depths	GL-15ft(5m),-50ft(15m), -80ft(24m) (No.8)	・diluvial layer , tertiary sand stone ・cyclic load with 3 pressure steps
3) Loggings	(Electrical) 35m	(No.8)	・using Normal Sonde , Micro Sonde ・water in the hole is needed
	(Caliper) 39m	(No.8)	・decision of measuring depth of load test and correction of diameter in Electrical Logging
4) P&S-wave Velocity Logging (Downhole Method)	99m (4 holes)	24m (No.2)	・measuring depth : 1m pitch ・monitoring for Q Value Logging is situated at surface near borehole
		14m (No.3)	
		23m (No.5)	
		38m (No.8)	
5) Suspension PS Logging	65m (3 holes)	17m (No.2)	・measuring depth : 1.0m pitch ・water in the hole is needed ・unmeasurable 2m from the top,and 6m from the bottom
		16m (No.5)	
		32m (No.8)	
6) V.S.P. Vertical Seismic Profiling	52m (2 holes)	14m × 1 offset (No.3)	・measuring depth : 1m pitch ・3 offsets are 0m , 10m , 20m , from the hole ・1 offset means 0m offset and PS Logging(Downhole)results are utilized
		38m × 3 offsets (No.8)	
7) Shallow Seismic Reflection Prospecting	620m (total measuring length)	620m× 1 line (near No.8)	・measuring points : 2.5m pitch ・shot interval : 5m ・vibration source : plank hammering ・1 shot 24channel measuring
8) Seismic Refraction Prospecting	2760m (total measuring length)	920m×2(main lines(A),(B))	・measuring points : 5m pitch ・shot interval : 55m ・vibration source : blasting ・charge :¼～½ lbs each
		460m (sub line (C))	
		460m (Q prospecting (Q))	
9) Q Value Analysis	(downhole method)	No.8	・spectral method , amplitude method , rise time method
	(Refraction)	(Q) line (ℓ=460m)	
10) Laboratory Test	(specific gravity , grain size)	4 samples	・ASTM & JIS-A standard
	(moisture content)	4 samples	・ASTM & JIS-A standard
	(unit weight)	4 samples	・ASTM & JIS-A standard
	(liquid limit & plastic limit)	3 samples	・JIS-A standard
	(dynamic deformation)	4 samples	・resonant column test , torsion test
	(triaxial ultrasonic wave velocity)	4 samples	

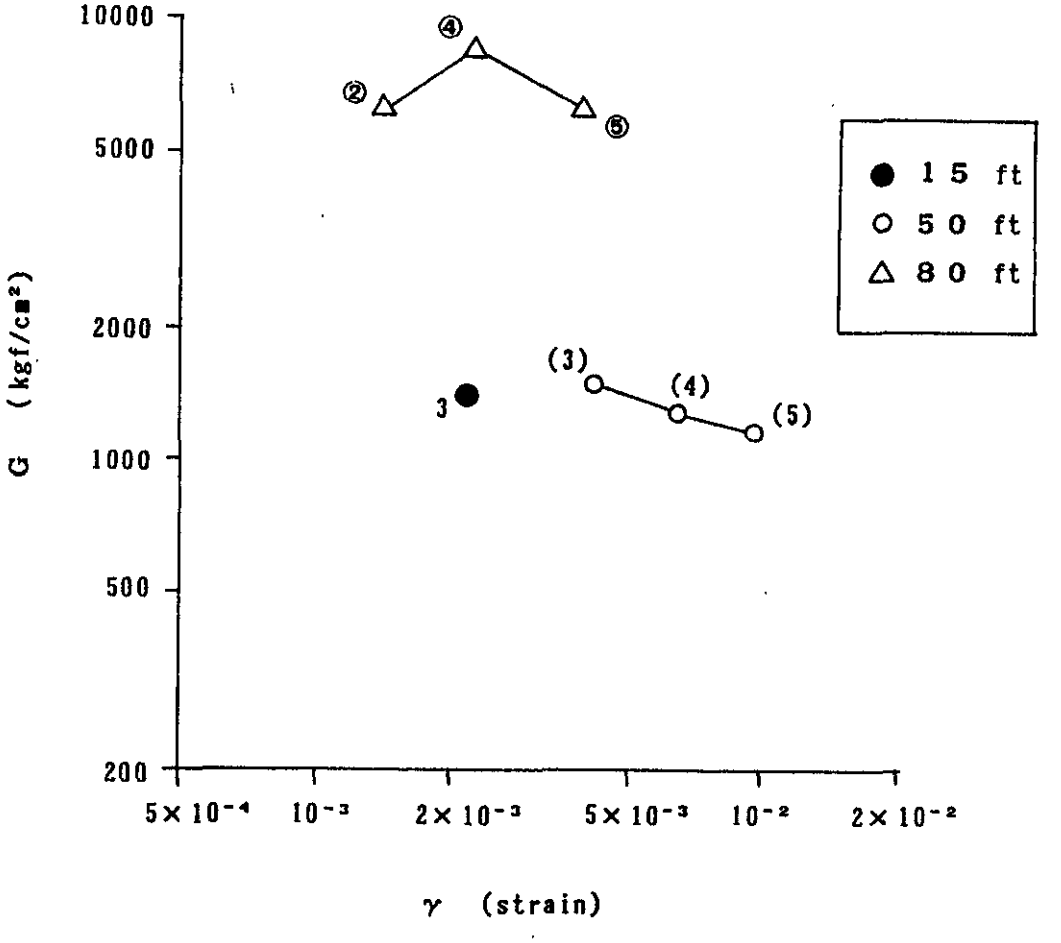

Fig. 12 Relationship with G and γ (Borehole Lateral Load Test)

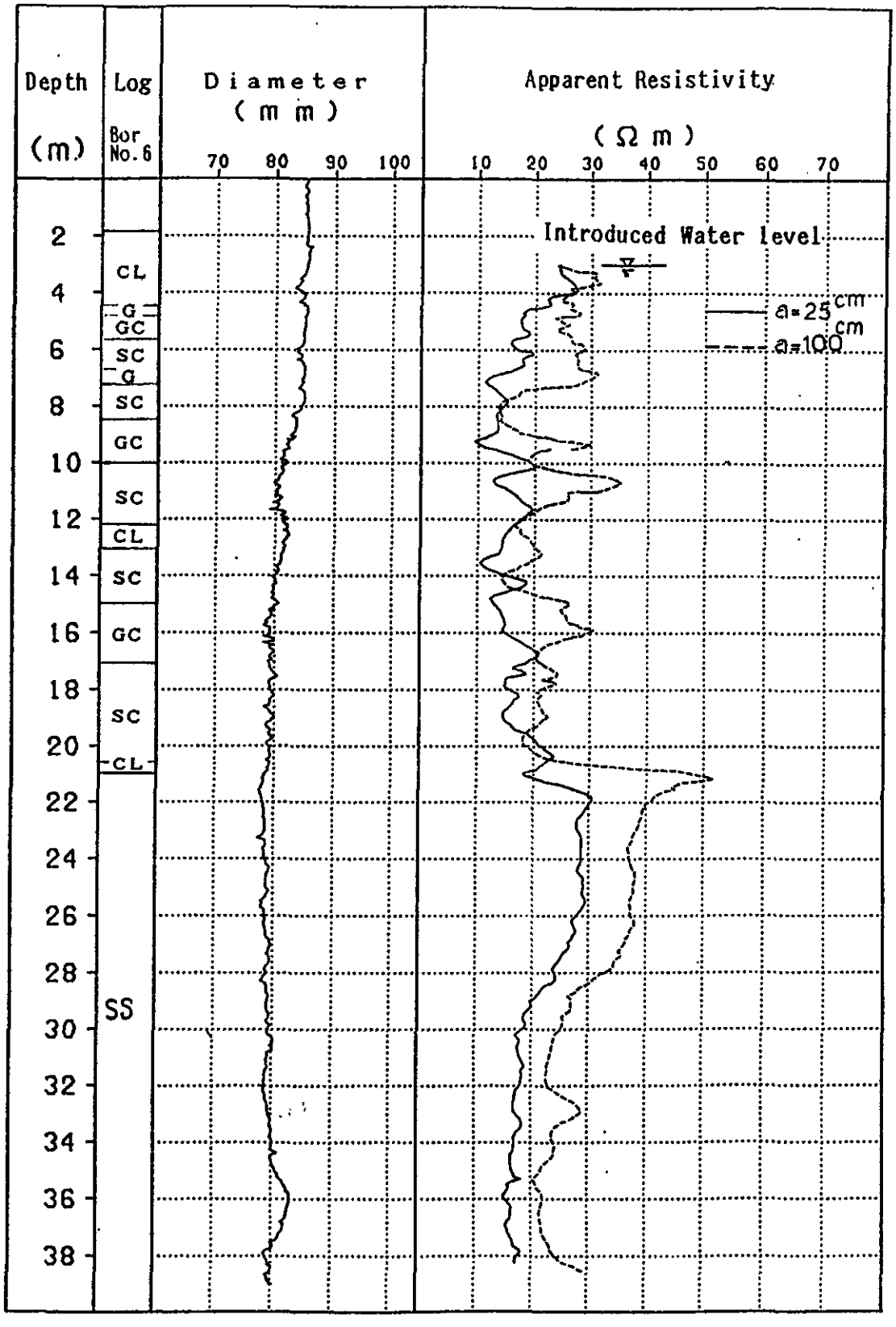

Fig. 1 5 Results of Caliper Logging & Electrical Logging Bor.No.8

Table 4 P & S-wave Velocity Logging Results (Borehole No. 2 :cased)

No	depth (m)	velocity (km/s)		Elastic Moduli
		P-wave	S-wave	
I	GL−0 GL−2	1.00	0.18	ρ=1.6, ν=0.483 G=530, E=1600
II	GL−2 GL−12	1.50	0.84	ρ=1.9, ν=0.272 G=14000, E=35000
III	GL−12 GL−24	2.60	1.10	ρ=2.2, ν=0.409 G=27000, E=76000

ρ [g/cm^3], G, E [kgf/cm^2]

ii. Borehole No. 3 (measuring depths: GL-0 to GL-14 m. :cased hole)

The travel time curves in Fig. 22 show that P and S-waves describe 3 layer ground structures, and that velocities have a tendency to increase with depth. Results are given in Table 5.

Table 5 P & S-wave Velocity Logging Results (Borehole No. 3 :cased)

No	depth (m)	velocity (km/s)		Elastic Moduli
		P-wave	S-wave	
I	GL−0 GL−2	0.58	0.22	ρ=1.6, ν=0.416 G=790, E=2200
II	GL−2 GL−10	0.85	0.42	ρ=1.8, ν=0.338 G=3200, E=8700
III	GL−10 GL−14	2.05	0.84	ρ=2.2, ν=0.399 G=16000, E=44000

ρ [g/cm^3], G, E [kgf/cm^2]

iii. Borehole No. 5 (measuring depths: GL-0 to GL-23 m. :cased hole)

The travel time curves in Fig. 23 show that P-waves describe a 2 layer ground structure, and S-waves describe a 3 layer ground structure. Wave velocities have a tendency to increase with depth.

Results are given in Table 6.

Table 6 P & S-wave Velocity Logging Results (Borehole No. 5 :cased)

P-wave			S-wave			Elastic Moduli
No	depth (m)	velocity (km/s)	No	depth (m)	velocity (km/s)	
I	GL－0 GL－19	2.80	I	GL－0 GL－2	(0.07)	ρ=1.6, ν=0.498 G=80 , E=240
			II	GL－2 GL－19	0.60	ρ=1.8, ν=0.219 G=7000, E=16000
II	GL－19 GL－23	2.05	II	GL－19 GL－23	1.00	ρ=2.2, ν=0.344 G=22000, E=60000

ρ [g/cm³], G , E [kgf/cm²]

iv. Borehole No. 8 (measuring depths: GL-0 to GL-38.5 m. :uncased hole)

The travel time curves in Fig. 24 show that P and S-waves describe 4 layer ground structures, and that wave velocities have a tendency to increase with depth. Results are given in Table 7.

Table 7 P & S-wave Velocity Logging Results (Borehole No. 8 : uncased)

No	depth (m)	velocity (km/s)		Elastic Moduli
		P-wave	S-wave	
I	GL−0 GL−1	(0.35)	(0.08)	ρ=1.6, ν=0.472 G=100, E=310
II	GL−1 GL−3	0.69	0.37	ρ=1.6, ν=0.298 G=2200, E=5800
III	GL−3 GL−21	1.00	0.63	ρ=1.8, ν=0.171 G=7700, E=17000
IV	GL−21 GL−38.5	2.50	1.10	ρ=2.2, ν=0.352 G=27000, E=75000

ρ [g/cm^3], G, E [kgf/cm^2]

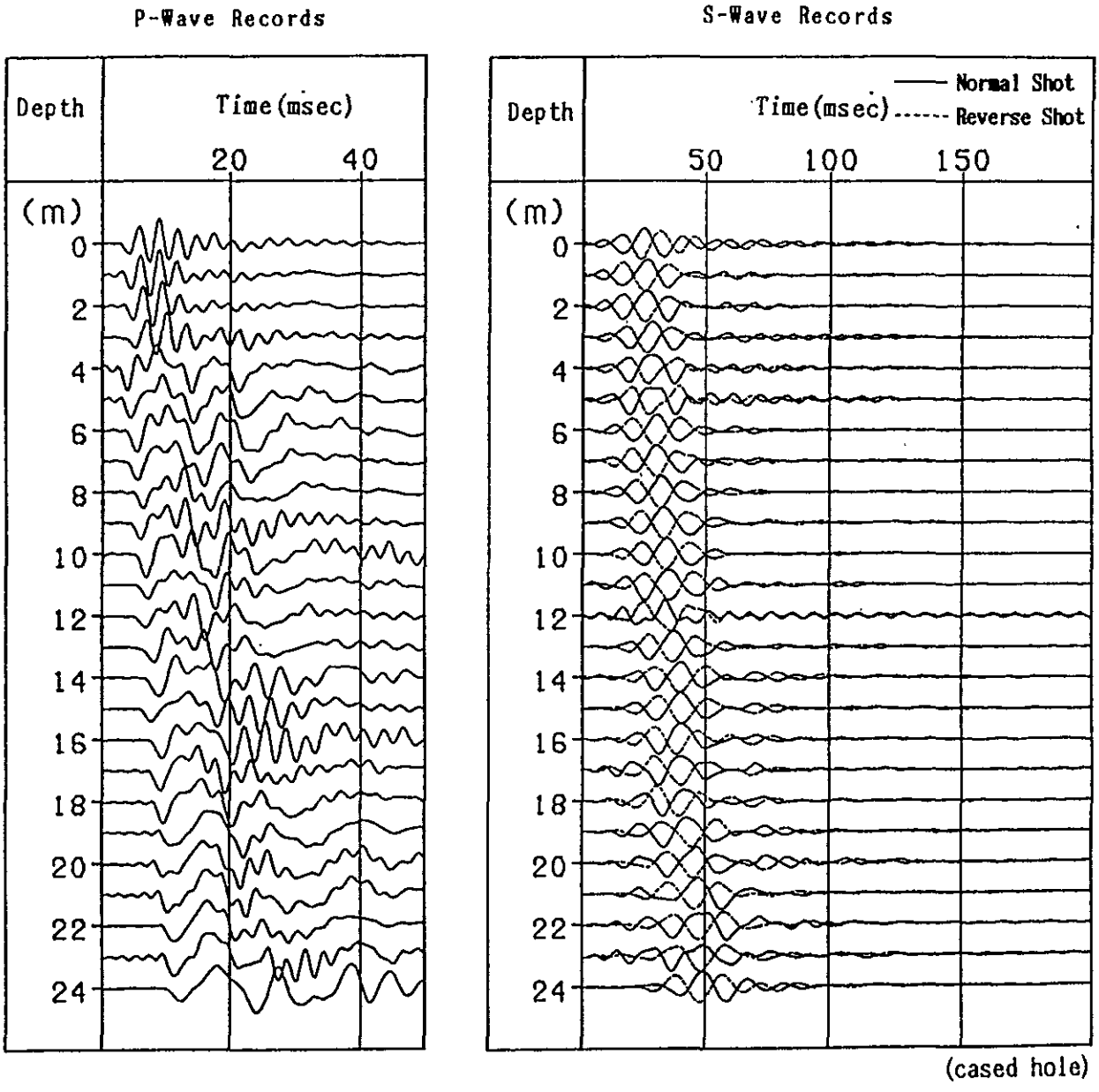

Fig. 1 7 Waveform by P&S-wave Velocity Logging (Downhole Method) Bor.No.2

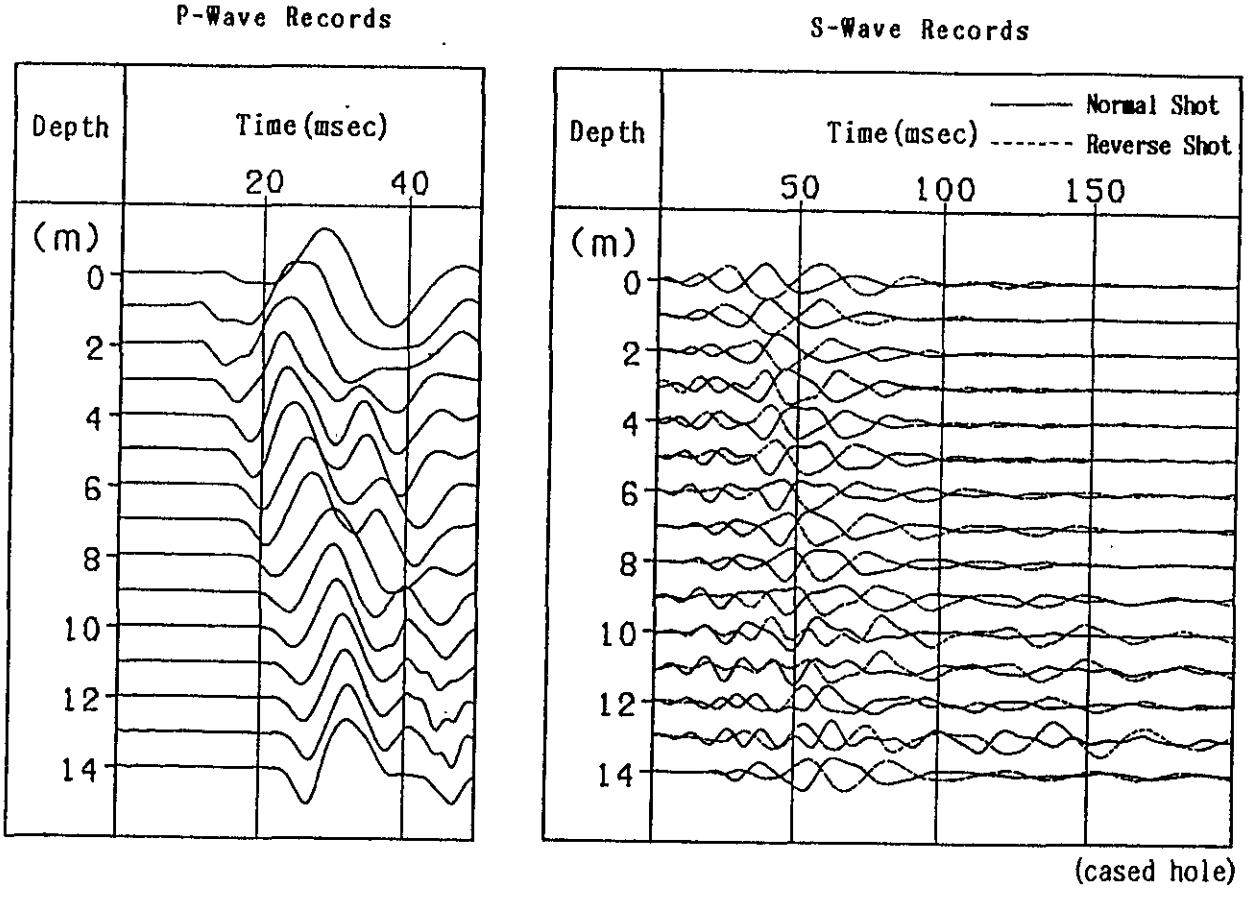

Fig. 1 8 Waveform by P&S-wave Velocity Logging (Downhole Method) Bor.No.3

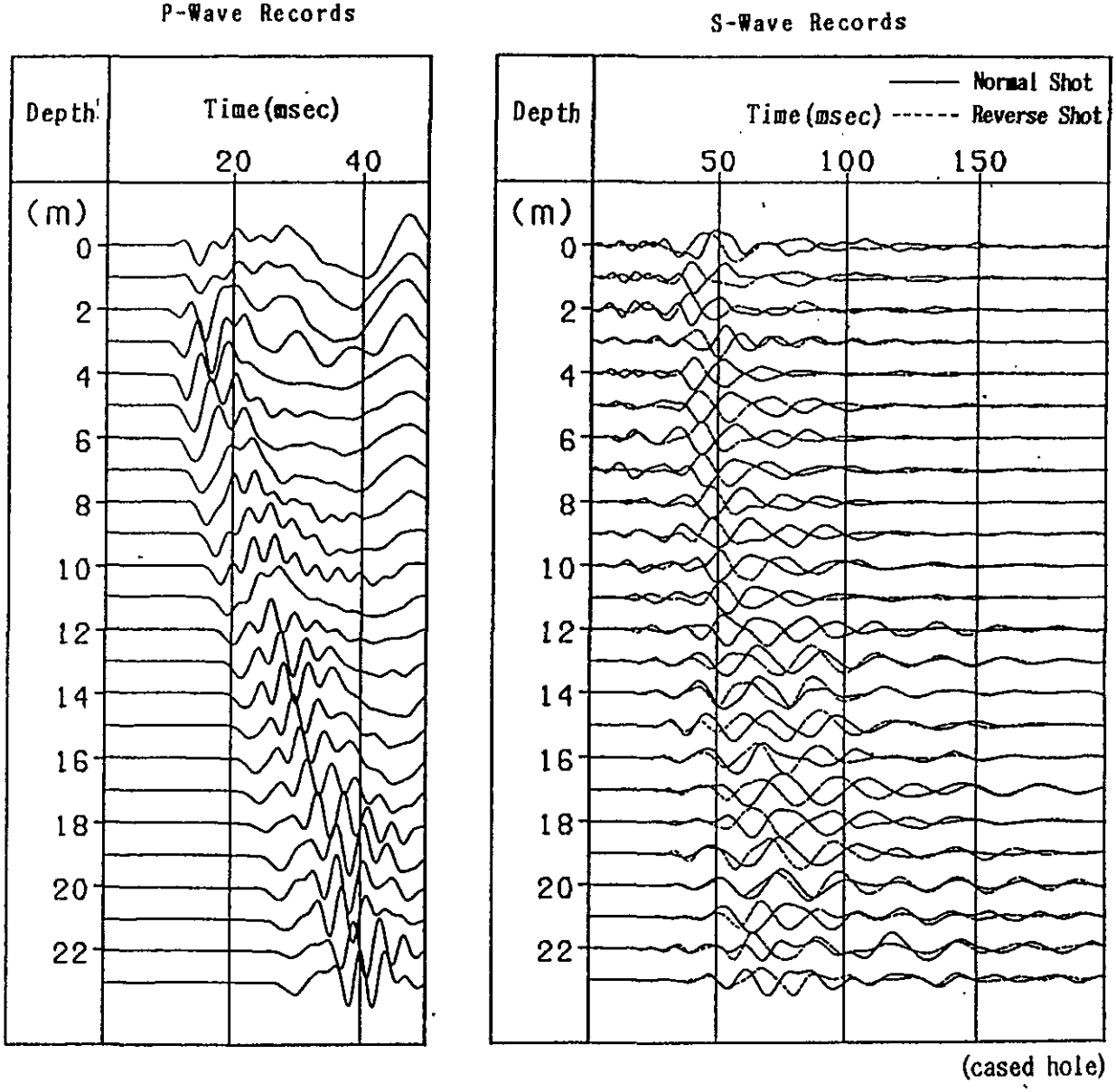

Fig. 1 9 Waveform by P&S-wave Velocity Logging (Downhole Method) Bor.No.5

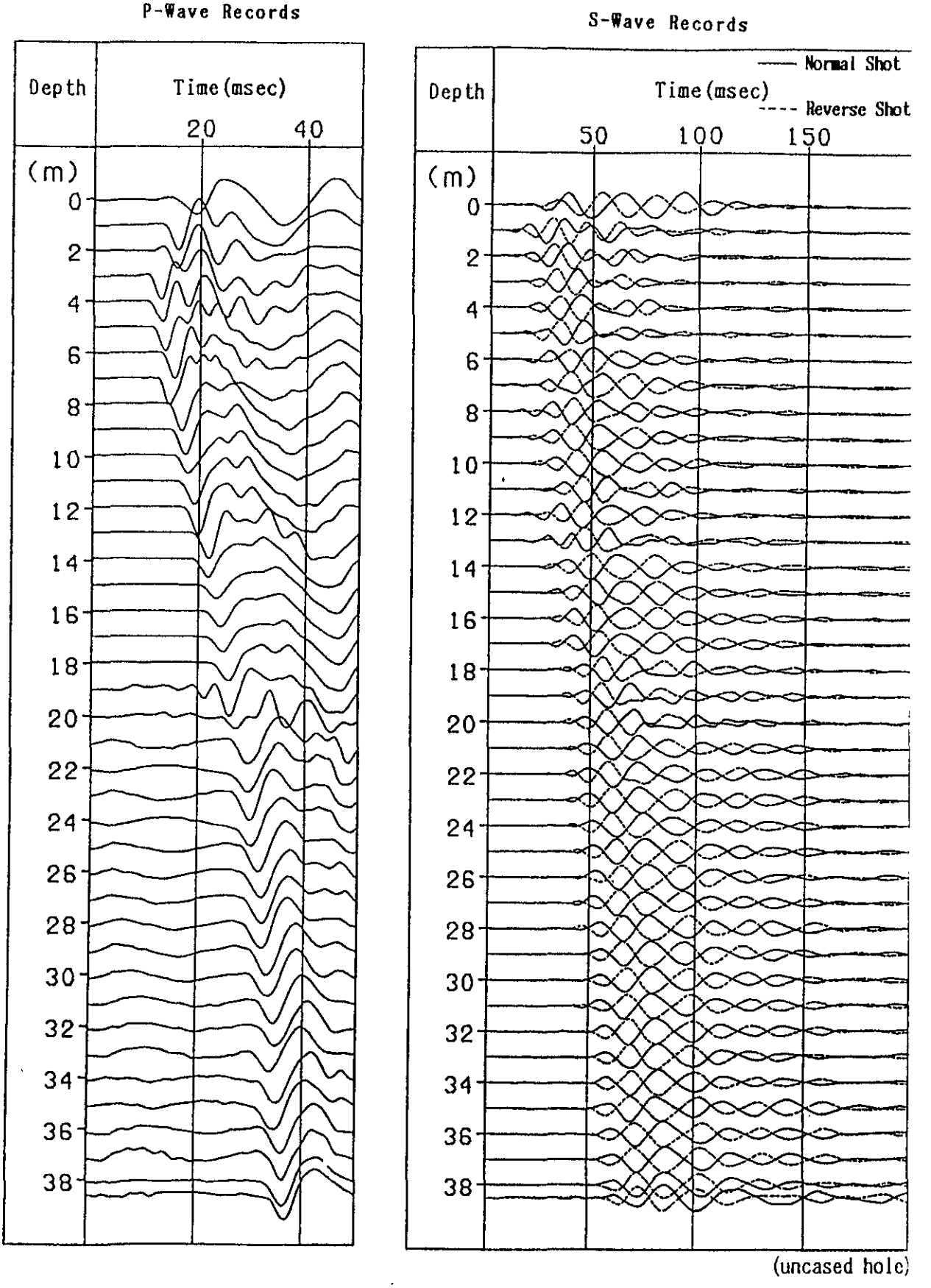

Fig. 2 0 Waveform by P&S-wave Velocity Logging (Downhole Method) Bor.No.8

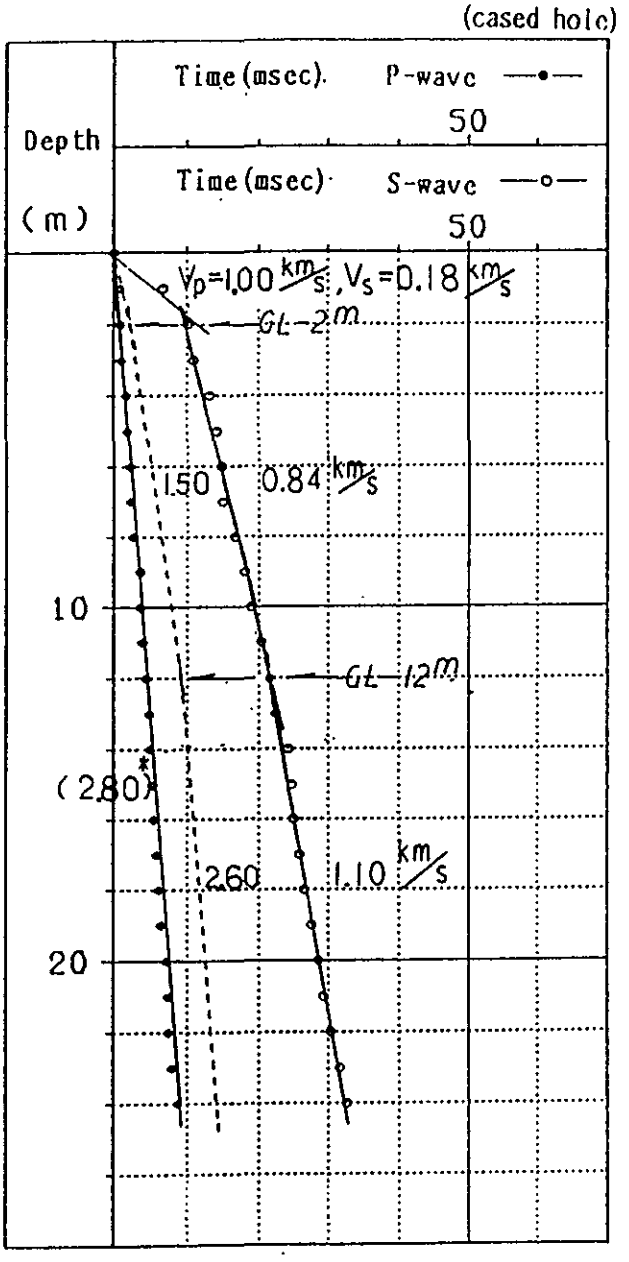

Fig. 2 1 Travel Time Curve by P&S-wave Velocity Logging (Downhole Method) Bor.No.2

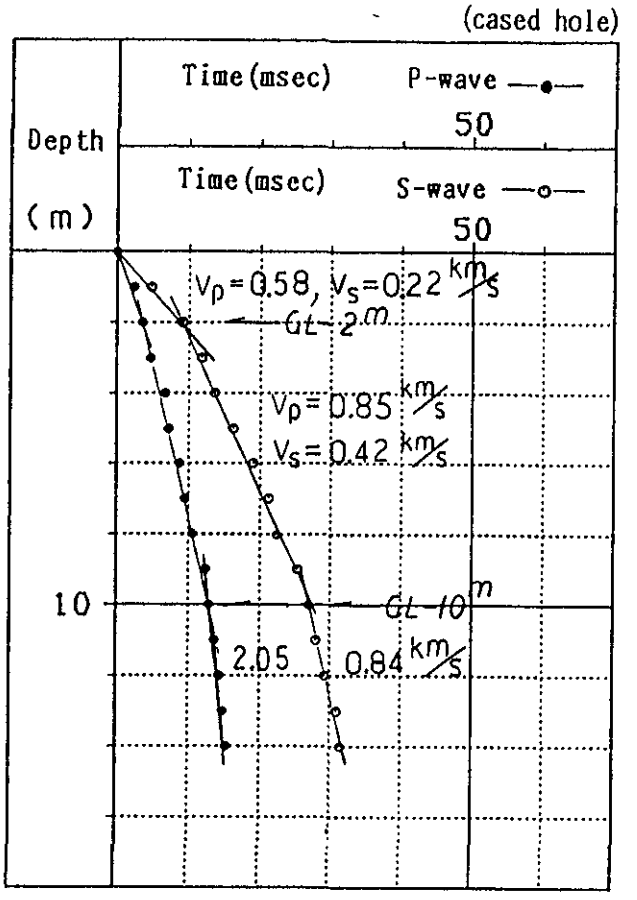

Fig. 2 2 Travel Time Curve by P&S-wave Velocity Logging (Downhole Method) Bor.No.3

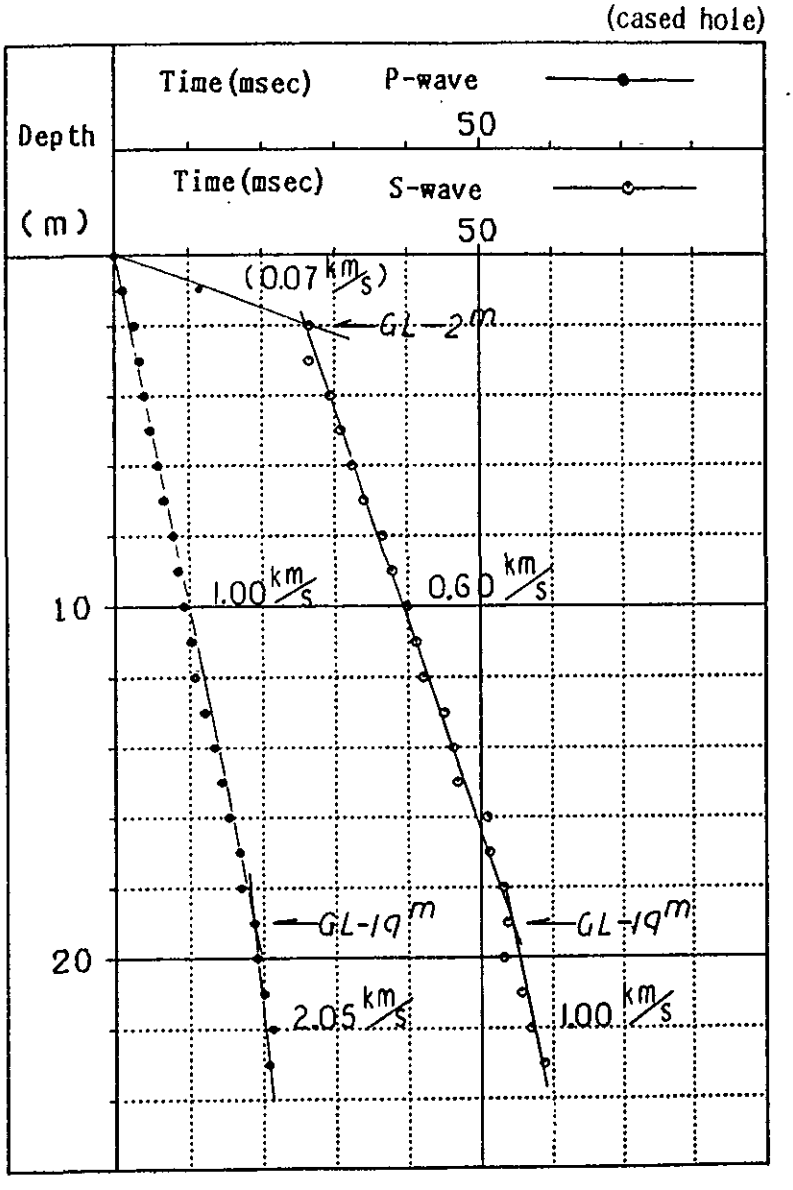

Fig. 2 3 Travel Time Curve by P&S-wave Velocity Logging (Downhole Method) Bor.No.5

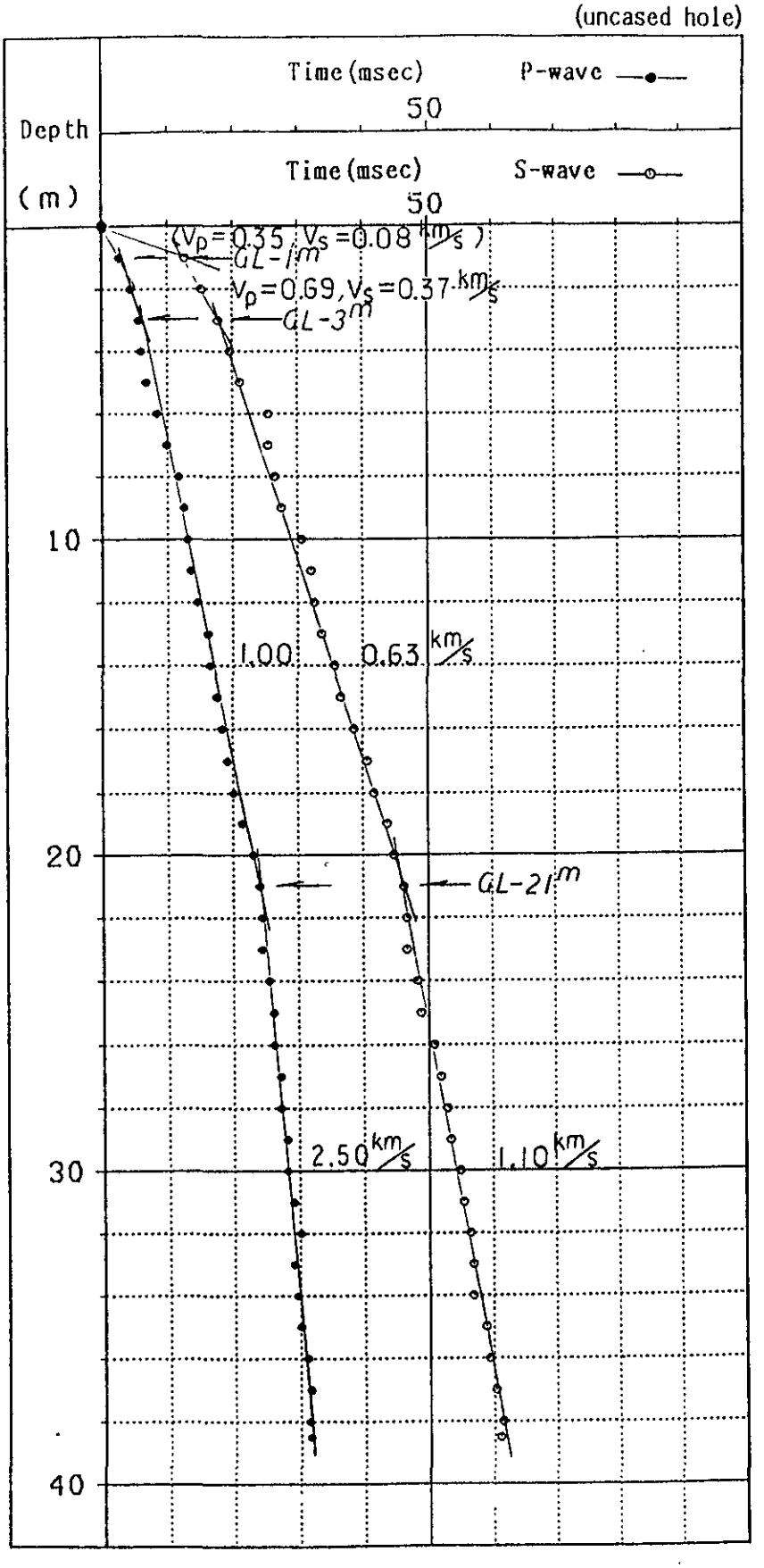

Fig. 2 4 Travel Time Curve by P&S-wave Velocity Logging (Downhole Method) Bor.No.8

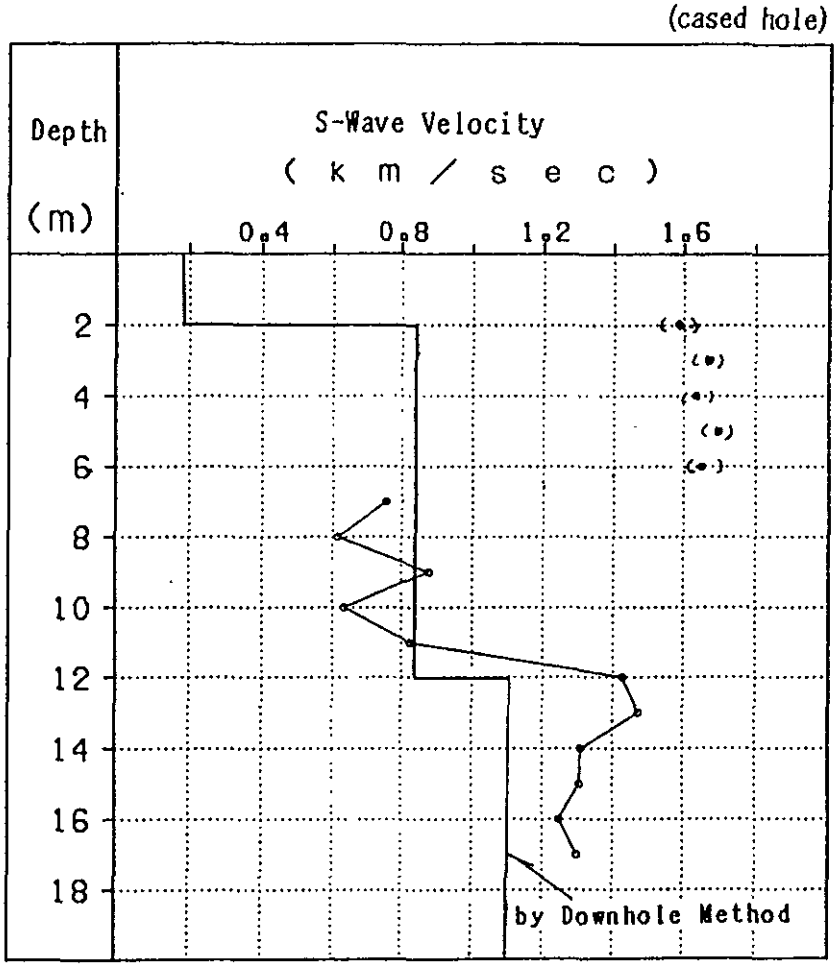

Fig.29 Results of Suspension P&S-wave Logging (Bor.No.2)

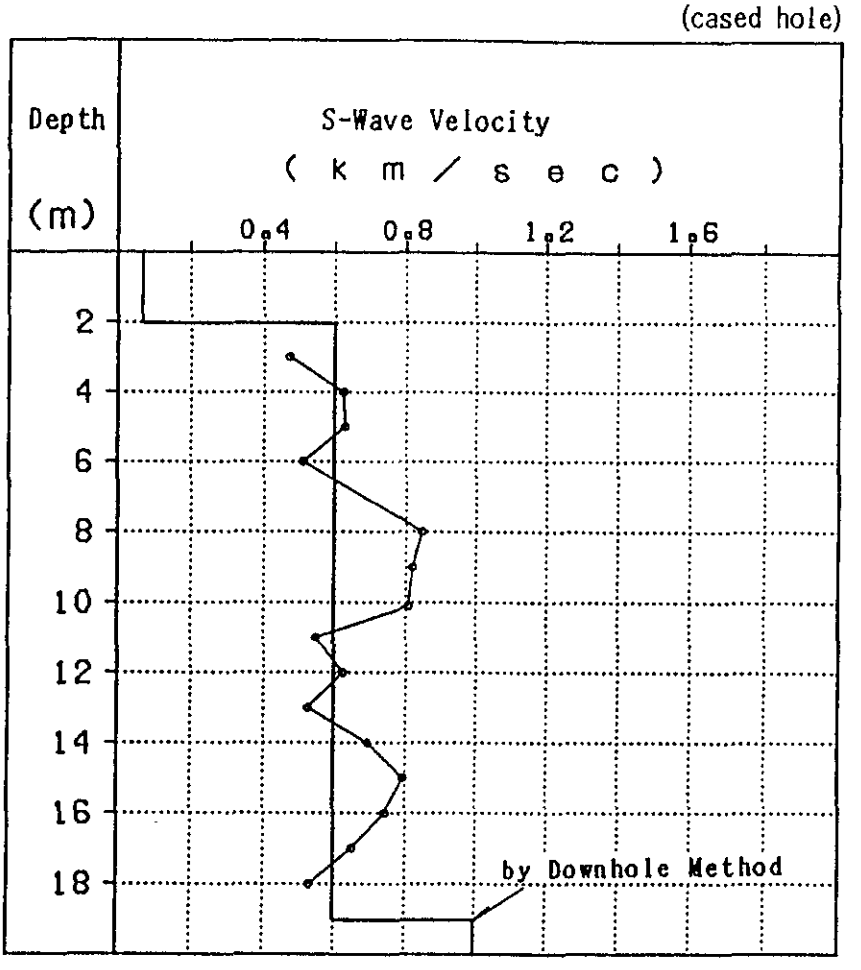

Fig. 30 Results of Suspension P&S-wave Logging (Bor.No.5)

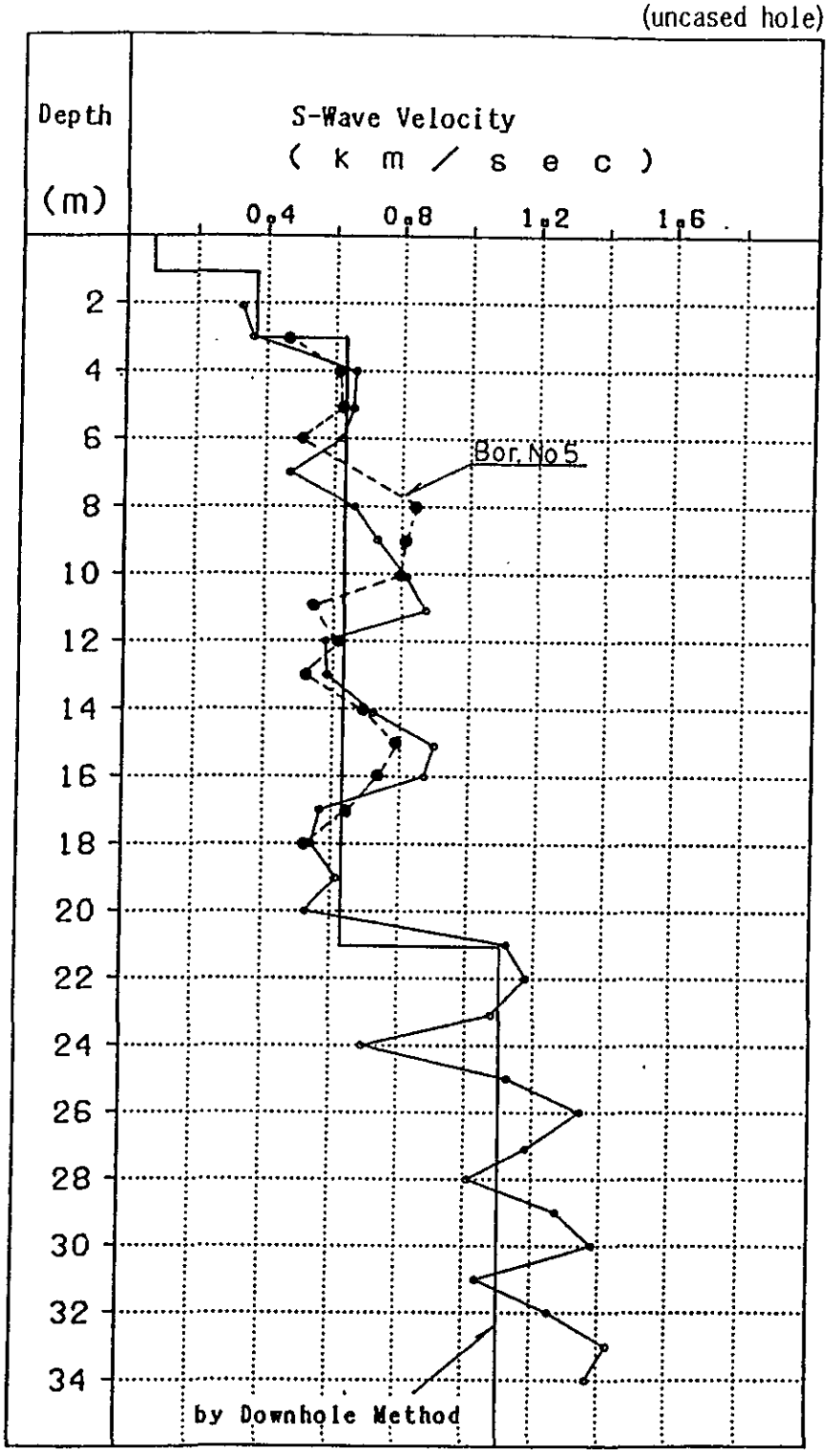

Fig. 3 1 Results of Suspension P&S-wave Logging (Bor.No.8)

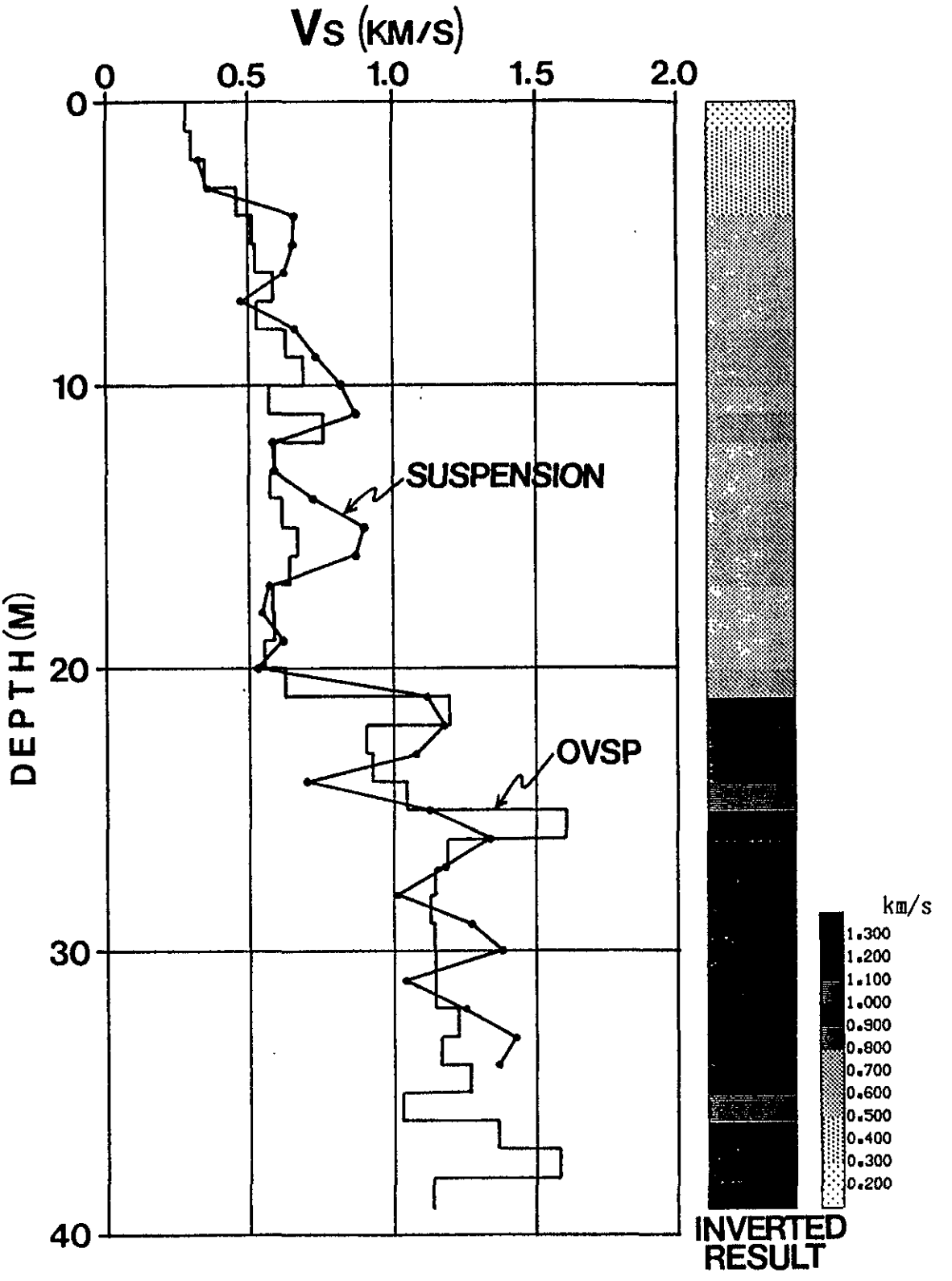

Fig. 38 Inverted Vs Profile from Offset VSP Data, Comparing with the Result of Suspension Log. (Br. 8)

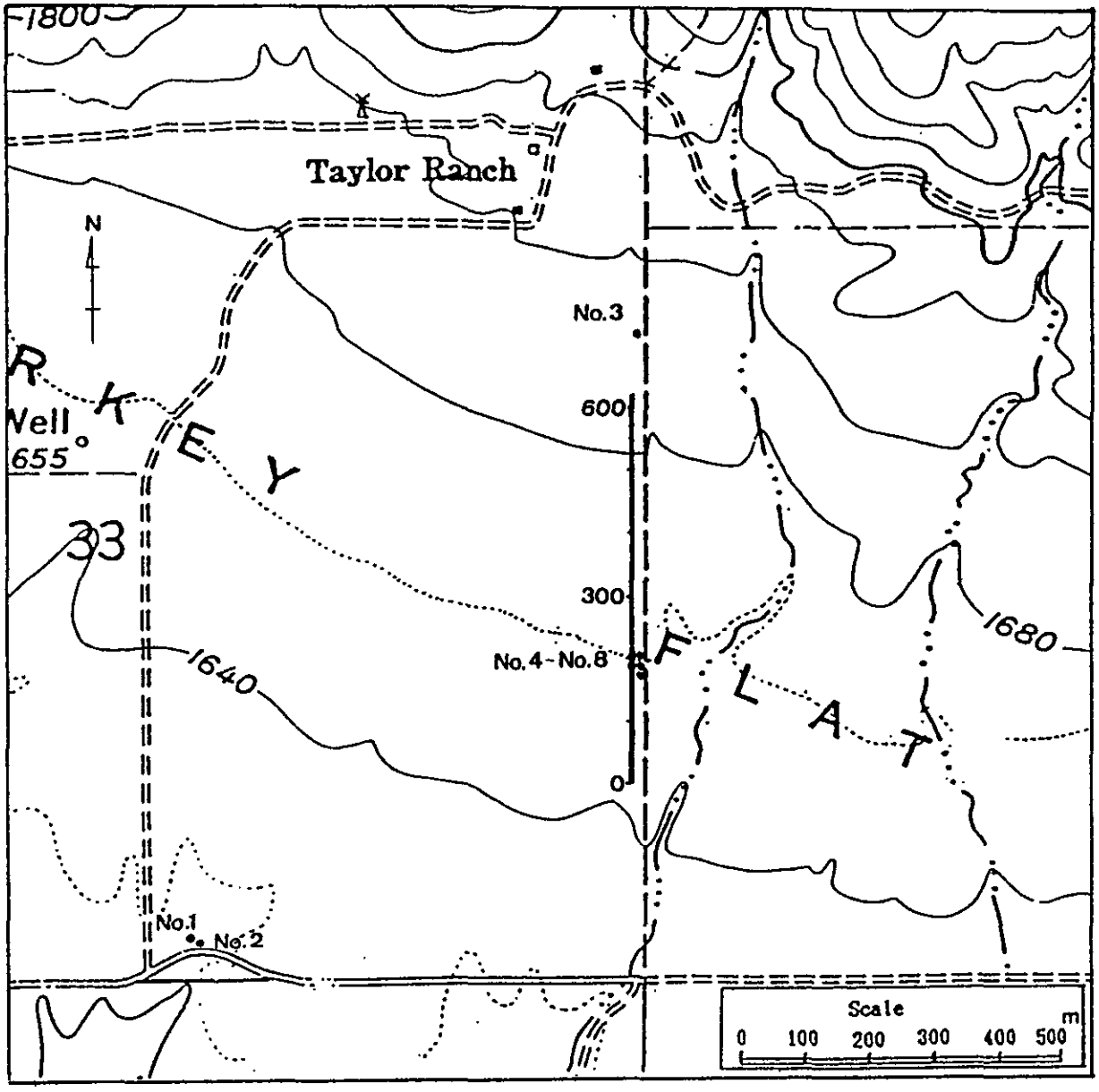

Fig. 4 0 Measuring line of shallow seismic reflection prospecting.

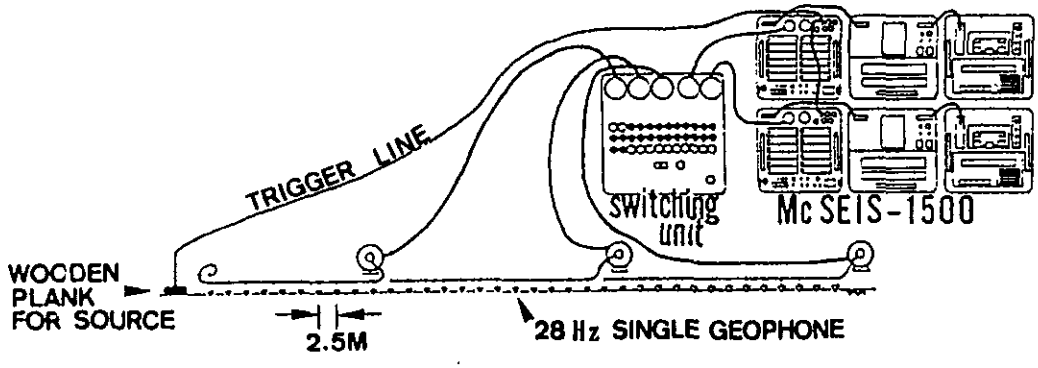

Fig. 4 1 Measuring system of shallow seismic reflection prospecting.

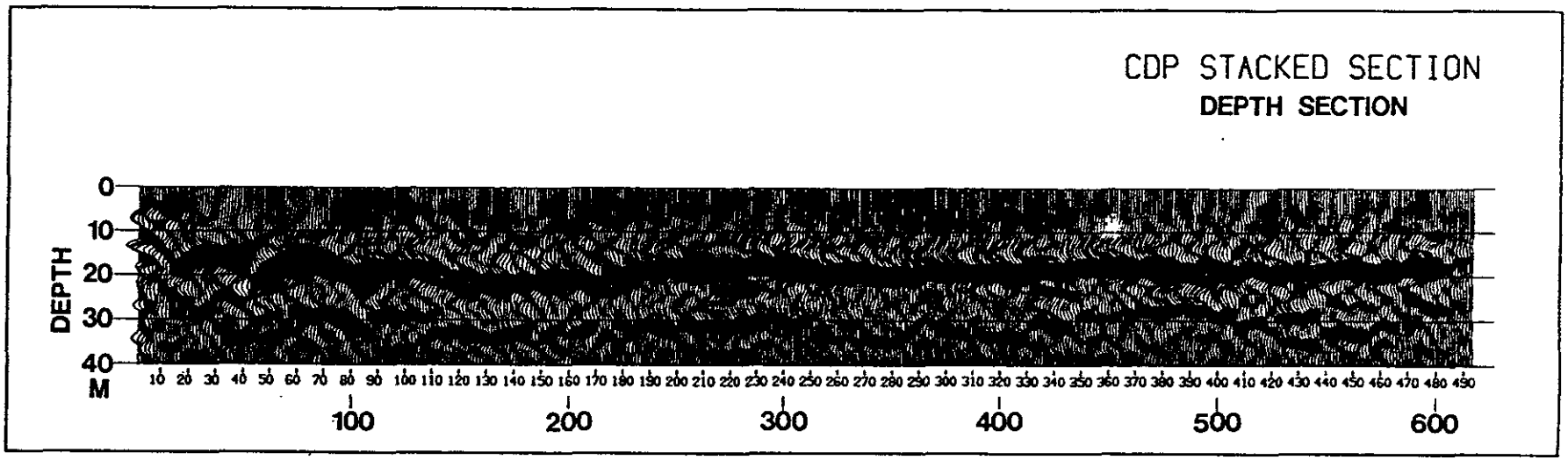

Fig. 4 7 Depth section after T-Z stretching with constant velocity 500m/s

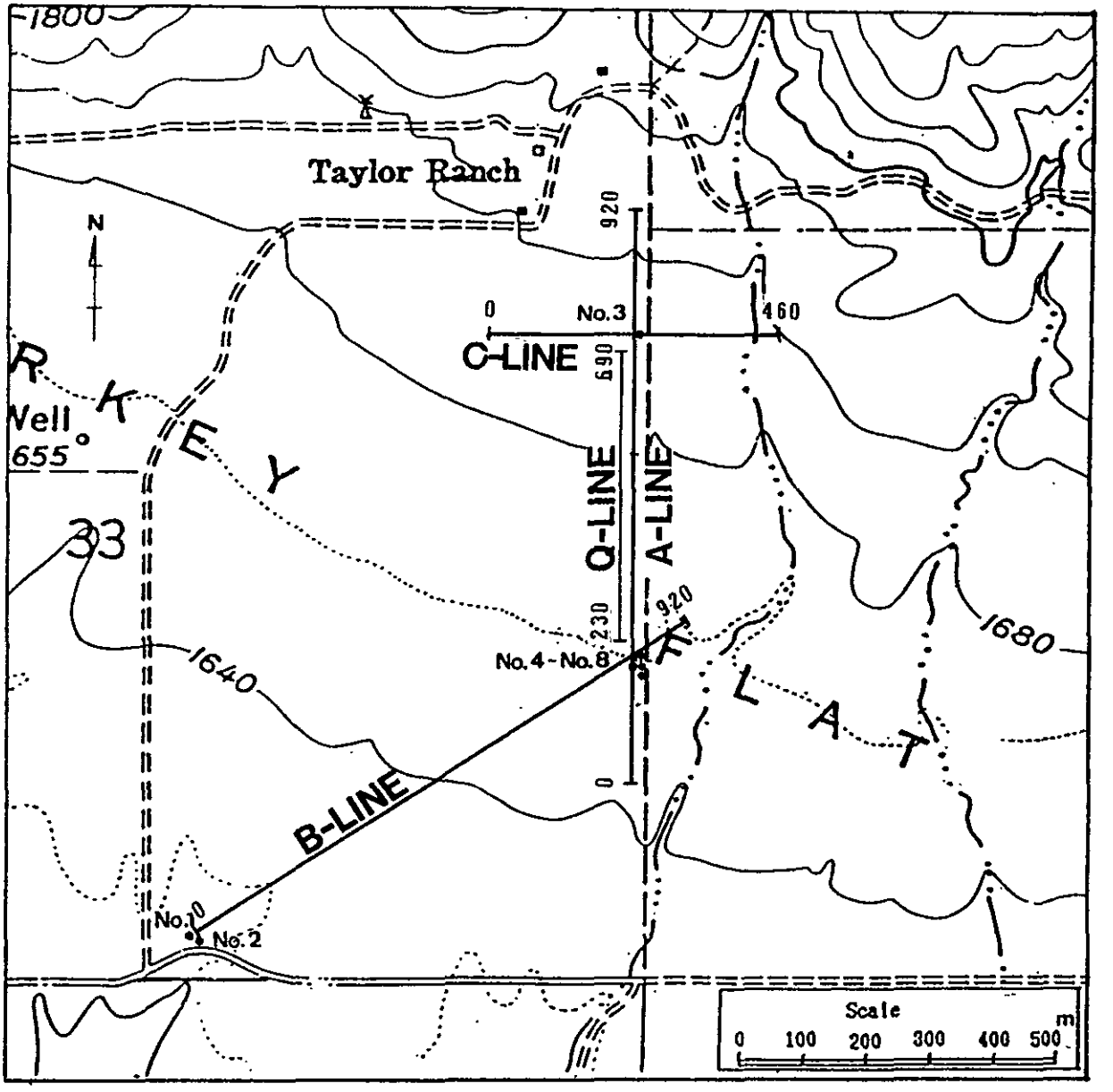

Fig. 5 0 Measuring Lines of Seismic Refraction Prospecting

A-LINE

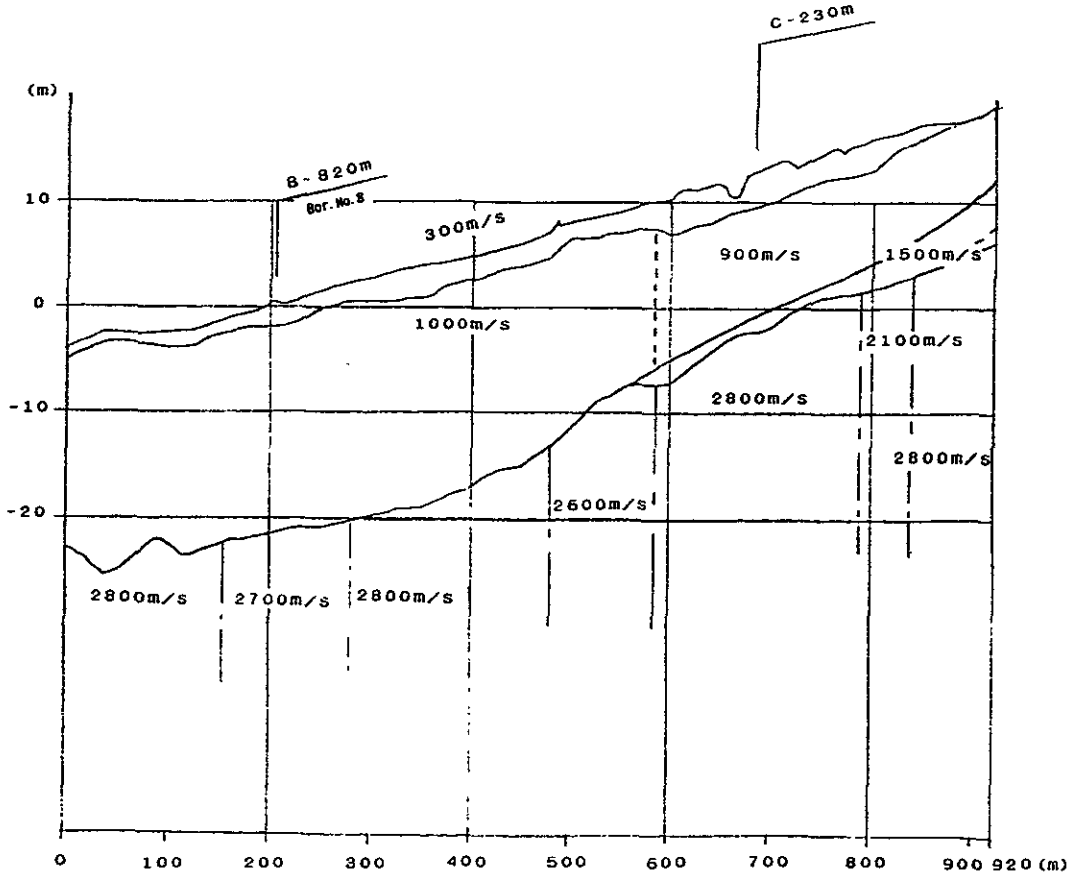

Fig. 52 Result of Refraction Prospecting
(P-wave Velocity Profile)

B-LINE

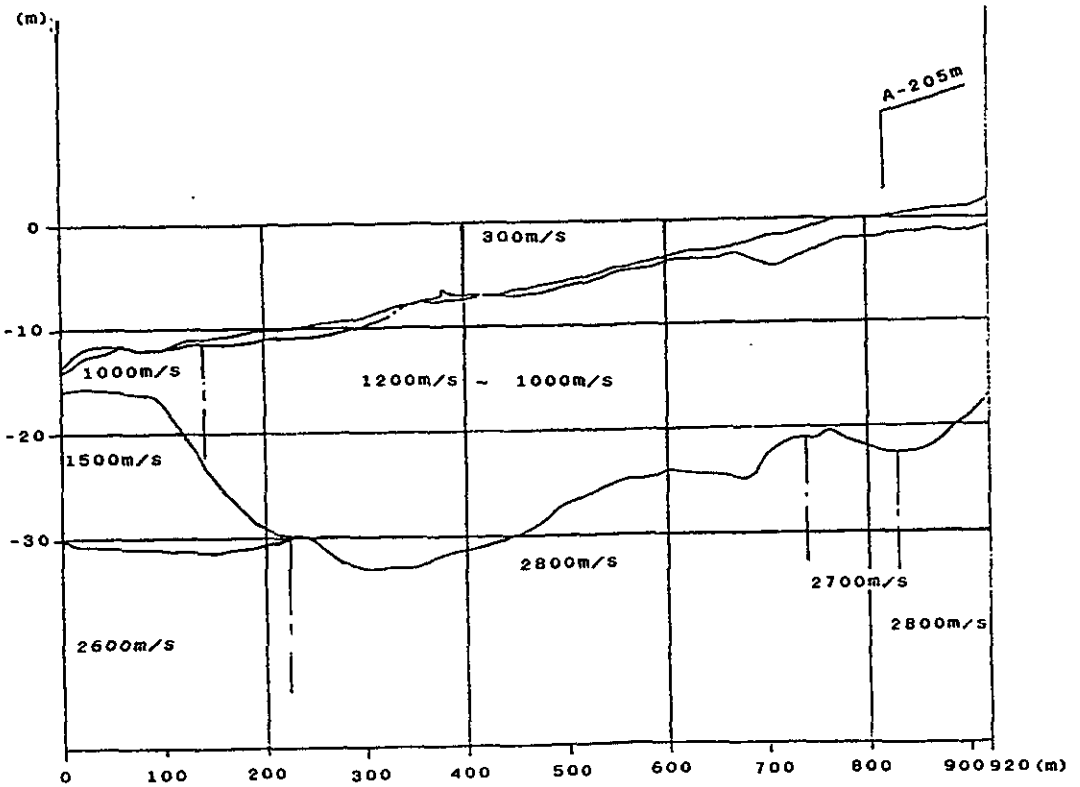

Fig. 53 Result of Refraction Prospecting
(P-wave Velocity Profile)

C－LINE

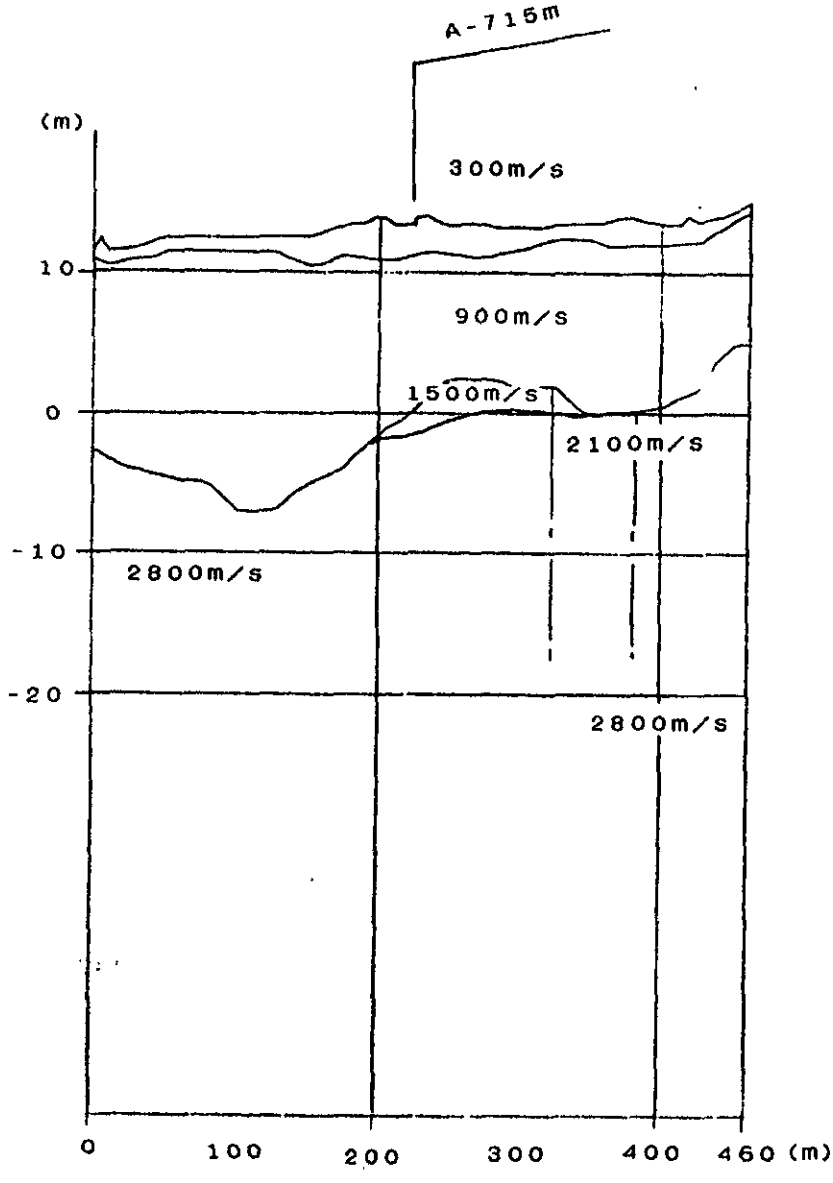

Fig. 54 Result of Refraction Prospecting
(P-wave Velocity Profile)

Table 10 Results of Q-value Analysis

Geology	Q	Analysis Method					
		Spectral ratio		Amplitude		Rise Time	
		downhole	reflection	downhole	reflection	downhole	reflection
Silt Layer	Q_P	—	—	—	—	10	11
	Q_S	10	—	—	—	25 ?	—
Sandstone Layer	Q_P	—	—	—	21	15	13
	Q_S	12	—	—	—	25 ?	—

Table 1 2 PHYSICAL SOIL TESTING RESULTS

SITE NAME: Turkey Flat

SAMPLE NO.			B-6-2	B-6-13		TF3-5	TF3-7
SAMPLE	U: UNDISTURBED D: DISTURBED		U	U		U	U
DEPTH		ft	7.0	60.0		15.0	30.0
NATURAL MOISTURE CONTENT		w %	25.4	19.1		21.8	16.5
SPECIFIC GRAVITY OF SOIL PARTICLE		Gs	2.70	2.70		2.69	2.71
BULK DENSITY		ρ_t g/cm³					
DRY DENSITY		ρ_d g/cm³					
NATURAL VOID RATIO		e					
DEGEE OF SATURATION		Sr %					
LIQUID LIMIT		wL %	45.2	NP		39.1	31.0
PLASTIC LIMIT		wP %	21.3	NP		23.1	21.3
PLASTICITY INDEX		IP %	23.9	—		16.0	9.7
GRAIN-SIZE ANALYSIS ( ): by ASTM	GRAVEL-SIZE FRACTION	%	1.5 (0.5)	5.0 (0.5)		2.0 (1.0)	3.0 (1.5)
	SAND-SIZE FRACTION	%	47.0 (48.0)	60.0 (64.5)		56.0 (57.0)	58.0 (59.5)
	SILT-SIZE FRACTION	%	37.0 (37.0)	23.0 (23.0)		27.5 (27.5)	26.0 (26.0)
	CLAY-SIZE FRACTION	%	14.5 (14.5)	12.0 (12.0)		14.5 (14.5)	13.0 (13.0)
	UNIFORMITY COEFFICIENT	Uc	50.0	83.3		91.2	76.0
CLASSIFICATION	in JAPAN [JSF M1-73]		(CL)	(SM_g)		(SC)	(SC_g)
	in U.S.A. [ASTM D2487-69]		SC	SW		SC	SC
UNCONFINED COMPRESSION TEST	UNCON. COMP. STRENGTH UNDISTURBED SPECIMEN	qu kgf/cm²					
TRIAXIAL COMPRESSION TEST	COHESION	C kgf/cm²					
	ANGLE OF SHEAR RESISTANCE	φ°					
DIRECT SHEAR TEST	COHESION	C kgf/cm²					
	ANGLE OF SHEAR RESISTANCE	φ°					
CONSOLIDATION TEST	PRECOMPRESSION LOAD	Pc kgf/cm²					
	COMPRESSION INDEX	Cc					
Permeability Test		K15 cm/S					

Fig. 6 4 GRAIN SIZE ANALYSIS

	Sample	Depth ft	Textural Classification	Gravel %	Sand %	Silt %	Clay %	60% Grain Size D_{60} mm	Effective Grain Size D_{10} mm	Uniformity Coefficient U_c	Max. Grain Size mm
1	B-6-2	7.0 ~ .	(CL) SC	1.5 (0.5)	47.0 (48.0)	37.0 (37.0)	14.5 (14.5)	0.115	0.0023	50.0	9.52
2	B-6-13	60.0 ~ .	(SMg) SW	5.0 (0.5)	60.0 (64.5)	23.0 (23.0)	12.0 (12.0)	0.275	0.0033	83.3	9.52
3		. ~ .									

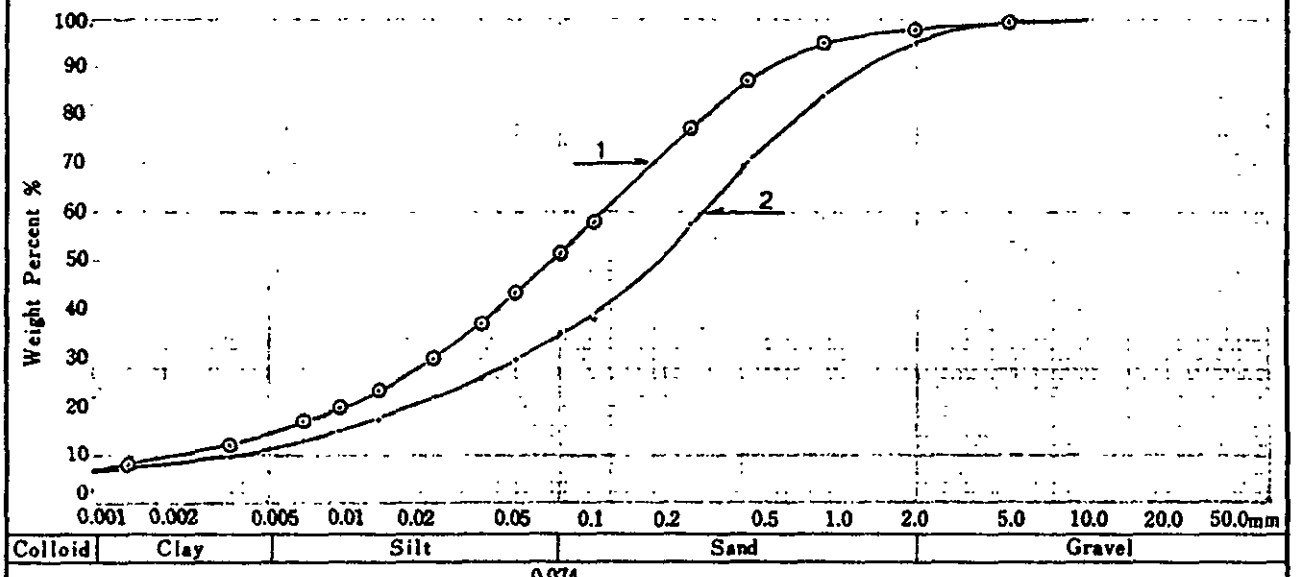

	Sample	Depth ft	Textural Classification	Gravel %	Sand %	Silt %	Clay %	60% Grain Size D_{60} mm	Effective Grain Size D_{10} mm	Uniformity Coefficient U_c	Max. Grain Size mm
1	TF3-5	15.0 ~ .	(SC) SC	2.0 (1.0)	56.0 (57.0)	27.5 (27.5)	14.5 (14.5)	0.155	0.0017	91.2	9.52
2	TF3-7	30.0 ~ .	(SC) SC	3.0 (1.5)	58.0 (59.5)	26.0 (26.0)	13.0 (13.0)	0.190	0.0025	76.0	9.52
3		. ~ .									

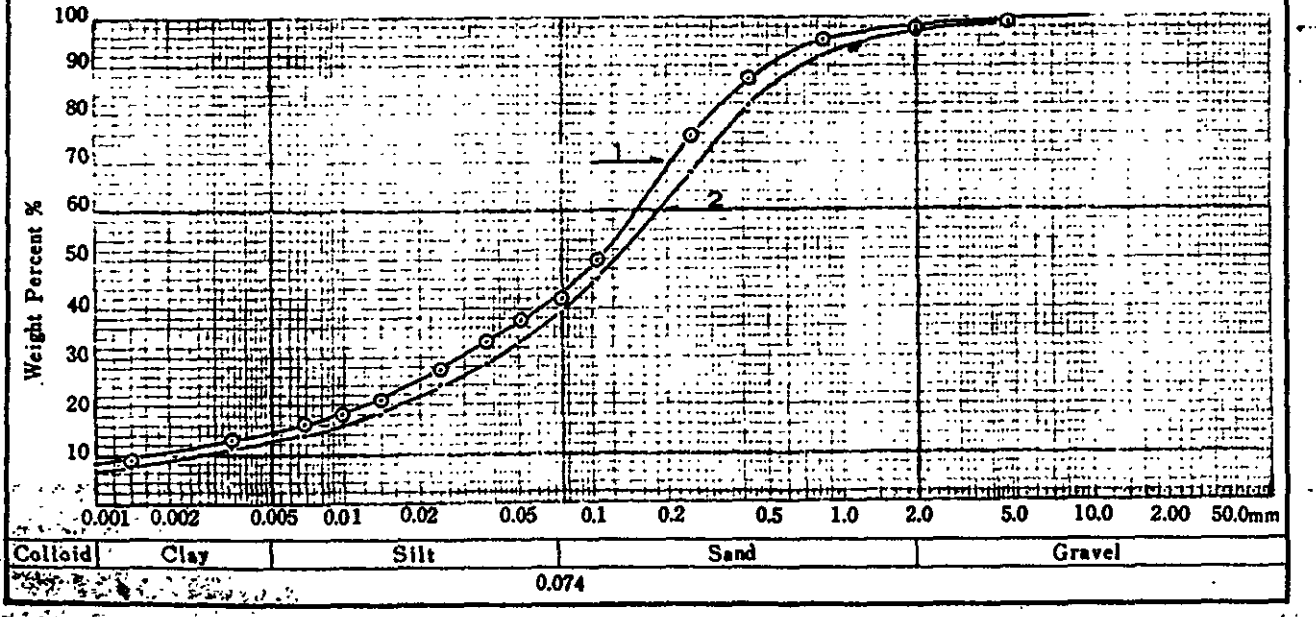

P

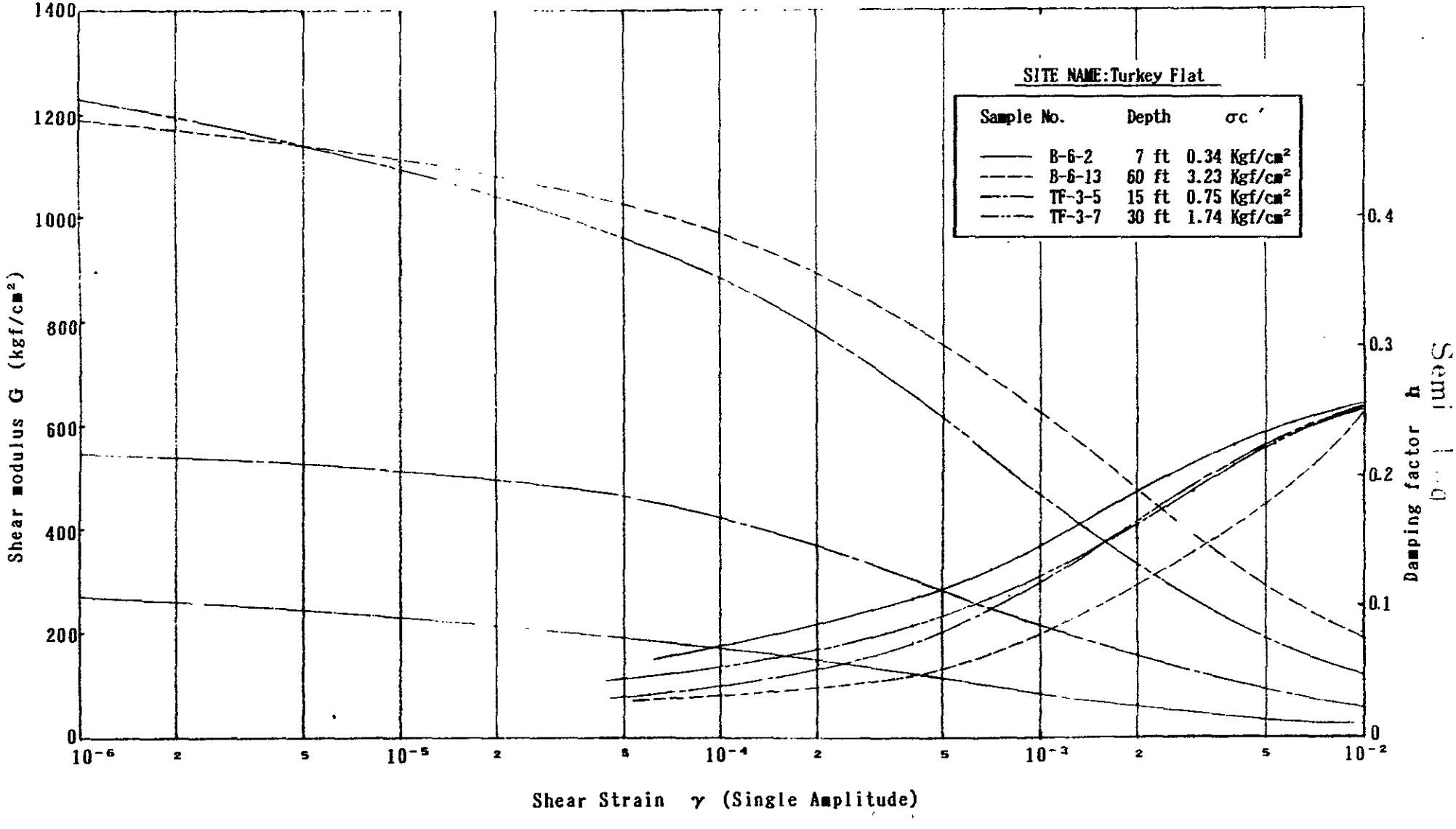

Fig.65 G～γ, h～γ Curve

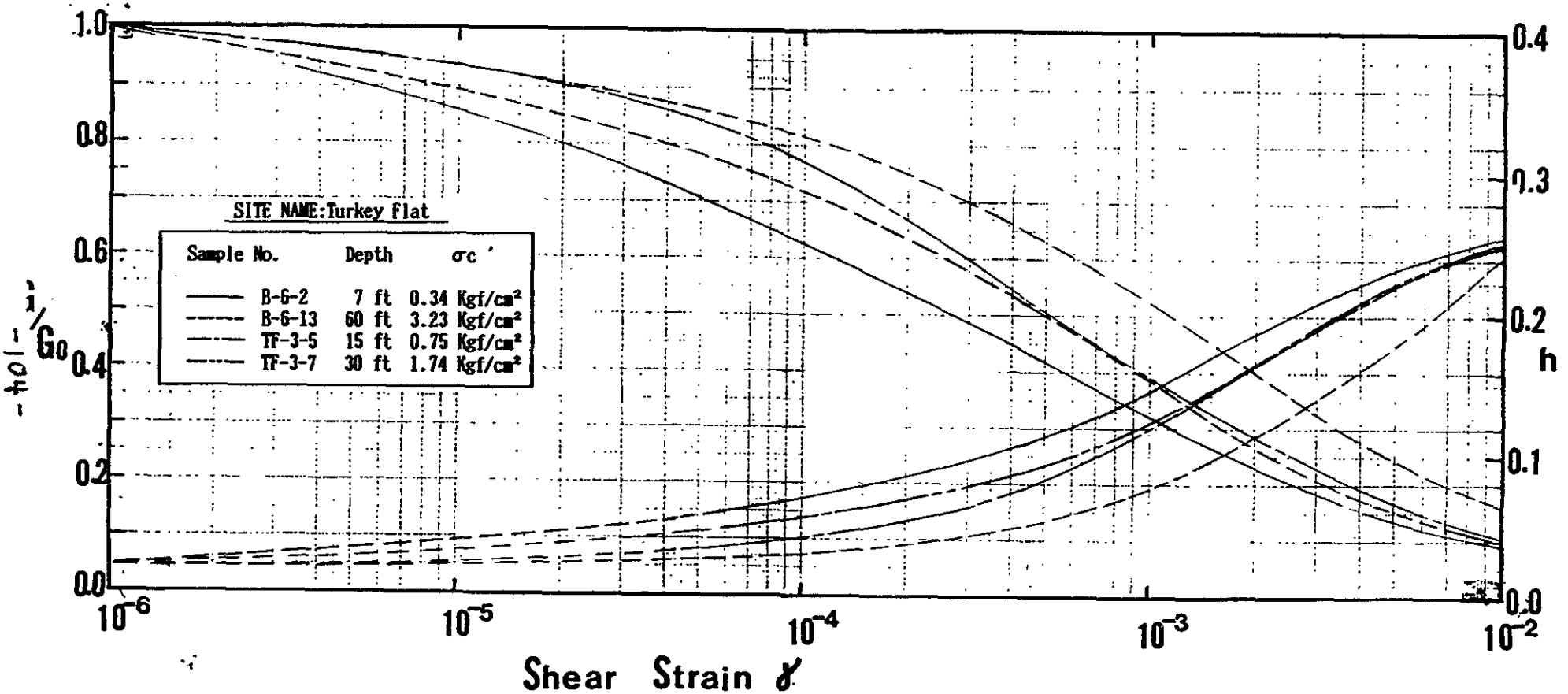

Fig.66 G/Go～γ, h～γ Curve

Table. 1 4 Result of Triaxial Ultrasonic Wave Velocity Measurement

Sample NO.	Depth(ft)	Diameter (cm)	Height (cm)	Unit weight (gf/cm³)	Moisture content (%)	Confining pressure (kgf/cm²)	Propagation time (μs)		Ultrasonic wave velocity (km/s)		Poisson's ratio
							Tp	Ts	Vp	Vs	
B-6-2	7.0	5.141	4.995	1.531	23.9	0.0	64.4	131.2	0.78	0.38	0.34
						0.4	64.4	130.4	0.78	0.38	0.34
B-6-13	60.0	4.862	4.040	1.641	17.1	0.0	60.6	119.2	0.67	0.34	0.33
						3.5	35.1	101.4	1.15	0.40	0.43
TF-3-5	15.0	5.095	3.295	1.698	22.9	0.0	28.0	61.2	1.18	0.54	0.37
						0.8	28.0	59.8	1.18	0.55	0.36
TF-3-7	30.0	5.128	5.558	1.935	18.2	0.0	59.1	162.0	0.94	0.34	0.42
						1.7	46.6	141.4	1.19	0.39	0.44

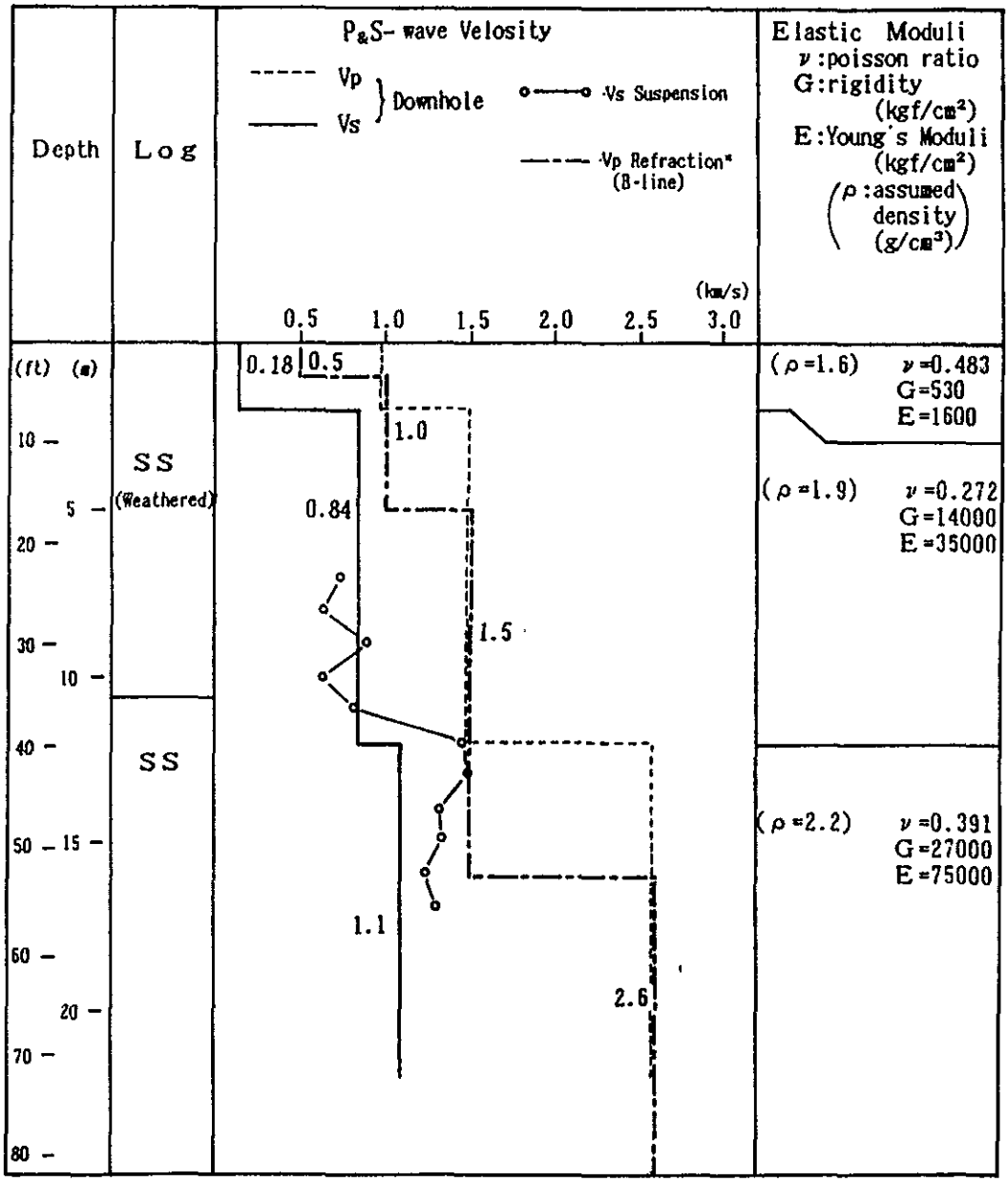

(*) B-line is 20m away from Bor. No. 2
SS: sand stone

Fig.69 Ground Conditions around Bor.No.2

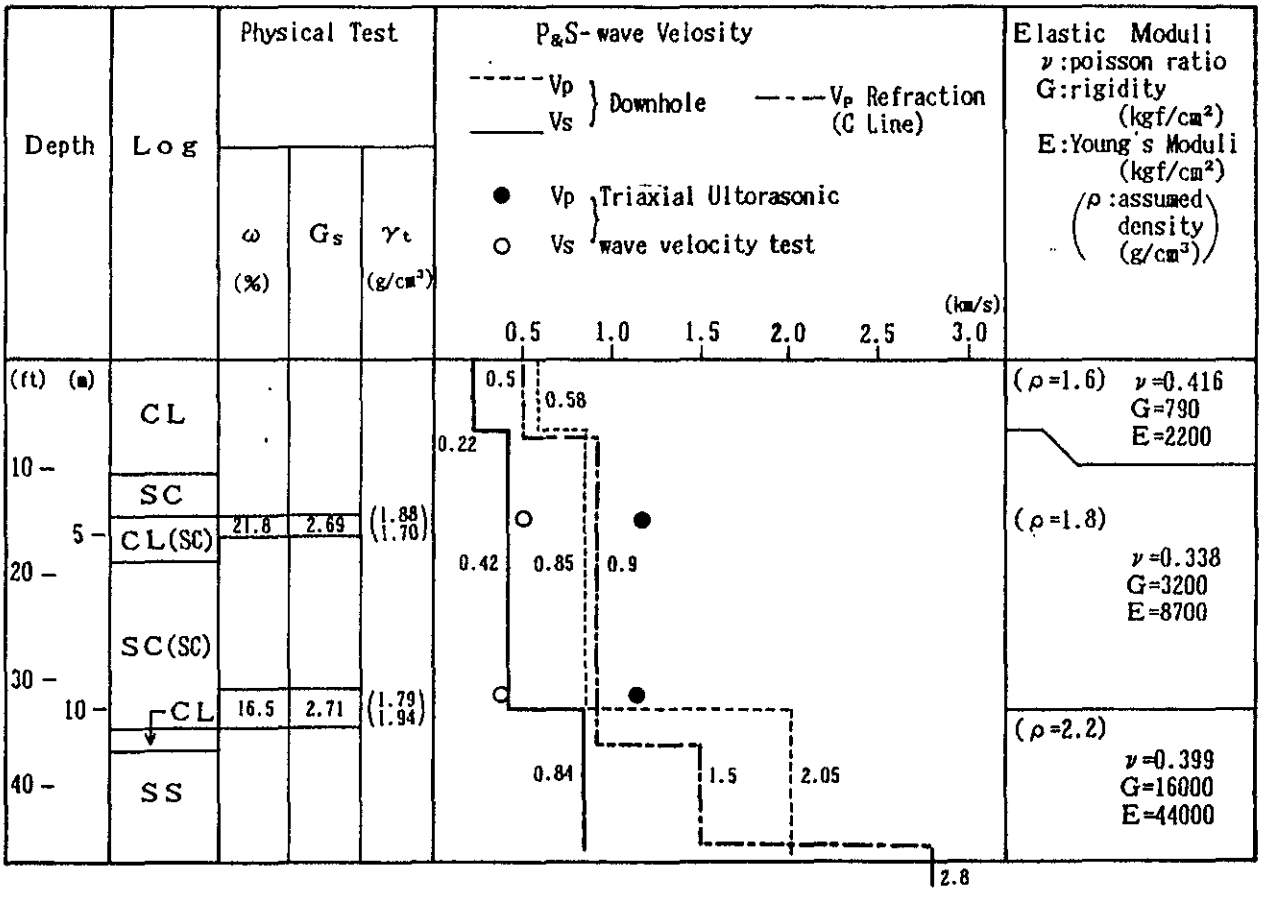

CL: low liquid limited clay
SC: clayey sand
SS: sand stone

Fig.70 Ground Conditions around Bor.No.3

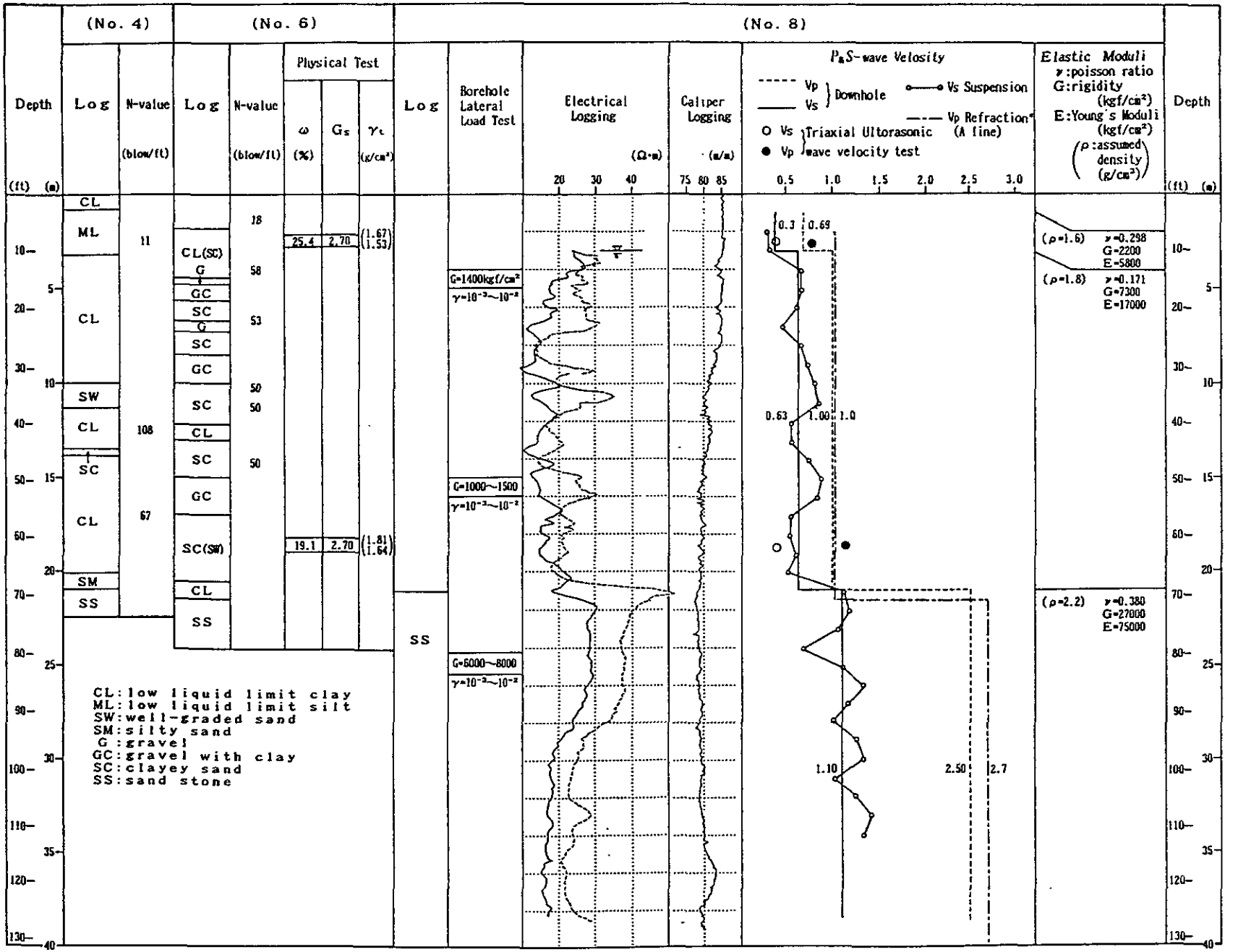

Fig.71 Ground Conditions around Bor.No.8

Table 16 Ground Model at Strong Motion Observation Point

Rock North (assumed)

	Vs (Vp) (km/s)	ρ (g/m³)	H (m)	DD Curve No
0	0.2 (0.6)	(1.6)	1	③
1	1.1 (2.8)	(2.2)	–	–

Rock South

	Vs (Vp) (km/s)	ρ (g/m³)	H (m)	DD Curve No
0	0.2 (0.6)	(1.6)	2	③
2	0.84 (1.5)	(1.9)	10	–
12	1.1 (2.6)	(2.2)	–	–

Valley North

	Vs (Vp) (km/s)	ρ (g/m³)	H (m)	DD Curve No
0	0.2 (0.6)	(1.6)	2	①
2	0.42 (0.90)	(1.8)	8	④
10	0.84 (1.5)	(1.9)	4	–
14	1.1 (2.8)	(2.2)	–	–

Valley Center

	Vs (Vp) (km/s)	ρ (g/m³)	H (m)	DD Curve No
0	0.2 (0.6)	(1.6)	2	①
2	0.63 (1.0)	(1.8)	19	②
21	1.1 (2.7)	(2.2)	–	–

Vs : S-wave Velocity

Vp : P-wave Velocity

ρ : unit volume mass

H : layer thickness

DD Curue : dynamic deformation characteristics curue

① NO.6 7ft

② NO.6 60ft

③ NO.3 15ft (after Fig.72)

④ NO.3 30ft

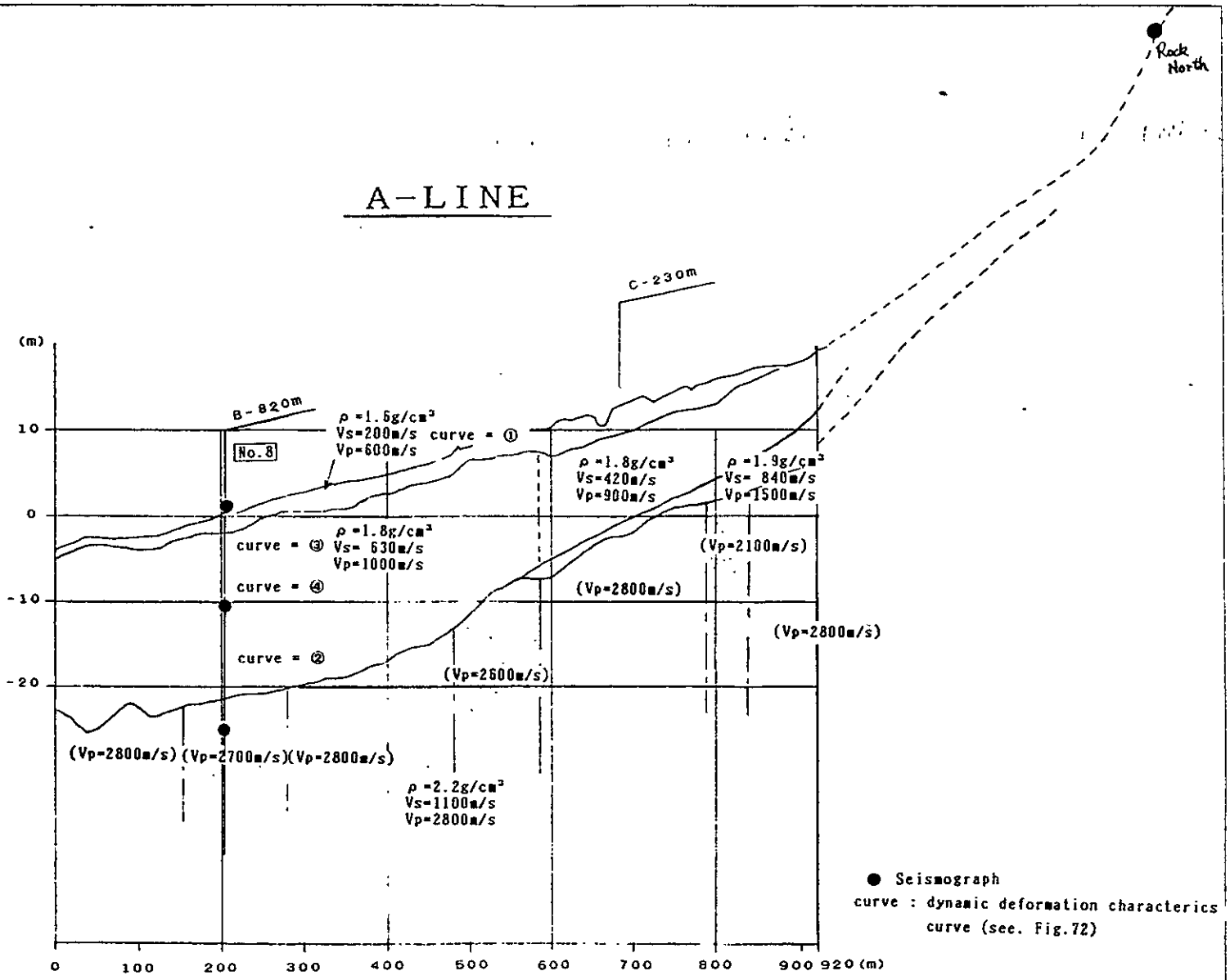

Fig.74 Cross Section of Numerical Model

B-LINE

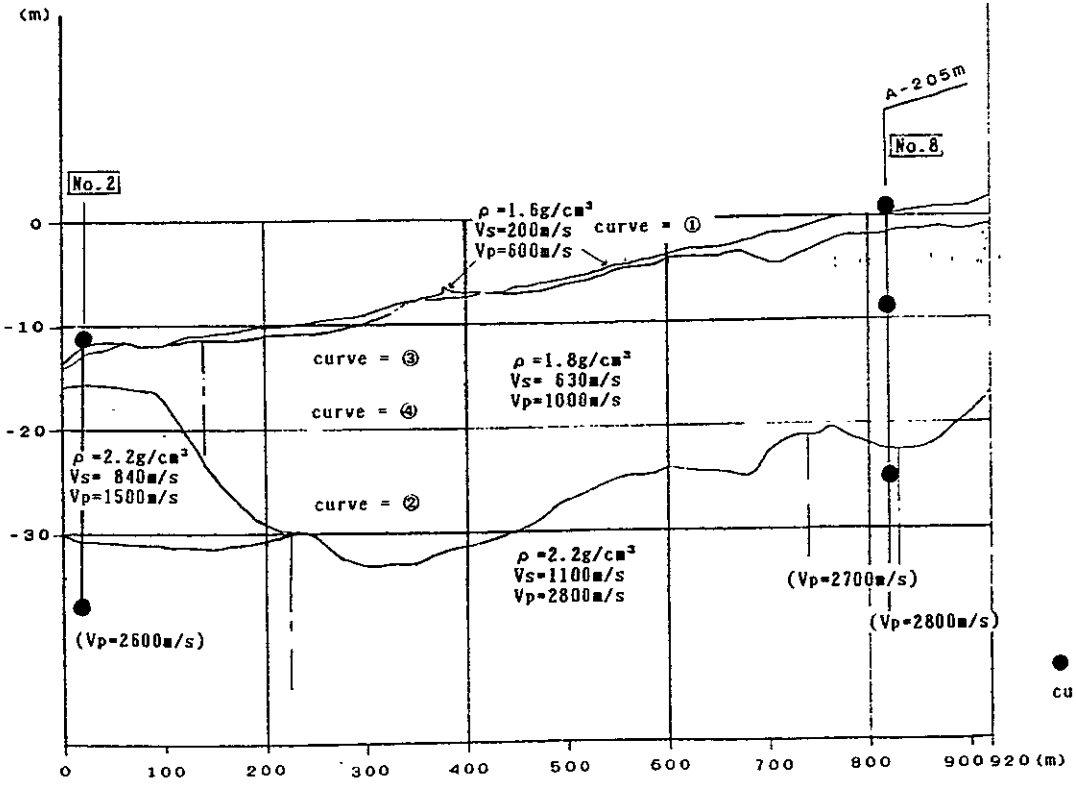

Fig.75 Cross Section of Numerical Model

C-LINE

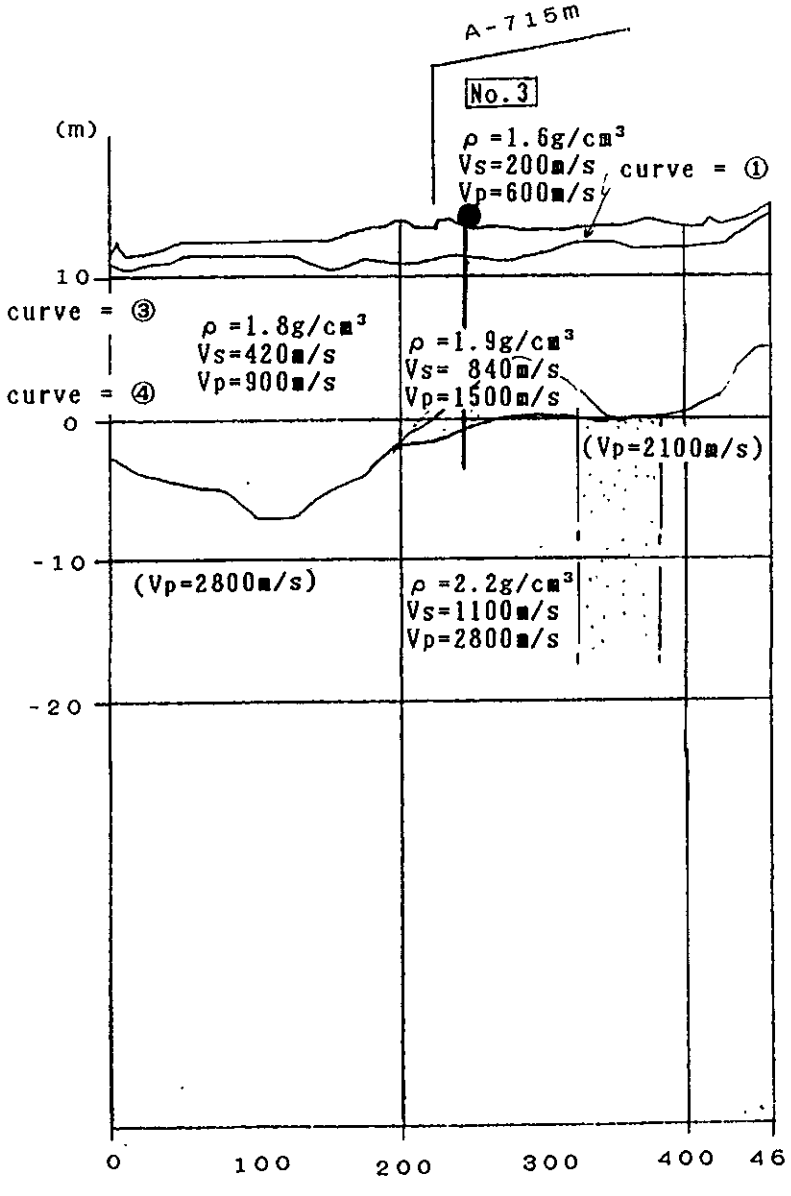

● Seismograph

curve : dynamic deformation characterics curve (see. Fig.72)

Fig.76 Cross Section of Numerical Model

PART 2
DEEP REFLECTION PROFILING

REPORT
ON A GEOLOGICAL INTERPRETATION OF THE SEISMIC REFLECTION PROFILE AT PARKFIELD TEST SITE

OCT. 1987

OYO CORPORATION

1. Introduction

We conducted a geological interpretation of a profile obtained by the seismic reflection exploration that was carried out to explore a somewhat deep structure of the test site at the same time as the Parkfield test. Using both the regional geological map around the test site by Dibblee (1980), and well logging data from the borehole VARIAN #1 located approximately 6 miles northwest from the seismic measuring line, the geological interpretation was conducted according to the following steps:

(1) From the regional geological map, the geological structures at the seismic measuring line and VARIAN #1 site were inferred, and the geological cross sections at both sites were constructed.

(2) Based on the geological cross section at the seismic measuring line obtained in (1), the geological interpretation of the reflection profile was conducted.

(3) Using the sonic log data taken in the borehole VARIAN #1, a synthetic reflection seismogram was calculated. After adjusting its time scale according to the ratio of the thicknesses of corresponding layers obtained from the geological cross sections at the seismic measuring line and VARIAN #1 site, the synthetic reflection seismogram was inserted into the reflection profile to clarify the origin of the reflection phases in the profile.

2. Inference of geological structure

Fig.1a shows the geological map and cross section (FF')around the test site, extracted from the Dibblee's geological map. The legend is given in Fig.1b. Fig.1a also shows the positions of the seismic measuring line and the borehole VARIAN #1.

It can be seen from this figure that the test site and VARIAN #1 site

are located in a synclinal structure as a result of strong folding between Gold hill fault and Maxim fault. The seismic measuring line intersects the synclinal axis.

In order to make it easy to see the structures at both sites, the geological map was enlarged (Fig.2). In addition to the synclinal axis, the figure shows strike lines for layers Te and Tm and their dips around both sites.

On the basis of these results, the geological cross sections (AA'and BB') of both sites were constructed, as shown in Fig.3.

3. Calculation of synthetic reflection seismogram

Fig.4 shows the five kinds of well logging data obtained in VARIAN #1.

Of these well logging data, the sonic log data were used to calculate a synthetic reflection seismogram, according to the following procedure:

(1) Since the reflection profile was expressed in two-way time, the original sonic log data were converted to two-way time data. That is, let d_i and V_i be the depth to the bottom of i-th layer and the velocity of i-th layer, respectively, then the interval transit time in this layer T_i is written as $T_i=(d_i-d_{i-1})/V_i$. So depth to two-way time coordinate transformation is expressed, as

$$d_i \rightarrow t_i=2\ \Sigma T_i.$$

(2) From the velocity value series V_i thus obtained, the reflection coefficient series R_i was calculated, as

$$R_i=(V_i-V_{i-1})/(V_i+V_{i-1}),$$

where the density was assumed to be constant.

(3) The synthetic reflection seismogram X was obtained by convolution of the reflection coefficient series R_i to the wavelet W which had the same characteristics as the final filter used in processing the

reflection data, i.e.,

$X=W*R$, (* means convolution operation).

The synthetic reflection seismogram thus obtained is shown in Fig.5. The figure also shows the sonic log data, depths and inferred geology expressed in two-way time.

4. Geological interpretation of reflection profile

A time profile obtained by the seismic reflection exploration is shown in Fig.6. Many reflection phases with good continuity can be seen up to the time of 0.6 seconds.

The approximate maximum thickness of each layer under the seismic measuring line in the geological cross section shown in the upper part of Fig.3 were determined as follows: Qoa 70 ft; Te 2000 ft; and Tm 1000 ft. From the refraction survey results in the Parkfield test and sonic log data in VARIAN #1, a velocity value of 3280 ft/sec (1km/sec) can be assumed for the layer Qoa, and for the layers Te and Tm 9843 ft/sec (3km/sec). Using these thicknesses and velocity values, two-way time to the bottom of each layer was calculated as follows: 43 msec for the layer Qoa, 449 msec for the layer Te and 652 msec for the layer Tm.

A geological interpretation of the reflection profile was conducted, based on the correlation between these two-way times and remarkable reflection phases in the reflection profile. This is given in Fig.7. In this figure, the solid lines indicate estimated layer boundaries and the two most remarkable reflection phases in layer Te. The depth to each reflector was calculated using the above velocity values, and shown over the each solid line.

In order to know what lithological variation two remarkable reflection phases in the layer Te correspond to, the part corresponding to the layer Te

was picked out from the synthetic reflection seismogram shown in Fig.5 and was inserted into the reflection profile. Time scale of the synthetic reflection seismogram inserted was adjusted according to the ratio of the thicknesses of layer Te below the seismic measuring line and that below VARIAN #1 site. The result is given in Fig.8. From this figure and Fig. 5, it can be inferred that these two remarkable reflection phases in layer Te correspond to the low velocity zone in the middle of the layer Te, which can be seen in VARIAN #1 sonic log data.

5. Conclusion

Using a geological map around the test site and well logging data from the borehole VARIAN #1, a geological interpretation of a seismic reflection profile was conducted.

Since VARIAN #1 was somewhat distant from the test site, the synthetic reflection seismogram made from the sonic log data obtained in this borehole could not be directly compared to the reflection profile. Therefore, the geological cross sections for both sites were inferred from the geological map, and on the basis of these cross sections, both synthetic and observed data were compared.

From the geological interpretation, it was found that the reflection profile showed the geological structure to a depth of approximately 3000 ft, that is, to the bottom of the layer Tm.

Reference

Dibblee,Jr.,T.W.(1980), "Geology along the San Andreas fault from Gilroy to Parkfield", in Studies of the San Andreas fault zone in northern California, R.Streitz and R.Sherburne Eds., California Division of Mines and Geology, Special Report 140, pp 3-18.

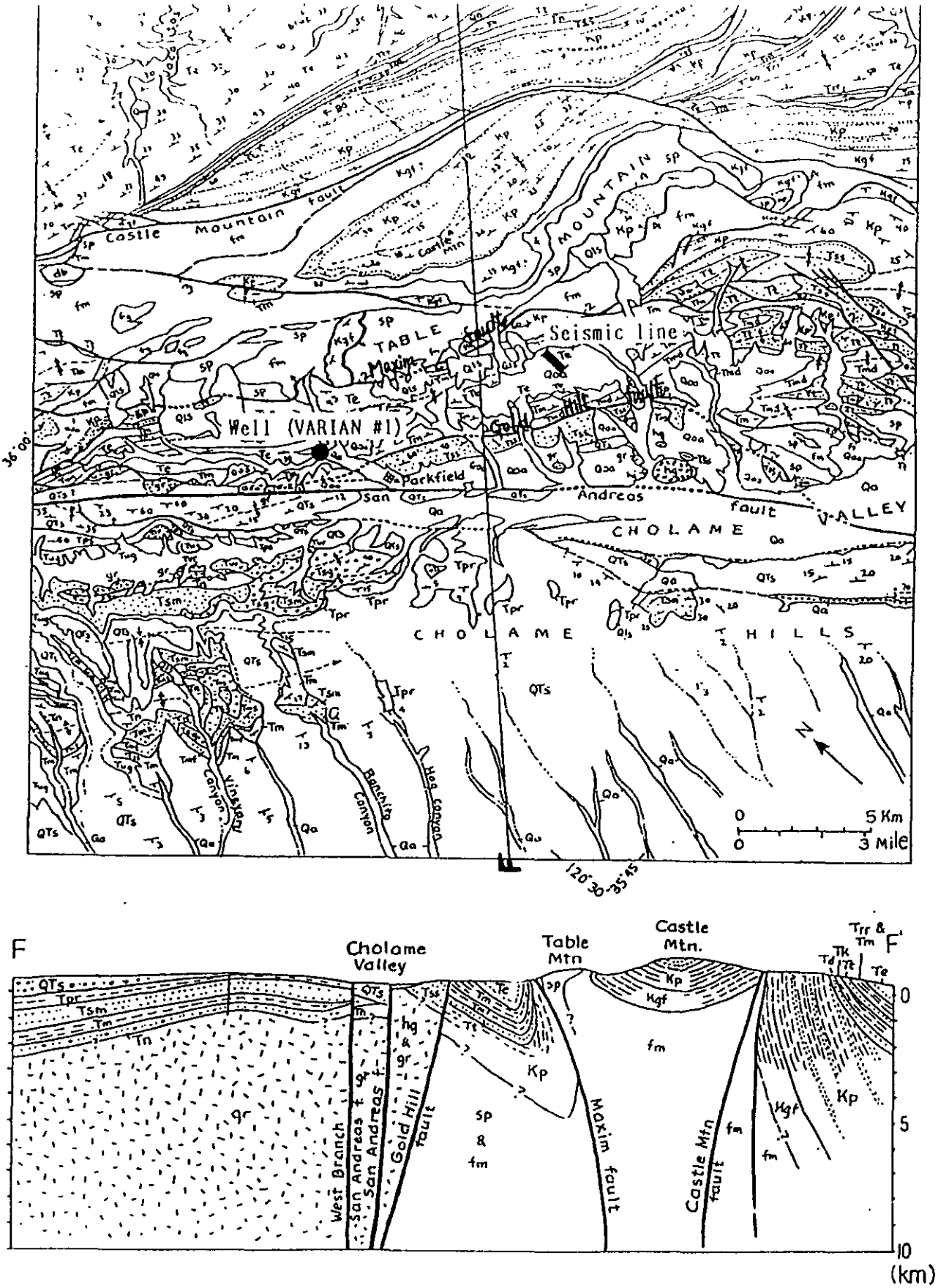

Fig.1a Geology around the test site (after Dibblee, 1980)

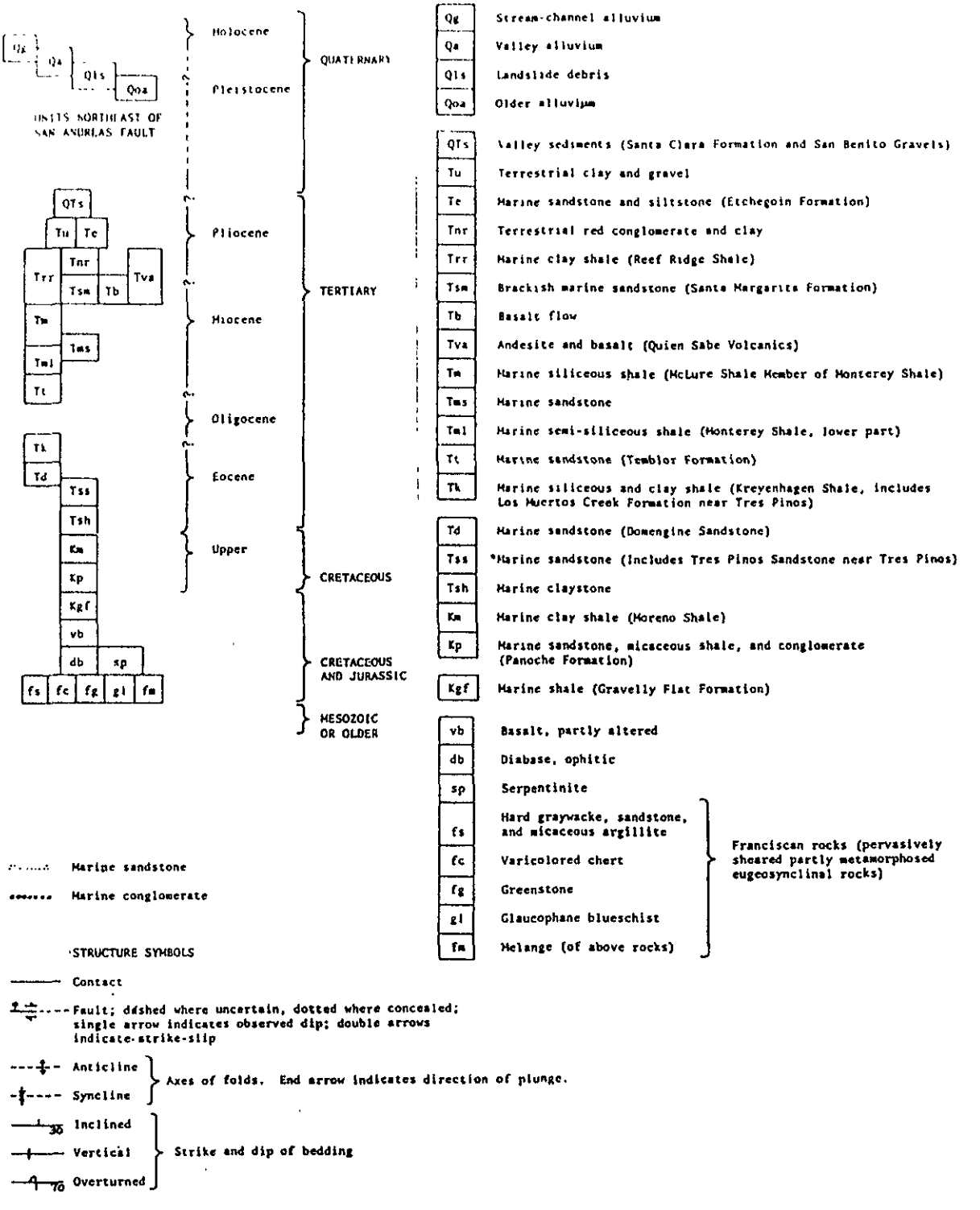

Fig.1b Description of geological units (after Dibblee, 1980)

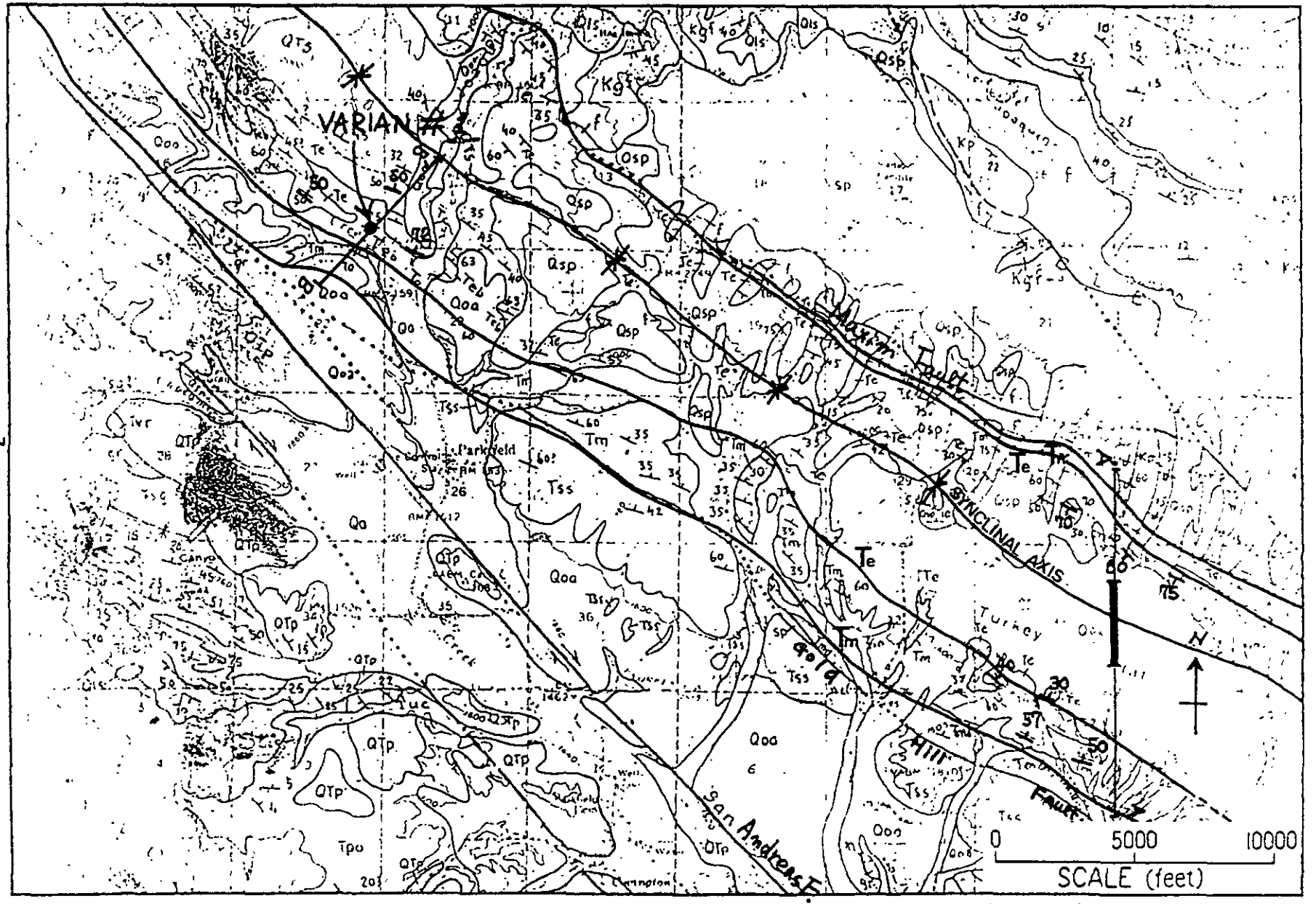

Fig.2 Synclinal structure extending through the seismic line and VARIAN #1

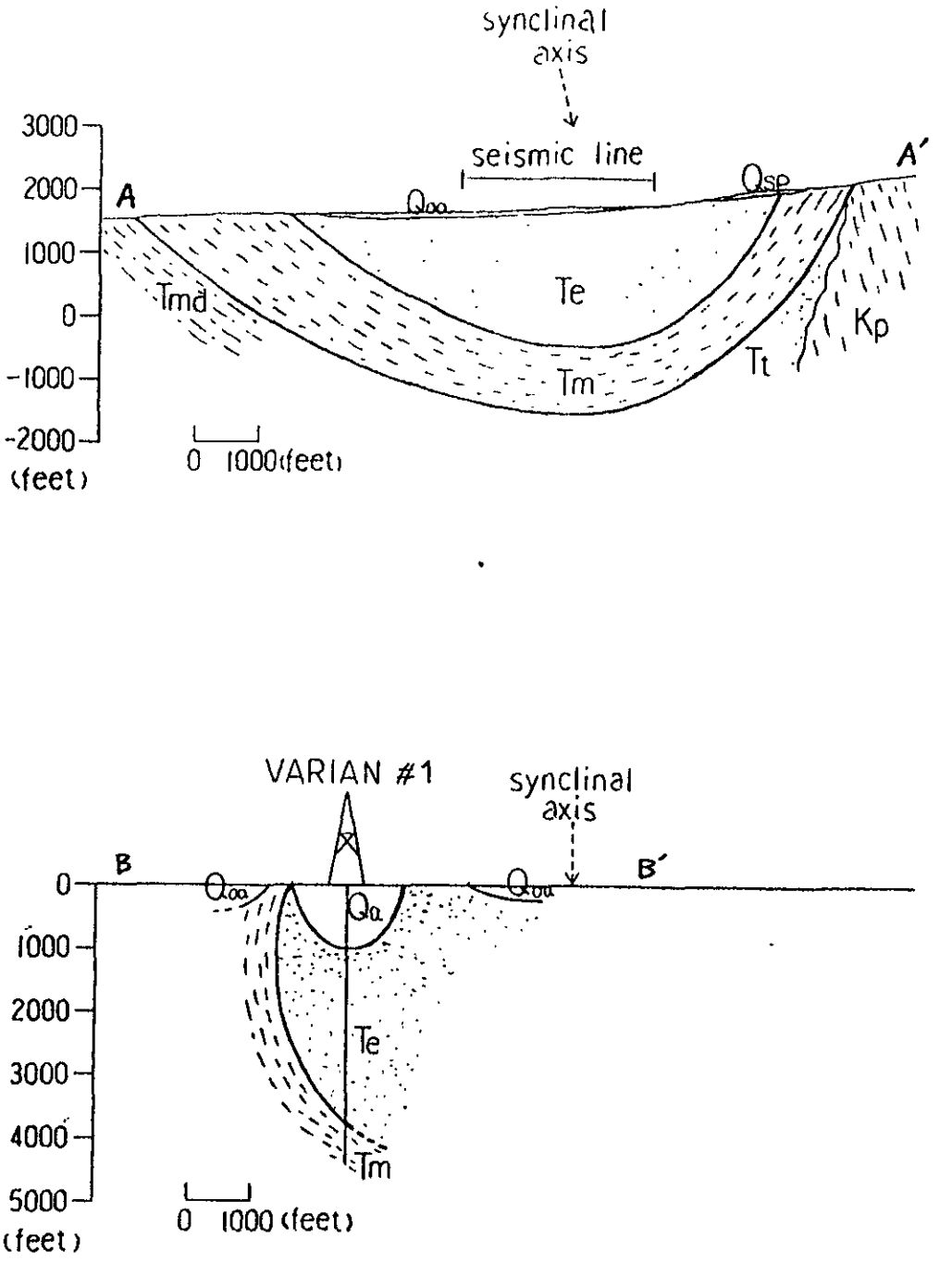

Fig.3 Geological cross sections at the seismic line and VARIAN #1

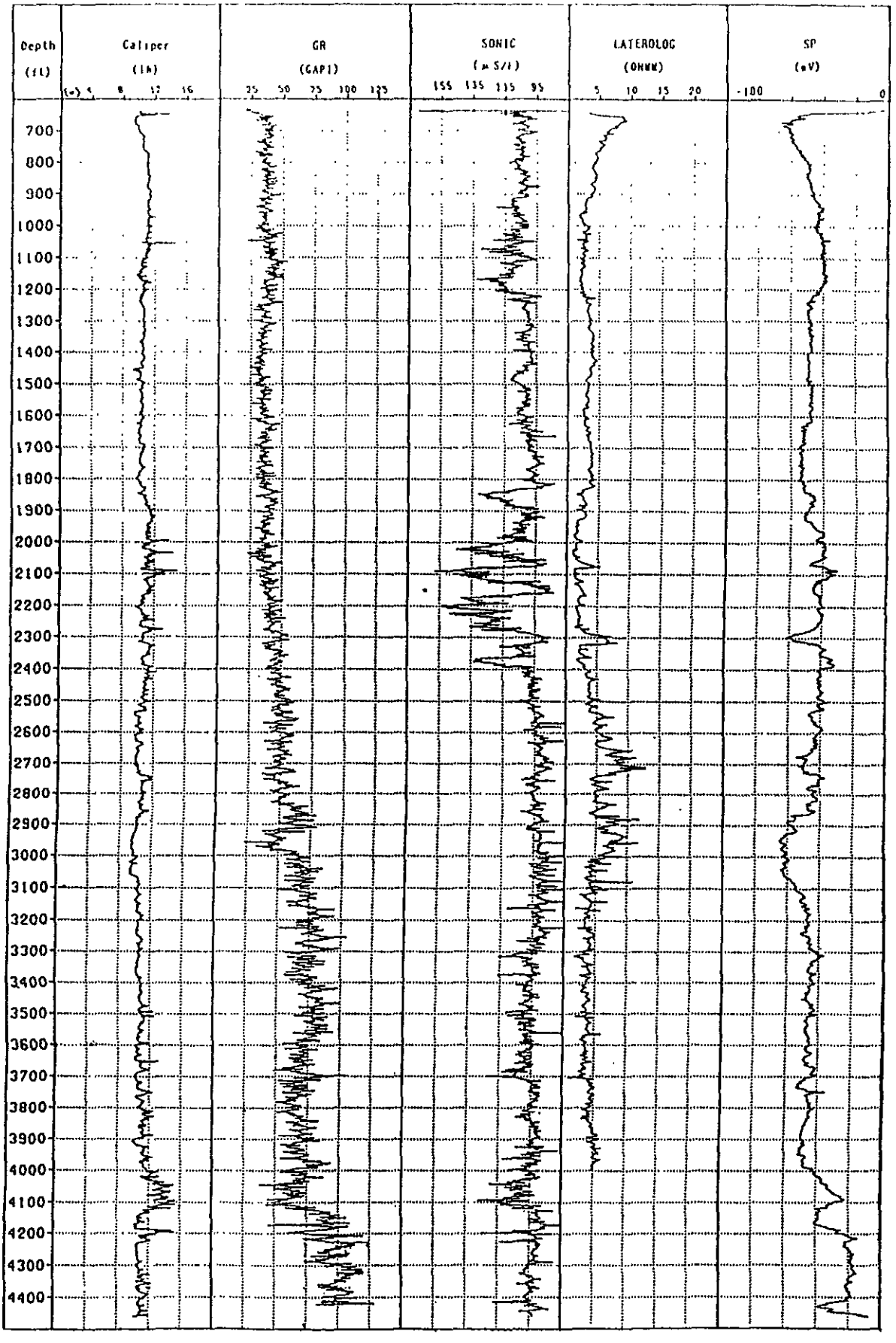

Fig.4 Well logging data obtained from VARIAN #1

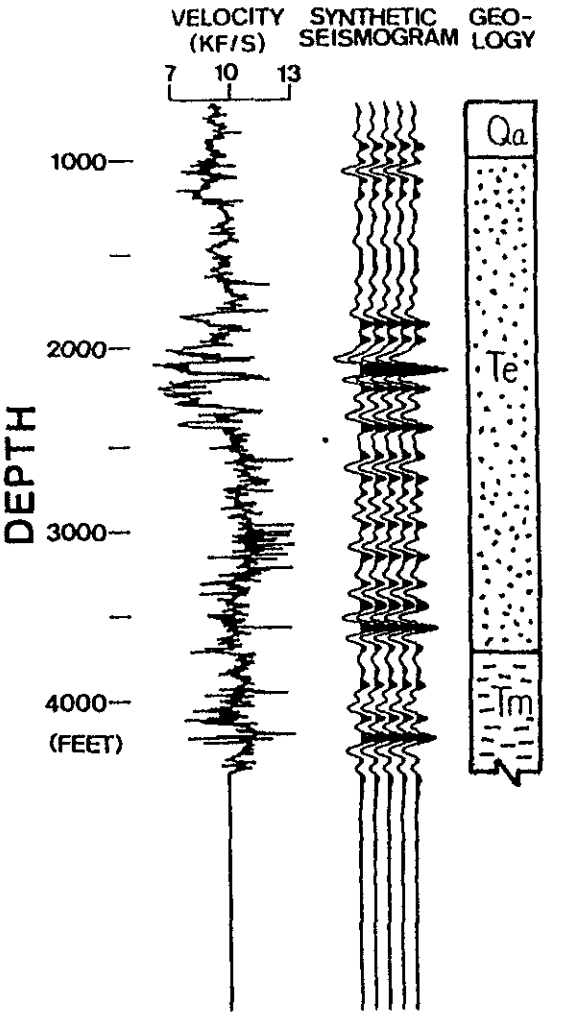

Fig.5 Synthetic reflection seismogram along with sonic log, depth and geology transformed into 2-way time scale

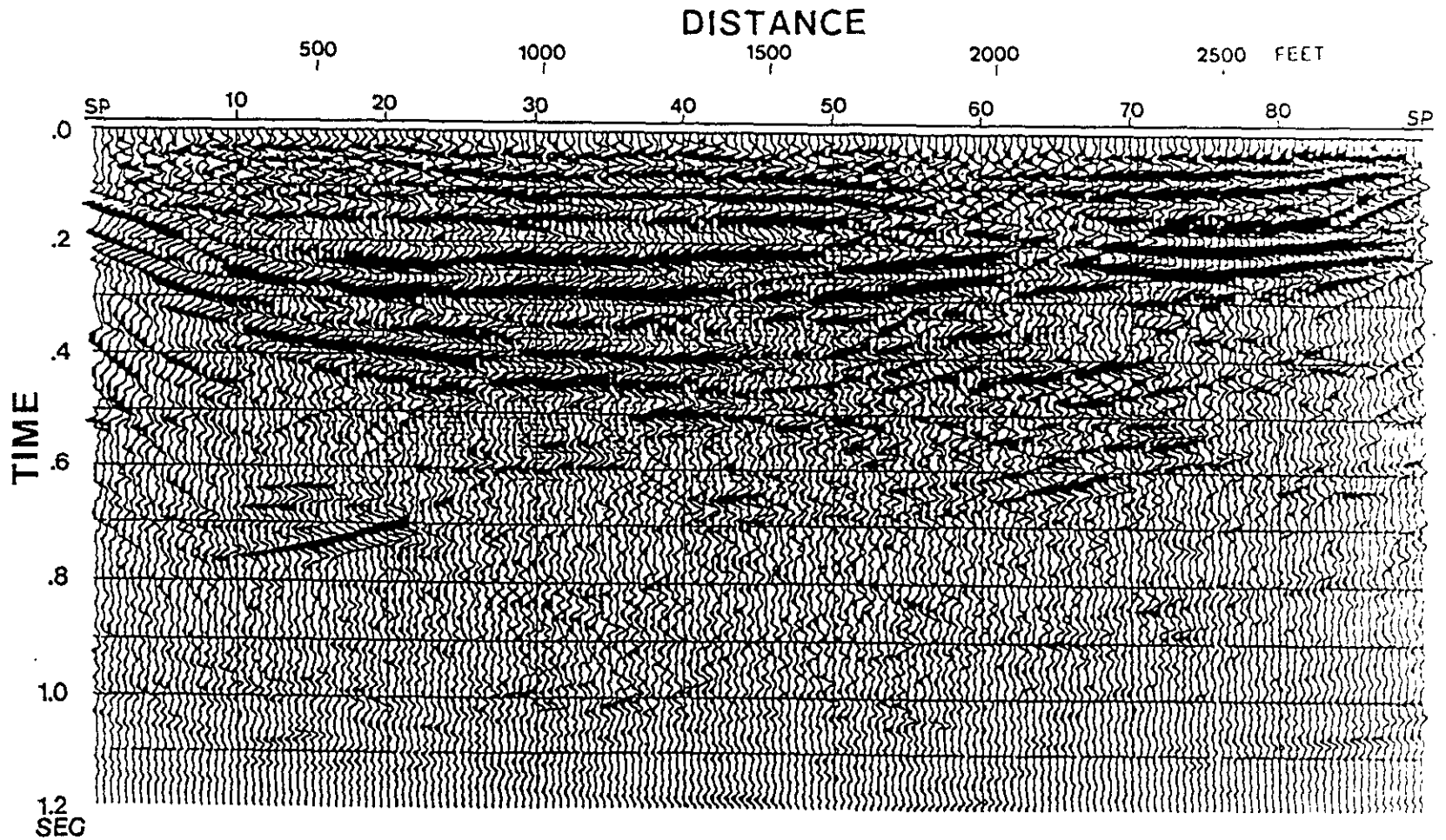

Fig.6 Seismic reflection profile

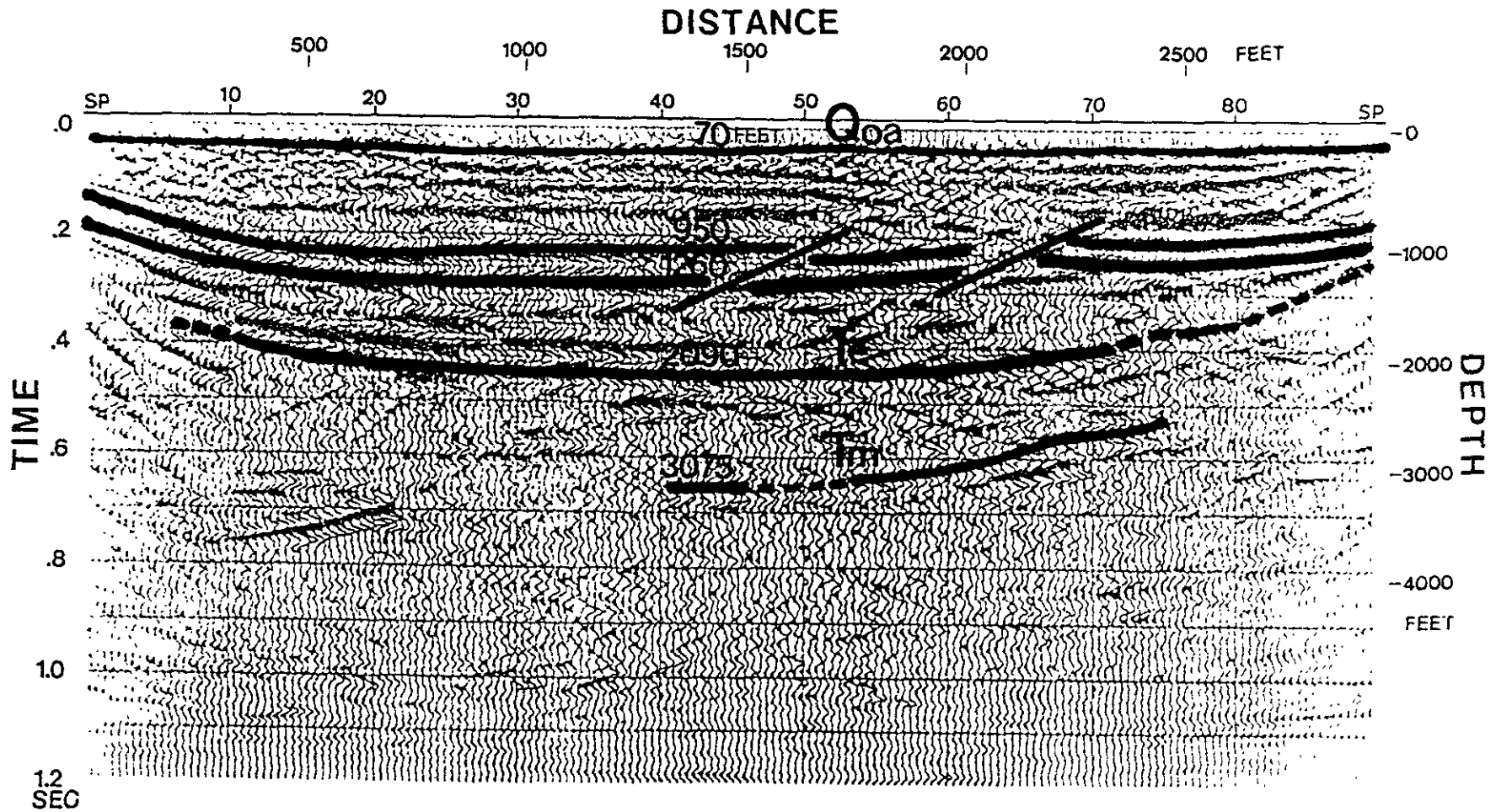

Fig.7 Geological interpretation of seismic reflection profile

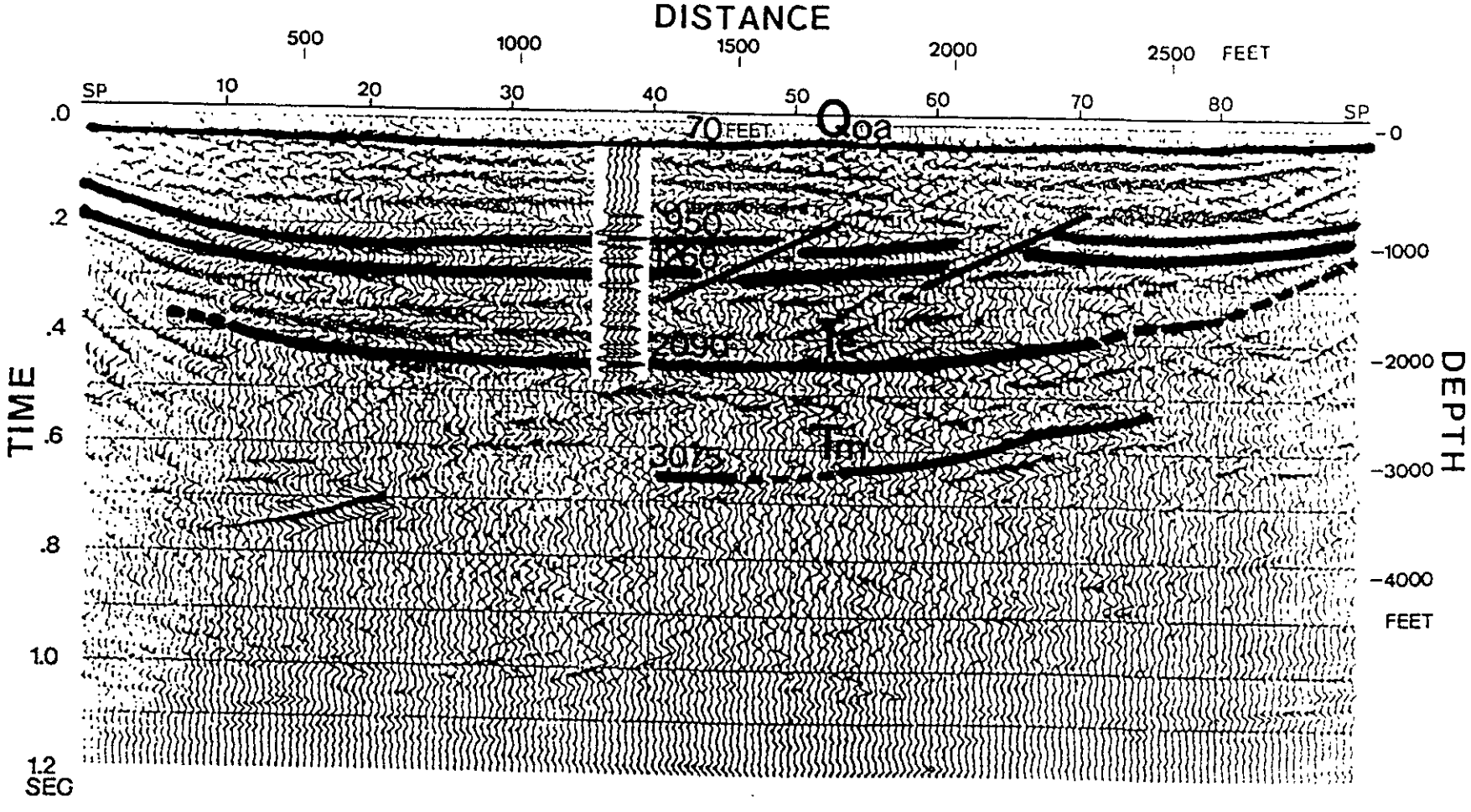

Fig.8 Comparison of synthetic seismogram with reflection profile

PART 3
LABORATORY TESTING OF ROCK SAMPLES

1987.10

[REPORT ON LABORATORY ROCK TESTING]

OYO Corporation

1. Testing Samples

The test covers sandstone obtaind from borehole TF-1 at Rock South. 8 samples from the upper part (to depth of 40 ft.) and 4 samples from the lower part (below 40 ft.) are used.

2. Types of Testing and Quantity of specimens

Cylindrical specimens whose diameter to length ratio is 1:1 are prepared. With these specimens, test for physical properties and ultrasonic wave velocity measurement are conducted. Table 1 shows types of testing and quantity of specimens.

3. Testing Method and Procedures

1) Test for Physical Properties

Using 12 specimens, following physical properties are obtained: Bulk density, Water content, Saturation ratio, Effective porosity and Water absorption.

2) Ultrasonic Wave Velocity Measurement

Measurements are conducted in unconfined condition by utilizing high frequency ultrasonic pulse transmission technique. New Sonic Viewer, manufactured by OYO Corporation, was used for this purpose.

① P and S wave velocities of 12 specimens are measured in natural water content condition.

② P and S wave velocities of each 4 specimens obtaind from the upper and the lower part are measured both in saturated and dry conditions.

③ P wave velocities of 4 specimens obtained from the upper part are measured in accordance with the change of water content by 10 steps for each specimen.

4. Testing Results

1) Description of Samples

(1) All samples are medium grain size sandstone

② The upper sandstone is light greyish brown, while the lower sondstone is bluish grey.

2) Physical Properties

Physical Properties are shown in Table 2. From these results, following characteristics are known.

① There is no remarkable difference on physical properties between the upper and lower sandstone.

② Saturated Bulk density is 2.20 ~2.23 g/cm^3 and dry one is 1.90~1.95 g/cm^3.

③ Effective porosity is 28.6 ~30.4%.

④ Water absorption is 14.8 ~16.0%.

3) Ultrasonic wave velocity

Ultrasonic wave velocities measured are shown in Table 2 and Table 3. Following characteristics are known.

① In saturated condition, Vp is in the range of 3.24 ~3.62km/s and Vs is 1.21 ~1.56 km/s with the upper sandstone, while Vp is 2.87~3.14 km/s and Vs is 0.83 ~1.09 km/s with the lower one.

② In dry condition, with the upper sandstone Vp is 1.96~2.39 km/s and Vs is 1.02~1.55 km/s, while with the lower one Vp is 1.15~1.68 km/s and Vs is 0.78~0.96 km/s.

③ Vp of the specimen varies in accordance with saturation ratio (Sr), especially within the range of Sr=60~100%.

[Notes]

A considerable time has elapsed since sampling was conducted, so it can be expected that the state of the specimens has changed during that time. Moreover, detailed information for the samples, such as sampling method, conditions of preservation etc., are unknown. Therefore we can not discuss the differences between the velocities obtained from PS logging and the laboratory testing.

Table 1 Types of Testing and Quantity of Specimens

unit :pieces

Types \ Location		TF-1 upper	TF-1 lower	Total
Physical Test		8	4	12
Ultrasonic Wave Velocity Measure-ment	natural	8	4	12
	saturated and dry	4	4	8
	change of water content	4	0	4

Table 2 Physical Properties and Ultrasonic Wave Velocities of the Test Specimens

Bor. No.	Depth (ft)	Specimen No.	Effective porosity (%)	Water absorption (%)	natural water content					Saturated			Dry		
					Bulk density (g/cm³)	Water content (%)	Saturation ratio (%)	Velocity (km/s)		Bulk density (g/cm³)	Velocity (km/s)		Bulk density (g/cm³)	Velocity (km/s)	
								Vp	Vs		Vp	Vs		Vp	Vs
TF-1	3~ 7	111	29.7	15.5	2.08	8.4	54.0	2.50	1.52	2.21	3.62	1.56	1.92	2.01	1.33
TF-1	3~ 7	112	29.9	15.6	2.10	9.5	60.9	2.15	1.32	2.22	3.53	1.35	1.92	2.01	1.03
TF-1	3~ 7	113	30.4	16.0	2.08	9.5	59.1	2.23	1.34	2.20	3.59	1.38	1.90	2.00	1.03
TF-1	16~20	121	29.7	15.6	2.06	8.3	53.2	2.23	1.42	2.20	3.36	1.44	1.91	2.00	1.25
TF-1	16~20	122	30.1	15.7	2.10	9.9	62.7	2.48	1.45	2.22	3.38	1.46	1.91	2.11	1.02
TF-1	16~20	123	28.6	14.8	2.08	7.9	53.0	2.32	1.53	2.22	3.36	1.51	1.93	2.39	1.55
TF-1	35~39	131	29.4	15.3	2.12	10.1	66.2	2.08	1.43	2.22	3.24	1.46	1.93	2.04	1.20
TF-1	35~39	132	28.8	14.8	2.13	9.3	63.1	1.99	1.19	2.23	3.26	1.21	1.95	1.96	1.12
TF-1	44~48	141	29.0	15.0	2.09	7.7	51.3	1.18	0.82	2.23	2.87	0.83	1.94	1.18	0.78
TF-1	62~66	151	29.7	15.5	2.08	9.0	58.1	1.68	1.03	2.21	3.14	1.09	1.91	1.68	0.96
TF-1	62~66	152	29.5	15.4	2.10	9.5	61.8	1.33	0.81	2.21	3.02	0.88	1.92	1.33	0.85
TF-1	62~66	153	29.7	15.6	2.07	8.4	53.9	1.17	0.82	2.20	2.97	0.87	1.91	1.15	0.79

*In saturated condition, Saturation ratio is 100 % and Water content is equal to Water absorption.
*In dry condition, Saturation ratio and Water content are 0 %.

Table 3 (1) Results of the Measurement of Ultrasonic Wave Velocity (change of water content by several steps)

Bor. No.	Depth (ft)	Specimen No.	Saturation ratio (%)	Water content (%)	Unit weight (g/cm³)	Vp (km/s)	Remarks
TF-1	3～ 7	112	100.0	15.6	2.22	3.53	saturated
			96.2	15.0	2.21	2.66	
			91.7	14.3	2.19	2.61	
			75.2	11.7	2.14	2.55	
			71.3	11.1	2.13	2.53	
			69.7	10.9	2.13	2.43	
			63.5	9.9	2.11	2.36	
			47.4	7.4	2.06	2.15	
			22.7	3.5	1.99	2.12	
			0.0	0.0	1.92	2.01	dry
	16～20	122	100.0	15.7	2.22	3.38	saturated
			94.5	14.8	2.20	2.74	
			91.4	14.4	2.19	2.69	
			76.8	12.1	2.15	2.69	
			73.5	11.5	2.14	2.53	
			72.1	11.3	2.13	2.51	
			66.9	10.5	2.12	2.48	
			53.4	8.4	2.08	2.19	
			29.6	4.6	2.00	2.38	
			0.0	0.0	1.91	2.11	dry

Table 3 (2) Results of the Measurement of Ultrasonic Wave Velocity (change of water content by several steps)

Bor. No.	Depth (ft)	Specimen No.	Saturation ratio (%)	Water content (%)	Unit weight (g/cm³)	Vp (km/s)	Remarks
TF-1	16～20	123	100.0	14.8	2.22	3.36	saturated
			96.4	14.3	2.21	2.85	
			91.9	13.6	2.19	2.78	
			75.3	11.2	2.15	2.78	
			72.0	10.7	2.14	2.61	
			70.4	10.4	2.13	2.53	
			66.4	9.9	2.12	2.50	
			55.4	8.2	2.09	2.28	
			32.8	4.9	2.03	2.40	
			0.0	0.0	1.93	2.39	dry
	35～39	132	100.0	14.8	2.23	3.26	saturated
			96.8	14.3	2.22	2.88	
			92.6	13.7	2.21	2.43	
			72.9	10.8	2.16	2.37	
			69.4	10.3	2.15	2.22	
			67.4	10.0	2.14	2.20	
			62.1	9.2	2.12	2.07	
			48.0	7.1	2.08	2.01	
			23.8	3.5	2.01	1.94	
			0.0	0.0	1.95	1.96	dry

APPENDIX G
QEST Consultants

REPORT of DOWNHOLE VELOCITY SURVEYS

at

TURKEY FLAT

by

QEST CONSULTANTS

2855 Telegraph Avenue
Suite 309
Berkeley, California 94705
415-849-2700

April 1987

Bruce B. Redpath

&

Richard C. Lee

REPORT of DOWNHOLE VELOCITY MEASUREMENTS
at
TURKEY FLAT
by
QEST CONSULTANTS
Berkeley, California

INTRODUCTION

As one of the participants in the CDMG program to compare methods of estimating the effects of surface geology on seismic motion, QEST Consultants has performed velocity measurements in two of the boreholes in the experimental array at Turkey Flat near Parkfield. Downhole shear- and compression-wave signals generated by sources on the surface were recorded at the Valley Center and South Rock locations. The measurements were made in the SINCO-cased holes provided for this purpose. In addition, measurements of the rate of attenuation of shear waves were attempted in the Valley Center hole to obtain an estimate of 'Q' for the alluvium.

INSTRUMENTATION

Our downhole transducer packages were fabricated by Slope Indicator Co.; the transducers contain Geo Space HS-J model L-1 geophone elements with a natural frequency of 10 Hz damped to 0.7 critical. A triaxial array of sensors is mounted on an assembly having fixed and spring-loaded wheels such that it tracks in one of the internal grooves of the SINCO casing, maintaining a fixed azimuthal orientation as it is moved up and down the hole. Mechanical lock-in is achieved by a nitrogen-inflated bladder.

Signals were amplified by Tektronix AM-502 differential amplifiers, monitored with a Gould digital oscilloscope, and recorded on a TEAC R61 FM data recorder. Zero-time for the hammer impact on the source is provided by a ceramic impact sensor.

All data reduction, including stacking, timing, plotting and frequency-domain analysis, was accomplished with a Norland 3001 digital signal analyzer.

RESULTS

Downhole shear-wave signals at Valley Center, generated by a wood-plank traction source, are plotted in Fig.1; corresponding travel times and velocities are shown in Fig.2. Travel times and velocities of compression-wave signals in the Valley Center hole are plotted in Fig.3.

The times of shear-wave arrivals plotted in Fig.2 represent the average of the first major peak and trough of the reversed-polarity signals. Each waveform is the result of stacking four separate impacts on the source. Times can generally be resolved to a precision of +/- 0.2 msec for shear waves, and +/- 0.1 msec for compression waves.

The shear signals observed in the borehole at the South Rock site are plotted in Fig.4. The source consisted of hammer blows against a steel

anvil bolted to the rock outcrop near the collar of the hole. Arrival times and velocities for the waveforms in Fig.4 are shown in Fig.5. Compression-wave times and velocities are plotted in Fig.6. We have computed an overall average for the compression-wave velocity in the rock, although the data points in Fig.6 show evidence of a finer velocity structure; the departure of any data point from the trend line in Fig.6 is 0.5 msec or less. The velocities in the near-surface rock are approximate values; we acknowledge that the shear and compression velocities shown for the top 5 ft are not compatible.

The attenuation of shear energy in the Valley Center hole is depicted in Fig.7 which shows the spectral slopes of the signals, referenced to the signal at 20 ft, as a function of (slant) depth. Spectral slopes, i.e. the rate of change of the logarithm of the spectral ratio with increasing frequency, were computed over a bandwidth of 20 to 150 Hz with no windowing of the signals. The rate of change of spectral slope with depth is equal to the attenuation constant 'k' in the attenuation operator $\exp(-kfR)$, where f is frequency (Hz) and R is the distance (ft) from the reference point to the measurement point. The factor Q is related to k by:

$$Q = \pi/kc$$

where c is the propagation velocity.

Spectral ratios between the measurement point and the reference point were computed separately for each direction of impact on the shear-wave source. The ratios were averaged and the spectral slope was determined for the average ratio. The values of spectral slope plotted in Fig.7 are characterized by more scatter than we would like, with some values being clearly questionable. The scatter is inherent in attempting to measure attenuation over close intervals with a narrow-band source on the surface. Nevertheless, the trend of the slopes is clear, and a least-squares fit results in a value for k of 2.1×10^{-4} sec/ft which, when combined with an average velocity of 2000 ft/sec, results in a value for Q of approximately 7.5 over the depth range of 10 to 60 ft. There is a suggestion that Q may increase between 40 and 60 ft, but the quality of the data is not adequate to resolve any such change. Estimates of the shear-wave attenuation for the South Rock site are still in progress.

The results of our velocity surveys are summarized in Table I.

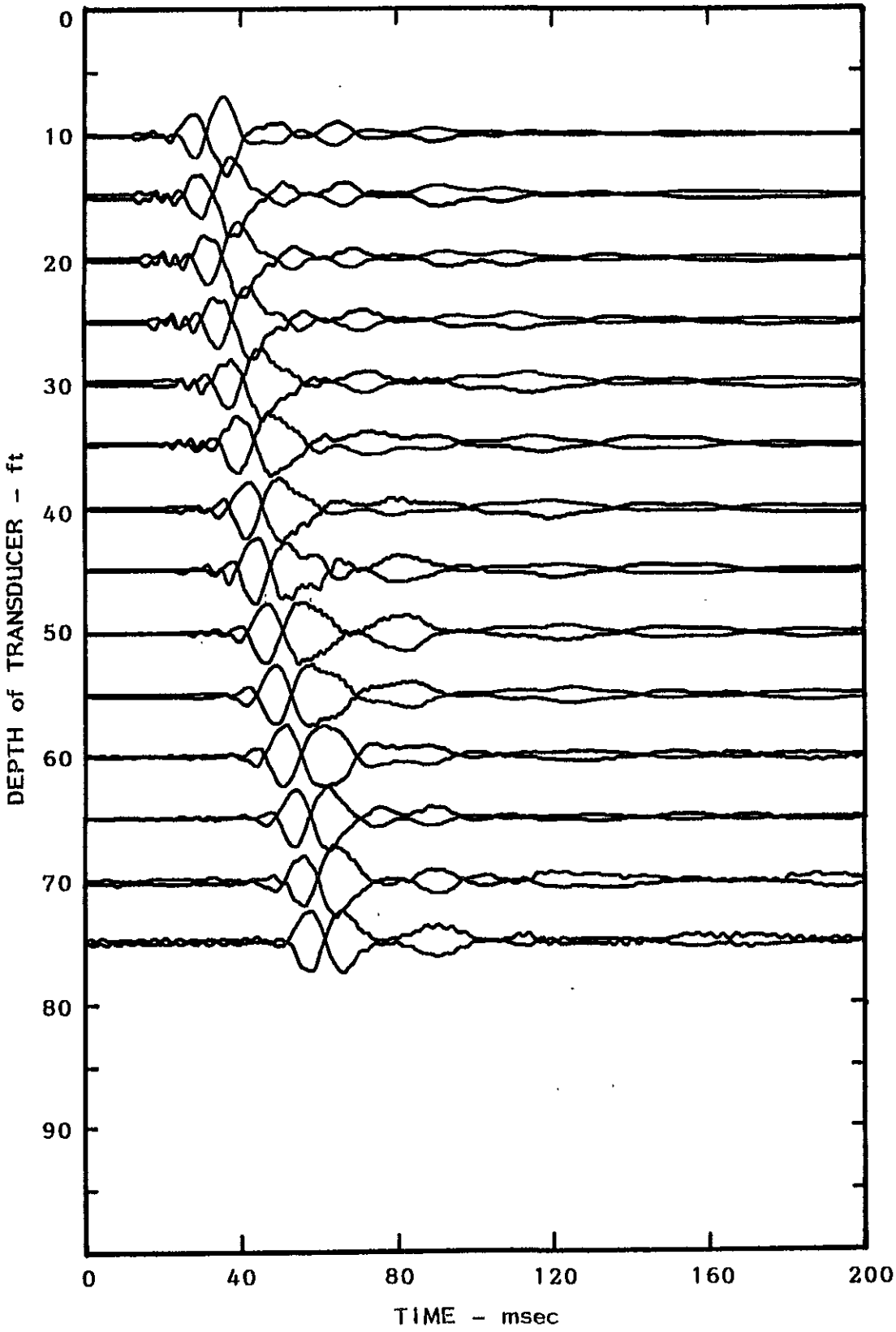

Fig.1 Signals recorded during downhole shear-wave velocity survey - Turkey Flat - Valley Center Site

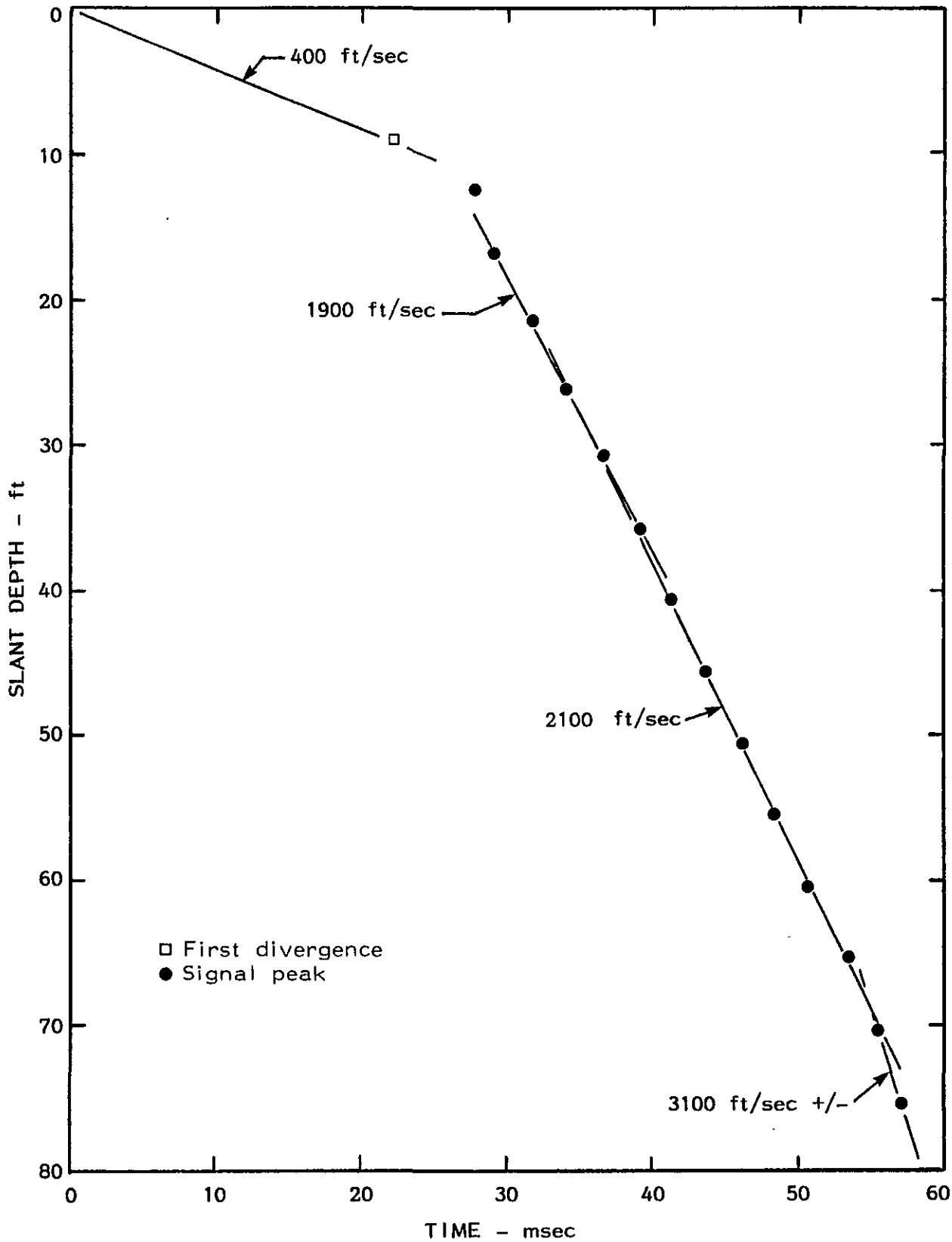

Fig.2 Travel times and velocities of shear-wave signals
Turkey Flat - Valley Center Site

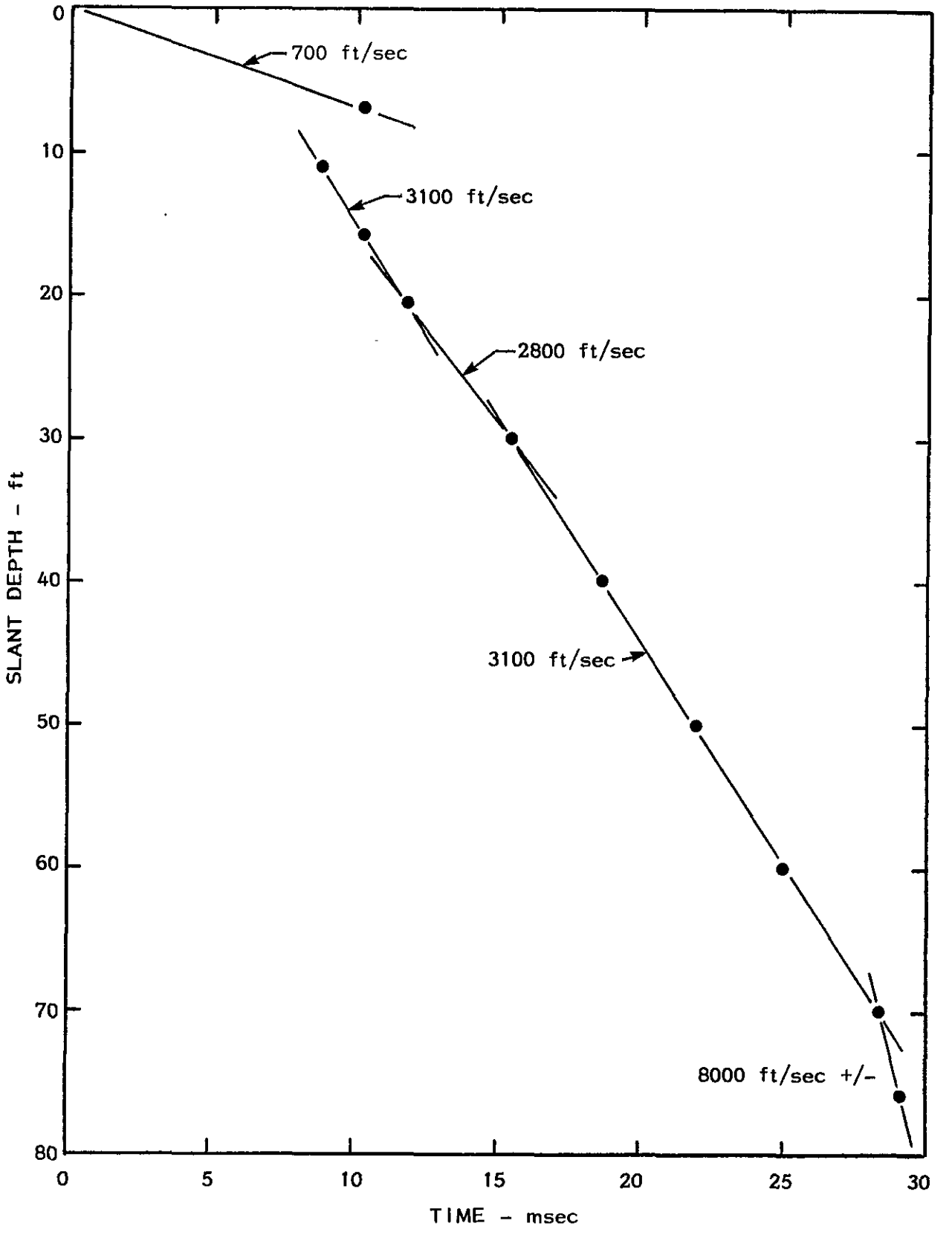

Fig.3 Travel times and velocities of compression signals
Turkey Flat - Valley Center Site

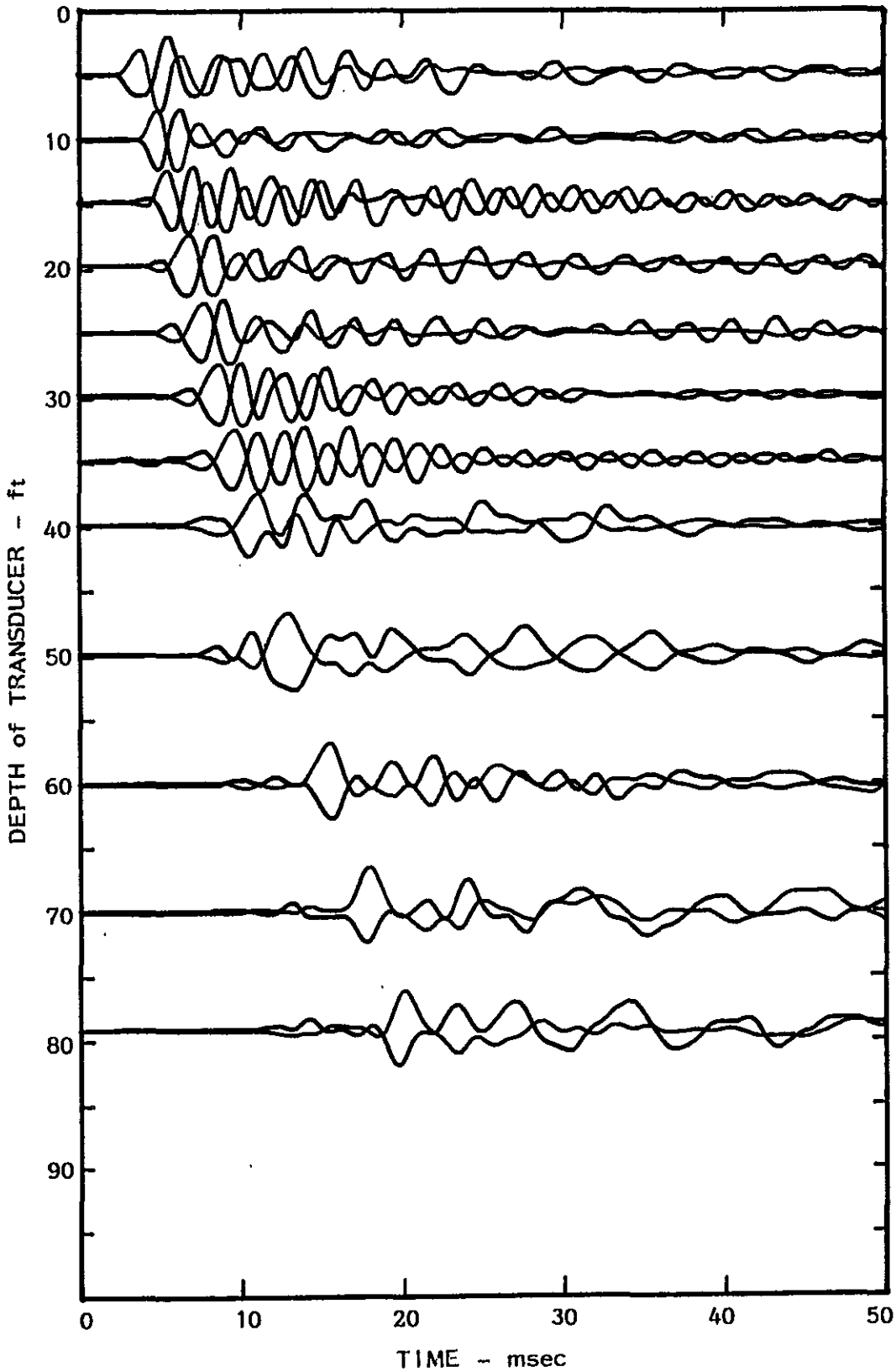

Fig.4 Signals recorded during downhole shear-wave velocity survey - Turkey Flat - South Rock Site

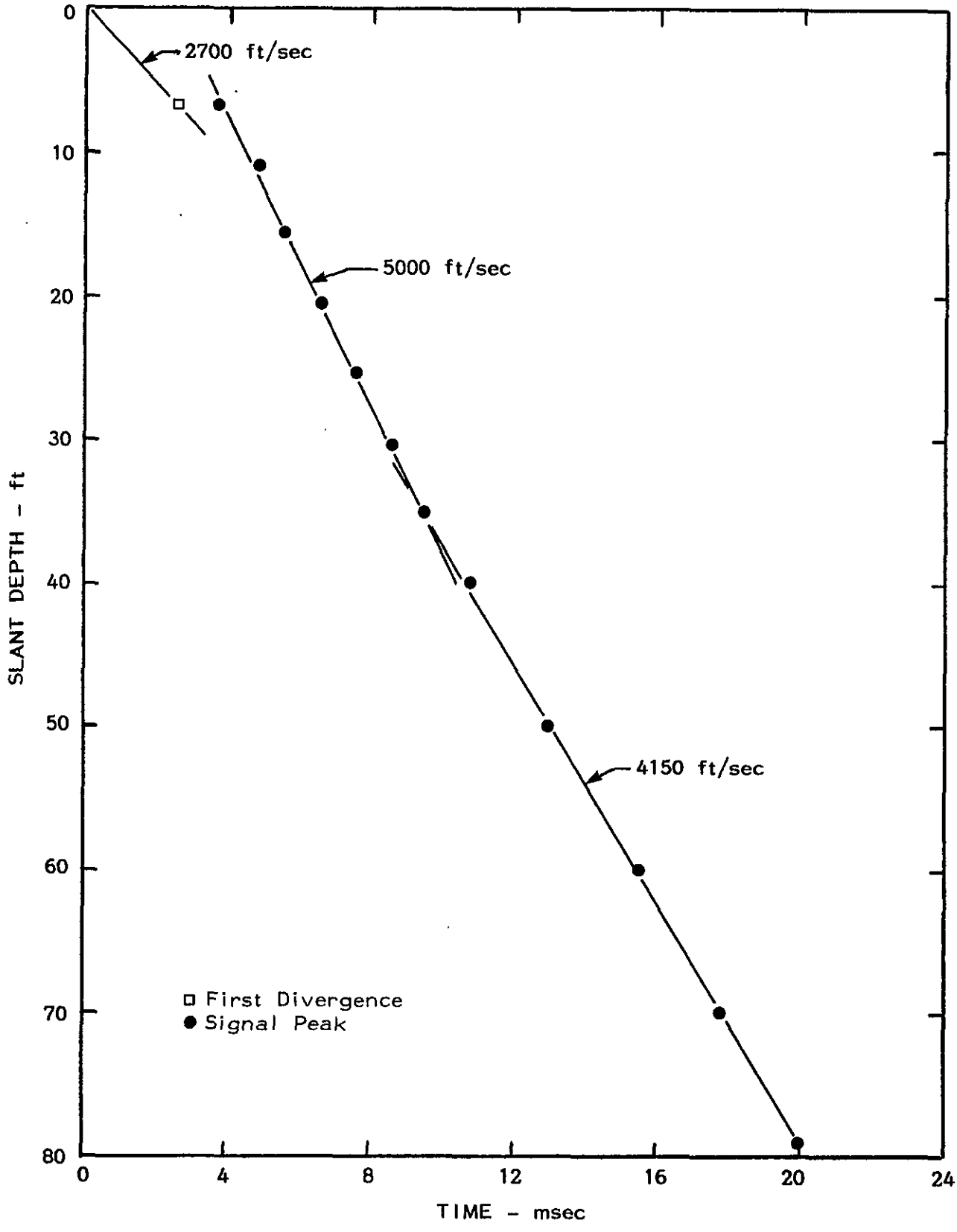

Fig.5 Travel times and velocities of shear-wave signals
Turkey Flat - South Rock Site

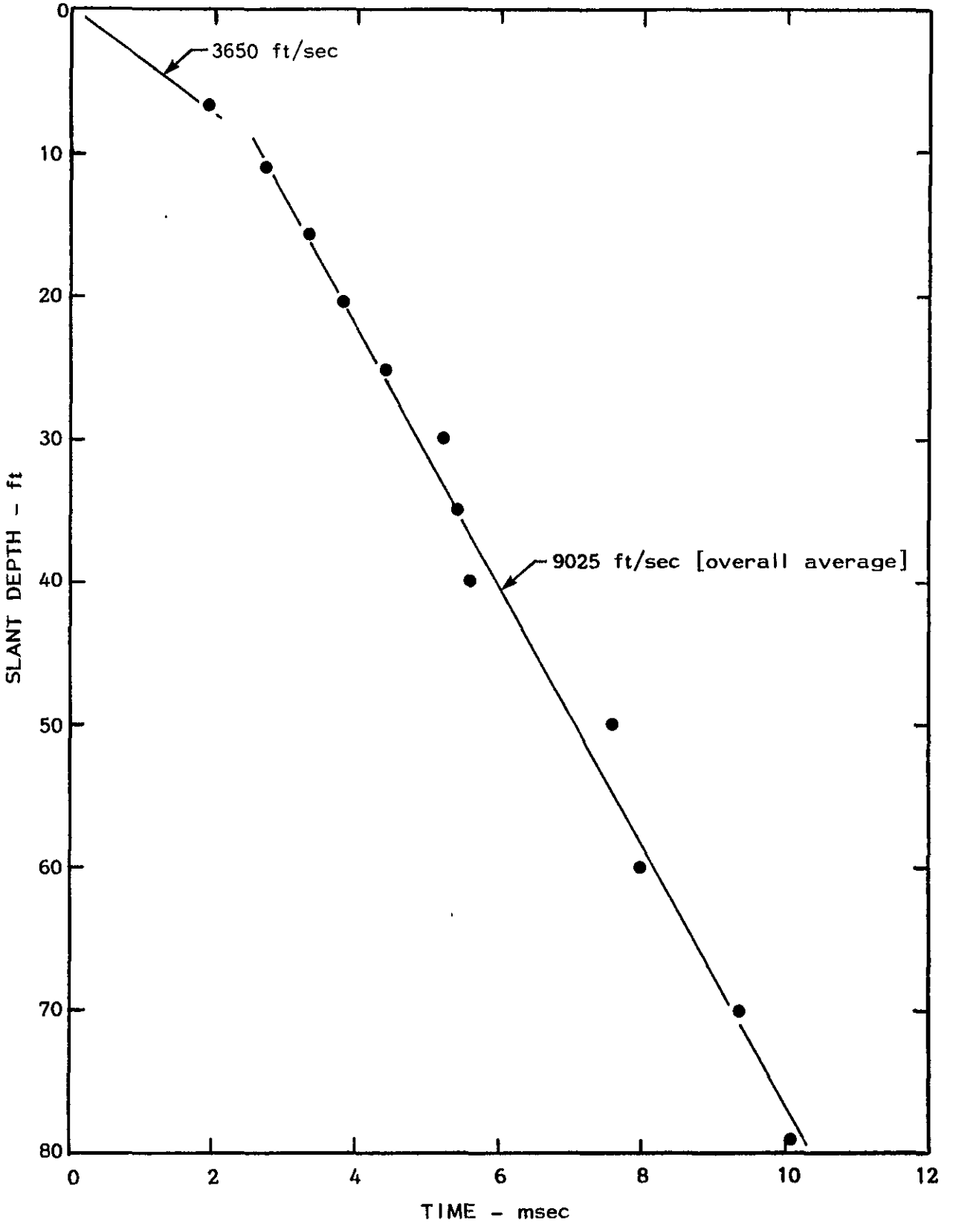

Fig.6 Travel times and velocities of compression signals
Turkey Flat - South Rock Site

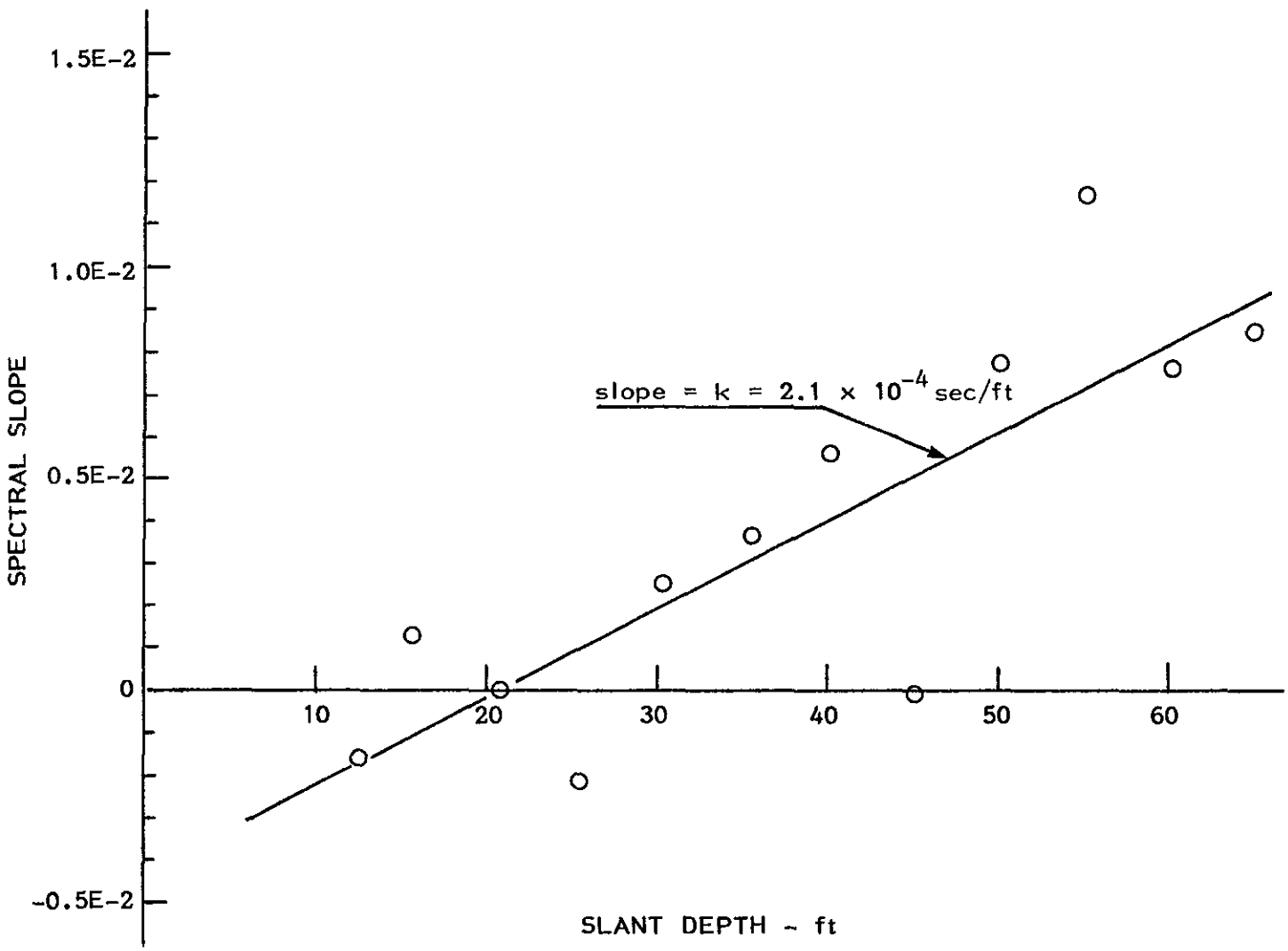

Fig.7 Slopes of spectral ratios of shear-wave signals, referenced to 20-ft depth, as a function of depth - Turkey Flat - Valley Center Site.

TABLE 1

TURKEY FLAT DOWNHOLE VELOCITIES
[QEST Consultants]

Valley Center Site				South Rock Site		
Depth	V_s	V_p	Q	Depth	V_s	V_p
0-5 ft	400	700	5	0-5	2700	3650
5-20	1900	3100	7.5	5-35	5000	9025
20-32	1900	2800	7.5	35-80	4150	9025
32-68	2100	3100	7.5			
68+	3100	8000	25+/-			

APPENDIX H
State of California (CDMG)

THREE PARTS:

1) **Downhole Velocity Surveys,**
2) **Borehole Deviation Surveys, and**
3) **Reconnaissance Seismic Surveys.**

PART 1
DOWNHOLE VELOCITY SURVEYS

DOWNHOLE VELOCITY MEASUREMENTS AT TURKEY FLAT, CA.

by

Chris Cramer

CALIFORNIA DEPARTMENT OF CONSERVATION
DIVISION OF MINES AND GEOLOGY
SEISMIC SHAKING ASSESSMENT UNIT
630 BERCUT DR.
SACRAMENTO, CA. 95814

INTERNAL REPORT NO. 87-1

JULY 1987

SUMMARY

Velocity estimates have been obtained by the Division of Mines and Geology (DMG) from velocity surveys down five bore holes (#2, 3, 4, 5, & 8) at three seperate sites at Turkey Flat (rock south, valley center, and valley north) (Figure 1). S-wave velocities in both soil and bedrock appear to increase more slowly with depth than P-wave velocities. Vp/Vs ratios at the top and bottom of the logged bore holes are 1.5 - 2.0, but range higher (2.5 - 3.0) at some depths due to the slower rise in S-wave velocities. Soil velocities average about 3200 ft/sec (975 m/sec) for P-waves and about 1700 ft/sec (520 m/sec) for S-waves while bedrock velocities average about 8700 ft/sec (2650 m/sec) for P-waves and about 4500 ft/sec (1370 m/sec) for S-waves. Velocity estimates can be in error by 10-20%.

This report first discusses data recording and processing methods employed by DMG. Then the downhole data and velocity results are presented.

METHOD

Data Recording:

The downhole records were originally recorded on an EG&G Geometrics model ES-1210 12-channel signal enhancement seismograph. Digital records were saved to cartridge tape using an EG&G Geometrics model G-724S digital magnetic tape recorder. After returning from the field, data on the cartridge tapes were transfered into a PR1ME 2250 computer for processing and analysis.

Two Mark Products L10-3D SWC (sidewall clamping) three component downhole seismometers were used to detect ground motions. One seismometer remained fixed at the top of the bore hole; the other was moved up the bore hole to make measurements at five foot intervals. These two seismometers were connected to the ES-1210 recorder so that two adjacent recorder channels were connected to each seismometer component.

Seismic waves were generated using a traction plank. P and S waves were generated at the same time by horizontally striking the end of an eight-foot wooden traction plank weighted by a vehicle. S-wave amplitude generally was larger than P-wave amplitude, but P-wave energy was

sufficient for P-wave travel-time measurements. A record for a given depth consists of three or more hits at one end of the plank stacked together (enhanced) on the odd channels of the recorder and three or more hits at the other end of the plank enhanced on the even channels of the recorder. Signal enhancement was needed to reduce random noise and enhance P and S arrivals. Sample intervals varied from bore hole to bore hole: .05 msec for bore hole 2, .1 msec for bore holes 3, 4 & 5, and .1 msec at depths above 55 feet and .2 msec at depths below 55 feet for bore hole 8.

Data Processing:

Downhole P and S arrivals were timed relative to the P-wave arrival on the tophole reference geophone. This removed travel-time variations due to systematic variation in recorder triggering on the solid-state trigger attached to the wooden mallet used to strike the end of the traction plank. Absolute P-wave travel-time to the tophole reference geophone was determined from seperate P-wave calibration shots from each end of the plank. (A metal sledge vertically stiking a metal plate was used in the calibration shots because this provided absolute P-wave travel-time to within a standard deviation of +/- 0.2 msec.)

P-wave arrivals were timed in the following manner. First, trace timing on all traces of a recorded shot were corrected to absolute time from the shot using the P-arrival on the co-recorded tophole vertical component. Then P-wave record sections were formed (see Appendix) and P-wave arrivals timed. Because two P-wave arrival times were available at each depth, one for a "shot" at each end of the plank, the two P-wave arrival times at each depth were averaged together.

S-wave arrivals were partially masked by the P-wave coda, particularly for the top part of the bore hole. Because of this, the digital data for the horizontal components were further processed to enhance the S-wave arrival. After being corrected to absolute time as described in the preceding paragraph, the trace for a given horizontal component from an enhanced "shot" at one end of the traction plank was subtracted from the trace for the same horizontal component for the "shot" at the other end of the traction plank. This procedure of stacking traces for a given horizontal conponent enhances the S-wave waveform and removes common P-wave waveforms, making for clearer timing of S-wave arrivals (Figure 2).

There are limitations on the accuracy of the downhole travel-time measurements made by this technique. First, amplifier gain must be sufficient to clearly record the weaker P-wave arrivals (vis-a-vis S-wave arrivals). Signal enhancement of multiple hits can help if they are properly stacked in terms of record start time. Second the seismic source must be repeatable from hit to hit and at both ends of the

plank. If source repeatability breaks down, 1) P-wave and S-wave travel-time scatter increases from less accurate correction of traces to absolute time since the shot and 2) S-wave enhancement is degraded due to the imperfect cancellation of P-waves and the less than optimal summing of S-waves. Both poor signal recording and source non-repeatability can lead to inaccurate and erroneous velocity estimates.

RESULTS

Downhole velocity measurements from bore hole 2 (rock south), bore hole 3 (valley north), and bore holes 4, 5, & 8 (valley center) are summarized in Table I. For bore hole 8, the travel-time measurements show more scatter than the measurements for the other four bore holes. This increased scatter for bore hole 8 is due to increased background noise from the inflatable-blatter clamping system (with air supply line leaks) used in bore hole 8 (because it was an uncased hole). A quieter bow-spring clamp system was used in cased holes 2-5. The increased scatter in the data for bore hole 8 results in the loss of detail in the velocity structure for that bore hole, but average velocities over tens of feet down the hole should still be reliable.

Velocities were estimated by least squares fitting offset-corrected arrival-times over specified depth intervals. Depths-to-layer-top were estimated independently for P-waves and S-waves from least-squares-fit velocities and intercept times. Hence P-wave and S-wave velocity boundaries may not exactly correspond for the same depth profile. Figures 3-7 (corresponding to bore holes 2, 3, 4, 5, & 8 respectively) show plots of offset-corrected P-wave and S-wave arrival-times and least-squares-fit velocities. P-wave and S-wave record sections for all five bore holes are in the Appendix.

A comparison of velocity estimates from bore holes 4 and 5 at the valley center site provides an idea of the repeatability of these velocity estimates. Generally differences in P-wave and S-wave velocities between these two bore holes range between 100 and 150 ft/sec with one S-wave velocity difference being 310 ft/sec. This translates into velocity variations of 10-20%. This agrees with the results of Beeston and McEvilly (1977). Thus individual velocity estimates in Table I could be in error by 10-20%.

S-wave velocities (Vs) increase more slowly with depth than P-wave velocities (Vp) at Turkey Flat. This shows up as an extra S-wave velocity layer in the velocity-depth models for each bore hole. For the valley bore holes (holes 3, 4 & 5), S-wave velocity increases from a slow surface velocity to a faster lower-soil-column velocity in a broad transition between 5 feet and 30 feet down the holes, while P-wave velocity increases sharply in one step at a depth between 5 and 10 feet

down the hole. This suggests that S-wave velocity may be exhibiting a gradient behavior with depth, unlike P-wave velocity which increases in sharp discrete steps.

At the rock south site (bore hole 2), S-wave velocity also increases more slowly than P-wave velocity. P-wave velocity transitions to 8600+ ft/sec in the top 20 feet of the hole, while S-wave velocity transitions to 4300+ ft/sec in the top 30 feet of the hole and to 5000+ ft/sec at 60 feet down the hole. This suggests that P-wave and S-wave velocities are affected differently by weathering of the sandstone bedrock or that some other factor is affecting S-wave velocity below 20feet from the surface.

Vp/Vs ratios generally vary between 1.5 and 2.0 except where S-wave velocity is increasing more slowly than P-wave velocity. A Vp/Vs ratio of 1.5 to 2.0 implies a Poisson's ratio of 0.10 to 0.33. More slowly increasing S-wave velocity causes the higher Vp/Vs ratios of 2.5 to 3.0 (Poisson's ratios of 0.40 to 0.44) observed in portions of the downhole sections.

Although the velocity profile for valley center bore hole 8 does not have the detailed velocity resolution of the other four bore holes due to increased data scatter from noisier records, the profile still provides good average velocities for the soil and bedrock portions of the velocity profile. The average soil column P-wave and S-wave velocities (second layer) for bore hole 8 agree well with corresponding layer velocities in bore hole 4 and 5: a second layer P-wave velocity of 3125 ft/sec in bore hole 8 agrees very well to the corresponding P-wave velocities of 3250 and 3125 ft/sec in bore holes 4 and 5, and an average S-wave velocity of 1740 ft/sec in bore hole 8 falls between the S-wave velocities of the corresponding double layers in both bore holes 4 and 5. Finally, the average P-wave and S-wave velocities for the bedrock below the valley in bore hole 8 correspond well with bedrock velocities in bore hole 2, particularly for the 30 to 55 foot depth range in bore hole 2.

REFERENCES

Beeston, H.E., and T.V. McEvilly, 1977, Shear wave velocities from downhole measurements: Earthquake Engineering and Structural Dynamics, v. 5, p. 181-190.

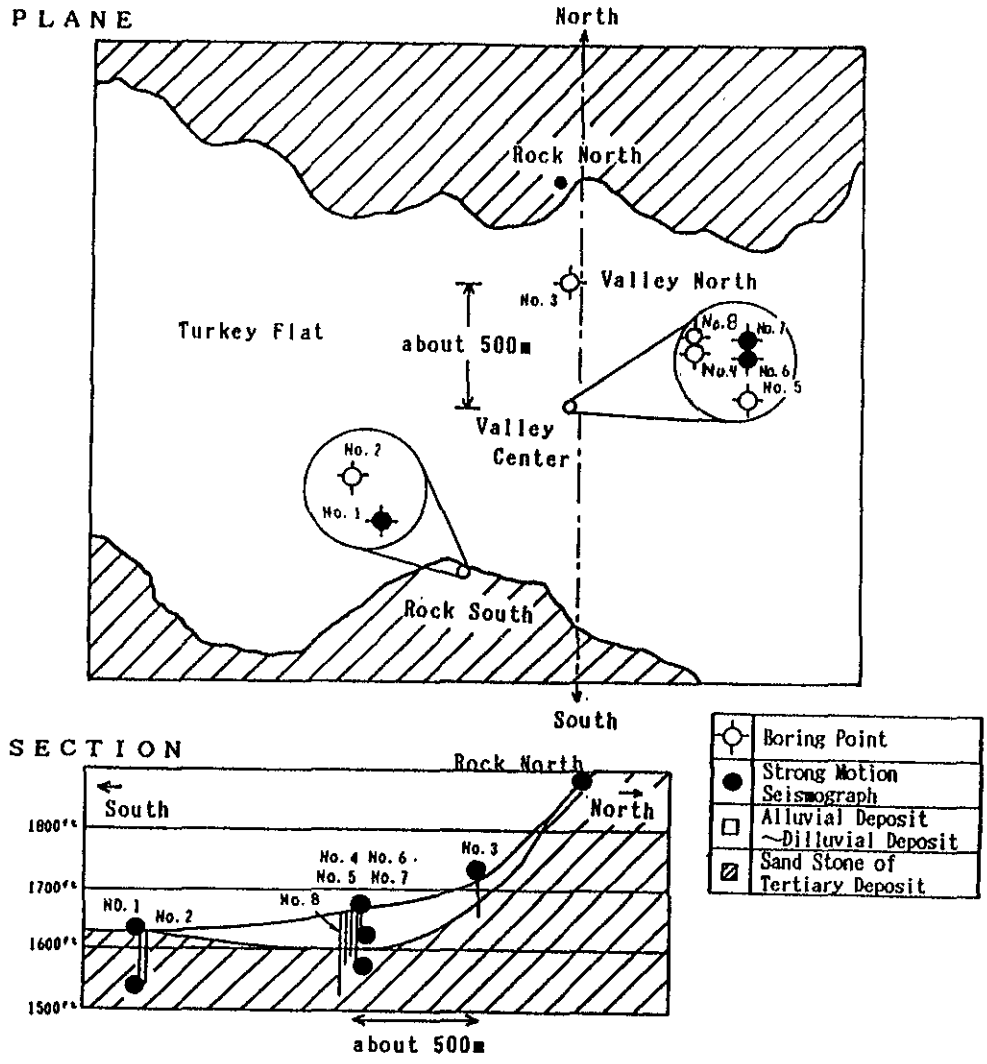

Description of Instrument and Test Borings

No.	Purpose	Depth (ft)	Diameter (inches)	Casing (inches)	Backfill
1	Test & Sensor	82	9	5-PVC	Pea Gravel[2]
2	Test	80	6	3.34-SINCO	Grout[1]
3	Test	47	9	5-PVC	Pea Gravel[2]
4	Test	73	8	5-PVC	Pea Gravel
5	Test	78	6	3.34-SINCO	Grout[1]
6	Test & Sensor	79	9	5-PVC	Pea Gravel[2]
7	Sensor	35	8	5-PVC	Pea Gravel
8	Test	132	3 1/8	Uncased	[2]

[1] A mixture of 5 parts cement to 1 part bentonite.
[2] A 3/4" piezometer tube installed in annulus.

Figure 1

FIGURE 2

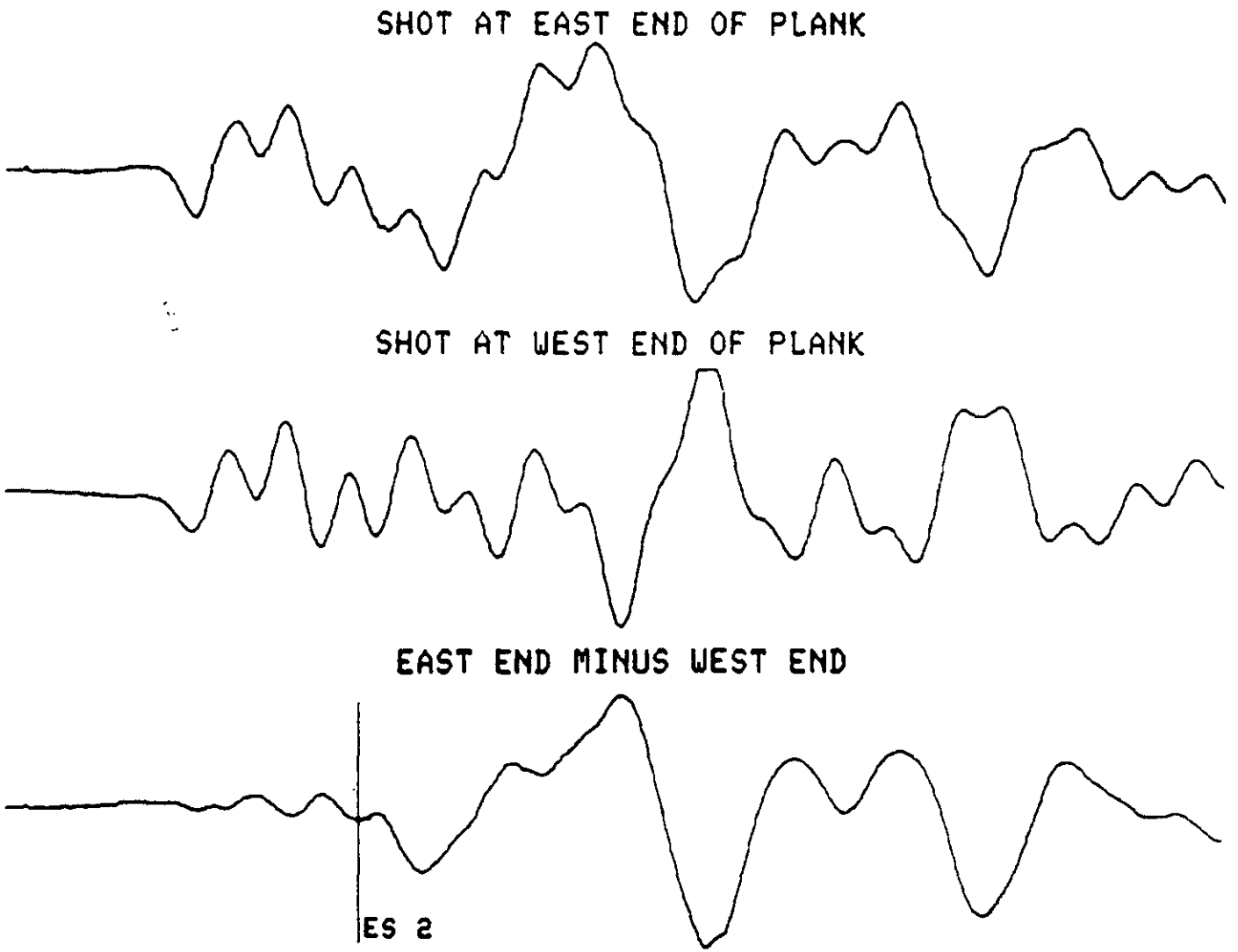
SHOT AT EAST END OF PLANK
SHOT AT WEST END OF PLANK
EAST END MINUS WEST END
ES 2

FIGURE 3A

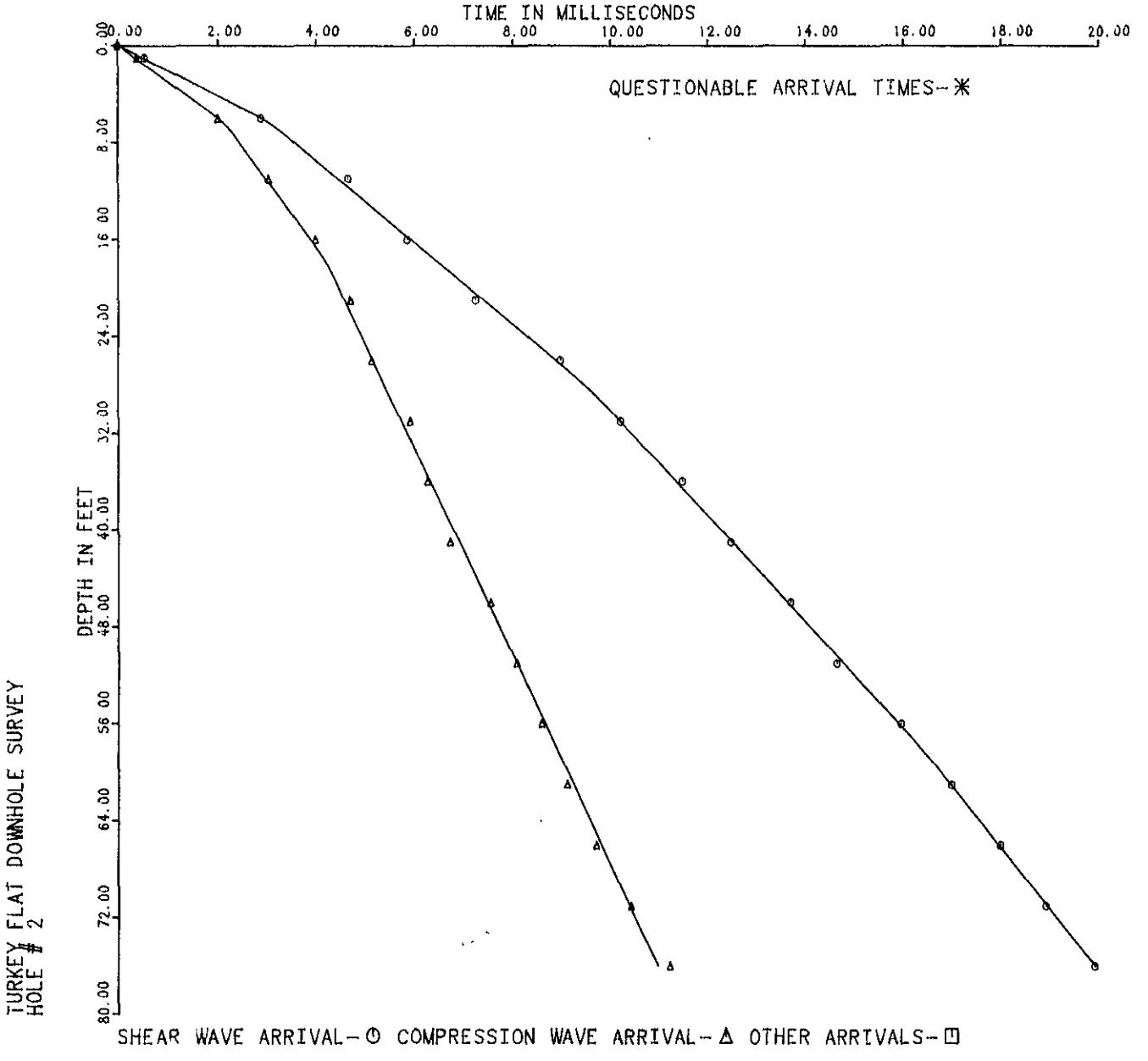
TIME IN MILLISECONDS
0.00
2.00
4.00
6.00
8.00
10.00
12.00
14.00
16.00
18.00
20.00
QUESTIONABLE ARRIVAL TIMES-✳
DEPTH IN FEET
0.00
8.00
16.00
24.00
32.00
40.00
48.00
56.00
64.00
72.00
80.00
TURKEY FLAT DOWNHOLE SURVEY
HOLE # 2
SHEAR WAVE ARRIVAL-⊙ COMPRESSION WAVE ARRIVAL-△ OTHER ARRIVALS-□

FIGURE 3B

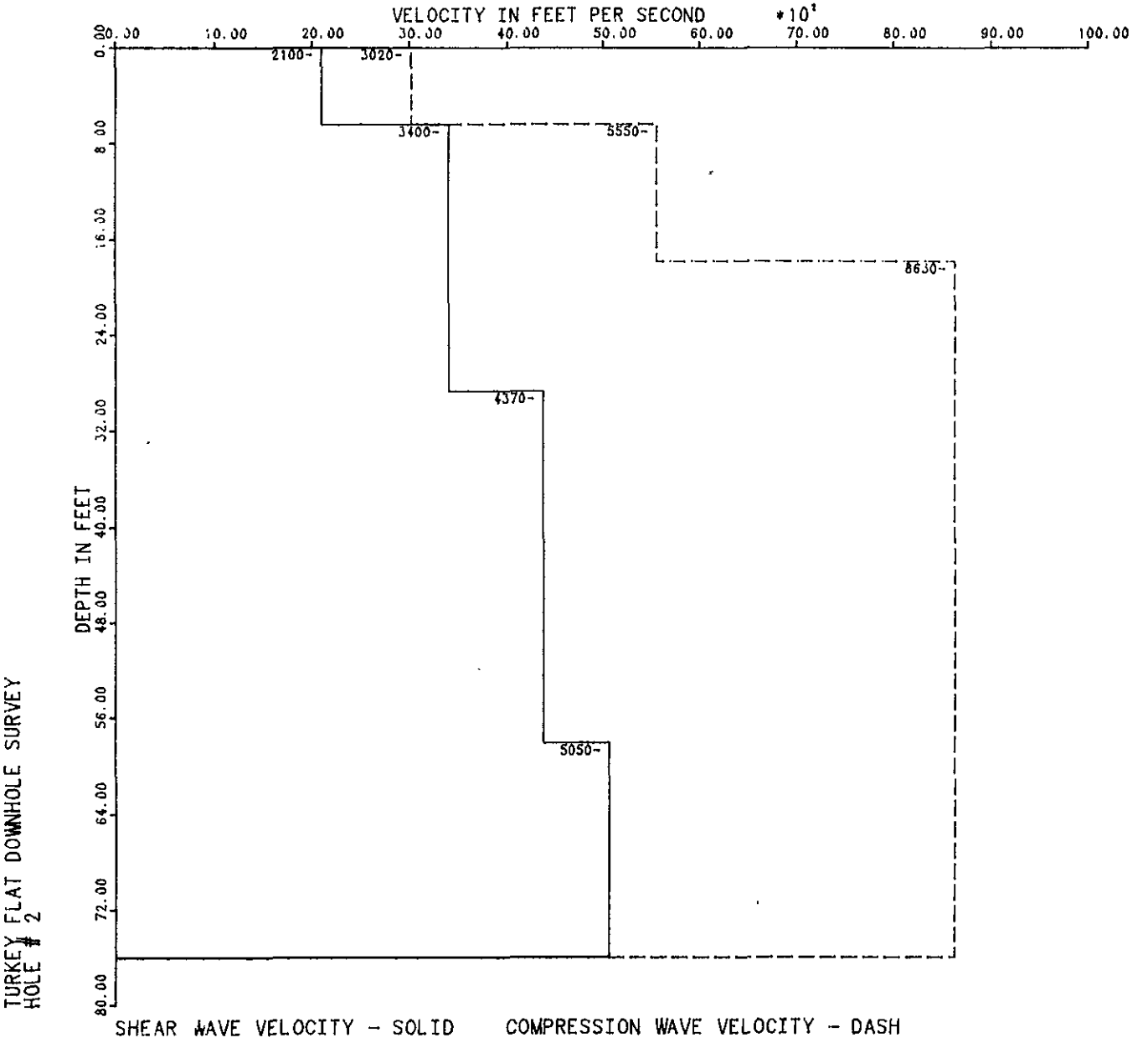
VELOCITY IN FEET PER SECOND *10³
0.00
10.00
20.00
30.00
40.00
50.00
60.00
70.00
80.00
90.00
100.00
2100
3020
3400
5550
8630
4370
5050
DEPTH IN FEET
0.00
8.00
16.00
24.00
32.00
40.00
48.00
56.00
64.00
72.00
80.00
TURKEY FLAT DOWNHOLE SURVEY
HOLE # 2
SHEAR WAVE VELOCITY - SOLID
COMPRESSION WAVE VELOCITY - DASH

FIGURE 4A

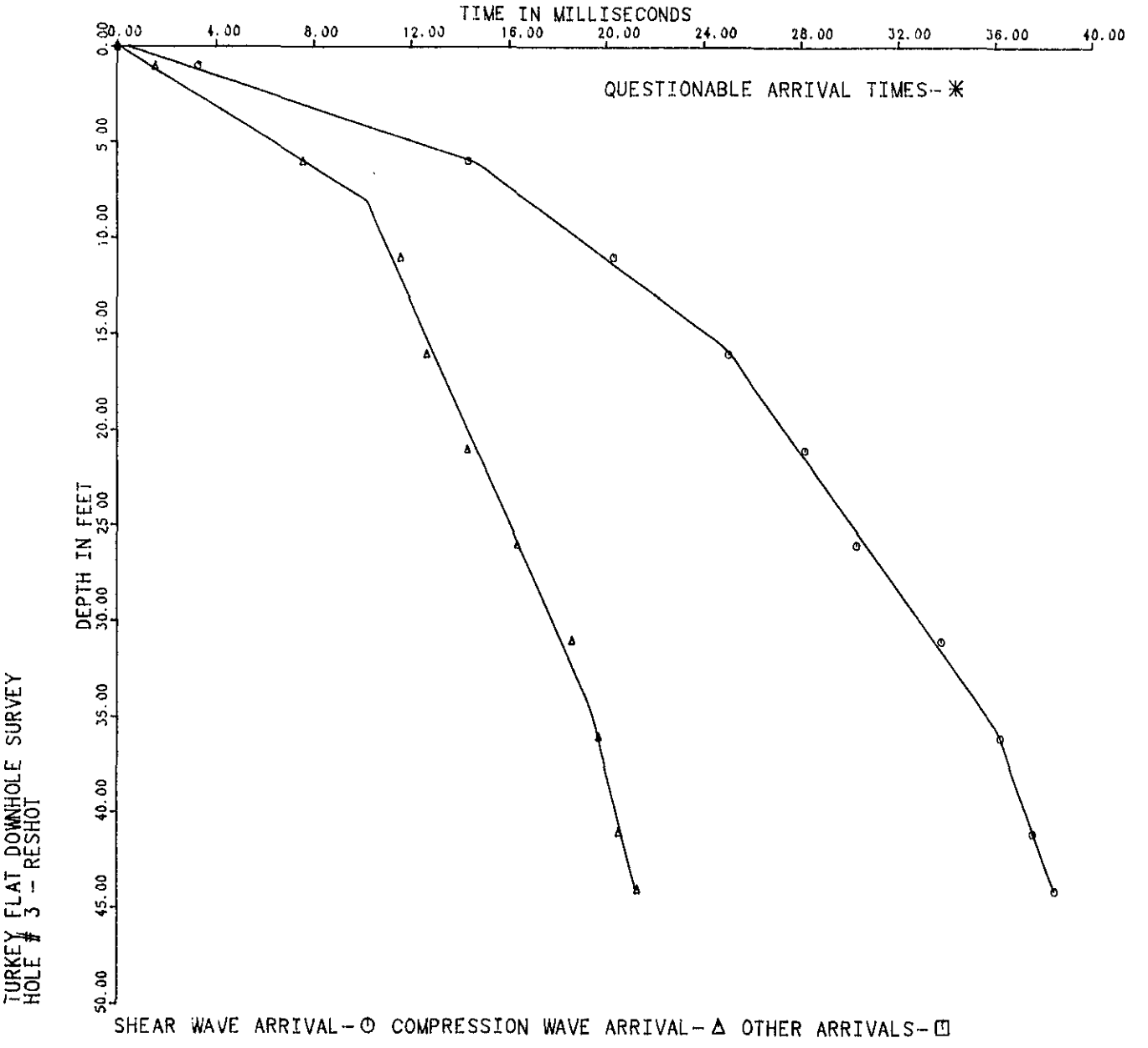
TURKEY FLAT DOWNHOLE SURVEY
HOLE # 3 - RESHOT
TIME IN MILLISECONDS
0.00
4.00
8.00
12.00
16.00
20.00
24.00
28.00
32.00
36.00
40.00
DEPTH IN FEET
0.00
5.00
10.00
15.00
20.00
25.00
30.00
35.00
40.00
45.00
50.00
QUESTIONABLE ARRIVAL TIMES-*
SHEAR WAVE ARRIVAL-O COMPRESSION WAVE ARRIVAL-Δ OTHER ARRIVALS-□

FIGURE 4B

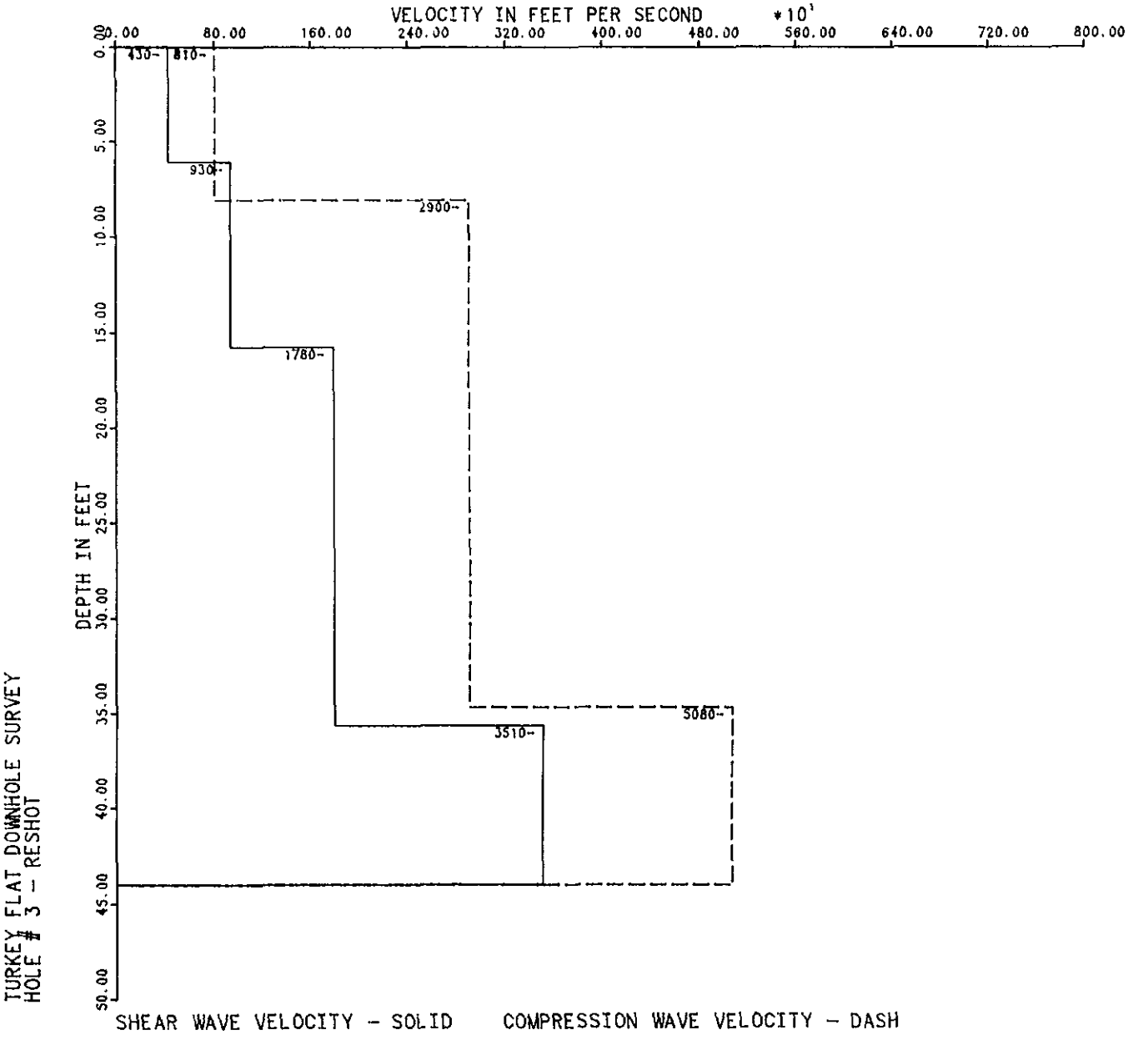
VELOCITY IN FEET PER SECOND *10¹
0.00
80.00
160.00
240.00
320.00
400.00
480.00
560.00
640.00
720.00
800.00
DEPTH IN FEET
0.00
5.00
10.00
15.00
20.00
25.00
30.00
35.00
40.00
45.00
50.00
430-
810-
930-
2900-
1780-
5080-
3510-
TURKEY FLAT DOWNHOLE SURVEY
HOLE # 3 - RESHOT
SHEAR WAVE VELOCITY - SOLID
COMPRESSION WAVE VELOCITY - DASH

FIGURE 5A

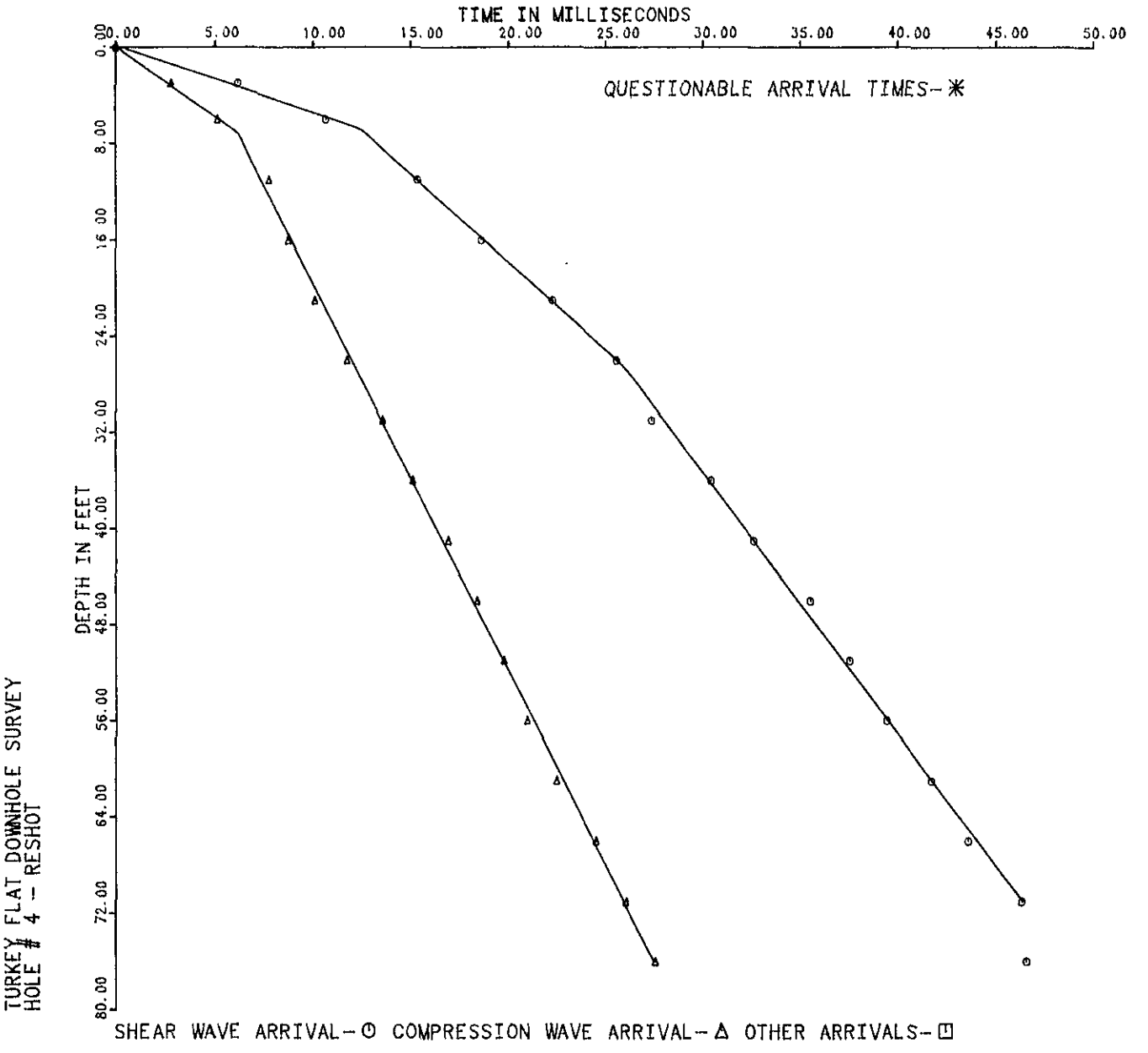
TIME IN MILLISECONDS
0.00
5.00
10.00
15.00
20.00
25.00
30.00
35.00
40.00
45.00
50.00
QUESTIONABLE ARRIVAL TIMES-✳
DEPTH IN FEET
0.00
8.00
16.00
24.00
32.00
40.00
48.00
56.00
64.00
72.00
80.00
TURKEY FLAT DOWNHOLE SURVEY
HOLE # 4 - RESHOT
SHEAR WAVE ARRIVAL-⏲ COMPRESSION WAVE ARRIVAL-△ OTHER ARRIVALS-⊡

FIGURE 5B

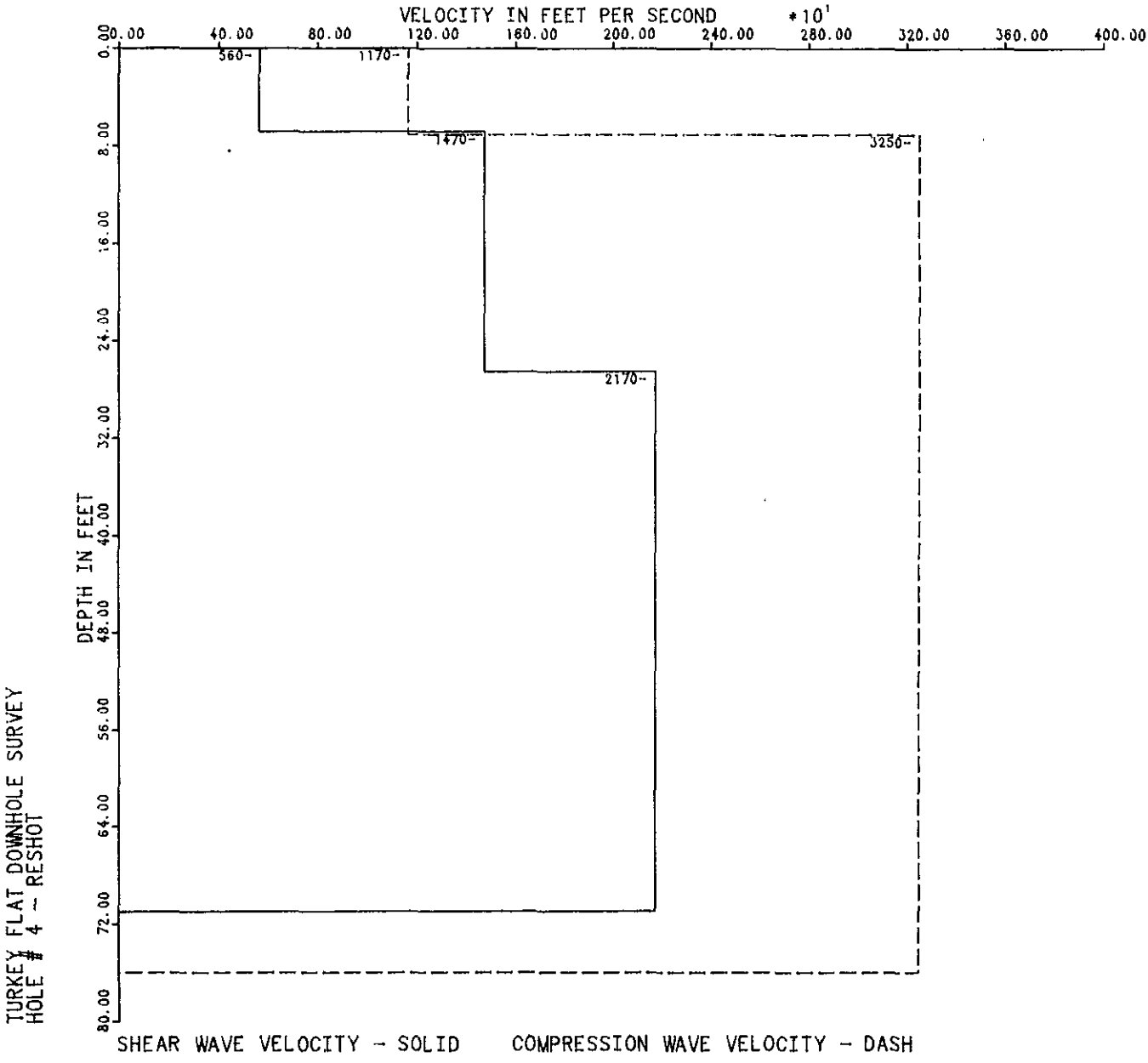
VELOCITY IN FEET PER SECOND *10¹
0.00
40.00
80.00
120.00
160.00
200.00
240.00
280.00
320.00
360.00
400.00
560-
1170-
1470-
3250-
2170-
DEPTH IN FEET
0.00
8.00
16.00
24.00
32.00
40.00
48.00
56.00
64.00
72.00
80.00
TURKEY FLAT DOWNHOLE SURVEY
HOLE # 4 - RESHOT
SHEAR WAVE VELOCITY - SOLID
COMPRESSION WAVE VELOCITY - DASH

FIGURE 6A

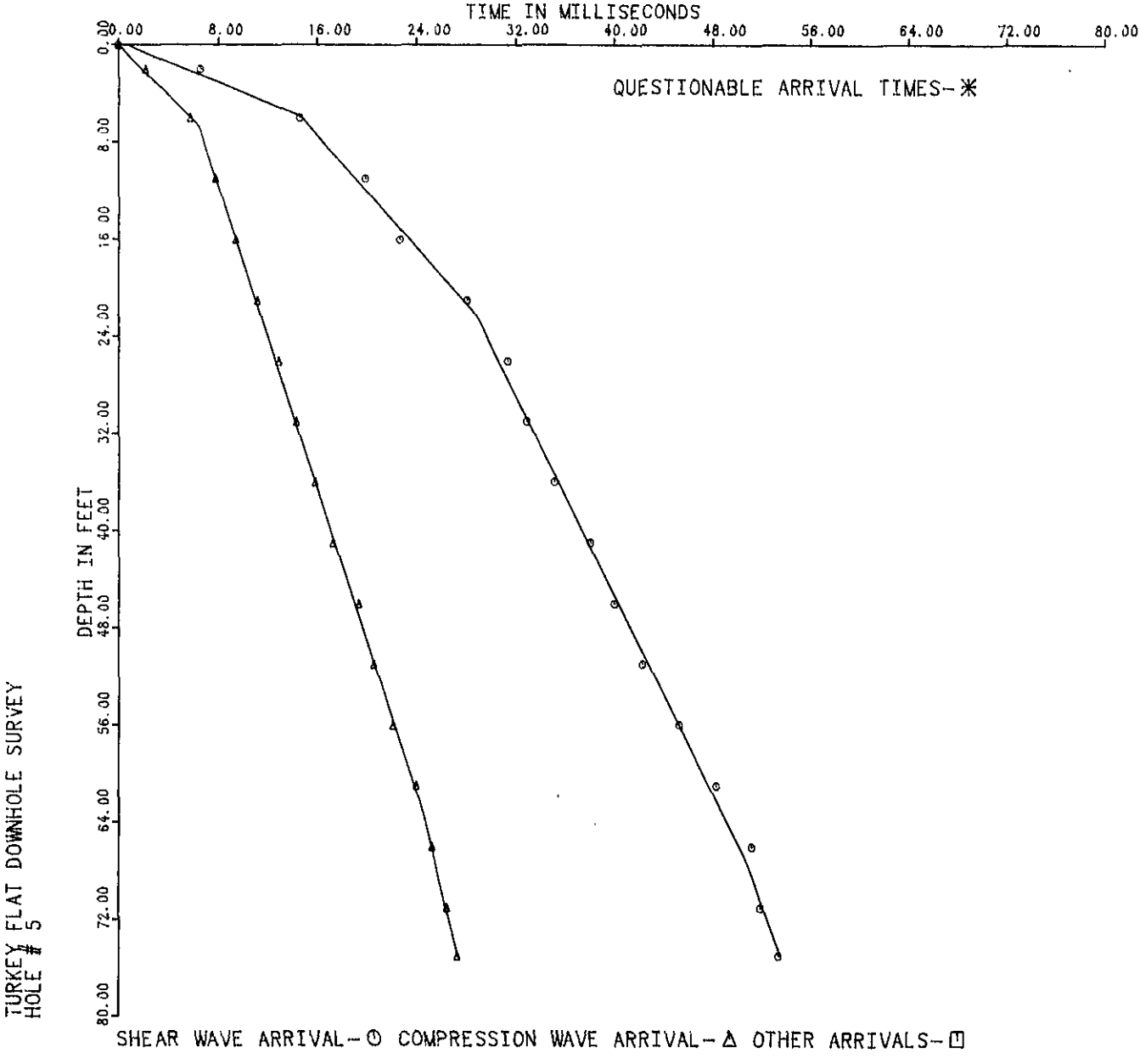
TIME IN MILLISECONDS
0.00
8.00
16.00
24.00
32.00
40.00
48.00
56.00
64.00
72.00
80.00
QUESTIONABLE ARRIVAL TIMES-✳
DEPTH IN FEET
0.00
8.00
16.00
24.00
32.00
40.00
48.00
56.00
64.00
72.00
80.00
TURKEY FLAT DOWNHOLE SURVEY
HOLE # 5
SHEAR WAVE ARRIVAL-⊙ COMPRESSION WAVE ARRIVAL-△ OTHER ARRIVALS-□

FIGURE 6B

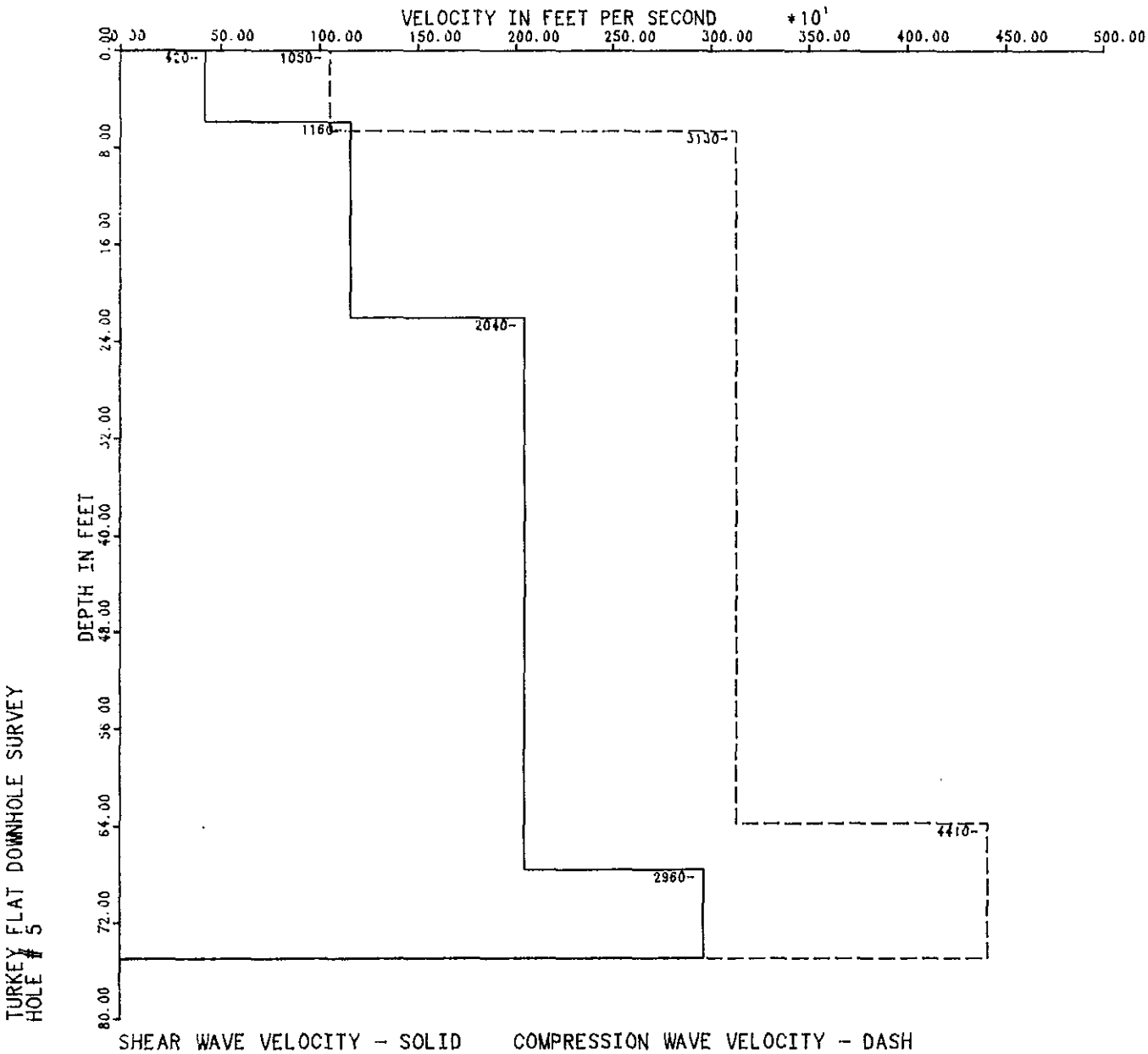
VELOCITY IN FEET PER SECOND *10¹
0.00
50.00
100.00
150.00
200.00
250.00
300.00
350.00
400.00
450.00
500.00
420
1050
1160
3130
2040
4410
2960
DEPTH IN FEET
8.00
16.00
24.00
32.00
40.00
48.00
56.00
64.00
72.00
80.00
TURKEY FLAT DOWNHOLE SURVEY
HOLE # 5
SHEAR WAVE VELOCITY - SOLID
COMPRESSION WAVE VELOCITY - DASH

FIGURE 7A

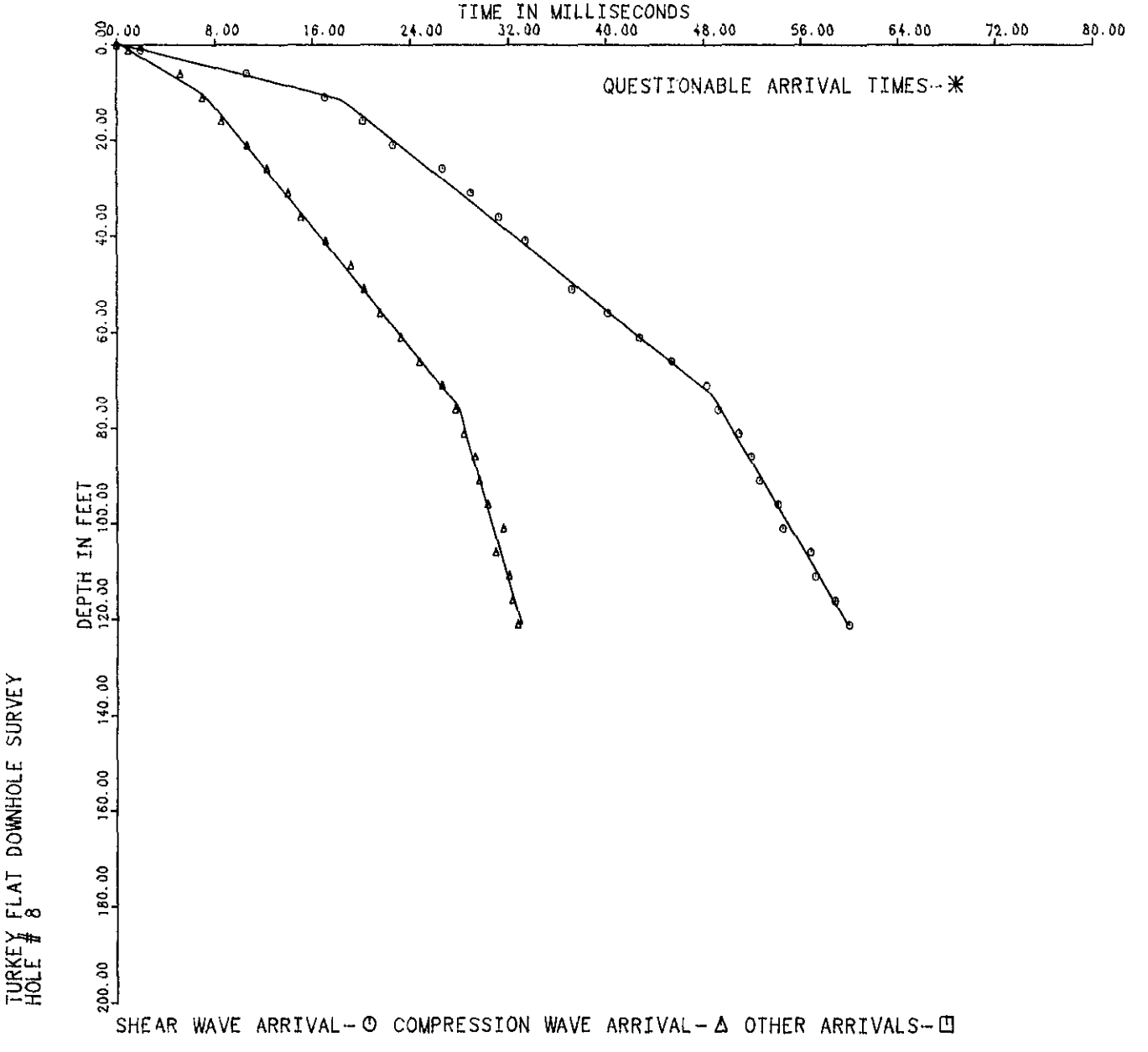
TIME IN MILLISECONDS
0.00
8.00
16.00
24.00
32.00
40.00
48.00
56.00
64.00
72.00
80.00
QUESTIONABLE ARRIVAL TIMES-*
DEPTH IN FEET
0.00
20.00
40.00
60.00
80.00
100.00
120.00
140.00
160.00
180.00
200.00
TURKEY FLAT DOWNHOLE SURVEY
HOLE # 8
SHEAR WAVE ARRIVAL-O COMPRESSION WAVE ARRIVAL-Δ OTHER ARRIVALS-□

FIGURE 7B

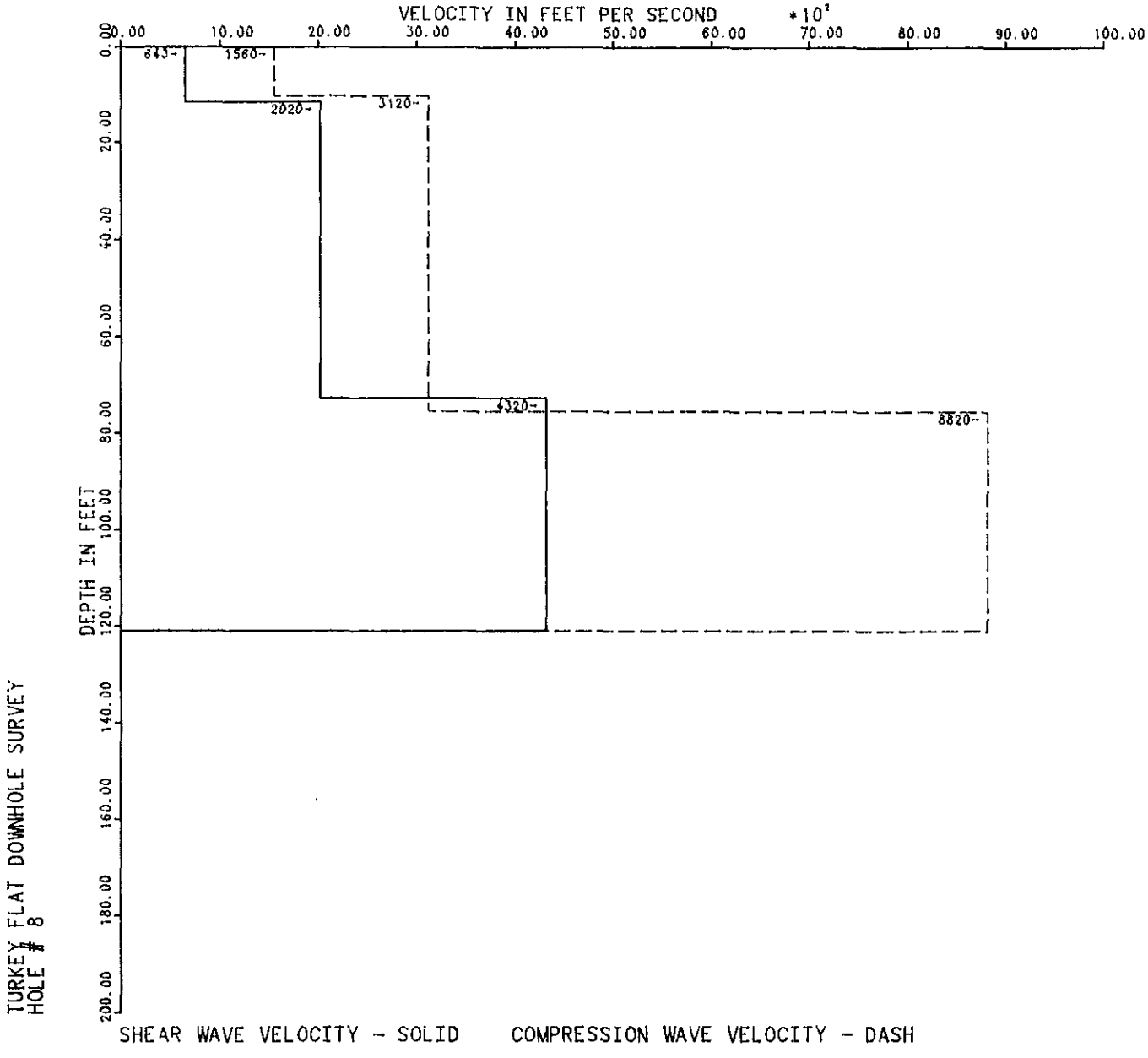
VELOCITY IN FEET PER SECOND *10²
0.00
10.00
20.00
30.00
40.00
50.00
60.00
70.00
80.00
90.00
100.00
DEPTH IN FEET
0.00
20.00
40.00
60.00
80.00
100.00
120.00
140.00
160.00
180.00
200.00
643
1560
2020
3120
4320
8820
TURKEY FLAT DOWNHOLE SURVEY
HOLE # 8
SHEAR WAVE VELOCITY - SOLID
COMPRESSION WAVE VELOCITY - DASH

TABLE I
DOWNHOLE VELOCITY ESTIMATES

	P-wave		S-wave			
Hole #	Depth-to-layer-top (ft)	P-velocity (ft/sec)*	Depth-to-layer-top (ft)	S-velocity (ft/sec)*	Vp/Vs ratio	Poisson's ratio
2	0.	3020.	0.	2100.	1.4	.00
	6.	5550.	6.	3400.	1.6	.18
	18.	8630.	29.	4370.	2.0	.33
			58.	5050.	1.7	.24
3	0.	810.	0.	430.	1.9	.31
	8.	2900.	6.	930.	3.1	.44
			16.	1783.	1.6	.18
	35.	5075.	36.	3510.	1.5	.10
4	0.	1170.	0.	560.	2.1	.35
	7.	3250.	7.	1475.	2.2	.37
			27.	2170.	1.5	.18
5	0.	1050.	0.	425.	2.5	.40
	7.	3125.	6.	1160.	3.0	.44
			22.	2040.	1.5	.10
	64.	4410.?	68.	3000.?	1.5	.10
8	0.	1560.	0.	760.	2.1	.35
	10.	3125.	9.	1740.	1.8	.28
	76.	8825.	72.	4320.	2.0	.33

* Velocity estimates could be in error by 10-20%.

APPENDIX

P-wave and S-wave record sections for Turkey Flat bore holes 2, 3, 4, 5, & 8 are presented in this appendix. For each hole, first the P-wave and then the S-wave record section is shown. P-wave record sections show both P-wave traces at each recording depth: one trace is for the "shot" at one end of the traction plank, and the other trace (inverted) is for the "shot" at the other end of the traction plank. The S-wave record sections show one processed trace corresponding to the horizontal component parallel to the traction plank (light trace) and two traces corresponding to right-side and left-side plank impacts (dark traces) at each recording depth. All P-wave and S-wave arrival picks are shown as a vertical line on the data trace.

TURKEY FLAT DOWNHOLE SURVEY
HOLE # 2 – P WAVE DATA – 10.0 FT OFFSET

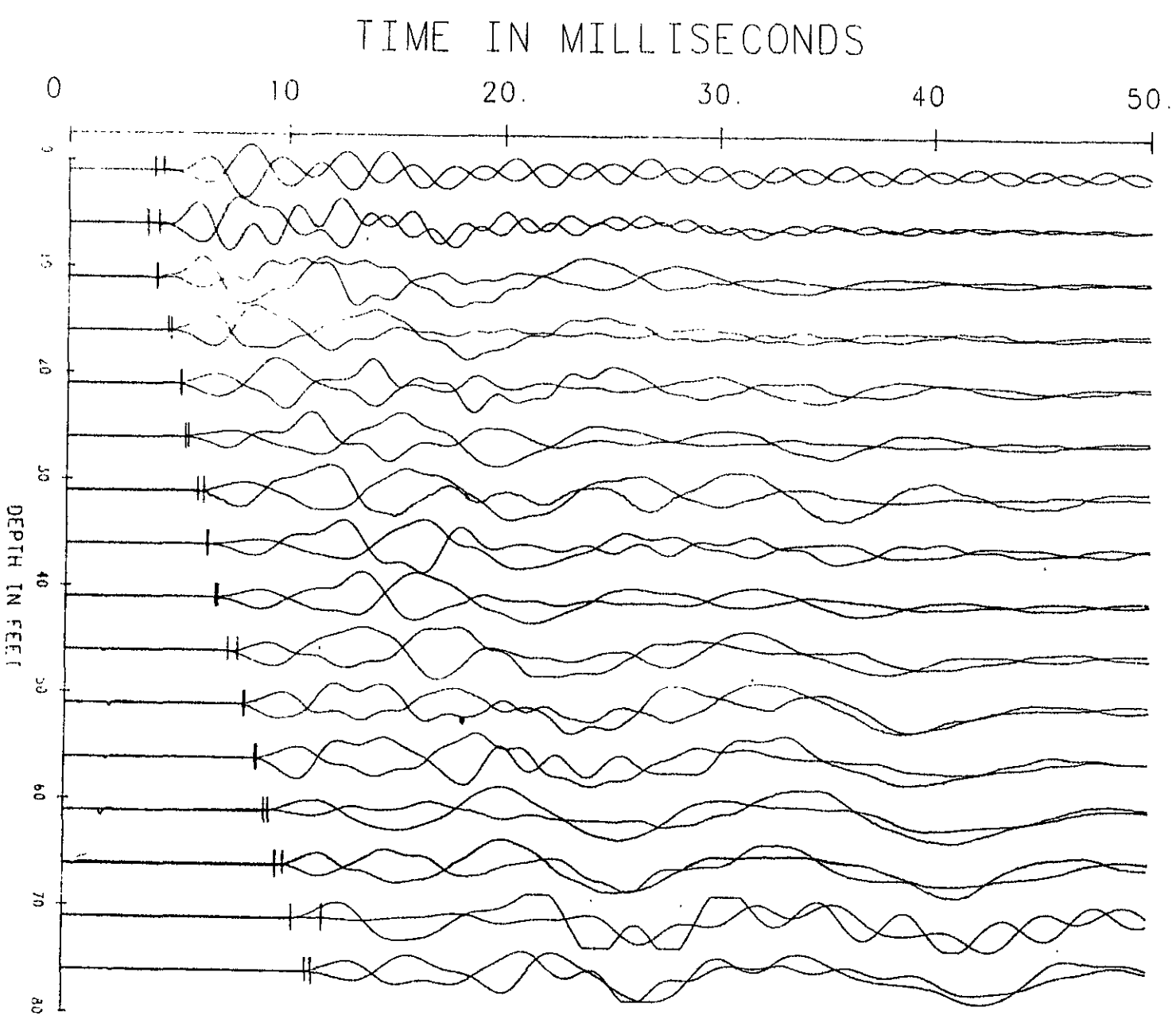

TURKEY FLAT DOWNHOLE SURVEY
HOLE # 2 - S WAVE DATA - 10.0 FT OFFSET

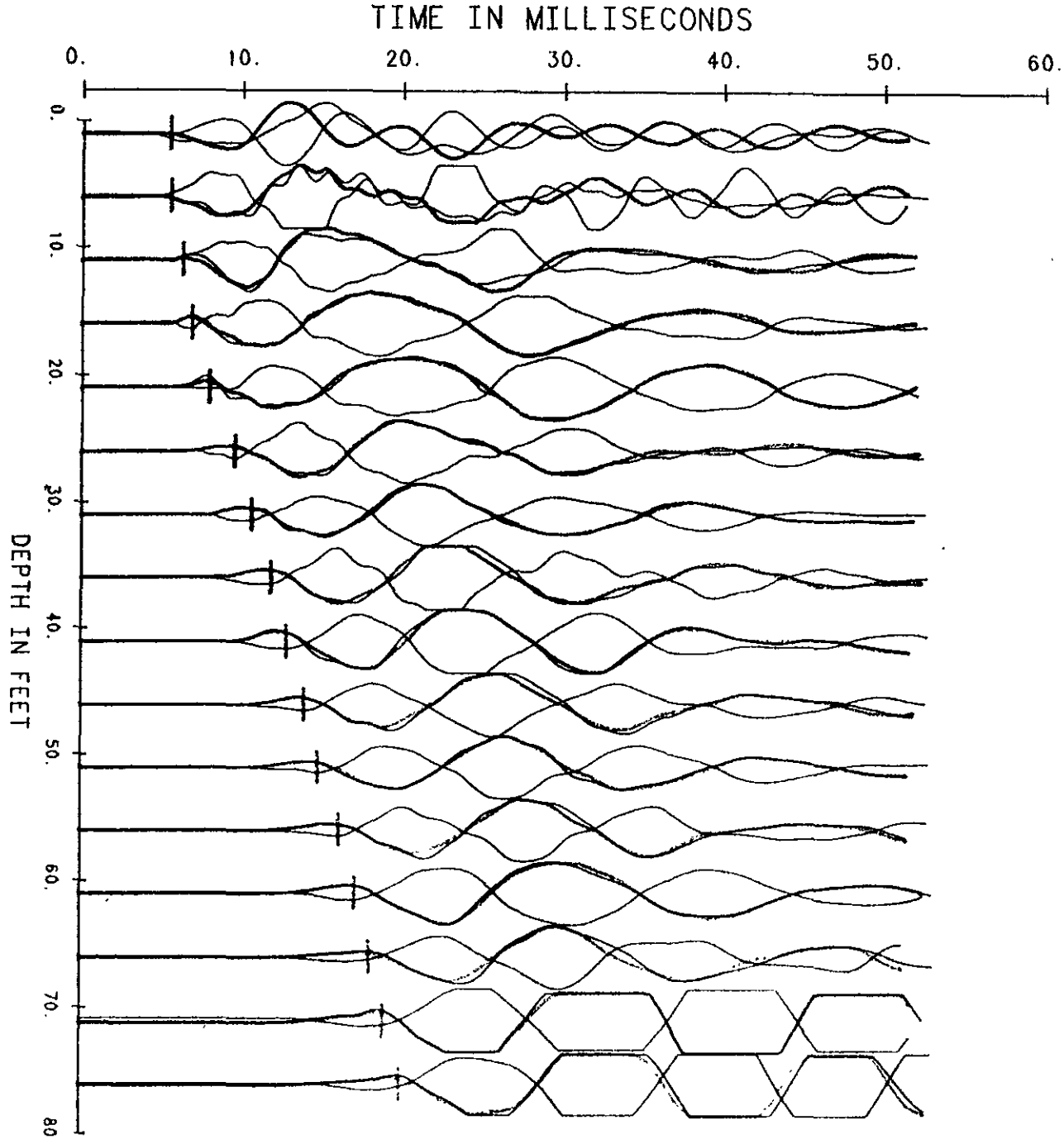

TURKEY FLAT DOWNHOLE SURVEY
HOLE # 3 - RESHOT - P WAVE DATA - 10.0 FT OFFSET

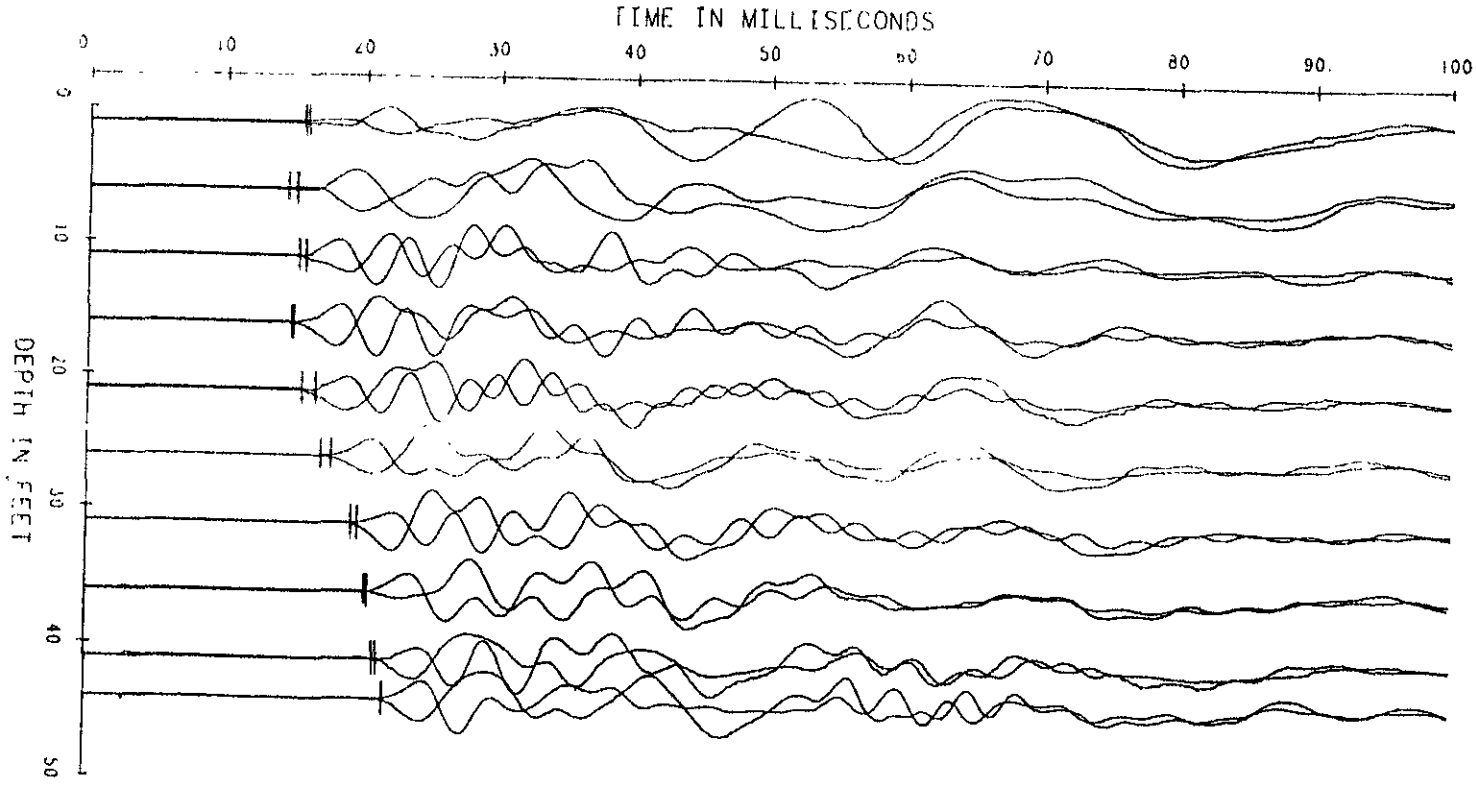

TURKEY FLAT DOWNHOLE SURVEY
HOLE # 3 - S WAVE DATA - 10.0 FT OFFSET

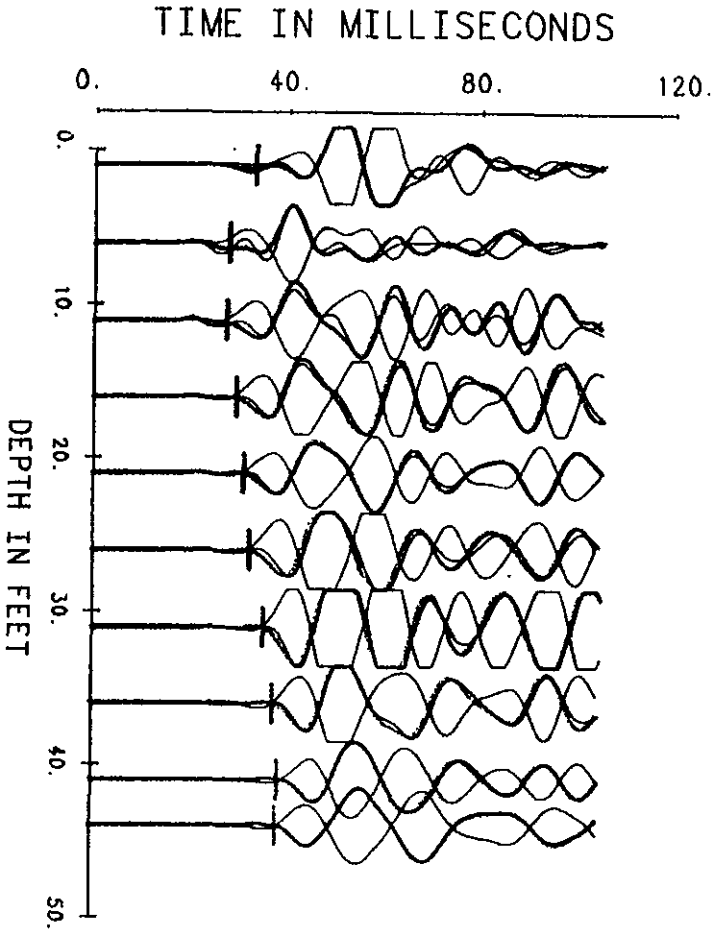

TURKEY FLAT DOWNHOLE SURVEY
HOLE # 4 - RESHOT - P WAVE DATA - 10 0 FT OFFSET

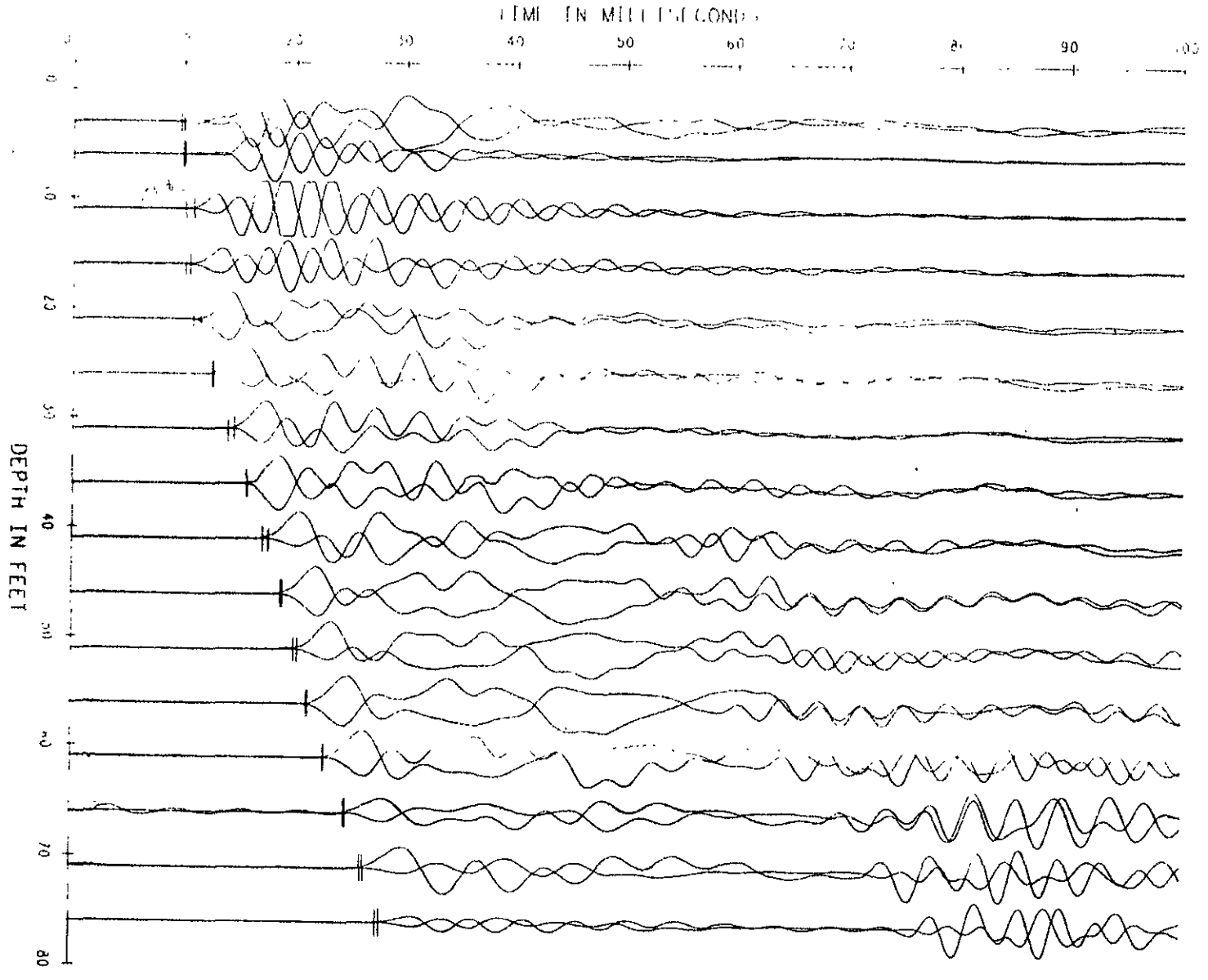

TURKEY FLAT DOWNHOLE SURVEY
HOLE # 4 - S WAVE DATA - 10.0 FT OFFSET

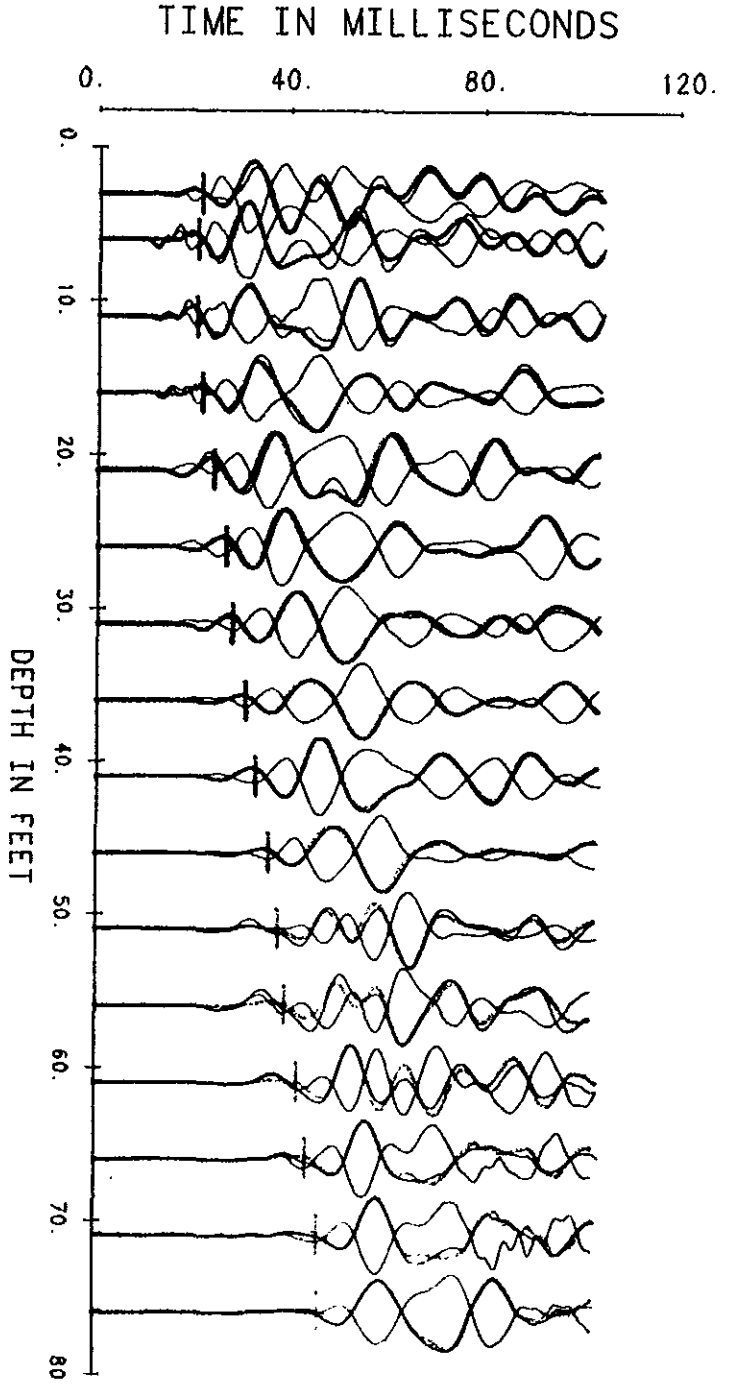

TURKEY FLAT DOWNHOLE SURVEY
HOLE # 5 - P WAVE DATA - 8 5 FT OFFSET

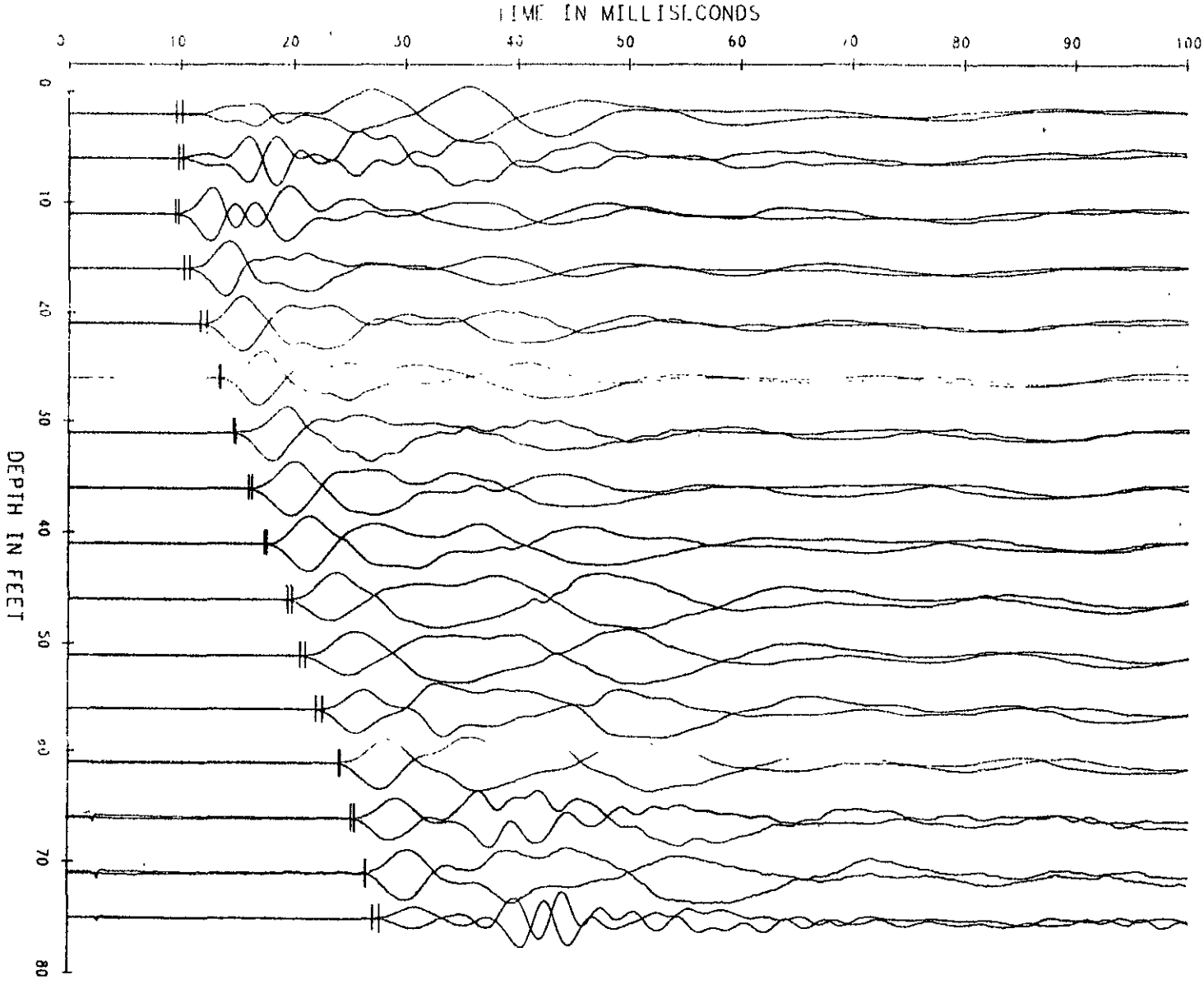

TURKEY FLAT DOWNHOLE SURVEY
HOLE # 5 – S WAVE DATA – 8.5 FT OFFSET

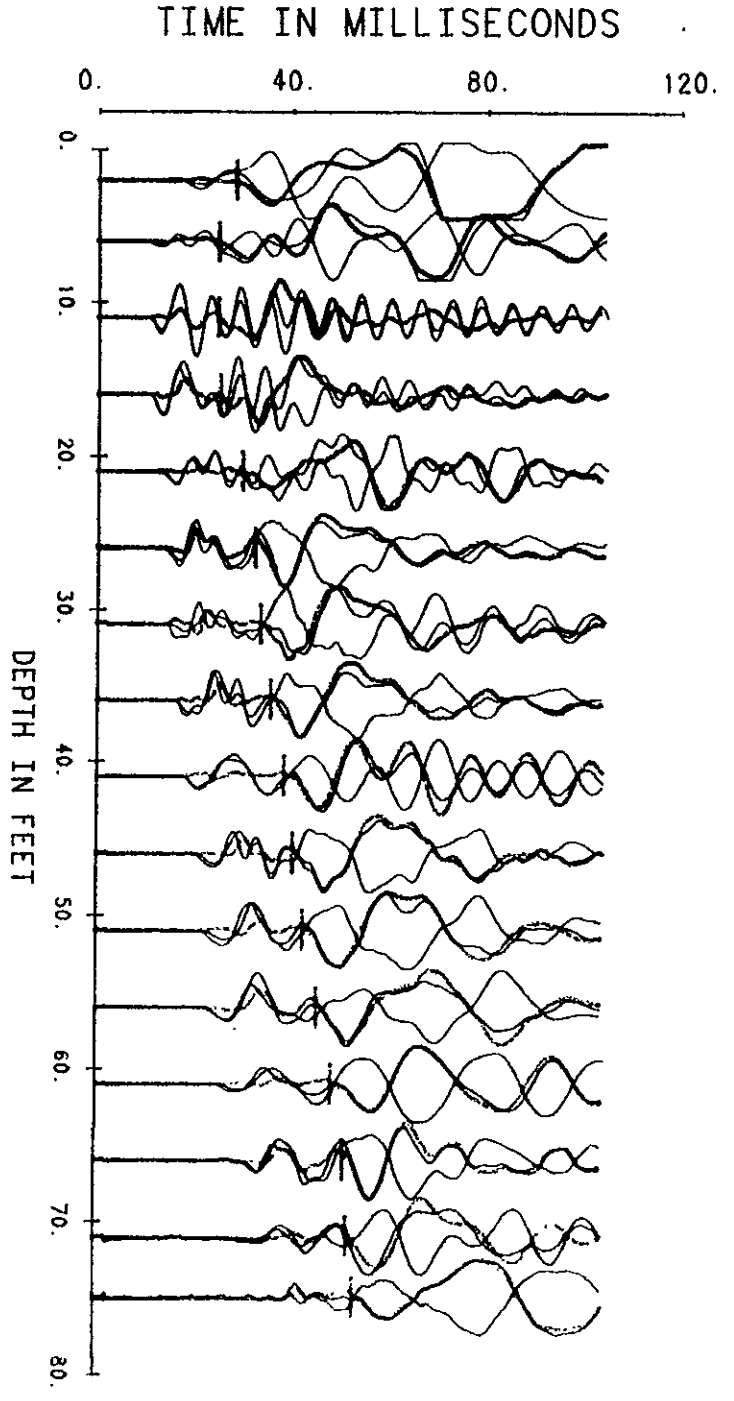

TURKEY FLAT DOWNHOLE SURVEY
HOLE # 8 - P WAVE DATA - 10 5 FT OFFSET

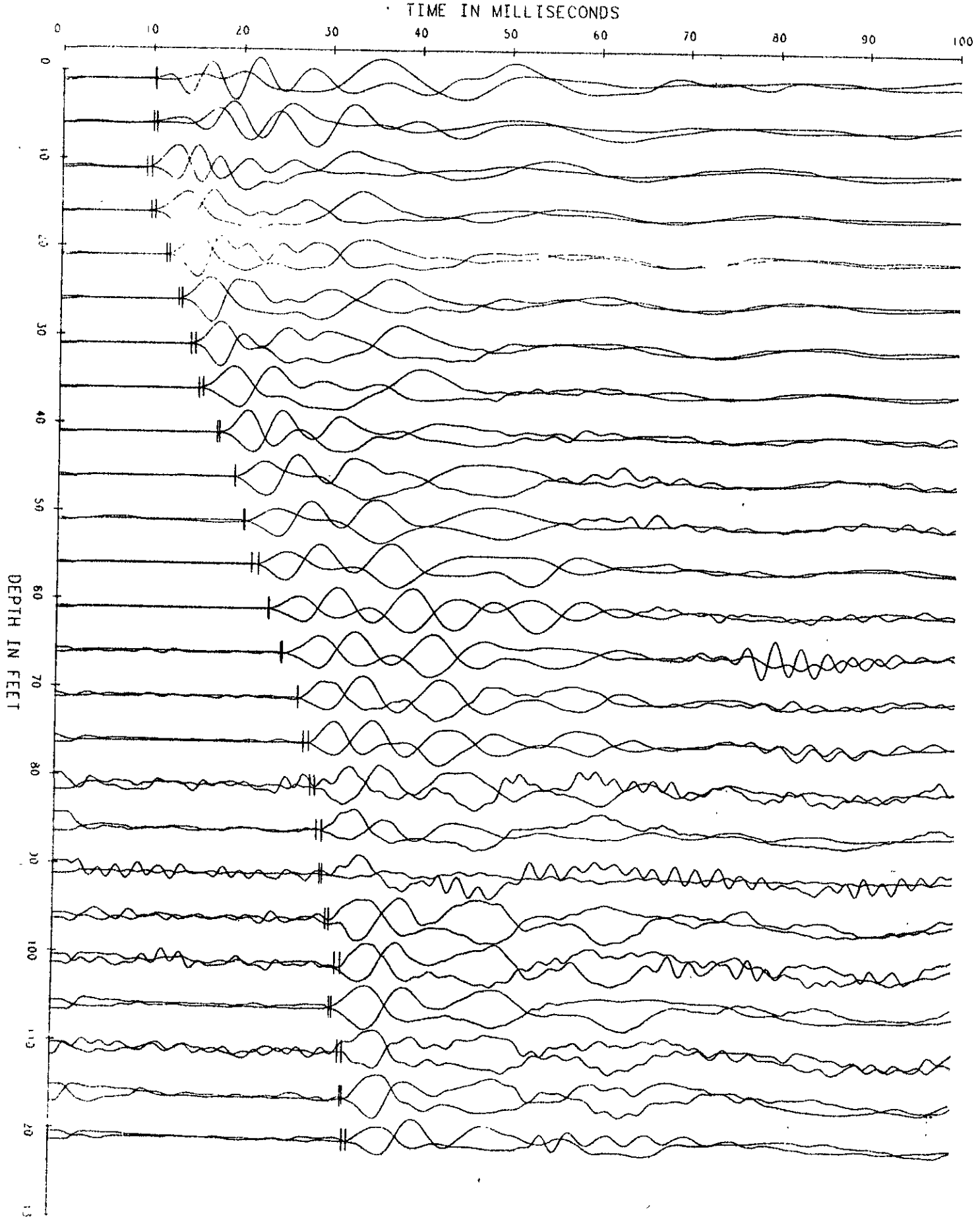

TURKEY FLAT DOWNHOLE SURVEY
HOLE # 8 - S WAVE DATA - 10.5 FT OFFSET

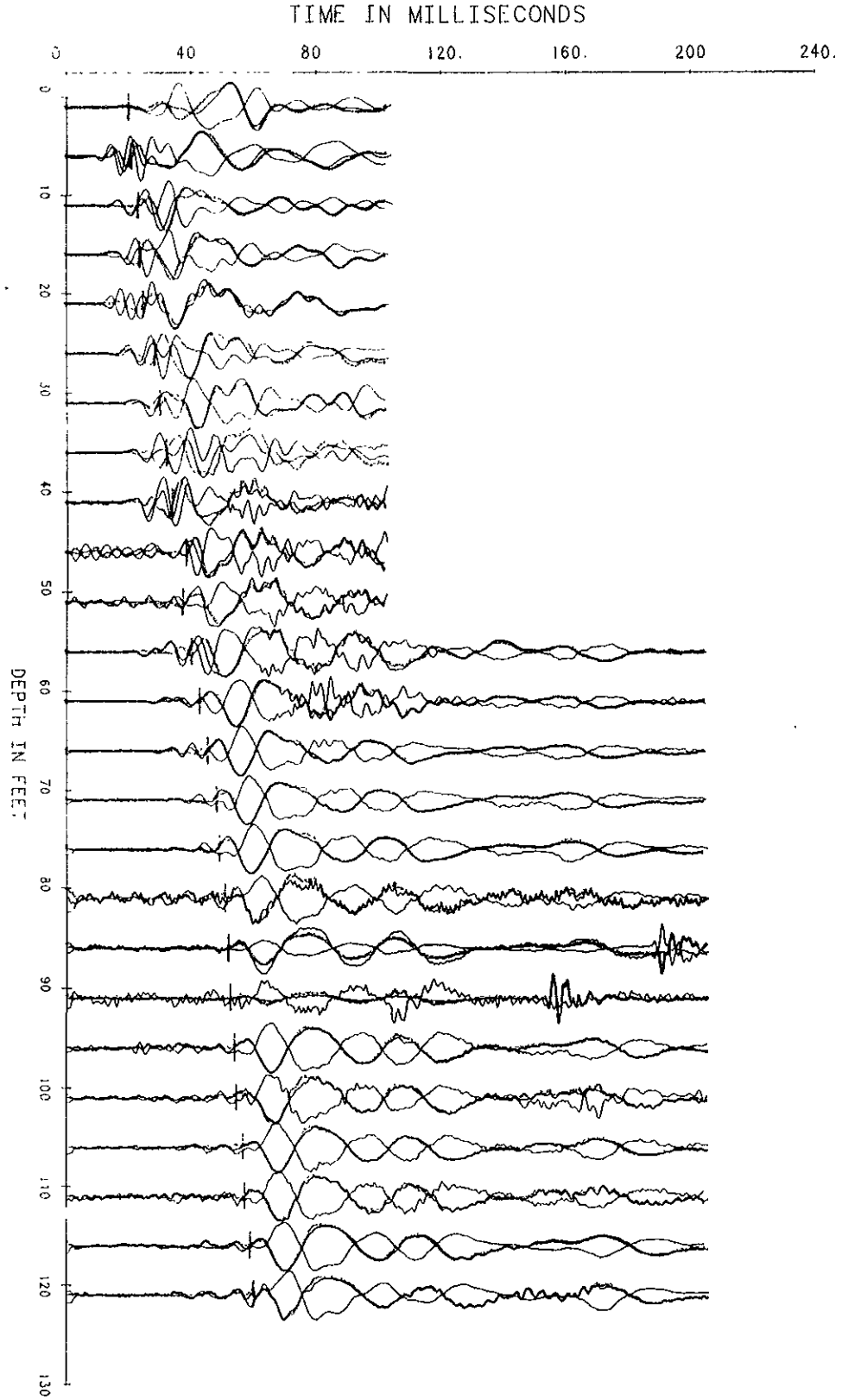

PART 2
BOREHOLE DEVIATION SURVEYS

Calculating the Survey

It is generally assumed that radius of curvature techniques provide the most accurate model for borehole survey calculations. However, radius of curvature calculations require use of computers or programmable calculators for their solution. For use on location, where a scientific calculator may be available, the angle averaging method is preferred. In most cases, the difference in bottom hole location between a survey calculated with radius of curvature techniques and the angle averaging method is not significant.

The angle averaging method assumes the borehole is parallel to the average of both the drift and bearing angles between adjacent survey stations. Once the two angles have been averaged, the calculation for each survey station is identical to the tangential method.

Survey data and computations should be recorded on a standard form, such as Eastman Whipstock's form illustrated in figure 13. Please refer to this form for the following.

The observed angles and observed directions are entered in columns 1 and 2.

Once the averaged angles and directions are figured and recorded in columns 5 and 11 respectively, the survey is then calculated as in the tangential method of calculation.

Measured depth (column 3) is the measurement taken with the top of the rotary table as the base and recorded on the disc envelope. Course length (column 4) is the difference between the last measured depth and the preceding one.

For figuring vertical depth (column 6), course deviation (column 10), latitude (columns 13 and 14) and departure (columns 15 and 16), use the following simplified formulas.

Vertical Depth = Course Length × Cosine (Average Drift Angle)

Course Deviation = Course Length × Sine (Average Drift Angle)

Check (when drift angle is less than 45°):

Course Deviation = Vertical Depth × Tangent (Drift Angle)

(when drift angle is more than 45°):

Vertical Depth = Course Deviation × Cotangent (Drift Angle)

Latitude (North or South) =

Course Deviation × Cosine (Average Drift Direction)

Departure (East or West) =

Course Deviation × Sine (Average Drift Direction)

Check (when drift direction is less than 45°):

Departure = Latitude × Tangent (Drift Direction)

(when drift direction is more than 45°):

Latitude = Departure × Cotangent (Drift Direction)

The north and south rectangular coordinates (columns 17 and 18) are the sums of the north or south coordinate differences (columns 13 and 14), respectively. The east and west rectangular coordinates (columns 19 and 20) are the sums of the east and west coordinate differences (columns 15 and 16), respectively.

True vertical depth (column 7) is an accumulative sum of the preceding vertical depths. By comparison with the measured depths, the total loss in depth in the hole can be ascertained at each measured depth.

At this point the true vertical depth and the rectangular coordinates have been derived for each point at which a single shot record was taken.

Column 12, Directional Difference, is the difference between the objective direction and the drift direction.

Column 9, Section Difference, is the product of the cosine of the directional difference multiplied by the course deviation.

Column 8, Vertical Section, is an accumulative sum of the section difference. Column 10, course deviation is the product of the sine of the drift angle multiplied by the course length.

To calculate the closure angle, divide the east or west rectangular coordinate (columns 15 or 16) by the north or south (columns 13 or 14). The answer is the tangent of the closure angle. Using Standard Field Tables, look up the tangent that matches closest with the calculation and read the degrees. To check, divide the north or south by the east or west. The quotient should be the cotangent of the same angle. The angle will be S-°E, S-°W, N-°E, or N-°W, depending on which columns the last rectangular coordinates are in.

To calculate closure distance, divide the east or west rectangular coordinate (column 19 and 20) by the sine of the closure angle. This will be larger than the last rectangular coqrdinate. To check, divide the north or south by the cosine of the closure angle, which should be the same closure distance.

Simplified formulas for closure angle and closure distance are:

$$\frac{\text{East or West}}{\text{North or South}} = \text{Tangent of the closure angle}$$

$$\frac{\text{East or West}}{\text{Sine of the closure angle}} = \text{Closure distance}$$

If Standard Field Tables are not available, the formula for figuring tangent will suffice:

$$\text{Tangent} = \frac{\text{Sine}}{\text{Cosine}}$$

A completed survey properly done by the angle averaging method should check extremely close to a computer printout using the radius of curvature method of calculation.

$\Delta V = \Delta D \cos \phi$

$\Delta H_N = \Delta D \sin \phi \cos Az$

$\Delta H_E = \Delta D \sin \phi \sin Az$

TF-1

EASTMAN WHIPSTOCK, INC.

COMPANY _____ FIELD _____ JOB NO. _____

LEASE _____ WELL NO. _____ DISTRICT _____

TYPE OF SURVEY _____ COMPUTATIONS _____ DATE _____

ENGINEER _____ OBJECTIVE _____ SHEET _____ OF _____

ϕ Declination 16° E Az ΔD

OBS ANGLE	OBS DIRECTION	MEASURED DEPTH		COURSE LENGTH (Ft)	AVG DRIFT ANGLE	VERTICAL DEPTH (Ft)	TRUE VERTICAL DEPTH (Ft)	VERTICAL SECTION	SECT'N DIFF.	COURSE DEVIAT'N	AVG. DRIFT DIRECTION	DIRECT'L DIFF	ΔCOORDINATE DIFFERENCES NORTH (+)	SOUTH (-)	EAST (+)	WEST (-)	RECTANGULAR COORDINATES NORTH (+)	SOUTH (-)	EAST (+)	WEST (-)
1	2	3		4	5	6	7	8	9	10	11	12	13	14	15	16	17	18	19	20
1¾°	25°NW	5-19	ft	19	351°	18.99	18.99						0.57		-0.09		0.57		- 0.09	
2°	33°NW	19-33	ft	14	343°	13.99	32.98						0.47		-0.14		1.04		- 0.23	
1⅛°	26°NW	33-47	ft	14	350°	14.00	46.98						0.32		-0.06		1.36		- 0.29	
⅔°	16°NW	47-61	ft	14	0°	14.00	60.98						0.16		0.00		1.52		- 0.29	
½°	75°NW	61-75	ft	14	316°	14.00	74.98						0.09		-0.08		1.61		- 0.37	

6-315R3

Calculating the Survey Sample Form
Figure 13

TF-2

EASTMAN WHIPSTOCK, INC.

COMPANY _____ FIELD _____ JOB NO. _____

LEASE _____ WELL NO. _____ DISTRICT _____

TYPE OF SURVEY _____ COMPUTATIONS _____ DATE _____

ENGINEER _____ OBJECTIVE _____ SHEET _____ OF _____

6 Declination 16° E AZ ΔD

OBS. ANGLE	OBS. DIRECTION	MEASURED DEPTH	COURSE LENGTH (Ft)	AVG. DRIFT ANGLE	VERTICAL DEPTH (Ft)	TRUE VERTICAL DEPTH (Ft)	VERTICAL SECTION	SECT'N DIFF.	COURSE DEVIAT'N	AVG. DRIFT DIRECTION	DIRECT'N DIFF.	Δ COORDINATE DIFFERENCES NORTH (Ft)	SOUTH	EAST (Ft)	WEST	RECTANGULAR COORDINATES NORTH (Ft)	SOUTH	EAST (Ft)	WEST
1	2	3	4	5	6	7	8	9	10	11	12	13	14	15	16	17	18	19	20
1½°	30° NE	0-14 Ft	10	46°	10.00	10.00						0.18		0.19		0.18		0.19	
1½°	32° NE	10-24 Ft	14	48°	14.00	24.00						0.25		0.27		0.43		0.46	
1½°	73° NE	24-38 Ft	14	89°	14.00	38.00						0.01		0.37		0.44		0.83	
1⅓°	89° NE	38-52 Ft	14	105°	14.00	52.00						-0.08		0.31		0.36		1.19	
1¼°	78° NE	52-66 Ft	14	89°	14.00	66.00						0.01		0.31		0.37		1.56	
1¼°	73° NE	66½-80½ Ft	14½	89°	14.50	80.50						0.01		0.32		0.38		1.94	

0-315R3

Calculating the Survey Sample Form
Figure 13

TF-3

EASTMAN WHIPSTOCK, INC.

COMPANY _____ FIELD _____ JOB NO. _____

LEASE _____ WELL NO. _____ DISTRICT _____

TYPE OF SURVEY _____ COMPUTATIONS _____ DATE _____

ENGINEER _____ OBJECTIVE _____ SHEET _____ OF _____

ϕ Declination 16°E Az

OBS. ANGLE	OBS. DIRECTION	MEASURED DEPTH (Ft)		COURSE LENGTH (Ft)	AVG. DRIFT ANGLE	VERTICAL DEPTH (Ft)	TRUE VERTICAL DEPTH (Ft)	VERTICAL SECTION	SECT'N DIFF.	COURSE DEVIAT'N	AVG. DRIFT DIRECTION	DIRECT'L DIF.	Δ COORDINATE DIFFERENCES NORTH (Ft)	SOUTH	EAST (Ft)	WEST	RECTANGULAR COORDINATES NORTH (Ft)	SOUTH	EAST (Ft)	WEST
1	2	3		4	5	6	7	8	9	10	11	12	13	14	15	16	17	18	19	20
2½°	S7°NW	4-18	ft	18	3½°	17.98	17.98						0.59		-0.52		0.59		-0.52	
1¾°	62°NW	18-32	ft	14	3¼°	13.99	31.97						0.30		-0.31		0.89		-0.83	
2½°	61°NW	32-46	ft	14	3½°	13.99	45.96						0.41		-0.43		1.30		-1.26	

G-315R3

Figure 13 Calculating the Survey Sample Form

TF-4 (Top of hole 1.5 ft below ground) (depths relative to ground level)

EASTMAN WHIPSTOCK, INC.

COMPANY _____ FIELD _____ JOB NO. _____

LEASE _____ WELL NO. _____ DISTRICT _____

TYPE OF SURVEY _____ COMPUTATIONS _____ DATE _____

ENGINEER _____ OBJECTIVE _____ SHEET _____ OF _____

ϕ Declination 16° E A2

OBS. ANGLE	OBS. DIRECTION	MEASURED DEPTH		COURSE LENGTH (Ft)	AVG DRIFT ANGLE	Δ VERTICAL DEPTH (Ft)	TRUE VERTICAL DEPTH (Ft)	VERTICAL SECTION	SECT'N DIFF.	COURSE DEVIAT'N	AVG. DRIFT DIRECTION	DIRECT'L DIFF.	Δ COORDINATE DIFFERENCES NORTH (Ft)	SOUTH	EAST (Ft)	WEST	RECTANGULAR COORDINATES NORTH (Ft)	SOUTH	EAST (Ft)	WEST
1	2	3		4	5	6	7	8	9	10	11	12	13	14	15	16	17	18	19	20
¼°	42° NW	8-22	ft	22.	334°	22.00	22.00						0.09		-0.04		0.09		-0.04	
⅓°	47° NW	22-36	ft	14.	329°	14.00	36.00						0.07		-0.04		0.16		-0.08	
⅞°	83° NW	36-50	ft	14.	293°	14.00	50.00						0.06		-0.15		0.22		-0.23	
¾°	67° NW	50-64	ft	14.	309°	14.00	64.00						0.12		-0.14		0.34		-0.37	
½°	10° NW	64-78½	ft	14.5	6°	14.50	78.50						0.13		0.01		0.47		-0.36	

G-315R3

Figure 13 Calculating the Survey Sample Form

TF-5

EASTMAN WHIPSTOCK, INC.

COMPANY _____ FIELD _____ JOB NO. _____

LEASE _____ WELL NO. _____ DISTRICT _____

TYPE OF SURVEY _____ COMPUTATIONS _____ DATE _____

ENGINEER _____ OBJECTIVE _____ SHEET _____ OF _____

ϕ Declination 16°E A2

OBS. ANGLE	OBS. DIRECTION	MEASURED DEPTH		COURSE LENGTH (Ft)	AVG. DRIFT ANGLE	VERTICAL DEPTH (Ft)	TRUE VERTICAL DEPTH (Ft)	VERTICAL SECTION	SECT'N DIFF.	COURSE DEVIAT'N	AVG. DRIFT DIRECTION	DIRECT'L DIFF.	Δ COORDINATE DIFFERENCES NORTH (Ft)	SOUTH	EAST (Ft)	WEST	RECTANGULAR COORDINATES NORTH (Ft)	SOUTH	EAST (Ft)	WEST
1	2	3		4	5	6	7	8	9	10	11	12	13	14	15	16	17	18	19	20
1°	76°NE	7-21	ft	21	92°	21.00	21.00						-0.01		0.37		-0.01		0.37	
2°	82°NE	21-35	ft	14	98°	13.99	34.99						-0.07		0.48		-0.08		0.85	
7/8°	65°NE	35-49	ft	14	81°	14.00	48.99						0.03		0.21		-0.05		1.06	
1¼°	89°NE	49-63	ft	14	105°	14.00	62.99						-0.08		0.30		-0.13		1.36	
1¾°	87°SE	63-77	ft	14	109°	13.99	76.98						-0.14		0.40		-0.14		1.76	

G-316R3

Calculating the Survey Sample Form
Figure 13

TF-6

EASTMAN WHIPSTOCK, INC.

COMPANY _____ FIELD _____ JOB NO. _____

LEASE _____ WELL NO. _____ DISTRICT _____

TYPE OF SURVEY _____ COMPUTATIONS _____ DATE _____

ENGINEER _____ OBJECTIVE _____ SHEET _____ OF _____

φ Declination 16°E A3

OBS. ANGLE	OBS. DIRECTION	MEASURED DEPTH		COURSE LENGTH (Ft)	AVG. DRIFT ANGLE	Δ VERTICAL DEPTH (Ft)	TRUE VERTICAL DEPTH (Ft)	VERTICAL SECTION	SECT'N DIFF.	COURSE DEVIAT'N	AVG. DRIFT DIRECTION	DIRECT'L DIFF.	Δ COORDINATE DIFFERENCES NORTH (Ft)	SOUTH	EAST (Ft)	WEST	RECTANGULAR COORDINATES NORTH (Ft)	SOUTH	EAST (Ft)	WEST
1	2	3		4	5	6	7	8	9	10	11	12	13	14	15	16	17	18	19	20
2°	50°NW	3-17	ft	17	326°	16.99	16.99						0.49		-0.33		0.49		-0.33	
1¾°	74°NW	17-31	ft	14	302°	13.99	30.98						0.23		-0.36		0.82		-0.69	
1°	64°NW	31-45	ft	14	312°	14.00	44.98						0.16		-0.18		0.98		-0.87	
⅓°	86°SW	45-59	ft	14	282°	14.00	58.98						0.02		-0.08		1.00		-0.95	
¼°	35°NE	59½-73½	ft	14.5	51°	14.50	73.48						0.04		0.05		1.04		-0.90	

G-315A3

Calculating the Survey Sample Form
Figure 13

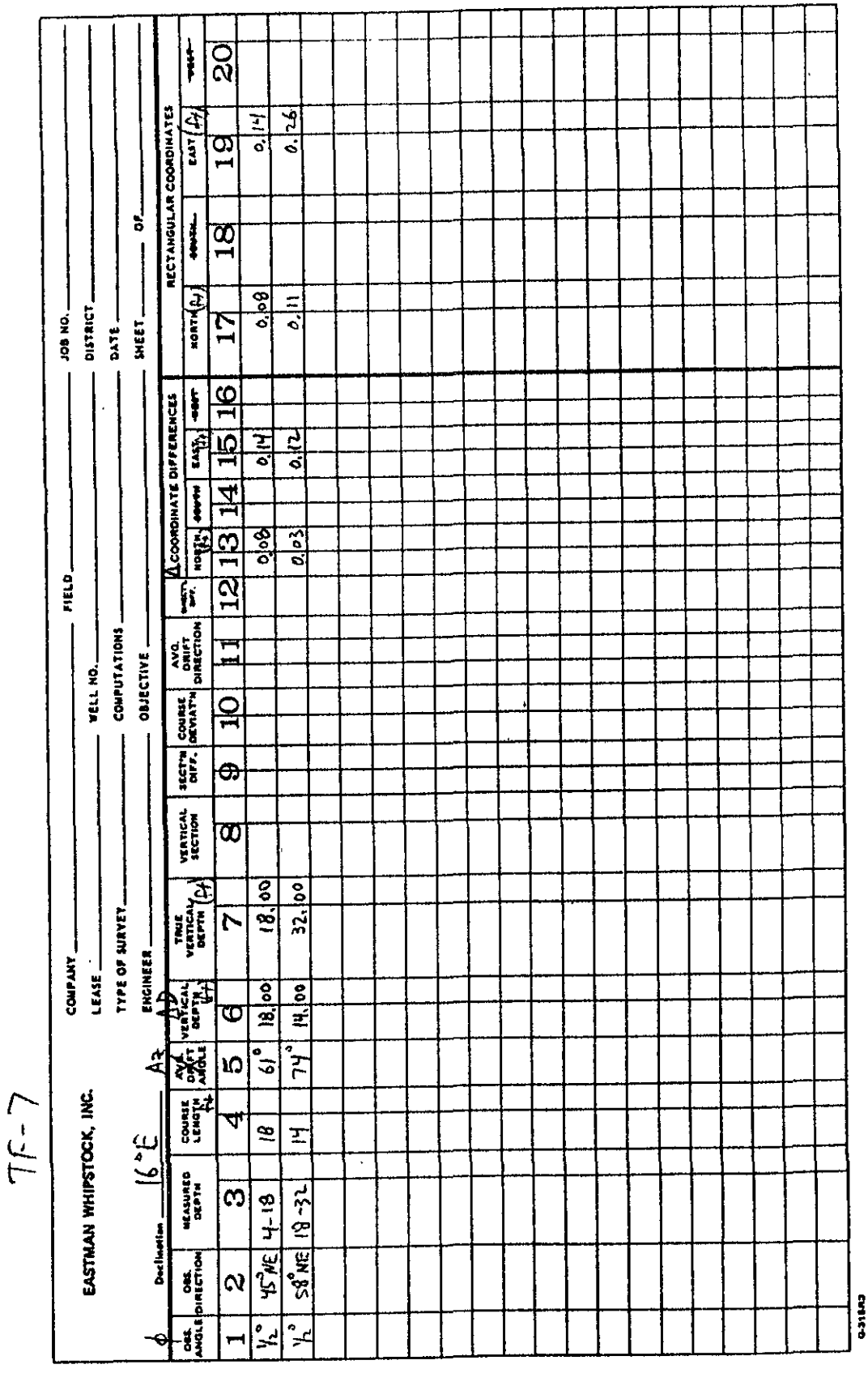

EASTMAN WHIPSTOCK, INC.

COMPANY _____ FIELD _____ JOB NO. _____

LEASE _____ WELL NO. _____ DISTRICT _____

TYPE OF SURVEY _____ COMPUTATIONS _____ DATE _____

ENGINEER _____ OBJECTIVE _____ SHEET _____ OF _____

Declination 16° E

TF-7

OBS. ANGLE	OBS. DIRECTION	MEASURED DEPTH	COURSE LENGTH	AVG. DRIFT ANGLE	VERTICAL DEPTHS	TRUE VERTICAL DEPTH	VERTICAL SECTION	SECT'N DIFF.	COURSE DEVIATN	AVG. DRIFT DIRECTION	SECT'N SEV.	COORDINATE DIFFERENCES NORTH (-)	COORDINATE DIFFERENCES EAST (-)	RECTANGULAR COORDINATES NORTH (+)	RECTANGULAR COORDINATES EAST (+)
1	2	3	4	5	6	7	8	9	10	11	12	13	14	15	16	17	18	19	20
½°	45° NE	4-18	18	61°	18.00	18.00						0.08		0.14		0.08		0.14	
½°	58° NE	18-32	14	74°	14.00	32.00						0.03		0.12		0.11		0.26	

0-31843

Calculating the Survey Sample Form
Figure 13

PART 3
RECONNAISSANCE SEISMIC SURVEYS

LINE-4

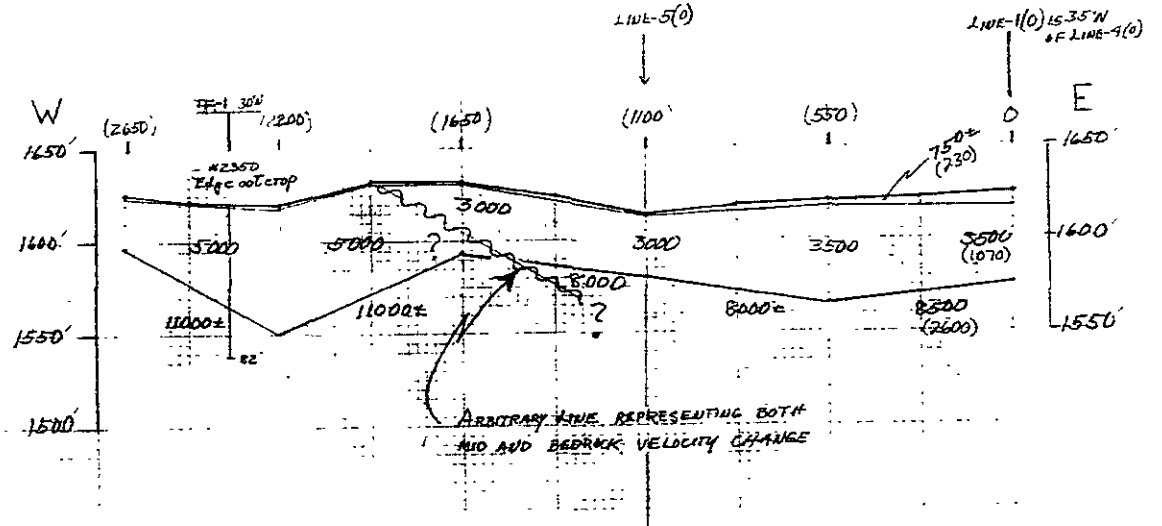

LINE-5

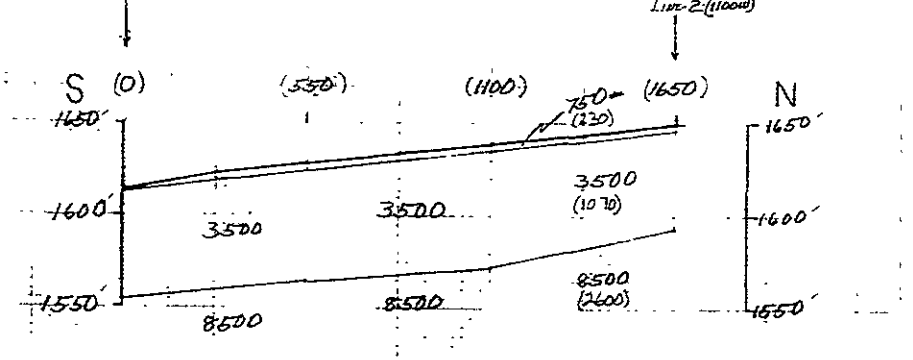

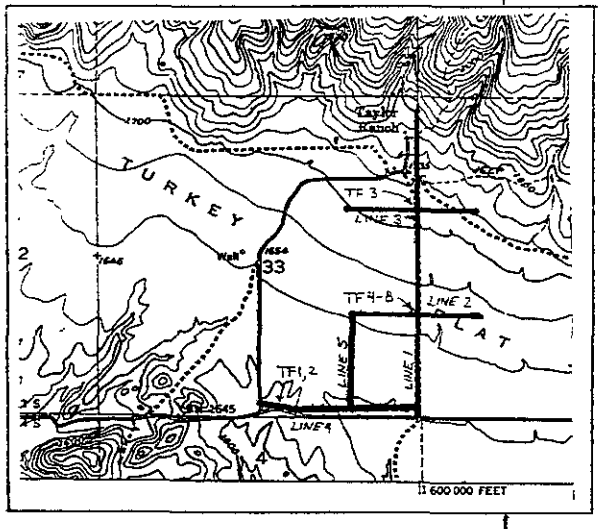

TURKEY FLAT
REFRACTION LINES

ELEVATIONS : FROM 25' CONTOURS
VELOCITY . FT/SEC (M/SEC)
LINES . 4, 5

DATE: 1/29/84

COMP: GWC

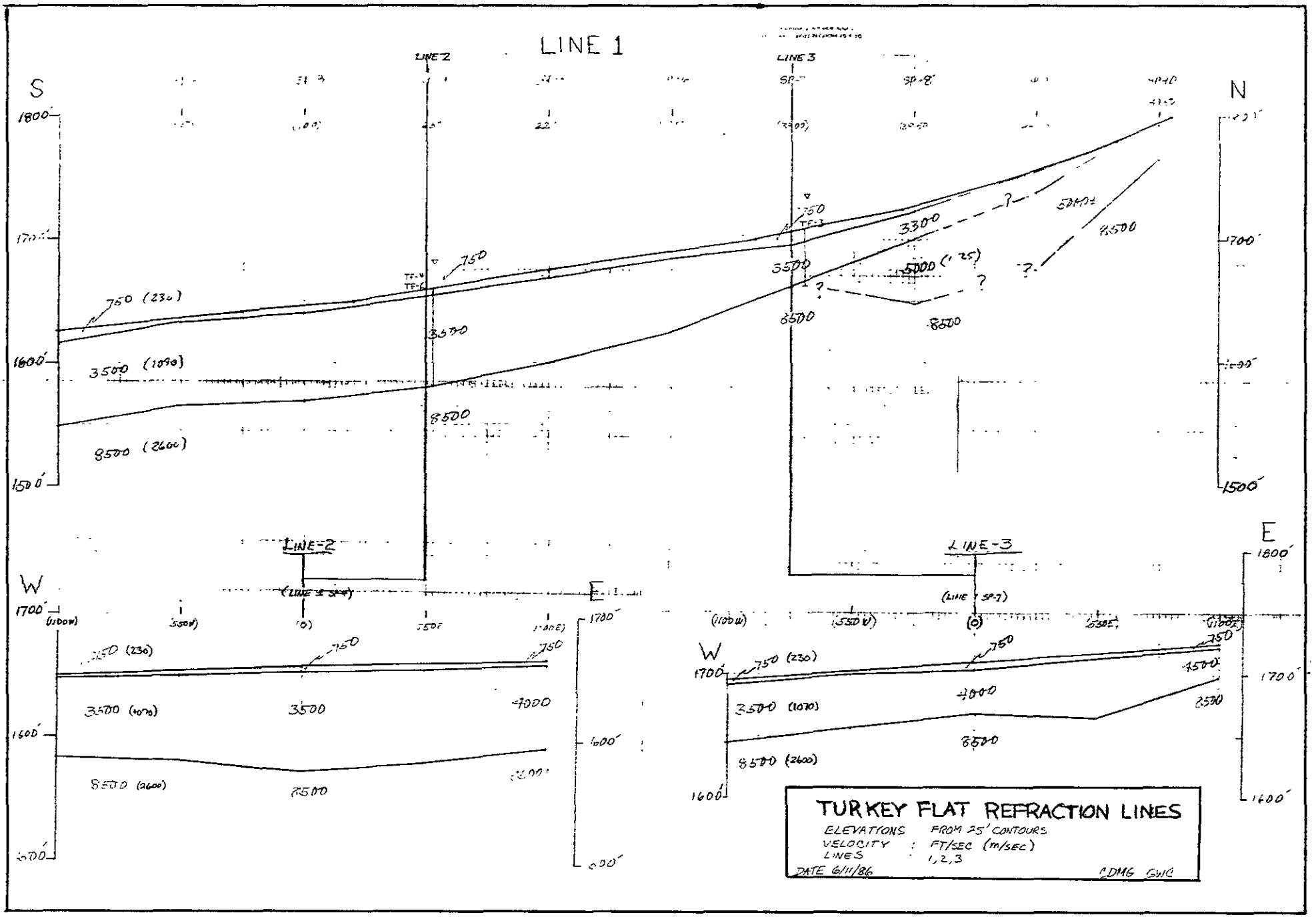

TURKEY FLAT REFRACTION LINES

ELEVATIONS FROM 25' CONTOURS
VELOCITY : FT/SEC (m/sec)
LINES 1, 2, 3

DATE 6/11/86 CDMG GWC

APPENDIX I
Woodward-Clyde Consultants

203 North Golden Circle Drive
Santa Ana, CA 92705
(714) 835-6886
(213) 581-7164
Telex 68-3420

Woodward-Clyde Consultants

21 May 1987

California Division of Mines and Geology
630 Bercut Drive
Sacramento, California 95814

ATTENTION: CHARLES R. REAL

SUBJECT: PARKFIELD DOWNHOLE SEISMIC MEASUREMENTS

Dear Mr. Real:

Woodward-Clyde Consultants is pleased to provide you with the attached results of our downhole seismic measurements. Time-distance graphs are shown for borings TF-1 through TF-6.

Measurements were obtained at each boring using the following methods. A steel bar was partially buried five feet from the boring and struck with a sledgehammer vertically and on either side to produce compressional and shear waves with opposite first motions. The downhole geophone consisted of a proprietary housing containing a triaxial geophone array clamped to the borehole wall using a pneumatic bladder. Amplification and recording was done using a EG & G ES-1225 seismograph. Values were obtained at five-foot intervals and have been time-shifted to correct for the source offset.

The results, as displayed on the attached drawings are self-explanatory. Notable features in this data set include: small but locally consistant velocity irreguliarities (e.g. lower velocity between 45 -50 feet in borings TF-5 and TF-6), and the presense of generally less than ten feet of surficial low velocity soils. Relatively constant velocity functions are shown on each plot since these appear to most meaningfully summarize the engineering significance of the results.

Please call me if you have any questions. I can be contacted at (714) 835-6886.

Very Truly Yours,

WOODWARD-CLYDE CONSULTANTS

Ronald Mees

RM/rp

Attachment

Woodward-Clyde Consultants

Sheet No. Of

Project

File

Phase Parkfield

Made by RLm Date 11-28-86

Subject Downhole Seismic Measurements

Checked by Date

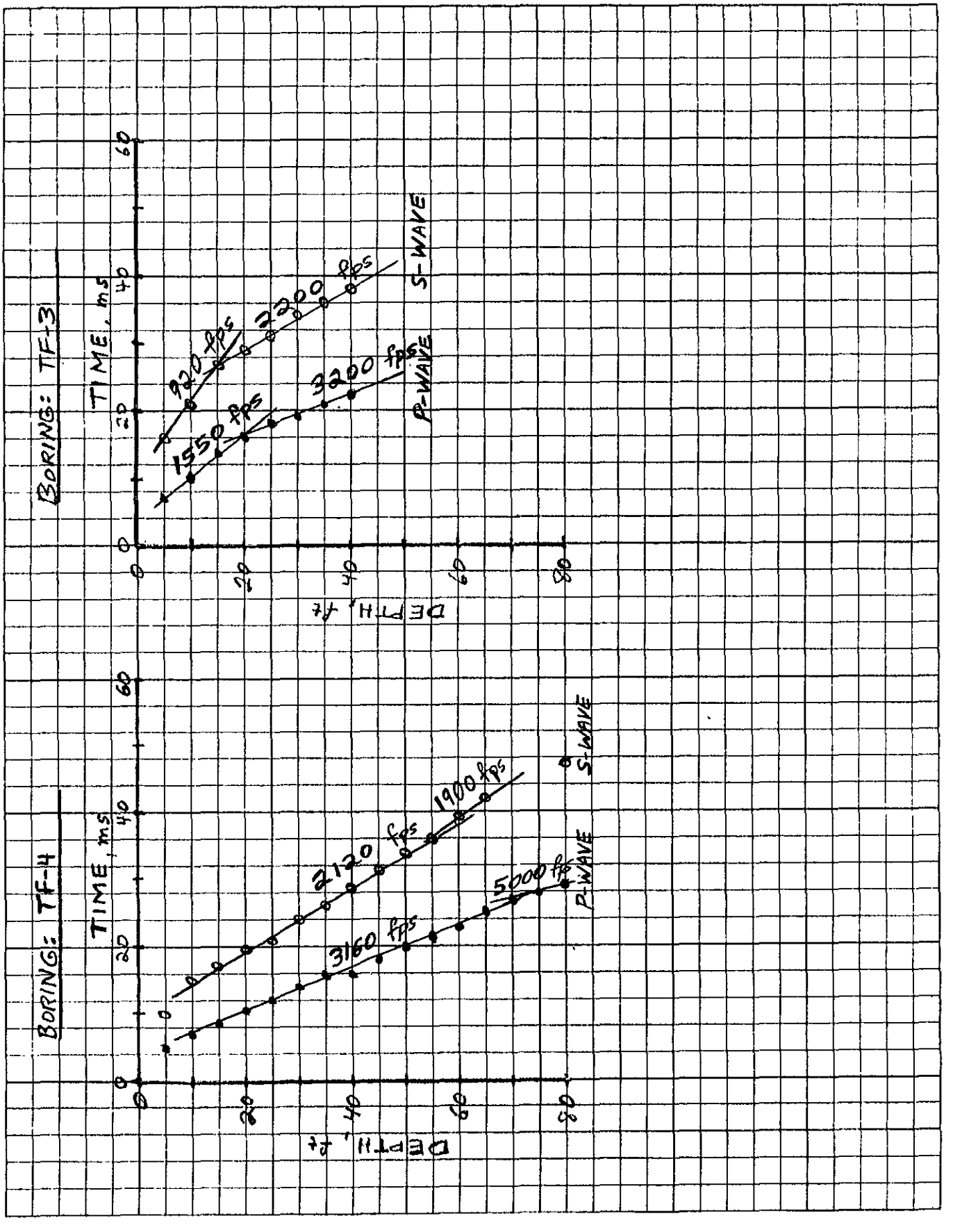

Woodward-Clyde Consultants

Sheet No. Of

Project

File

Phase Parkfield

Made by RLm Date 11-28-86

Subject Downhole Seismic Measurements

Checked by Date

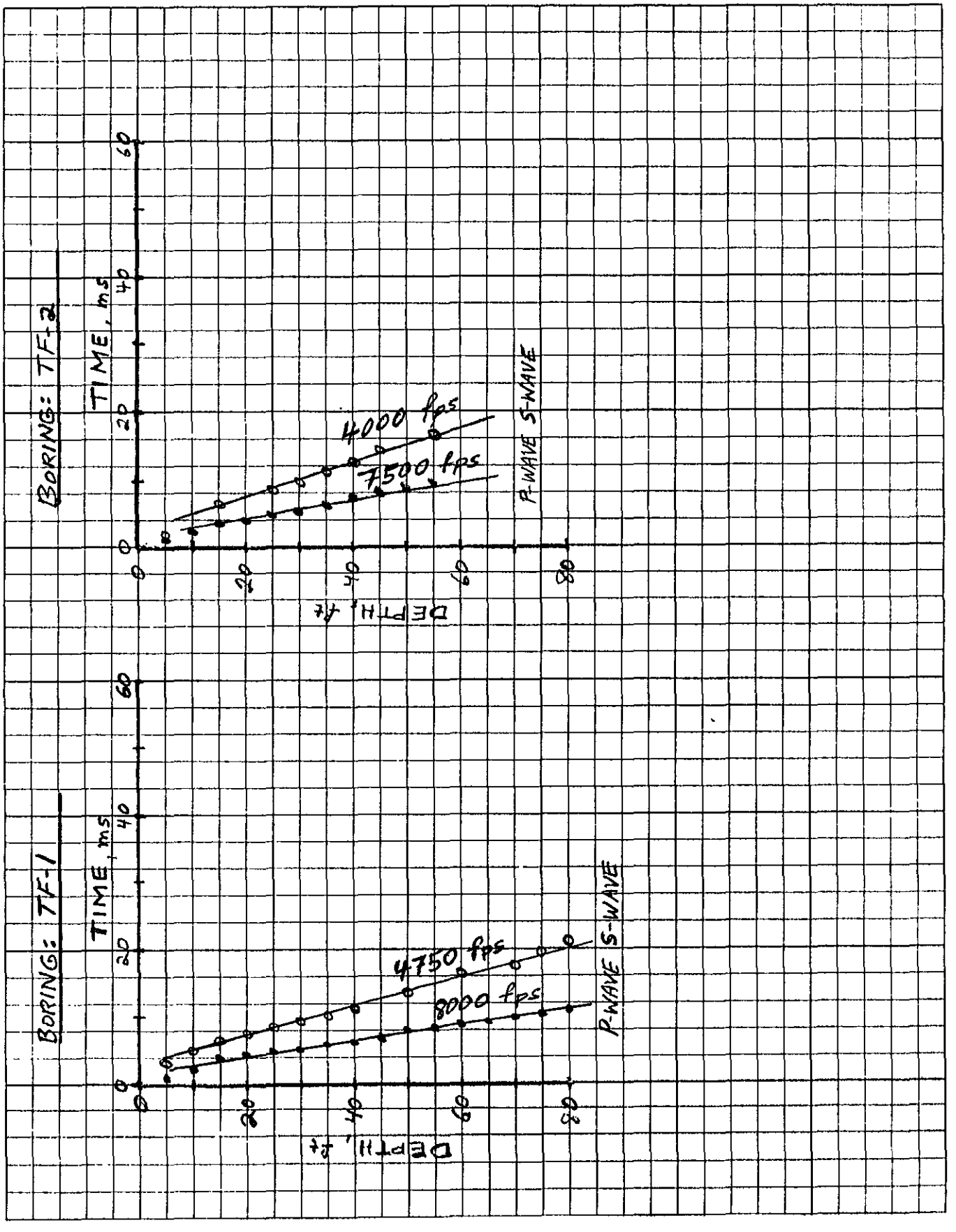

Woodward-Clyde Consultants

Sheet No. Of

Project

File

Phase Parkfield

Made by RLm Date 11-28-86

Subject Downhole Seismic Measurements

Checked by Date